Mechanistic Investigations on Bacterial Enzymes from Sulfur Metabolism and Terpene Biosynthesis

Kumulative Dissertation

zur

Erlangung des Doktorgrades (Dr. rer. nat.)

der

Mathematisch-Naturwissenschaftlichen Fakultät

der

Rheinischen Friedrich-Wilhelms-Universität Bonn

vorgelegt von

Anuj Kumar Chhalodia

aus Muzaffarnagar (India)

Bonn, 2024

Angefertigt mit Genehmigung der Mathematisch-Naturwissenschaftlichen Fakultät
der Rheinischen Friedrich-Wilhelms-Universität Bonn

Gutachter/Betreuer: Prof. Dr. Jeroen S. Dickschat
Gutachter: Prof. Dr. Dirk Menche

Tag der Promotion: 02.10.2024
Erscheinungsjahr: 2024

Die vorliegende Arbeit wurde in der Zeit vom 15.07.2019 bis zum 30.07.2024 am Kekulé- Institut für Organische Chemie und Biochemie der Rheinischen Friedrich-Wilhelms- Universität Bonn unter der Leitung von Prof. Dr. Jeroen S. Dickschat angefertigt.

Acknowledgement

First and foremost, I would like to express my deepest gratitude to my supervisor, Prof. Dr. Jeroen S. Dickschat. Your invaluable guidance, support, and insightful feedback have been instrumental in the completion of this thesis. Your dedication and hardwork have inspired me throughout this journey, and I am immensely grateful for the countless hours you have invested in mentoring me. Thank you for your patience, encouragement, and for always challenging me to strive for excellence. This thesis would not have been possible without your continuous support and belief in my abilities. Additionally, I would like to extend my thanks for making me a better long-distance bike rider.

I would like to express my deepest gratitude to Prof. Dr. Dirk Menche for spending time to read and referee my doctoral thesis, as well as Prof. Dr. Nikolay Kornienko and PD Dr. Christiane Dahl for their kindness in joining my thesis examination committee.

I would like to extend my heartfelt thanks to my labmates, with whom I spent most of my time and shared many enjoyable moments during my PhD journey. Special thanks go to Dr. Jan Rinkel and Dr. Lukas Lauterbach for teaching me the biological techniques at the beginning of my PhD journey. Additionally, I would like to thank Dr. Anwei Hou, Dr. Houchao Xu, Dr. Lin-Fu Liang, Zhiyong Yin, Dr. Zhiyang Quan, Heng Li, Dr. Geng Li, Dr. Binbin Gu, Kizerbo A. Taizoumbe, Dr. Georges B. Tabekoueng, Alain Tumma, Dr. Fulong Lin, Neran Reuber, and Alina Oseguera Jaramillo for creating a supportive and productive lab environment.

In addition, I would like to thank NMR department, HPLC pool, and Mass department for measuring lot of samples without which this thesis would not have been possible. I would like to extend my gratitude to technical staff for their help.

Finally, I would like to thank my parents, my grandmother, my grandfather, my buaji (Mrs. Mamta and Mrs. Prem), my fufaji (Mr. Manoj and Mr. Subash), my brother and my sisters for their continuous motivation and support in my difficult time and for making me what I am today. I would like to express my deepest gratitude to Meghana Shekar, Dr. Shah Alam and Dr. Sumaiya Afsar for their continuous support and help. Additionally, I would like to thank my friends Sudip Dey, Sandeep Kumar, Gourav Arora, and Avnish Singh.

Preamble

This cumulative doctoral thesis, titled “Mechanistic Investigations on Bacterial Enzymes from Sulfur Metabolism and Terpene Biosynthesis,” consists of eight chapters focusing on sulfur metabolism and terpene biosynthesis. Chapter 1 provides a detailed introduction to the biosynthesis of dimethylsulfonium propionate (DMSP) in plants and bacteria, along with the enzymes involved in sulfur metabolism. Chapters 2–7 each contain a brief introduction and summary of the associated publications. Chapter 8 offers a comprehensive summary of the work presented in this thesis and discusses how the reported scientific advances could influence future research. The corresponding publications are included in Appendices A–F.

Table of contents

1. Dimethylsulfonium propionate (DMSP) 1
   - 1.1 Marine sulphur cycle 2
2. Biosynthesis of DMSP 4
   - 2.1 Biosynthesis of DMSP in plants 4
   - 2.2 Biosynthesis of DMSP in bacteria 5
   - 2.3 Biosynthesis of DMSP in algae 6
   - 2.4 Biosynthesis of DMSP in dinoflagellates 7
3. DMSP cleavage 8
   - 3.1 Phytoplankton cleavage 8
   - 3.2 Bacterial cleavage 9
   - 3.2.1 DMSP lysis pathway 9
   - 3.2.2 DMSP lyase DddD 10
   - 3.2.3 DMSP lyase DddL 11
   - 3.2.4 DMSP lyase DddP 11
   - 3.2.5 DMSP lyase DddQ 13
   - 3.2.6 DMSP lyase DddW 15
   - 3.2.7 DMSP lyase DddK 17
   - 3.2.8 DMSP lyase DddY 18
   - 3.2.9 DMSP lyase DddX 19
   - 3.2.10 DMSP lyase DddU 20
   - 3.2.11 DMSP lyase enzyme Alma1 20
   - 3.3 DMSP demethylation pathway 21
   - 3.3.1 DMSP demethylase (DmdA) 21
   - 3.3.2 3-Methylmercaptopropionyl-CoA ligase (DmdB) 23
   - 3.3.3 MMPA-CoA dehydrogenase (DmdC) 24
   - 3.3.4 MTA-CoA hydratase (DmdD) 25
4. Substrate tolerance of *Roseobacter* clade marine bacteria and DMSP lyase 26
5. Identification of volatiles from six marine *Celeribacter* strains 29

6.	Breakdown of 3-(allylsulfonio)propanoates in bacteria from the *Roseobacter* group yields garlic oil constituents	35
7.	Discovery of dimethylsulfoxonium propionate lyases – a missing enzyme relevant to the global sulfur cycle	43
8.	Functional characterisation of twelve terpene synthases from actinobacteria	49
9.	The Stereochemical Course of DmdC, an Enzyme Involved in the Degradation of Dimethylsulfoniopropionate	57
10.	On the Substrate Scope of Dimethylsulfonium Propionate Lyases toward Dimethylsulfoxonium Propionate Derivatives	63
11.	Summary and outlook	69
12.	References	75
13.	Appendices A–F	87

Chapter 1

Introduction

1. Dimethylsulfonium propionate (DMSP)

The discovery that red algae, particularly *Polysiphonia fastigiata* and *P. grescens* emit dimethylsulfide (DMS, **6**),[1] resulted in the identification of dimethylsulfonium propionate (DMSP, **5**) as its precursor.[2] DMSP (**5**) exists in a zwitterionic form and is found in marine surface waters, typically in concentrations of less than 1 nanomolar.[3] It serves various functions in different organisms, including regulating cell volume osmotically and acting as an antioxidant, predator deterrent, and cytoprotectant.[4,5] While micro and macroalgae are the primary producers of DMSP (**5**), certain plants also contribute to its formation. It plays a crucial role in the marine sulfur cycle and acts as a source of reduced sulfur for marine microbes. Notably, marine phytoplankton emerge as the predominant DMSP (**5**) producers, thereby serving as the primary source of atmospheric DMS (**6**) emissions.[6,7]

Marine enzymes possess the ability to break down DMSP (**5**) with the formation of DMS (**6**) and methanethiol (**11**) via different pathways. Nine enzymes (DddW, DddQ, DddP, DddK, DddL, DddU, DddX, DddY, and Alma1) derived from marine bacteria and algae have been identified, facilitating the cleavage of DMSP (**5**) into DMS (**6**) via the lysis pathway. Additionally, four enzymes (DmdA-D) are known for their role in converting DMSP (**5**) into methanethiol (**11**) through the demethylation pathway.[8,9] A detailed discussion about the DMSP (**5**) degradation pathways will be presented in section 3.2. It has been reported that only 2-21% of water-soluble DMSP (**5**) undergoes conversion into DMS (**6**) via the lysis pathway, while approximately 80% of DMSP (**5**) is transformed into methanethiol (**11**) via the demethylation pathway. This implies that its release from the oceans is largely influenced by the phytoplankton community (Figure 1).[10,11]

Despite of its significance in the biogeochemical sulfur cycle and its pivotal role in global ecology, marine DMS (**6**) is released into the atmosphere from the oceans at an annual rate of approximately 2×10^7 tons.[8,12] Upon release, DMS (**6**) undergoes oxidation in the atmosphere, leading to the formation of sulfur compounds such as sulfates (**13**), sulfur dioxide (**14**) and dimethyl sulfoxide (DMSO, **8**). These compounds serve as nuclei for cloud condensation, and rain down to earth to close the sulfur

cycle.[7] DMS (**6**) also increases the sulfur burden in the atmosphere, impacting DMSP (**5**) production in oceans, a phenomenon explained by the CLAW hypothesis.[13]

The CLAW hypothesis proposes a link between solar radiation and atmospheric DMS (**6**) concentrations, suggesting that increased solar radiation leads to higher ocean temperatures, promoting the growth of DMSP (**5**) producing marine phytoplankton and consequently increasing total DMSP (**5**) production. This increase in amount of DMSP (**5**) results in elevated atmospheric DMS (**6**) levels, leading to cloud formation, which then decreases solar radiation. This decrease in solar radiation slows down marine phytoplankton growth, leading to a reduction in DMSP (**5**) production–a negative feedback loop. However, Lovelock proposed the anti-CLAW hypothesis, suggesting that rising global temperature cause ocean surface warming, which in turn, increases stratification and decreases nutrient flux, hindering the growth of DMSP (**5**) producing phytoplankton and reducing atmospheric DMS (**6**) levels.[6,14] This hypothesis provides a positive feedback between global temperature and DMS (**6**) production.

In 2018, Thume et al. uncovered an additional molecule closely related to DMSP (**5**) known as dimethylsulfoxonium propionate (DMSOP, **7**), synthesized by marine bacteria and algae. DMSOP (**7**) is characterized as a zwitterionic metabolite present in nanomolar concentrations, adding a novel aspect to the biochemical story. This discovery results in the enzymatic ability of marine bacteria to break down DMSOP (**7**) into dimethyl sulfoxide (DMSO, **8**) and acrylate (**9**) (Figure 1). Isotope labeling experiments suggest DMSOP (**7**) may originate from DMSP (**5**) via enzymatic oxidation. Although, the enzymes responsible for DMSP (**5**) oxidation to DMSOP (**7**) and its cleavage to DMSO (**8**) remain unknown.[15] Our recent study has addressed an important missing link after discovering the enzymes responsible for cleaving DMSOP (**7**) into DMSO (**8**) and acrylate (**9**).[16] A detailed discussion will be presented in chapter 4. However, an essential link remains open, no enzyme has been identified for oxidizing DMSP (**5**) into DMSOP (**7**).

1.1 Marine sulfur cycle

DMSP (**5**), abundant in sulfur, is estimated to contribute significantly, ranging from 3% to 10% of the carbon and 30% to 100% of the sulfur supply for catabolic bacteria. The process of DMSP (**5**) biosynthesis initiates with the uptake of inorganic sulfate (**1**) from seawater by algae and phytoplankton.

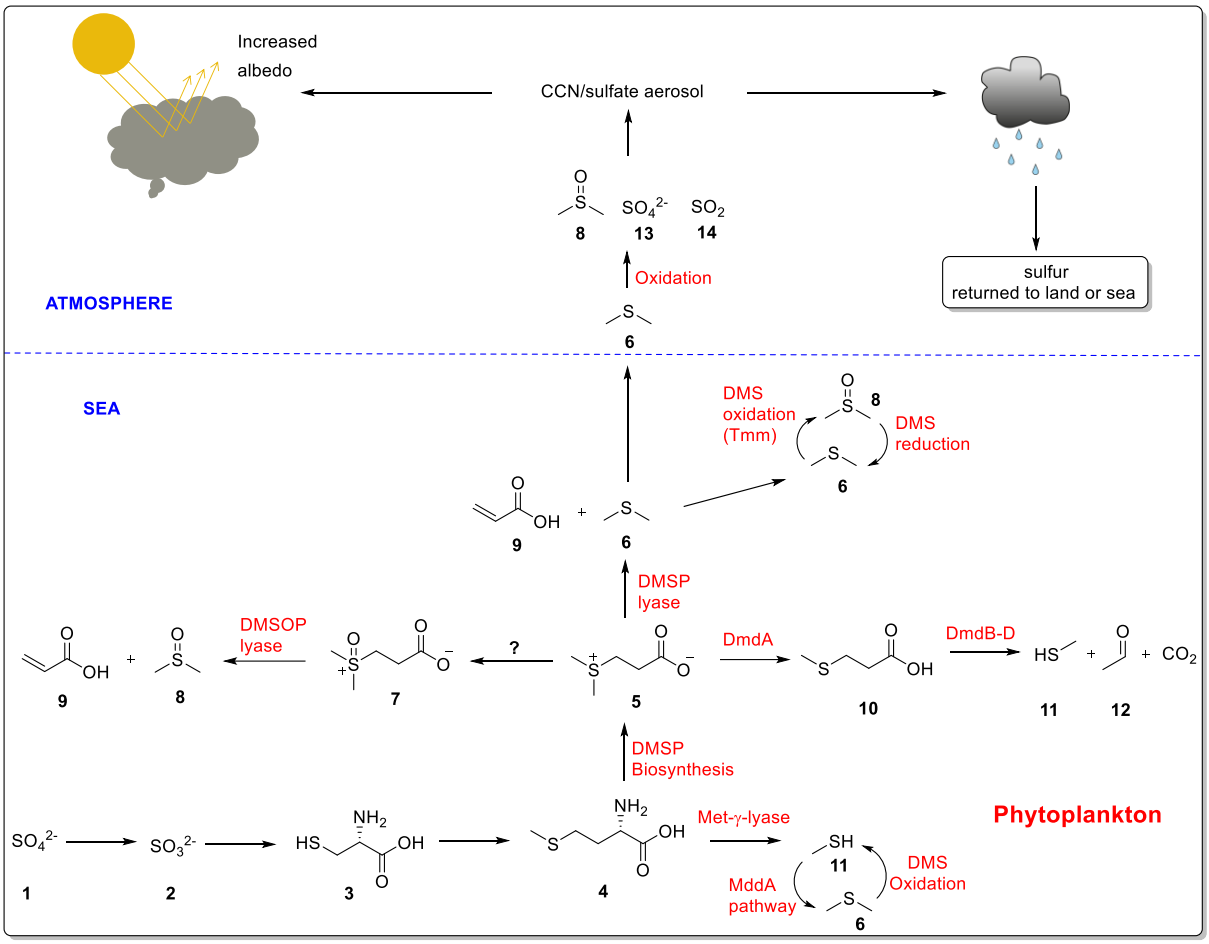

Figure 1. The biogeochemical cycle of DMSP (**5**), MeSH (**11**) and DMS (**6**) in seawater and the atmosphere.

Sulfate (**1**) undergoes conversion into sulfite (**2**), and subsequently into sulfur-based amino acids such as cysteine (**3**) and methionine (**4**), eventually leading to the formation of **5**. Enzymes further oxidize **5** into **7**; however, as discussed in section 1, the identity of these enzymes remains unknown. Through the action of DMSP lyases, **5** undergoes a degradation resulting in the formation of **6** and **9**, while compound **7** breaks down into **8** and **9**. DMSP lyases play a key role in these conversions. Particularly, the release of DMS (**6**) into the atmosphere from the ocean holds a significant climatic importance. The DMSP demethylation enzymes facilitate the breakdown of **5** into **11** and **12**, while methionine γ-lyase directly transforms **4** into **11**. MddA (methanethiol S-methyltransferase) further converts **11** into **6**. As a result, **6** undergoes oxidation, leading to the formation of sulfate aerosols. These aerosols serve as nuclei for cloud condensation, ultimately returning to the land or ocean through phenomena like acid rain (Figure 1).[17]

2. Biosynthesis of DMSP

The ability to produce **5** is widespread across various kingdoms of life, with genetic information for its biosynthesis present in organisms ranging from red algae[2] to green algae,[18] coastal plants,[19] diatoms,[20] coccolithophores,[20] dinoflagellates,[21] and even corals.[22] Remarkably, while some organisms such as coccolithophores and diatoms utilize a similar biosynthetic pathway for **5**, that is observed in red and green algae, others like dinoflagellates employ a distinct pathway. This suggests that the evolution of the biosynthetic pathway for **5** in plants, green algae, and dinoflagellates occurred independently, underscoring the diverse origins and adaptations within this fundamental biochemical process across different taxa.

2.1 Biosynthesis of DMSP in plants

The DMSP (**5**) biosynthesis pathway in plants like *Wollastonia biflora* and *Spartina alterniflora* begins with L-methionine (**4**) as the precursor (Figure 2). Although the initial and final steps are the same in both plants, intermediate steps vary. In both species, the first step involves the methylation of **4** to produce S-methyl-L-methionine (**15**). In *W. biflora*, after the formation of **15**, the pathway includes transamination-decarboxylation, leading to the formation of 3-(dimethylsulfonio)propionaldehyde (**18**), via a highly unstable intermediate 4-(dimethylsulfonio)-2-oxobutyrate (**17**), which has never been observed.[19,23-24] On the other hand, in *S. alterniflora*, **15** decarboxylates to form 3-(dimethylsulfonio)propylamine (**16**), followed by oxidative deamination to produce **18**. However, both plants undergo a final oxidation step to yield **5**.

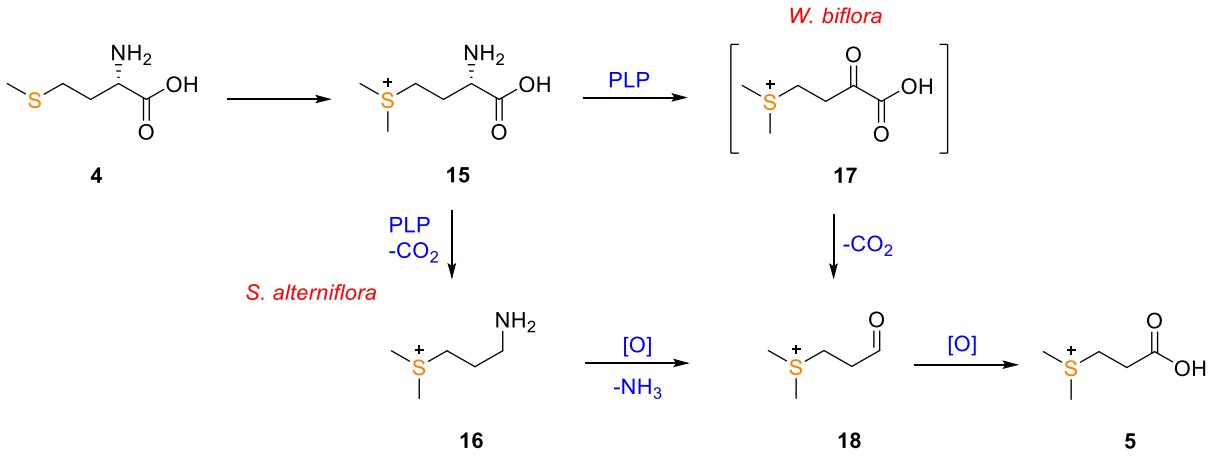

Figure 2. Biosynthesis of **5** in plants species *W. biflora* and *S. alterniflora*.

In *W*. *biflora*, the initial methylation step was examined via a pulse-chase experiment utilizing [^{14}C]-**4**. These results demonstrated a rapid conversion of [^{14}C]-**4** to **6**, alongside the formation of labeled acrylate (**9**).This suggests that **5** is derived from **4** through a sequence of methylation, deamination, decarboxylation, and oxidation steps (Figure 2).[25] Methionine *S*-methyltransferase responsible for the methylation of **4**, was isolated from *W*. *biflora* leaves and identified as a tetramer.[26]

Feeding experiments with [^{14}C]-**15** and [$^{13}CH_3$, C^2H_3]-**15** resulted in the efficient conversion into [^{14}C]-**5** and [$^{13}CH_3$, C^2H_3]-**5**, confirming **15** as the direct precursor for **5** (Figure 2).[19] The transamination step was confirmed by feeding [*methyl*-$^2H_3$,^{15}N]-**15** to leaf discs, which increased the ^{15}N abundance in glutamate, consistent with transamination.[24] In *S. alterniflora*, feeding [^{35}S]-**4** to leaves led to the formation of **15**, indicating similarity in the methylation step across both plants. Furthermore, feeding experiments with [^{35}S]-**15** and [^{35}S]-**16** led to the formation of **5** via the highly unstable intermediate **18**, demonstrating that the final step in the biosynthetic pathway is the same for both plants.[23]

2.2 Biosynthesis of DMSP in bacteria

To date, a diverse range of marine bacteria has been identified as capable of converting **4** into **5** through the methionine transamination pathway.[27,28] The key enzyme DsyB, responsible for this process, was first discovered in marine Alphaproteobacteria (*Labrenzia aggregata* LZB033).[27] Further understanding of the DMSP (**5**) biosynthetic pathway has been achieved through the isolation and characterization of four enzymes—MSMT, SMMDC, DMSPAAT, and DMSPADH from the bacterium *Streptomyces mobaraensis* (Figure 3). Bacterial MSMT (methionine S-methyltransferase), which shares 24% amino acid sequence identity with MSMT of *W. biflora* and *S. alterniflora*, catalyzes the transfer of a methyl group from SAM to **4**, resulting in the formation of **15**. Notably, the binding mechanism of methionine to bacterial MSMT differs from that observed in plants (*W. biflora* and *S. alterniflora*). Following that, the PLP-dependent decarboxylase enzyme SMMDC (S-methylmethionine decarboxylase) fulfills a critical role in the pathway. SMMDC shares about 50% of its amino acid sequence identity with bacterial diaminopimelic acid decarboxylase and less than 30% with plant proteins. Despite this, it efficiently catalyzes the decarboxylation of **15**, resulting in the production of **16**.

Interestingly, DMSPAAT (DMSP aminotransferase) with 60% amino acid sequence identity to the putative bacterial transaminase (WP_10376337370 from *Roseovarius confluentis*) and less than 35% to plant enzymes, transfers an amine group from **16** to pyruvate, forming intermediate **18**. Intermediate **18** decays rapidly to **6** and acrolein (**19**), indicating that DMSPAAT alone does not yield **5**. To catalyze the final step of biosynthesis of **5**, a reaction involving SMMDC, DMSPAAT, and DMSPADH (DMSPaldehyde dehydrogenase), along with NAD^+, was conducted, that resulted in an 80% conversion of **15** into **5**.[28]

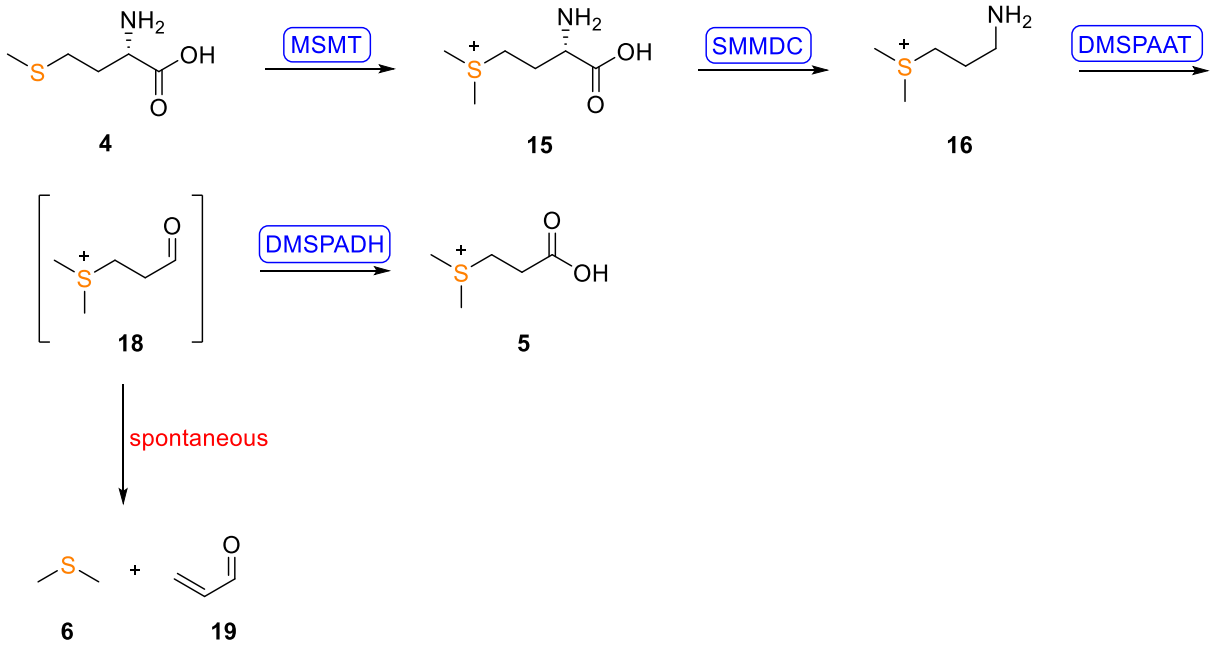

Figure 3. Biosynthetic pathway of **5** in *Streptomyces mobaraensis*.

2.3 Biosynthesis of DMSP in algae

In 1935, Haas's discovery revealed that certain marine algae, including *Polysiphonia fastigiata* and *P. grescens*, produce **6** when exposed to air,[1] Challenger and Simpson were the first to isolate **5** from these red algae, identifying it as the precursor for **6**.[2] Presently, a variety of marine organisms including bacteria, algae, phytoplankton, diatoms, and coccolithophores are recognized for their capacity to generate **5**.

In 1962, initial experiments aiming at the biosynthesis of **5** in red algae using labeled **4** were conducted. Feeding experiments using [^{35}S]-**4** and [*methyl*-^{14}C]-**4** indicated that the methyl group and sulfur of **5** originate from **4**, while feeding of [2-^{14}C]-**4** demonstrated that the carboxyl group arises from the C_α position of **4**. These findings

are consistent with the hypothesis proposing that the conversion of **4** to **5** involves deamination, decarboxylation, oxidation, and methylation steps.[18]

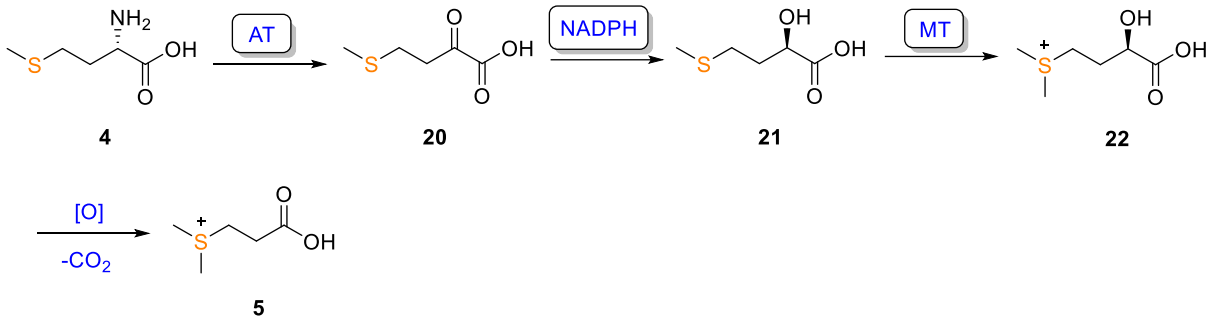

Figure 4. Biosynthetic pathway of **5** in green and red algae.

Subsequently, detailed investigations on the algal DMSP (**5**) biosynthetic pathway were conducted through feeding of [^{35}S]-**4** to the green algae *Enteromorpha intestinalis* (*Ulva intestinalis*). *In vitro* experiments using cell-free extracts revealed the involvement of a 2-oxoglutarate-dependent aminotransferase (AT) in the transamination step, while the reduction of 4-(methylthio)-2-oxobutanoic acid (**20**) to 2-hydroxy-4-(methylthio)butanoic acid (**21**) was found to be NADPH-dependent. The methylation step was mediated by a SAM-dependent methyltransferase (MT), producing 4-(dimethylsulfonio)-2-hydroxybutanoate (**22**) (Figure 4).[29]

Based on kinetics experiments with [^{35}S]-**4** and the identification of isolated intermediates, a proposed biosynthetic pathway for **5** was established (Figure 4). Initially, **4** undergoes transamination to produce **20**, which is then reduced to form **21**. Subsequently, *S*-methylation of **21** generates **22**, which undergoes oxidative decarboxylation to produce **5**.[29] This pathway notably differs from that observed in plants, as intermediates **15**, **16**, and **18** (Figure 2) known from plant DMSP (**5**) biosynthesis were not observed in the algal DMSP (**5**) biosynthesis.[30]

2.4 Biosynthesis of DMSP in dinoflagellates

A distinct biosynthetic pathway for **5** is observed in dinoflagellates. However, the complete understanding of the biosynthetic pathway in these organisms remains a subject of ongoing exploration. The dinoflagellate *Crypthecodinium cohnii* is a known producer of **5**. Research conducted by Uchida et al. in 1996, through the feeding of [^{35}S]-**4** and [*methyl*-^{14}C]-**4** to *C*. *cohnii*, demonstrated that sulfur, the methyl group, and carbons 2 and 3 of **4** were efficiently incorporated into **5**. This supports the hypothesis that **5** is derived from **4** through decarboxylation, deamination, and methylation

processes. Interestingly, the common feeding of **4** together with the plant intermediate **15** did not hinder the incorporation of **4** into **5**, whereas feeding of **4** with methylmercaptopropionic acid (**10**) inhibited this process. These findings suggest that the biosynthesis of **5** involves the decarboxylation of **4** to produce 3-(methylthio)propylamine (**23**), followed by transamination and oxidation to yield **10**. Further methylation by SAM results in the formation of **5** (Figure 5).[8,21,31]

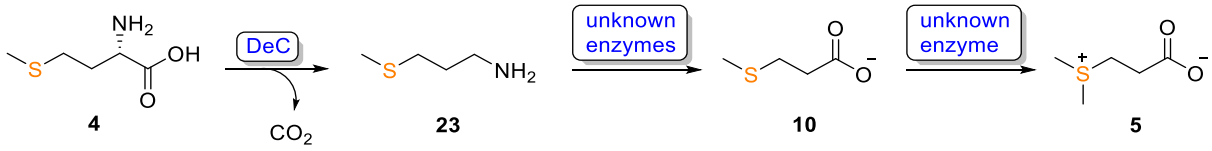

Figure 5. Biosynthesis of **5** in dinoflagellates.

The decarboxylation process appears important in the biosynthesis of **5**, prompting the isolation of a methionine decarboxylase (DeC) from *C. cohnii*. This enzyme plays a crucial role in converting **4** into **23** by facilitating decarboxylation and release of CO_2.[32] Despite this finding, several key enzymes essential for the biosynthesis of **5** in dinoflagellates have yet to be identified.

3. DMSP cleavage

3.1 Phytoplankton cleavage

In the complex marine ecosystem, marine bacteria play an important role as primary degraders of **5**, while phytoplanktonic organisms serve as the primary synthesizers. However, it is noteworthy that phytoplankton is also involved in the degradation of **5** through the lysis pathway.[33]

In 2009, Yost and Mitchelmore made the significant discovery that four out of five strains of the dinoflagellate *Symbiodinium microadriaticum* possessed DMSP lyase activity, despite with varying rates among strains.[34] Coccolithophores are also known to produce **5**, but lack DMSP lyase activity. However, only those coccolithophores closely related to *Emiliania huxleyi* and *Gephyrocapsa oceanica* are capable of degrading **5**.[35] Numerous studies have suggested that in *E. huxleyi*, **5** is stored in the cytoplasm, potentially serving as a signaling molecule.[36]

Notably, DMSP lyases were first identified in *Ulva curvata* (red algae) and *Polysiphonia paniculata* (green algae),[37,38] although it remains unclear whether the lyase genes from these two algae are related to each other.

3.2 Bacterial cleavage

Marine DMSP (**5**) undergoes non-enzymatic hydrolysis, producing **6** and **9** (Figure 6), yet its half-life in water is remarkably long, about 8 years. This slow rate of hydrolysis makes it challenging to determine the turnover number of **5**.[39] This evidence resulted in the discovery of DMSP lyase enzymes and suggested that marine bacteria are the primary degraders of **5**. Hence, in 1995, the first bacterial DMSP lyase (E.C. 4.4.1.3) was isolated from *Alcaligenes faecalis* M3A by Souza and Yoch.[40] Steinke and co-workers further investigated this enzyme for its DMSP lyase activity, conducting *in vitro* and *in vivo* enzyme reactions using crude cell extract or enzyme extract. The discovery of this DMSP lyase paving the way for the subsequent isolation of various lyase enzymes from different organisms.[41]

Genes encoding enzymes for the cleavage of **5** are widespread in marine bacteria and are even present in some fungi. Compound **5** can be catabolized by enzymes through two crucial pathways: the lysis pathway and the demethylation pathway.[42] In the lysis pathway, **5** is cleaved into **6**, while in the demethylation pathway, it is cleaved into water-soluble **10**, and acetaldehyde (**12**). Therefore, these pathways are of great interest and it is important to know how these pathways are regulated in marine bacteria like *Ruegeria pomeroyi*, which encodes the genes for both pathways.[43]

However, understanding the bacterial switch mechanism between the lysis pathway and the demethylation pathway is challenging, as it is influenced by numerous external factors like carbon source, temperature, and UV dose.[44] Additionally, a hydrolyase is known to degrade **5** into **6** and **25**, further adding to the complexity of DMSP metabolism.[45]

3.2.1 DMSP lysis pathway

Marine bacteria plays a crucial role in the cleavage of **5**, yielding **9** and **6**, a poorly water-soluble gas that is extensively released into the atmosphere from oceans. To date, a total of nine enzymes responsible for the degradation of **5** have been identified. Eight of these enzymes originate from bacterial sources: DddL from *Sulfitobacter* EE-36,[46] DddP from *Roseovarius nubinhibens* ISM,[47] DddQ from *Ruegeria pomeroyi* DSS-3,[48] DddY from *Alcaligenes faecali*s M3A,[49] DddW from *R. pomeroyi* DSS-3,[50] DddK from *Pelagibacter* HTCC1062,[51] DddX from *Psychrobacter* sp. D2,[52] and DddU from *Amylibacter cionae* H-12.[53] In addition, Alma1 was identified in the

coccolithophore *E. huxleyi*.[54] These DMSP lyases exhibit varying degrees of efficiency because of different activity, degrading only 2% to 21% of **5** into **6** through the lysis pathway.[10]

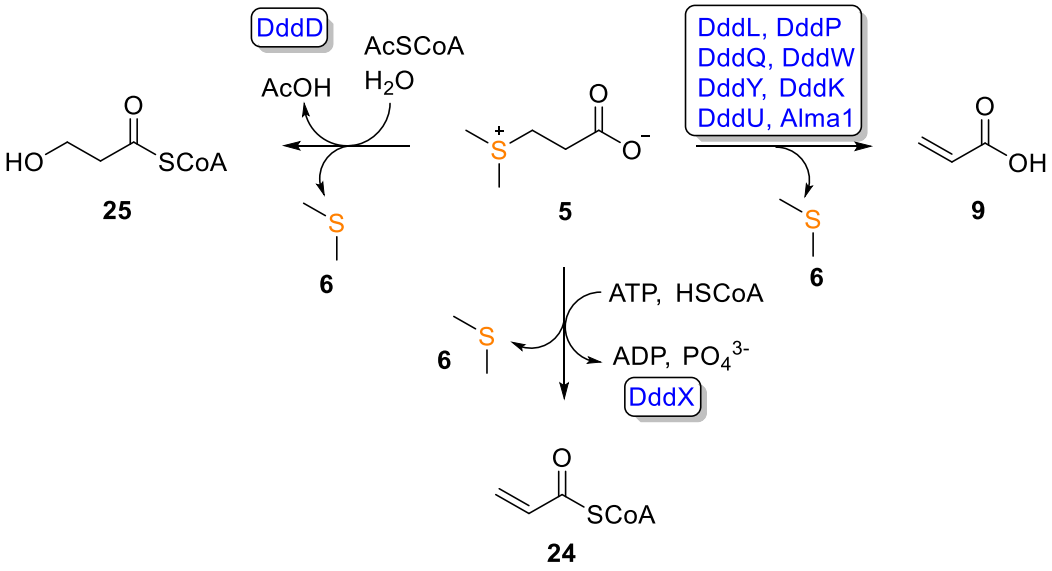

Figure 6. Degradation of **5** via the lysis pathway and the hydrolysis pathway.

3.2.2 DMSP lyase DddD

DddD, originating from *Marinomonas* sp. MWYL1, was the first DMSP lyase enzyme to be identified. DddD is predominantly present in Gammaproteobacteria, notably Oceanospirillales and Pseudomonadales, as well as in selected Proteobacteria like Rhizobiales, Rhodobacterales, and Burkholderiales. These bacterial strains are commonly isolated from environments abundant in **5**, such as coral reefs, marine seaweeds, and saltmarsh sediments.[42,55-58]

DddD exhibits the unique ability to hydrolyze **5** into **6** and 3-hydroxypropionate-CoA (**25**) (Figure 6), rather than the typical **6** and **9**. Based on its amino acid sequence, DddD has been classified as a type III acyl coenzyme A transferase, sharing 26% amino acid sequence identity with the γ-butyrobetainyl-CoA: carnitine CoA-transferase (CaiB) from *E. coli*. CaiB is known for transferring coenzyme A from γ-butyrobetainyl-CoA to carnitine, although it fails to catalyze the thioesterification of carnitine with coenzyme A.[59] The similarity in homology between CaiB and DddD suggests a mechanism for the cleavage of **5** by DddD via a hydrolysis pathway.[45] The proposed catalytic mechanism of DddD suggests that initially, compound **5** and acetyl-CoA react to form a **5**–enzyme intermediate complex. This intermediate can then proceed via two pathways: (1) hydration of the **5**–enzyme intermediate followed by HSCoA attack to

produce **25**, or (2) initial HSCoA attack to form dimethylsulfonium propionate-CoA (**26**) followed by hydrolysis to yield **25** (Figure 7).[60] However, the exact mechanism of DddD remains unclear.

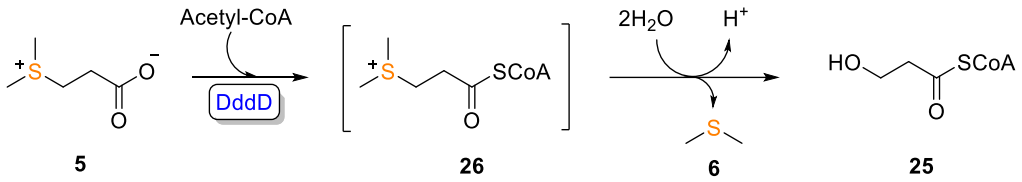

Figure 7. DMSP cleavage mechanism by DddD.

Previously, it was thought that the cleavage activity for **5** was rare in *Endozoicomonas* bacteria. However, a recent discovery of DddD from *Candidatus Endozoicomonas ruthgatesiae* strain 8E has shown its ability to degrade **5** into **6**. This finding highlights the widespread occurrence of the cleavage activity of **5** in *Endozoicomonas*.[61]

3.2.3 DMSP lyase DddL

Although *Sulfitobacter* sp. EE-36 and *Roseovarius nubinhibens* ISM lacked a DddD homolog, both organisms produced **6** from **5**, suggesting the presence of alternative enzymes that facilitated the cleavage of **5**.[45,62] This finding prompted further investigation, leading to the discovery of DddL in *Sulfitobacter* EE-36. The DddL enzyme, initially isolated from the Alphaproteobacterium *Sulfitobacter* EE-36, was found to exhibit DMSP (**5**) cleavage activity when expressed heterologously in *E. coli*. Deleting the *dddL* gene in *Sulfitobacter* EE-36 resulted in the inability to produce **6** from **5**. Interestingly, the amino acid sequence identity of the DddL enzyme shows no resemblance to any previously identified DMSP lyase enzymes.[46]

3.2.4 DMSP lyase DddP

In 2009, a new gene called *dddP* was discovered in the marine Alphaproteobacterium *Roseovarius nubinhibens* ISM. Cloning and expression of *dddP* gene in *E. coli* unveiled its ability to convert **5** into **6**. Notably, DddP is categorized within the extensive M24 metallopeptidase family, distinguishing it from other known lyase enzymes. Unlike most M24 metallopeptidases, which typically hydrolyse the C-N bond, DddP exhibits a distinct capability to cleave the C-S bond.[47,63] This unique enzymatic function classifies DddP into a specialized subgroup within the M24 metallopeptidase family, indicating its specific role in cleaving non-peptide substrates via C-S bond cleavage.[47]

Interestingly, close homologs of DddP are found not only in Alphaproteobacteria but also in certain ascomycete fungi such as *Aspergillus* and *Fusarium*.

Feeding experiments using [1-^{13}C]-**5** and [1-^{14}C]-**5** resulted in the production of **6** and labeled **9**, providing evidence of DddP activity as a DMSP lyase.

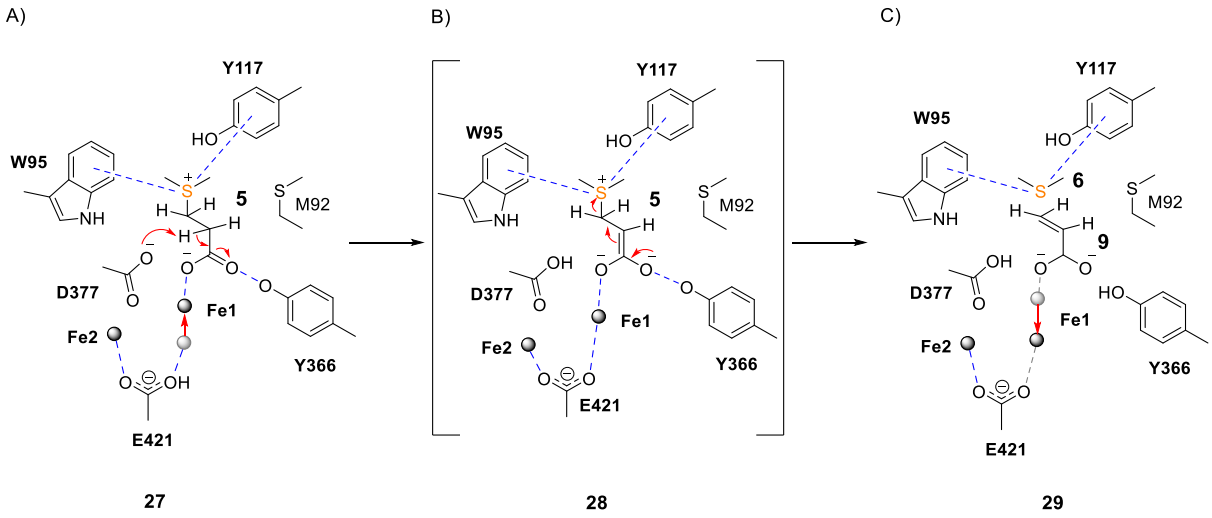

Figure 8. Proposed mechanism for the cleavage of **5** by DddP from *Ruegeria lacuscaerulensis*. A) Fe ions form an electrostatic bond with the carboxyl group of **5**. B) Asp377 residue acts as a base and forms an unstable intermediate **28**. C) The Asp377 residue triggers the elimination reaction, leading to the release of **6** and **23** from **5**.

The crystal structure analysis of DddP from *R. denitrificans* Och 114 and *Ruegeria lacuscaerulensis* ITI_1157 has revealed that DddP is a homodimeric metalloenzyme containing two Fe ions at its active site. Therefore, the mechanism for the cleavage of **5** by DddP has been proposed. Initially, the specific active site residues are Asp (295, 297, 307), His371, and Glu (406, 421), along with a water molecule coordinated with the two Fe atoms. As compound **5** enters the active site, one Fe atom forms an electrostatic bond with the carboxylate group of **5**, stabilizing the molecule, while Trp95, Tyr117, and Tyr366 bind to its sulfur atom to form intermediate **27** (Figure 8A). This interaction initiates a cascade effect: the C_α hydrogen of **5** and the carboxylate side chain of Asp377 were activated, weakening the bond between Fe and Glu421. Acting as a nucleophilic base, Asp377 attacks the C_α of **5**, resulting in the formation of an unstable intermediate **28** (Figure 8B). Consequently, the C_α hydrogen is released, and the C-S bond undergoes rapid polarization, leading to its cleavage into **6** and the formation of **9** (Figure 8C, **20**).[63,64]

3.2.5 DMSP lyase DddQ

The DddQ lyase enzyme, discovered in *R. pomeroyi* DSS-3, plays an important role in the breakdown of **5** in marine bacteria. Belonging to the cupin superfamily, its discovery demonstrated the mechanism of degradation of **5**.[48] Notably, *R. pomeroyi* DSS-3 contains not only the *dddQ* gene but also the *dddP* gene.

The crystal structure of DddQ reveals that this enzyme forms dimers arranged asymmetrically. However, contrary to this finding, gel filtration analysis revealed that DddQ actually exists as a monomer when in a liquid environment.

Atomic absorption spectroscopy deepened the understanding of the DddQ enzymatic activity. It unveiled that DddQ is indeed a metalloenzyme, containing Zn^{2+} ions (approximately 0.42 equiv.) at its active site.[65] Surprisingly, an excess of Zn^{2+} actually hinders DddQ activity, as additional ions bind to the active site.[65-69] Further studies elucidated that not only zinc but also other metal ions like Cu^{2+} and alkaline earth metal cations suppress DddQ activity, while Co^{2+} and Mn^{2+} ions enhance it by substituting the catalytic Zn^{2+} ion for the cleavage of **5**.[66,68]

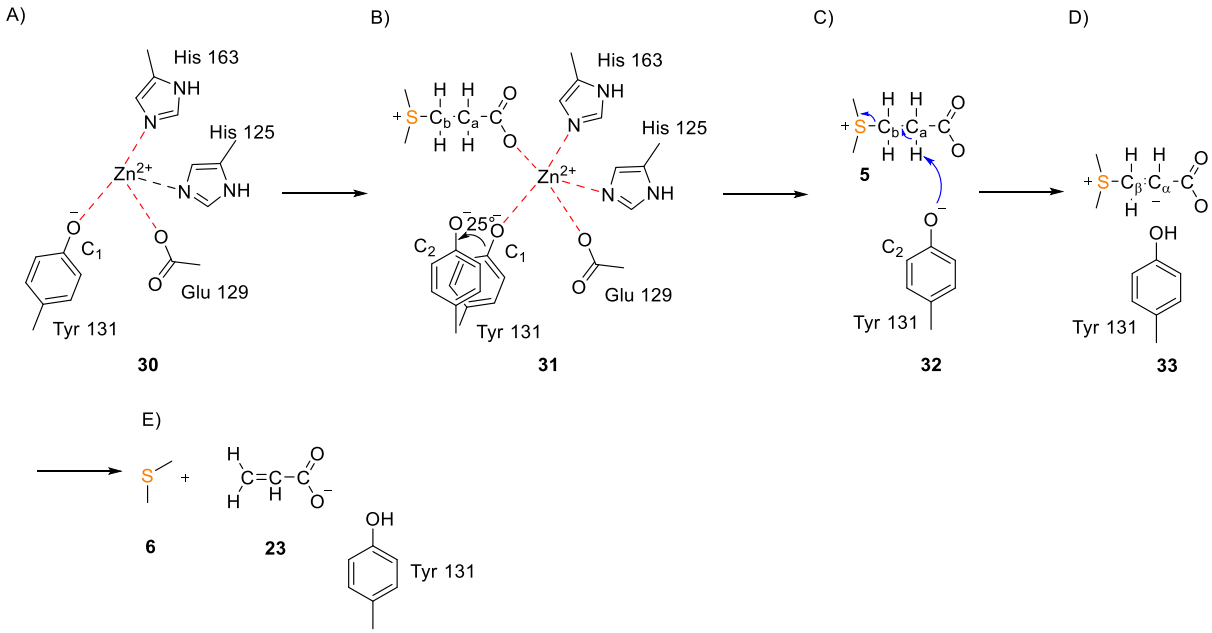

Figure 9. A proposed mechanism for the cleavage of **5** by DddQ to generate **6** and **9**. A) Zn^{2+} binds with His163, His125, Glu129, and Tyr131 to create intermediate 30. B) Zn^{2+} binds with carboxylate group of **5** and shifts Tyr131 by 25°. C) Tyr131 attacks on the C_α of **5**. D) Tyr131 abstracts the C_α proton of **5** to form intermediate **33**. E) Intermediate **33** degrades to release **6** and **9**.

Additionally, upon closer examination of the DddQ structure, molecular dynamics (MD) simulations indicate that two loops, namely loop 1 (Lys74–Thr78) and loop 2 (Asn184–Arg188), function as a gateway for **5** to enter the active site. In the open state, the gap between the two loops provides sufficient space for **5** to enter. Once **5** has entered the binding pocket, loops 1 and 2 move closer to each other, transitioning into a closed state. This conformational change likely enhances the subsequent breakdown of **5**. Upon completion of the catalytic reaction, loops 1 and 2 revert to the open state to release the products.

Therefore, the mechanism for the cleavage of **5** by DddQ has been proposed: the oxygen atom of the carboxylate group of **5** forms a coordinate bond with Zn^{2+}, displacing Tyr131 and causing a 25° deviation in its position to form intermediate **31** (Figure 9B). Consequently, Tyr131 shifts closer to **5**, interacting with the C_α proton to generate intermediate **32** (Figure 9C). This interaction facilitates the abstraction of the C_α proton, leading to the formation of a C_α carbanion (Figure 9D). The generated carbanion initiates an attack on C_β, causing a weakening of the S-C_β bond in **5**, resulting in the formation of **6** and **9** (Figure 9E).[65]

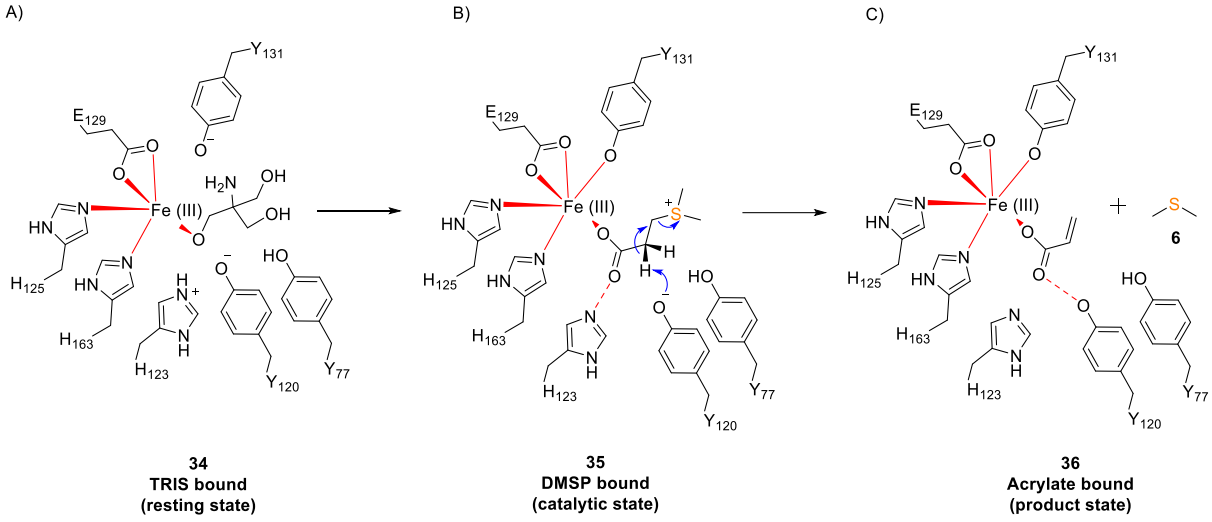

Figure 10. Proposed mechanism for the cleavage of **5** by DddQ. A) Tris molecule bound to Fe^{3+} to form intermediate **34**. B) Compound **5** displaces the Tris molecule and coordinates with the Fe^{3+} ion via the carboxylate oxygen in a monodentate manner, forming intermediate **35**. C) Tyr120 abstracts the C_α proton of **5**, leading to the release of **6** and **9**.

Subsequent reports revealed that DddQ isolated from *R*. *lacuscaerulensis* ITI_1157 contains approximately Fe^{3+} (0.5 equiv.) and minor amounts of Zn^{2+} (<0.1 equiv.) at its active site. Notably, a Tyr131 residue is coordinated to the iron. Each DddQ structure comprises two molecules, each with iron present at the active site with full occupancy. Furthermore, the crystal structure of DddQ indicates that, in the absence of **5**, Fe(III)-DddQ binds with Tris molecule from the buffer to form intermediate **34** (Figure 10A), and also arranged in an open conformation, with Tyr131 positioned away from the metal center. Upon the addition of **5**, the molecule coordinates in a monodentate manner through its carboxylate oxygen to make intermediate **35**. Tyr131 then moves to coordinate with iron, while three residues–His123, Tyr131, and Tyr120–assist in attaching **5** by interacting with the second carboxylate oxygen (Figure 10B). This arrangement of **5** prepares the substrate for catalysis. With **5** appropriately positioned, Tyr120 closely interacts with the adjacent carbon hydrogen, resulting in the elimination of **6** and **9** (Figure 10C).[70]

3.2.6 DMSP lyase DddW

A novel gene *dddW*, which encodes for DMSP lyase, was first isolated from *R*. *pomeroyi* DSS-3. This enzyme cleaves **5** into the environmentally important volatile gas **6**. Heterologous expression of DddW in *E*. *coli* confirmed its function as a DMSP lyase. This was evidenced by the complete conversion of labeled [1-^{14}C]-**5** into **6** and labeled **9**.[50]

It is a metalloenzyme containing iron cofactor within its active site and belongs to the cupin superfamily. DddW is present in a dimeric form, with each monomer requiring one Fe^{2+} ion for binding.[71,72] The metal cofactor plays an important role in catalyzing DddW activity towards **5**. Interestingly, experiments revealed that the culture of recombinant DddW in the absence of metal ions leads to the formation of insoluble protein.

However, when grown in the presence of a mixture of metal ions, including Mn^{2+}, Fe^{3+}, Co^{2+}, Ni^{2+}, Cu^{2+}, and Zn^{2+}, in equal proportions, soluble protein is produced. This highlights the importance of metal ions in modulating DddW activity and emphasise the intricate mechanisms governing its function. The presence of Zn^{2+} metal ions entirely suppresses the activity, primarily because Zn^{2+} tends to favour a tetrahedral geometry. Consequently, the four metal coordination sites may be occupied by the

four active site residues (3-His-1-Glu), thereby hindering the binding of **5**. Stoichiometric studies have revealed that DddW exhibits the greatest affinity for binding Fe^{2+}, given its lower position in the Irving Williams Series.[71]

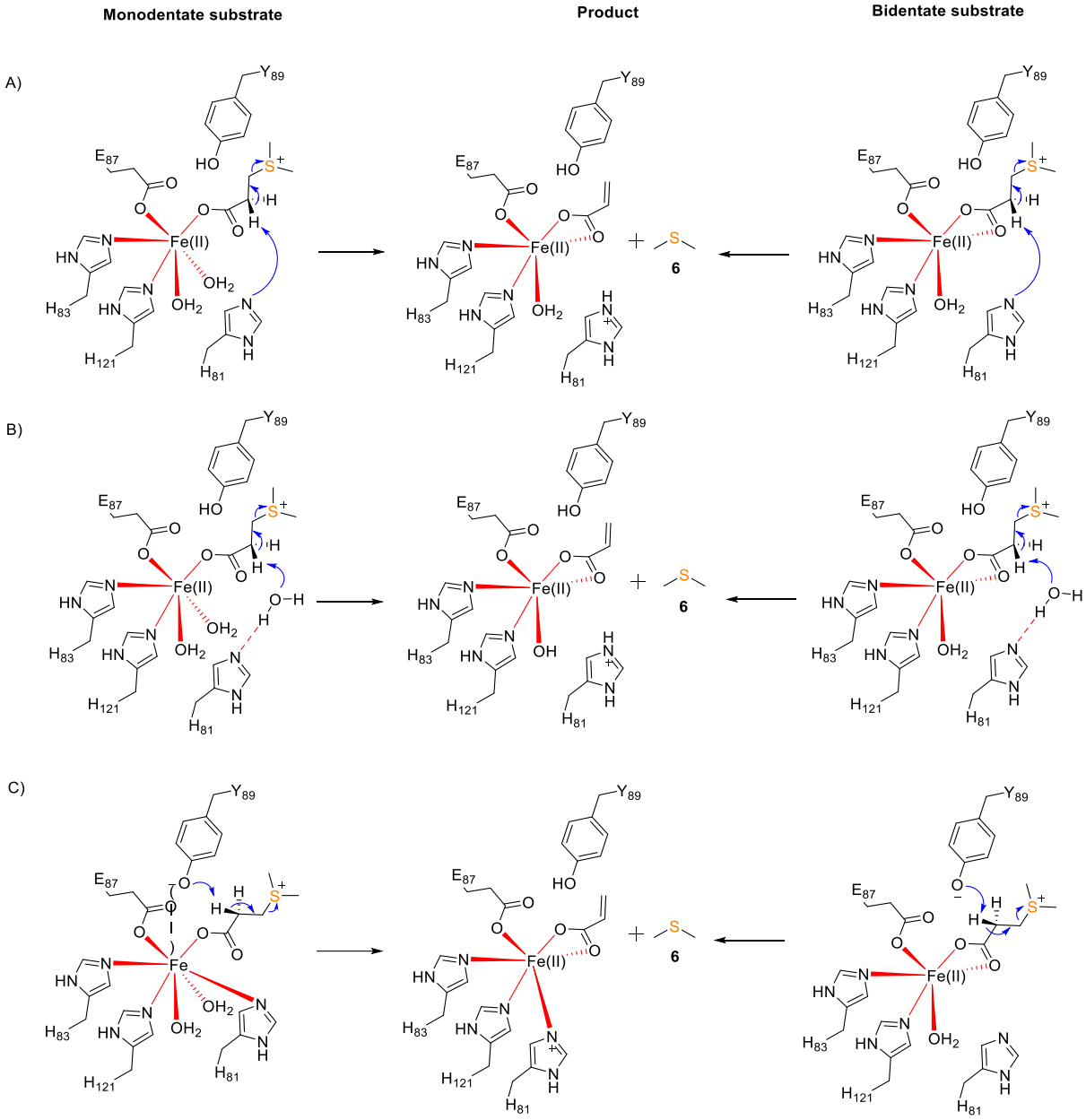

Figure 11. Proposed mechanism for Fe dependent DddW. DddW binds to cofactor Fe^{2+} to which **5** can bind in monodentate or bidentate mode. A) His81 acts as a nucleophile and abstracts the proton from **5** to form **6** and **9**. B) A water molecule activated by His81 acts as nucleophile and removes the proton from **5** to produce **6** and **9**. C) Tyr89 initiates the elimination reaction to cleave **5** into **6** and **9**.

The proposed mechanism for the cleavage of **5** involves specific residues–H81, H83, E87, and H121 coordinating with the Fe metal center. Compound **5** can bind either in

a monodentate or bidentate manner, with the remaining coordination sphere around the Fe ion being occupied by water molecules. His81 acts as a base, abstracting a hydrogen atom from the C_α of **5** to generate **9** (Figure 11A). Alternatively, a hypothetical water molecule may be activated by His81, subsequently acting as a nucleophile to abstract the proton from C_α of **5**, resulting in the formation of **6** and **9** (Figure 11B). Additionally, Tyr89, located near the active site, has the potential to act as a nucleophile, abstracting a proton to facilitate the cleavage of **5** (Figure 11C).[71]

3.2.7 DMSP lyase DddK

DddK is the first cupin fold containing DMSP lyase initially discovered from *Pelagibacter ubique* HTCC1062. This enzyme efficiently cleaves **5** into **6** and **9**.[51] Similar to DddW and DddQ, DddK is also a metalloenzyme and it exists as a dimer in solution with two molecules arranged asymmetricly.[73-74]

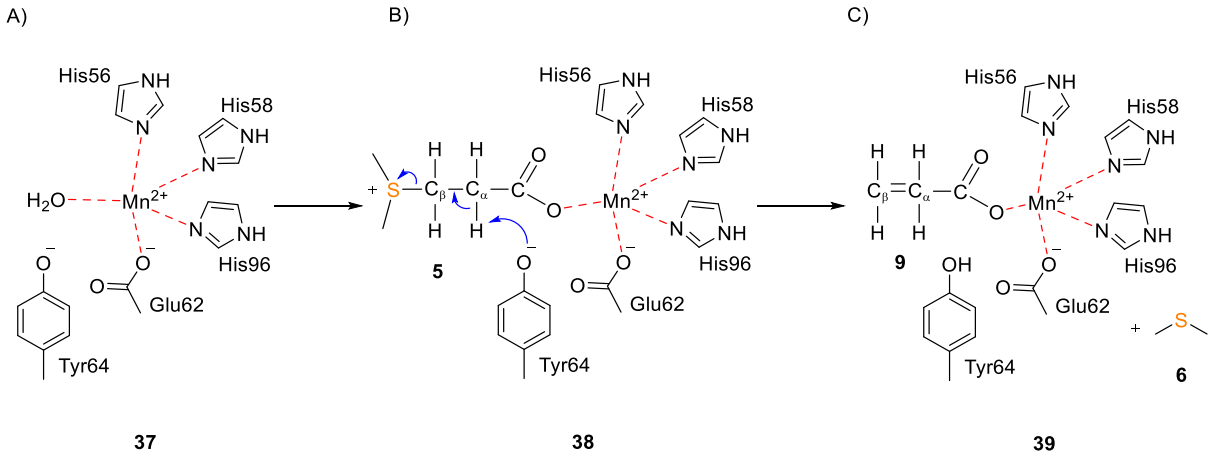

Figure 12. Catalytic mechanism of DddK for the cleavage of **5**. A) The Mn^{2+} is coordinated with His56, His58, His96, Glu62 and water molecule. B) Compound **5** enters the active site, displaces the water molecule, and coordinates with Mn^{2+} to form intermediate **38**. C) Tyr64 abstracts the proton from C_α of **5** to release **6** and **9**.

Inductively coupled plasma atomic emission spectrometry analysis has revealed the elemental composition of DddK, indicating the presence of Mn^{2+} (~0.34 equiv.), Fe^{2+} (~0.24 equiv.), and trace amounts of Co, Zn, and Ni (~0.05 equiv. each).[73] Studies have also shown that DddK utilizes various metal cofactors for the cleavage of **5**. Interestingly, when Ni^{2+} and Mn^{2+} are present as cofactors, DddK exhibits the highest activity due to the distorted octahedral coordination environment.[73,74]

Based on the obtained crystal structure, a mechanism for the cleavage of **5** has been proposed. Initially, His56, His58, Glu62, His96, and a water molecule coordinate to Mn^{2+}, thereby facilitating the formation of intermediate **37** (Figure 12A). Upon entering the active site, **5** coordinates with Mn^{2+} and displaces a water molecule (Figure 12B). In proximity to the active site, Tyr64 plays a crucial role, acting as a base to abstract a proton from the C_α of **5**. This action leads to the formation of the C_α carboanion intermediate **38**, which subsequently initiates an attack on C_β, ultimately breaking the C-S bond and resulting in the elimination of **6** and **9** (Figure 12C). Remarkably, the same elimination mechanism is also observed for DddK isolated from SAR11 bacteria.[73]

3.2.8 DMSP lyase DddY

The DMSP lyase DddY, encoded by the *dddY* gene, was initially isolated from Betaproteobacterium *Alcaligenes faecalis* M3A. However, it is not limited to this strain alone; it is also found across a wide range of bacterial phyla including Alpha, Beta, Gamma, Delta, and Epsilon proteobacteria. Cloning and expression of *dddY* into *E. coli* have demonstrated its remarkable ability to efficiently convert [1-^{13}C]-**5** into **6** and labeled **9**, confirming its role as a DMSP lyase. Notably, knockout of the *dddY* gene from *Alcaligenes faecalis* M3A completely abolished the formation of **6** from **5**.[49]

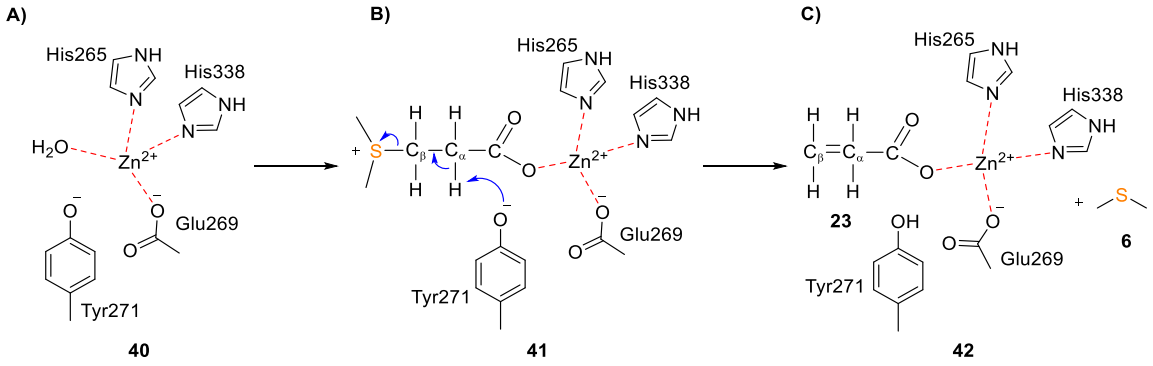

Figure 13. Catalytic mechanism for the cleavage of **5** by DddY. A) Zn^{2+} ion coordinated with His265, Glu269, His338 and a water molecule to form intermediate **40**. B) Compound **5** displaces the water molecule and coordinates with the Zn^{2+} ion, while Tyr271 serves as a base to abstract the C_α proton of **5**. C) Tyr271 triggers the elimination reaction, leading to the release of **6** and **9**.

Furthermore, the elucidation of the crystal structure of DddY from the Gamma proteobacterium *Acinetobacter bereziniae* revealed that it belongs to the cupin

superfamily. According to inductively coupled plasma atomic emission spectrometry, DddY predominantly contains Zn^{2+} ions (approximately 0.68 equiv.) and iron (approximately 0.18 equiv.).[75]

Based on the obtained crystal structure, a proposed mechanism for the cleavage of **5** suggests that DddY consists of an N-terminal domain (Ala22–Val190), known as the cap domain, composed of α-helices, and a C-terminal catalytic domain (Ser191–Pro401) with a β-barrel fold structure. Both domains are coordinated with Zn^{2+} ions present at the active site, further emphasizing their role in the cleavage of **5**. In the absence of **5**, Zn^{2+} ions are coordinated with residues His265, Glu269, His338, and a water molecule, forming a stable complex **40** (Figure 13A). Upon the entry of **5**, it displaces the water molecule and binds to Zn^{2+}, forming an intermediate **41** (Figure 13B). Tyr271 positioned close to the active site, functions as a base and facilitate the removal of a proton from the C_α of **5**. This process generates a C_α carbanion, which subsequently initiates an attack on C_β, leading to the cleavage of C_β-S bond and release of **6** and **9** (Figure 13C).[75]

3.2.9 DMSP lyase DddX

Recently, the discovery of DddX in *Psychrobacter* sp. D2 revealed its capability to catalyze the conversion of **5** into **6**. DddX stands out as an ATP-dependent enzyme belonging to the acyl-CoA synthetase superfamily, distinguishing it from other known DMSP lyase enzyme families.

Structural analysis of DddX with ATP has shown that it forms a tetramer consisting of four monomers, arranged asymmetrically. Residues Tyr181, Asp208, and Glu432 are situated in close proximity to the active site, with Glu432 serving as the base for cleaving **46** (Figure 13D). Based on structural insights, a proposed cleavage mechanism for **5** is as follows: Initially, His292 undergoes phosphorylation by ATP to form **43**, followed by the transfer of a phosphoryl group from **44** to **5**, resulting in the formation of **45** (Figure 13A-C). Subsequently, **45** is attacked by HSCoA to generate intermediate **46**, whereupon Glu432 initiates the elimination reaction by abstracting a proton from the C_α position of **46**. This process leads to cleavage of **5** into **6** and **24** (Figure 13D-E).[52]

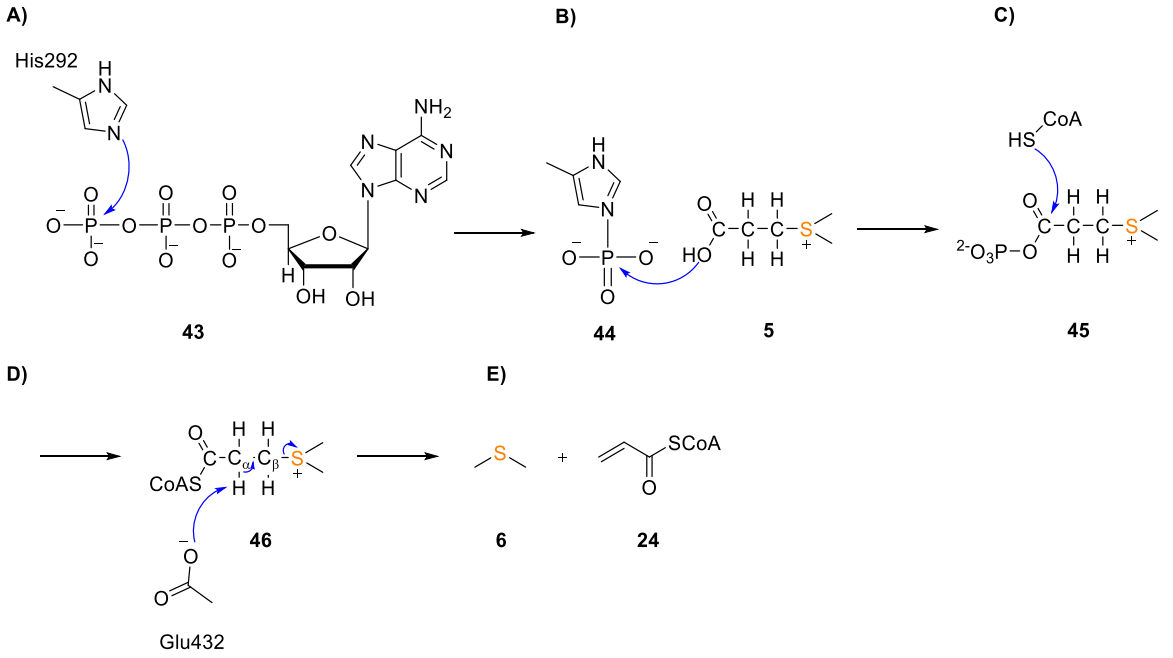

Figure 14. Proposed mechanism for cleavage of **5** by DddX. A) His292 attacks on ATP to form **44**. B) The phosphoryl group is transferred to **5**, generating **45**. C) HSCoA attacks to form **46**. D) Glu432 abstracts the proton from C_α of **46**. E) Compound **6** and **24** formed as a cleavage product.

3.2.10 DMSP lyase DddU

The novel DMSP lyase DddU was identified from *Amylibacter cionae* H-12 and belongs to the cupin superfamily, sharing <15% amino acid sequence identity with other known DMSP lyases. Although less abundant in marine bacteria compared to DddP and DddK, DddU is more prevalent than DddW, DddY, and DddL. DddU efficiently catalyzes the conversion of **5** into **6** and **9**, confirming its role as a DMSP lyase.[53]

Using AlphaFold2, the structure of DddU from *Phaeobacter inhibens* P66 was predicted, revealing a β-barrel fold surrounded by α-helices, resembling the structures of other cupin superfamily members.[76] DddU employs a catalytic mechanism similar to DddQ, with His146, Glu150, Tyr152, and His185 residues playing important role. Tyr152 acts as a base, abstracting a proton from the C_α position of **5**, initiating the elimination reaction and resulting in the release of **6** and **9** (Figure 6).[53]

3.2.11 DMSP lyase enzyme Alma1

Alma1, the first algal DMSP lyase from *Emiliania huxleyi*, belongs to the redox-sensitive aspartate racemase superfamily, exists as a homotetramer with typical

DMSP lyase activity. It shares 45% amino acid sequence identity with *Sym*-Alma1 from dinoflagellate *Symbiodinum*-A1.

Its heterologous expression in *E*. *coli* confirms its ability to convert [1-^{13}C]-**5** into **6** and labeled **9**. Alma1 catalyzes proton abstraction from the Cα position of **5**, initiating a β-elimination reaction to release **6** and **9**.[54]

3.3 DMSP demethylation pathway

As outlined previously, marine bacteria utilize two pathways to break down **5**: the DMSP cleavage pathway, which yields **6** and **9** (Figure 6), and the demethylation pathway, leading to the production of MeSH (**11**).[77,78] The demethylation pathway involves four enzymes, collectively known as DmdA, DmdB, DmdC, and DmdD/AcuH (Figure 15), which work together to convert **5** into **11** and **12**.

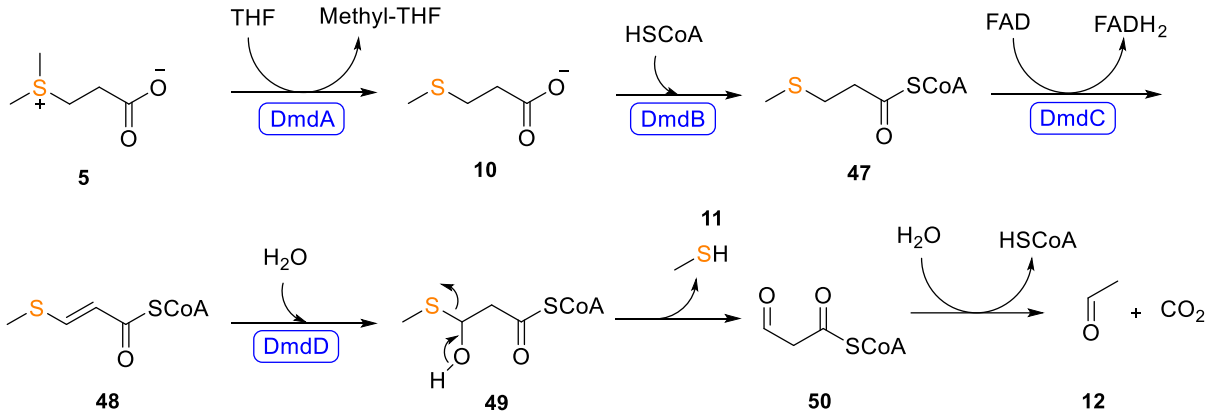

Figure 15. Degradation of **5** via demethylation pathway.

Initially, the methyl transferase DmdA removes the methyl group from **5** and transfers it to tetrahydrofolate (FH_4), yielding **10** and 5-methyl-FH_4.[79,80] Next, free acid **10** is converted into **47** by the coenzyme A ligase DmdB via ATP activation. Intermediate **47** is then dehydrogenated by the FAD-dependent dehydrogenase DmdC to yield **48**. Finally, **48** undergoes hydrolysis by the enoyl-CoA hydratase DmdD, producing **49**, which further breaks down into **11** and **50**. Upon hydrolysis, **50** decarboxylates to yield **12** and CO_2.[81,82]

3.3.1 DMSP demethylase (DmdA)

The gene dmdA, responsible for encoding the DmdA enzyme, was initially isolated from *R*. *pomeroyi* DSS-3.[79] Initially, DmdA was categorized as a member of the glycine cleavage family protein (GcvT). However, further analysis revealed significant

differences between DmdA and GcvT, with only a 25% amino acid sequence identity shared between them. While both enzymes catalyze the cleavage of a carbon-sulfur bond, their substrates vary. GcvT cleaves a bond between a remnant of glycine and a sulfur-containing cofactor (lipoic acid), whereas DmdA cleaves a bond between a methyl group and the sulfur atom of **5**.[83,84]

DmdA catalyzes the removal of a methyl group from **5** to produce **10** which is subsequently demethylated again to form mercaptopropanoic acid or can be demethiolated to **11** and **9**.[78,85] Knockout of the *dmdA* gene from *R. pomeroyi* DSS-3 makes the mutant incapable to produce **11** indicating that this gene is important for the cleavage of **5** via the demethylation pathway.[79]

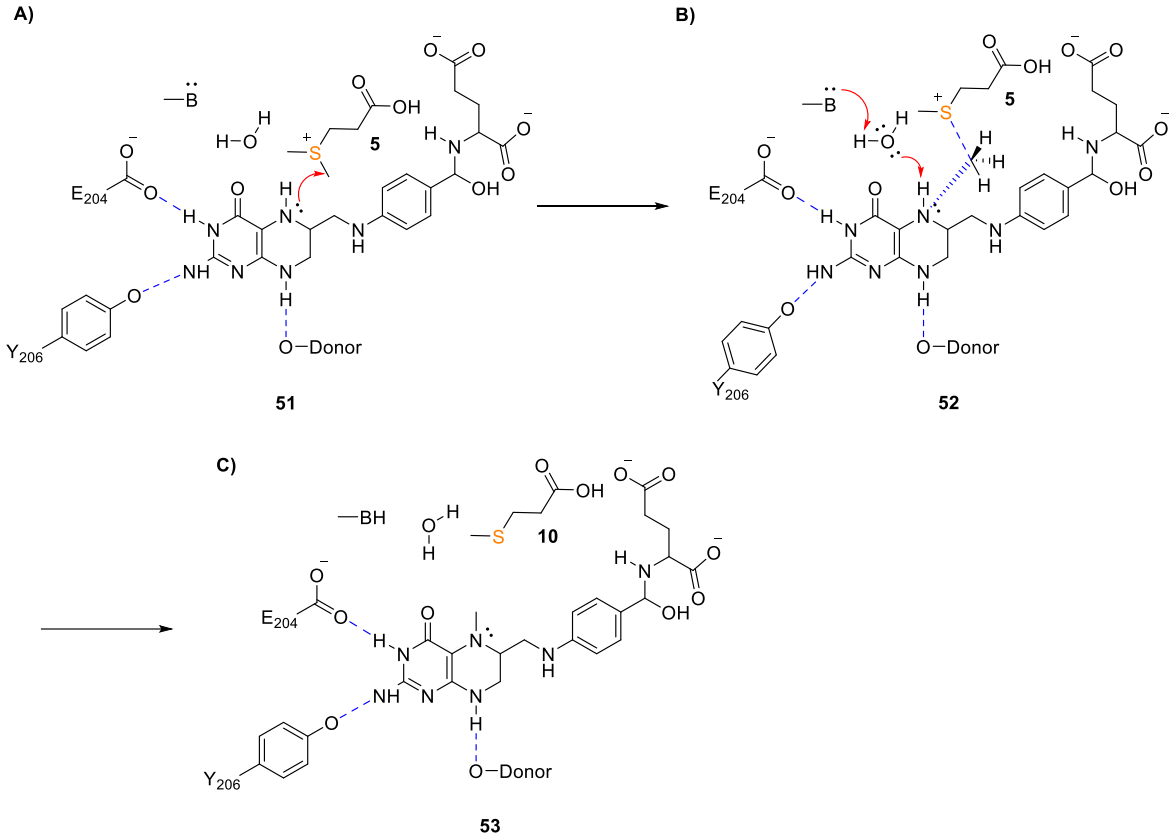

Figure 16. Proposed mechanism for the methyl transfer reaction catalyzed by DmdA.

A crystal structure of DmdA from *Pelagibacter* ubique with **5** demonstrated that DmdA exists as a dimer and the interaction of DmdA with FH_4 appears to be highly conserved, as two conserved residues, Y206 and E204 are positioned in such a way as to form hydrogen bonds with FH_4 to form intermediate **51** (Figure 16A). The binding of **5** in the active site removes the coordinated water molecule, and residue E204 forms hydrogen bonds with FH_4 or H_2O molecules as shown in intermediate **52** (Figure 16B).

Compound **5** possesses a sulfonium atom, enhancing the reactivity of the methyl group as a leaving group. This facilitates the formation of an S_N2 intermediate, characterized by concerted methyl and proton transfers, mediated by a water molecule within the active site. Therefore, it results in formation of **10** and N5-methyl-FH_4 (Figure 16C, **53**).[80] There are some similar enzymes like glycine-N methyltransferase, and phenylethanolamine-N methyltransferase that also support this methyl transfer mechanism because these enzymes facilitate the same substrate binding through hydrogen bonding.[86-88]

3.3.2 3-Methylmercaptopropionyl-CoA ligase (DmdB)

After the discovery of the DmdA enzyme, another significant finding emerged with the isolation of the *dmdB* gene, encoding the DmdB enzyme, from *R. pomeroyi* DSS-3. DmdB belongs to the acyl-CoA ligase family.[89] The heterologous expression of *dmdB* into *E. coli* demonstrated its capability to exhibit MMPA-CoA ligase activity, facilitating the conversion of **10** into **47** (Figure 15).[82] During catalysis, the acyl-CoA ligase undergoes various conformational changes, including an open conformation, an adenylate-forming conformation in which the C-terminal domain of the enzyme rotates ~90°, and a thioester-forming conformation where the C-terminal domain undergoes an additional 140° rotation subsequent to the initial one.[90-93]

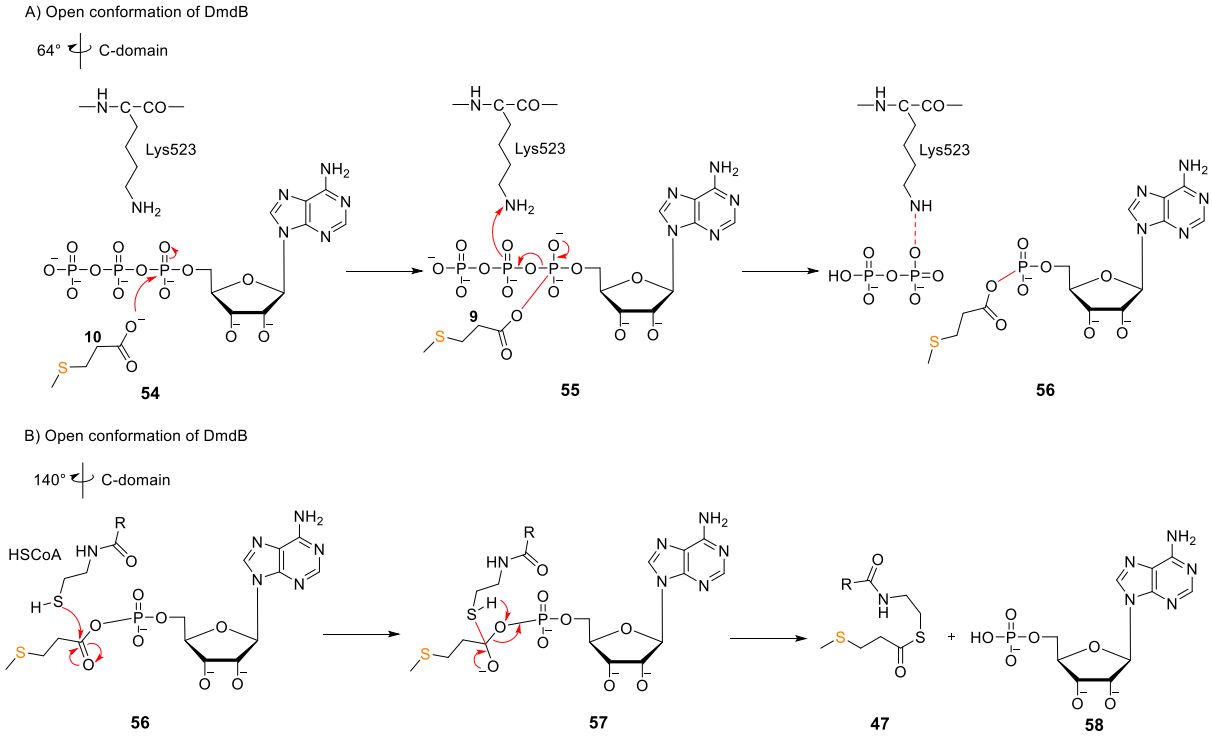

Figure 17. Catalytic mechanism for DmdB to generate **47**.

The crystal structure analysis of DmdB from *R*. *lacuscaerulensis* in complex with **10** revealed that DmdB exists as a dimer, with each monomer consisting of two chains, A and B. Chain A exhibits an open conformation as it lacks **10**, whereas chain B, containing ADP, forms adenylate conformation. Investigation into the catalytic mechanism of DmdB highlighted the conservation of Lys523, which plays a pivotal role in catalysis. DmdB undergoes two significant conformational changes during its catalytic cycle. Initially, ATP binding induces a 64° rotation of the C-domain, transitioning DmdB from an open to an adenylate conformation (Figure 17A). Subsequently, upon the entry of **10** into the active site, residues His231, Trp235, and Gly302 coordinate to facilitate its attack on the phosphate atom of ATP. This process generates intermediate **55**, which swiftly converts into **56**, preparing it for the subsequent attack of HSCoA. A further 140° rotation of the C-domain brings **56** and coenzyme A into proximity, leading to the thioester conformation (Figure 17B). The stabilization of HSCoA is facilitated by residues Asp435, Lys438, Gly440, Gly441, Glu442, Trp443, and Glu474, allowing the sulfur atom of HSCoA to initiate attack on the carbonyl carbon of **56**, leading to the formation of **47** via intermediate **57** and the release of **58**.[89]

3.3.3 MMPA-CoA dehydrogenase (DmdC)

The enzyme DmdC, derived from *R. pomeroyi* DSS-3, has been identified as a FAD-dependent acyl-CoA dehydrogenase. Its function involves catalyzing the dehydrogenation process, accompanied by the anti-elimination of hydrogen from **47** to yield **48**.[82,89,94] A detailed discussion about the stereochemical course of DmdC will be presented in chapter 6.

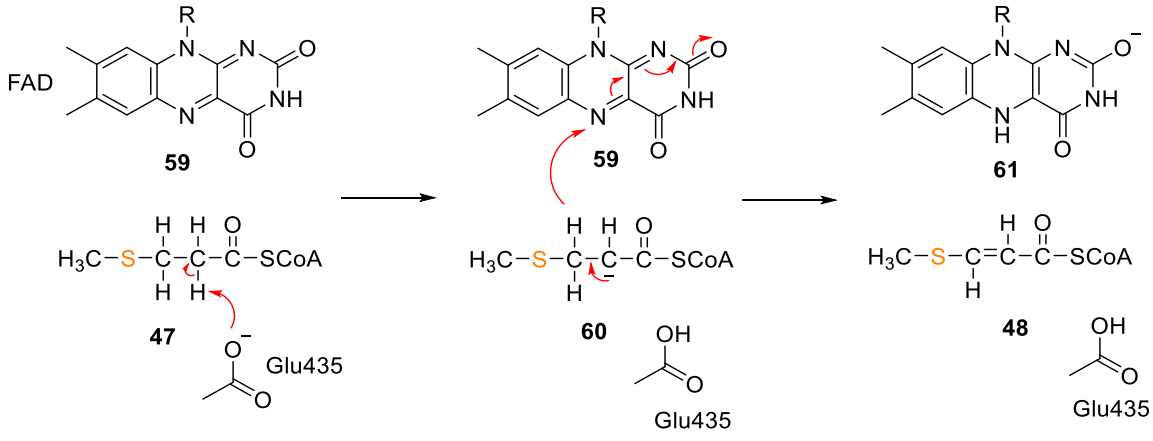

Figure 18. Catalytic mechanism of MMPA-CoA dehydrogenase DmdC.

On the basis of previous studies on acyl-CoA dehydrogenases, a catalytic mechanism for DmdC from *Roseobacter* has been proposed.[95-97] Within the active site, FAD (**59**) is stabilized by Met161, Thr170, Ser197, and Tyr434 residues, with Phe195 and Glu435 playing crucial roles in FAD binding and DmdC activity. The substrate **47** is positioned between **59** and Glu435. Glu435 acts as a base, initiating the anti-elimination reaction by abstracting the *pro-R* proton from the C_α of **47**, generating C_α carbanion intermediate **60**. The C_α carbanion subsequently attacks the C_β, weakening the C_β-H bond, while the *pro-S* hydride is transferred to the N5 position of **59**, resulting in the formation of **48** and **61** (Figure 18).[94]

3.3.4 MTA-CoA hydratase DmdD

DmdD, a member of the crotonase superfamily, was isolated from *R. pomeroyi* DSS-3, and it catalyzes the final step in the demethylation pathway of **5**, liberating **11**. This enzyme facilitates the hydration and hydrolysis of **48** to yield **11**, **12**, and CO_2. Interestingly, the release of **11** occurs spontaneously as a consequence of hydration of **48** by DmdD, evidenced by the enzyme inability to release **11** from **47**.[82,98]

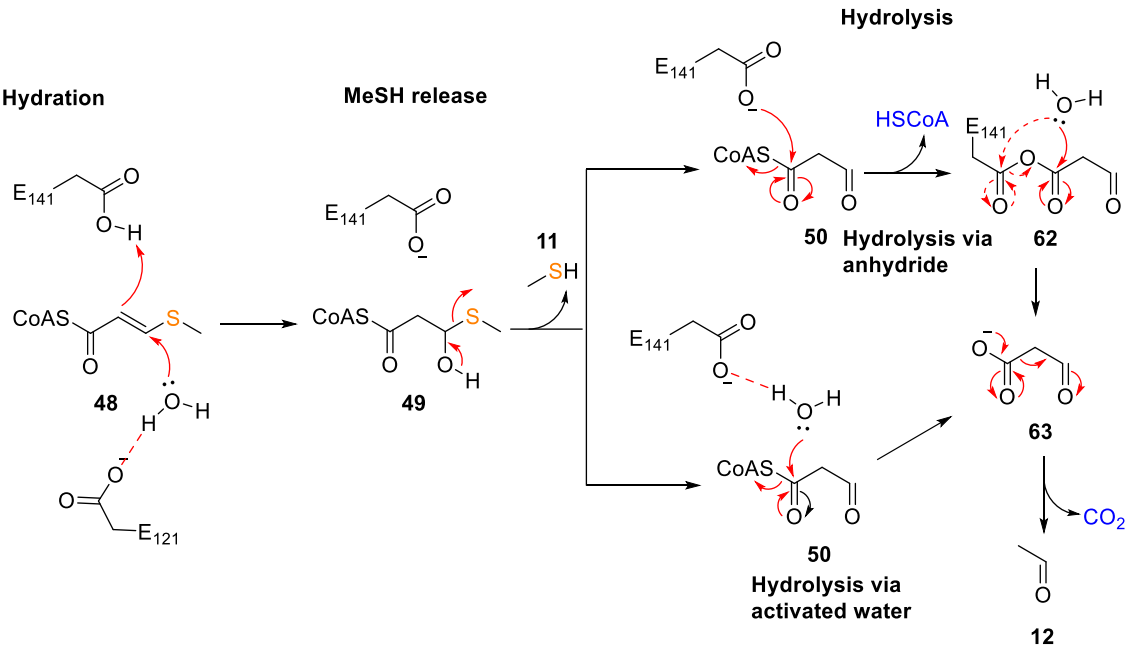

Figure 19. Catalytic mechanism of hydration and hydrolysis by DmdD.

The crystal structure of DmdD suggests it exists as a hexamer composed of a dimer of trimers, bearing structural resemblance to other crotonases. DmdD employs a mechanism similar to canonical crotonase enzymes in catalyzing the hydrolysis and hydration of **48**. The Glu121 residue acts as a base, activating a water molecule to

attack Cβ of **48**, forming intermediate **49**, which subsequently leads to the production of **11** and **50**. Simultaneously, Glu141 either directly attacks the carbonyl carbon of the HSCoA of **50** to form an anhydride **62**, subsequently attacked by water to generate intermediate **63**, or Glu141 activates a water molecule to catalyze the hydrolysis of **50** to **63**. Intermediate **63** undergoes decarboxylation, resulting in the formation of **12** and CO_2.[98]

4. Substrate tolerance of *Roseobacter clade* marine bacteria and DMSP lyase

The *Roseobacter* clade bacteria represent a crucial group known for both production and degradation of **5**.[99] Notably, four strains from the *Roseobacter* clade, including *Phaeobacter inhibens*, *Oceanibulbus indolifex*, *Dinoroseobacter shibae*, and *R. pomeroyi* DSS-3, have been extensively studied for their degradation pathways (Figure 20).

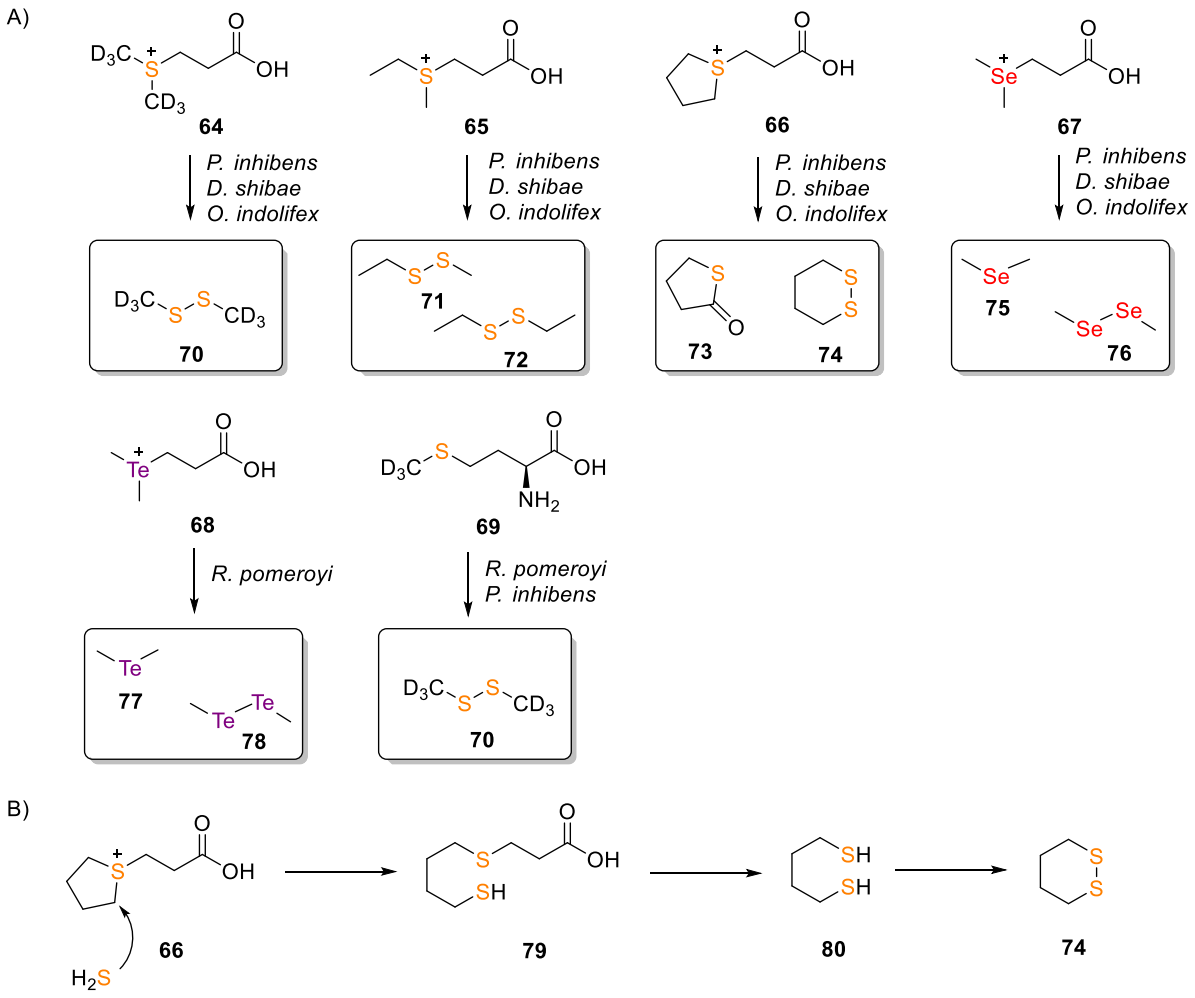

Figure 20. A) Volatiles produced from analogs of **5** catabolized by *P. inhibens*, *O. indolifex* and *D. shibae*. B) Mechanism for the formation of **74** from **66**.

Through the synthesis and feeding of various analogs of **5**, in which the sulfur atom is replaced by selenium and tellurium, a variety of sulfur, selenium, and tellurium volatiles have been observed from these strains. Specifically, volatiles **6**, **75**, and **77** are formed via the lysis pathway, while volatiles **70**, **71**, **72**, **76**, and **78** are generated through the demethylation pathway followed by oxidation.[100,101] In a similar manner, allyl DMSP analogs were synthesized and fed to *P. inhibens*, *O. indolifex*, and *D. shibae*, leading to the formation of sulfur volatiles resembling to those found in garlic.[102] A detailed discussion of these results will be provided in Chapter 3.

Interestingly, feeding the heterocyclic analog **66** to *P*. *inhibens* and *O*. *indolifex*, resulted in the formation of **73** and **74**. Volatile **74** originates from the nucleophilic ring opening of **66**, catalyzed by the attack of H_2S, leading to the sequential formation of **79**, **80** through lysis, and **74** through oxidation.[103] These findings contribute significantly to understand the bacterial metabolism.

Moreover, deeper investigations into the *dmdA* knockout mutant of *R*. *pomeroyi* DSS-3 and *P*. *inhibens* revealed interesting outcomes upon feeding [$^2H_6$]-**5**. This feeding experiment resulted in the formation of [$^2H_3$]-**11**, indicating the activation of an alternate demethylation pathway. Furthermore, feeding [*methyl*-$^2H_3$]-**4** and ^{34}S-labeled sulfate or thiosulfate to *P*. *inhibens* led to the production of [$^2H_3$]-**11** but not [^{34}S]-**11**, suggesting the involvement of methionine γ-lyase in the formation of **11**.[101]

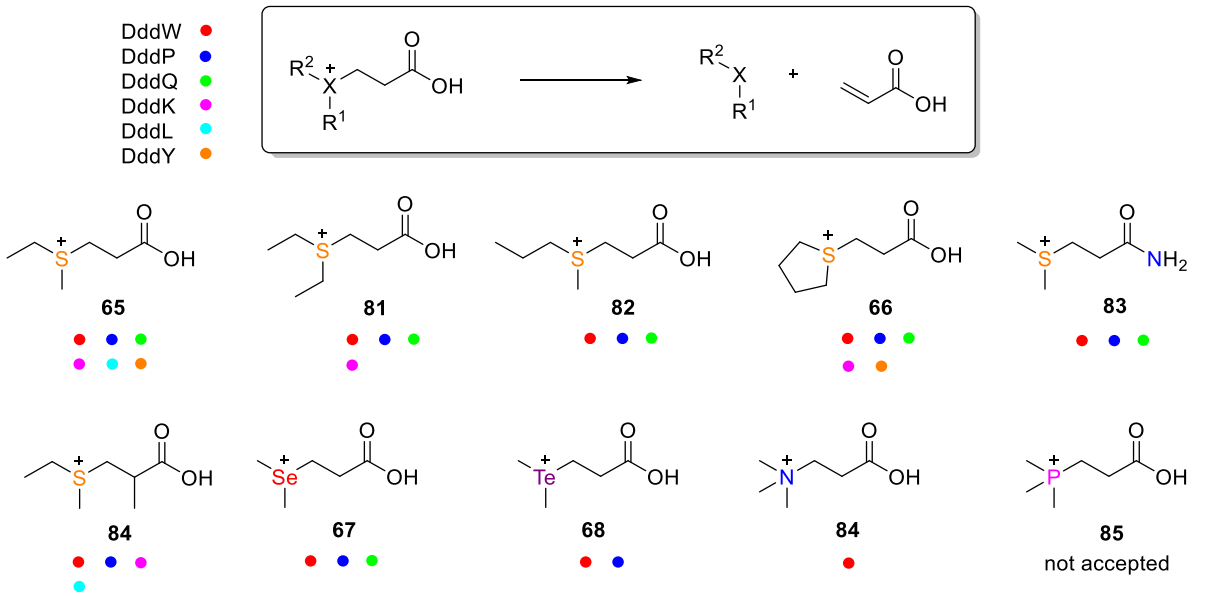

Figure 21. Substrate scope of DMSP (**5**) analogs. Colour dots represent the corresponding enzyme.

The genomes of *R*. *pomeroyi* DSS-3 and *P*. *inhibens* encode three DMSP lyases: DddW, DddQ, and DddP. Feeding experiments involving **5** and various analogues of **5** to *R*. *pomeroyi* and related species showcased broad substrate flexibility for breakdown via the lysis pathway. However, the specific contributions of individual enzymes remained unknown. To address this, a series of **5** analogues were synthesized and tested for substrate tolerance *in vitro*. In general, all three DMSP lyases exhibited a wide substrate spectrum. Compounds such as **5**, **69**, and **84**, were accepted as substrates, while **83** and **84** were efficiently converted by DddW only, and none of the enzymes showed activity towards **85**. Notably, both DddW and DddP demonstrated activity towards both enantiomers (*R*) and (*S*)-**84**, whereas DddQ did not accept **84**.[104]

In the similar way, DddK, DddL and DddY enzymes were also tested for the substrate specificity. The substrate **81** is only accepted by DddK, whereas **68** is not accepted by DddL. However, **84** is not the substrate for DddK and DddY.[105]

The extent to which DMSP lyases can accommodate DMSOP (**7**) analogs as substrates remains largely unexplored. To address this, a comprehensive study involving the synthesis and testing of various DMSOP (**7**) analogs has been conducted.[106] A detailed analysis of these results will be presented in Chapter 7.

Chapter 2

Identification of volatiles from six marine *Celeribacter* strains

Anuj Kumar Chhalodia, Jan Rinkel, Dorota Konvalinkova, Jörn Petersen and Prof. Dr. Jeroen S. Dickschat*

Beilstein J. *Org*. *Chem*. **2021,** *17,* 420–430.

Headspace extract analysis of six *Celeribacter* strains and the synthesis of one reference compound **129** were performed by me. The feeding experiments with isotopically labelled compounds and the synthesis of another reference compound **128** were performed by Jan Rinkel and Dorota Konvalinkova.

The publication “Identification of volatiles from six marine *Celeribacter* strains” can be found in Appendix A.

Introduction

The *Roseobacter* group bacteria are among the most prevalent species found in marine ecosystems.[99,107] These bacteria are known for their ability to metabolize the sulfur compound DMSP (**5**) into either compound **6** or **11** via different pathways (Figure 22A), as discussed in sections 3.2 and 3.3.[108] Isotope labeling experiments conducted in laboratory cultures have also confirmed that *Roseobacter* group bacteria efficiently degrade **5** into sulfur volatiles.[100,101]

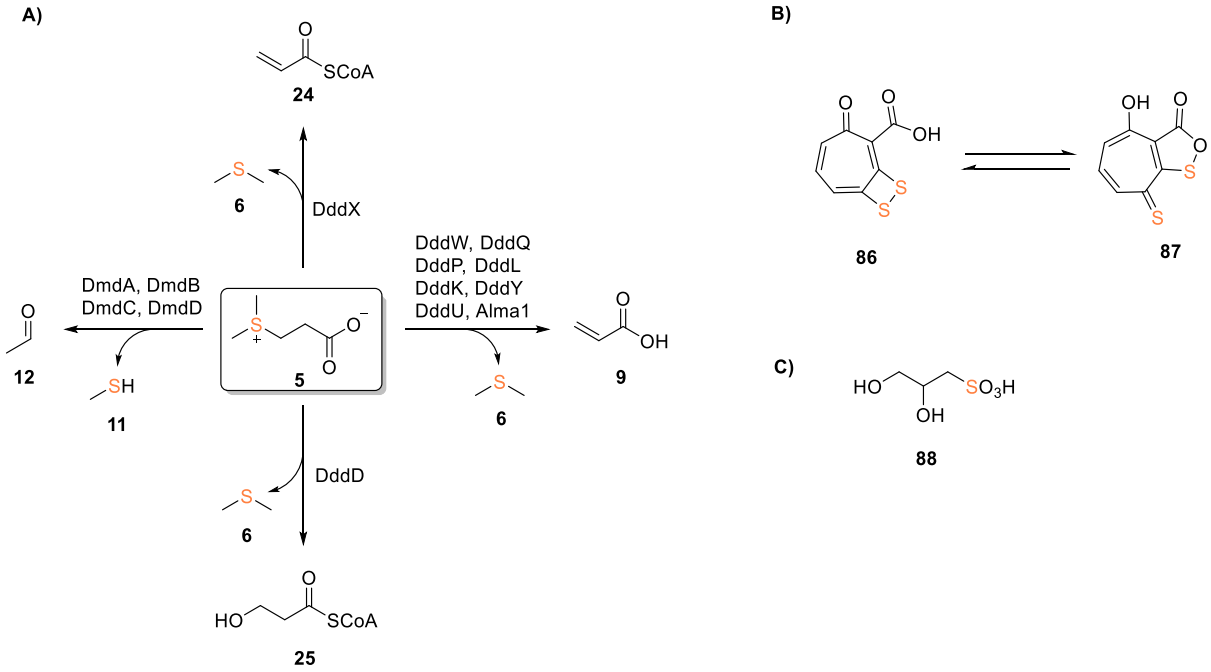

Figure 22. A) Degradation of **5** via the lysis pathway, the hydrolysis pathway and the demethylation pathway. B) Structure of tropodithietic acid in equilibrium with its tautomer thiotropocin. C) Structure of 2,3-dihydroxypropane-1-sulfonic acid (DHPS).

Furthermore, studies have shown that the sulfur metabolite 2,3-dihydroxypropane-1-sulfonic acid (DHPS, Figure 22C), produced by the marine diatom *Thalassiosira pseudonana*, is efficiently incorporated into sulfur volatiles.[103,108-109] In addition, the biosynthesis pathway of tropodithietic acid (TDA), an antibiotic containing sulfur produced by *Phaeobacter piscinae* DSM 103509^T has been investigated using feeding experiments with *P. inhibens* (Figure 22B). These experiments showed that TDA is formed from phenylalanine via phenylacetyl-CoA and the phenylacetyl-CoA catabolon.[110,111]

These feeding experiments provided insights into the mechanism of sulfur incorporation and emphasized the importance of sulfur metabolism for marine bacteria

belonging to the *Roseobacter* group. In this chapter, we have presented the sulfur volatiles produced by six *Celeribacter* strains within the *Roseobacter* group.

Summary

We investigated the volatile profiles of six *Celeribacter* strains, specifically looking at sulfur compounds. These strains include *Celeribacter marinus* DSM 100036^T, *Celeribacter neptunius* DSM 26471^T, *Celeribacter manganoxidans* DSM 27541^T, *Celeribacter baekdonensis* DSM 27375^T, *Celeribacter halophilus* DSM 26270^T, and *Celeribacter indicus* DSM 27257^T. Our analysis revealed 42 volatiles, of which six were sulfur compounds (Figure 23). The structures of these 42 compounds were determined by comparing their mass spectra with our database and matching retention index values with those found in the literature. Many of these compounds are well-known in the literature. The headspace extracts from three strains—*C. marinus*, *C. neptunius*, and *C. manganoxidans*—contained a higher number of volatiles compared to those from the other three strains—*C. baekdonensis*, *C. halophilus*, and *C. indicus*—which had fewer compounds. All six strains produced methylated pyrazines (**89-91**), and some also produced hydroxypentanones (**92-94**), which are known precursors to pyrazines.[113] Additionally, various aldehydes (**95-101**) with different carbon atom numbers were identified in smaller quantities in most strains. Similarly, most strains emitted a range of γ-lactones (**102-108**), furans (**111-113**), along with 3-methylbutan-4-olide (**109**) and 4-methylhex-5-en-4-olide (**110**), except for *C. halophilus*. Cyclohexanol (**114**), along with aromatic compounds (**115-121**), was uniquely produced by *C. marinus*. However, compounds **122** and **123** were identified as non-enzymatic products resulting from the degradation of menaquinones.[112] Sulfur compounds (**124**-**127**) were present in the headspace extracts of all strains. Moreover, compound **128** was present in three strains (*C. marinus*, *C. neptunius*, and *C. baekdonensis*), and its mass spectrum was not found in our database. To elucidate its structure, compound **128** was synthesized using BF_3•OEt_2, by reacting bis(benzothiazol-2-yl)disulfane with dimethyl disulfide. The mass spectrum and retention index of synthetic **128** matched to the compound produced by three strains. Compound **129**, with a retention index (*I*) of 1177 detected in both *C. marinus* and *C. manganoxidans*, did not distinguish between the *E* and *Z* isomers. To determine its structure, the *E* and *Z* isomers of **129** were synthesized through Michael addition of sodium thiomethoxide to ethyl propiolate. HPLC separation and GC/MS analysis

showed retention index values of *I*=1177 for (*E*)-**129** and *I*=1200 for (*Z*)-**129**, confirming that the compound in the strain extracts was (*E*)-**129**.

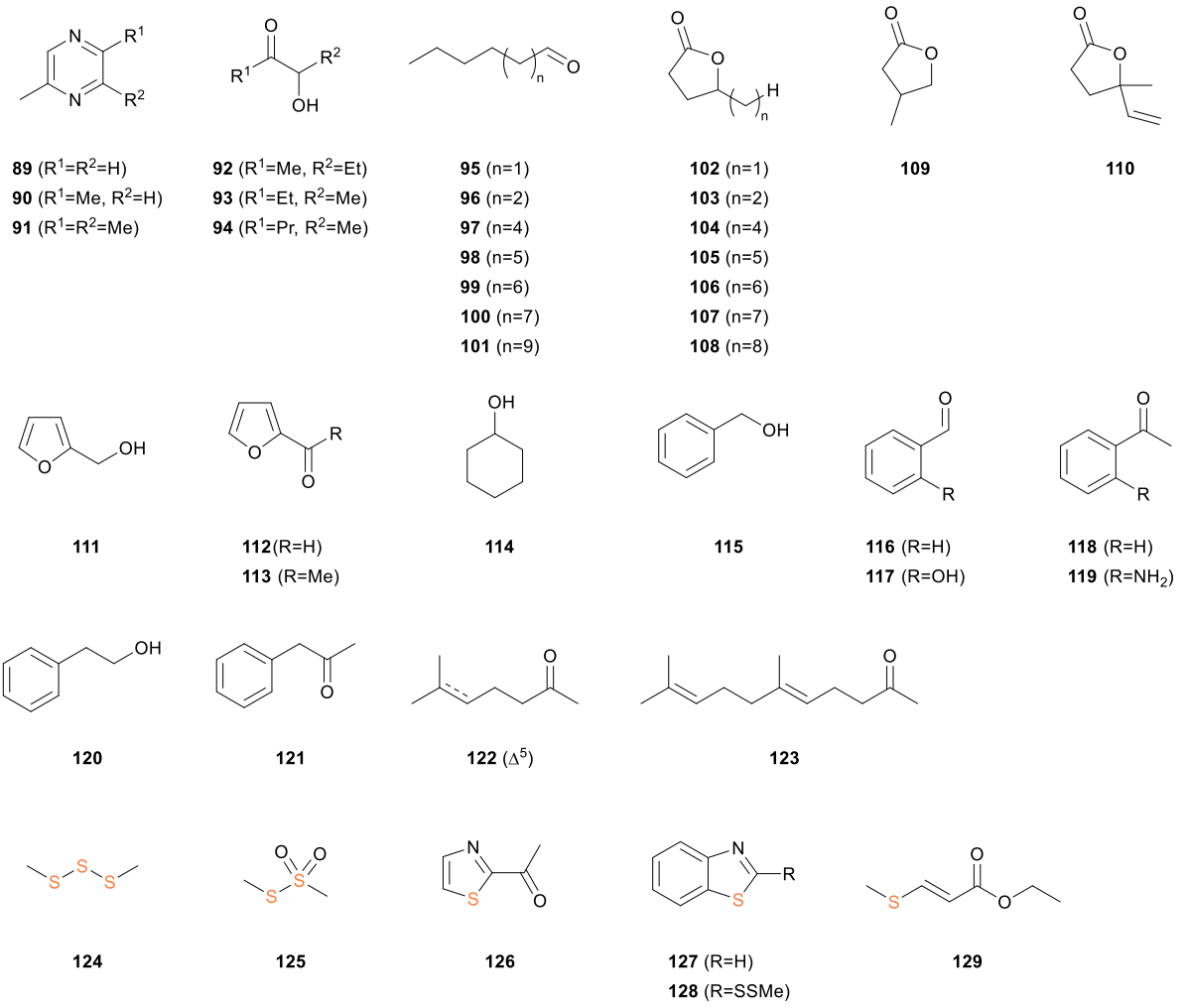

Figure 23. Volatile compounds emitted by six *Celeribacter* strains.

To explore the biosynthesis of sulfur compounds, a series of feeding experiments was conducted using isotopically labeled precursors. Remarkably, when (*methyl*-$^{2}H_3$)-**4** was fed, highly efficient incorporation into **124**, **125**, and the methyl group of **128** was observed. Similarly, feeding of (*methyl*-^{13}C)-**4** led to comparable levels of incorporation into **124**, **125**, and the methyl group of **128**. Additionally, feeding of [^{34}S]-**5** resulted in incorporation into the MeSH group of **124**, both sulfur atoms of **125**, but only into one sulfur atom of **128**.

The selective incorporation into one sulfur atom of **128** prompted further investigations into its natural origin, as there was no incorporation observed into the other two sulfur atoms. Despite conducting several feeding experiments with primary metabolites such

as ($^{13}C_6$)glucose, ($^{13}C_5$)ribose, and (indole-$^{2}H_5$)tryptophan), no incorporation into **128** was observed. This led to the conclusion that its origin is non-biological.

An intriguing discovery was made that 2-mercaptobenzothiazole, commonly used in the sulfur vulcanization of rubber, could spontaneously react with bacterial-origin **11** in the presence of oxygen to generate **128**. This provides a plausible explanation for its formation.

Chapter 3

Breakdown of 3-(allylsulfonio)propanoates in bacteria from the *Roseobacter* group yields garlic oil constituents

Anuj Kumar Chhalodia and Prof. Dr. Jeroen S. Dickschat*

Beilstein J. *Org*. *Chem*. **2021**, *17,* 569–580*.*

The publication “Breakdown of 3-(allylsulfonio)propanoates in bacteria from the *Roseobacter* group yields garlic oil constituents” can be found in Appendix B.

Introduction

The sulfur compounds found in garlic include allyl propyl disulfide (**130**), diallyl disulfide (**131**), diallyl trisulfide (**132**), diallyl tetrasulfide (**133**), 2-vinyl-4H-1,3-dithiine (**134**) and 3-vinyl-3,4-dihydro-1,2-dithiine (**135**) (Figure 24A).[114] These compounds are formed when alliin (**138**), a non-volatile compound present in garlic and related plants, undergoes degradation by pyridoxal phosphate (PLP) dependent alliinase, as shown in Figure 24B.[115] Alliinase catalyzes this reaction, converting **138** into allyl sulfenic acid (**139**), pyruvic acid (**140**), and ammonia. Compound **139** then undergoes dimerization, losing water in the process, to form allicin (**137**). Allicin (**137**) further undergoes hydrolysis, leading to the formation of allylsulfinic acid (**142**) and allyl thiol (**141**) (Figure 24B). These compounds then undergo a series of spontaneous reactions, resulting in the formation of sulfur compounds, as illustrated in Figure 24A.[116,117]

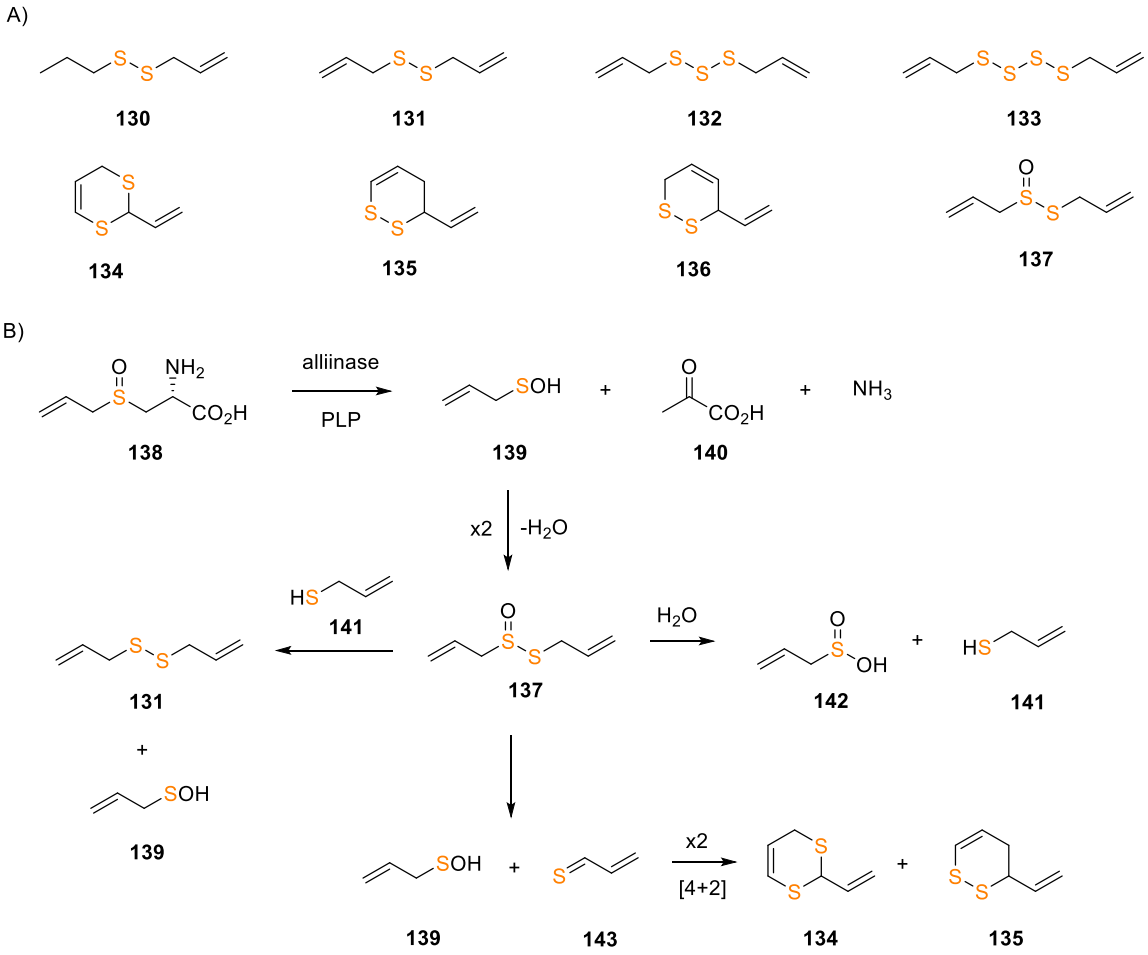

Figure 24. Compounds known from garlic produced from the oxidation of alliin.

Various bacteria and fungi release sulfur compounds[118,119] and marine bacteria from the *Roseobacter* group are especially known for this.[120-122] These sulfur compounds

are largely derived from **5**, a metabolite produced abundantly by algae.[45] The *Roseobacter* group of bacteria is known to encode DMSP lyase and enzymes for DMSP demethylation, which break down **5** and its analogs into various compounds, as summarized in section 4.[100,101] This has been demonstrated by feeding of (*methyl*-$^{2}H_{6}$)-**5** to *P. inhibens* DSM 17395 and *R. pomeroyi* DSM 15171, resulting in the production of **70** from the oxidation of ($^{2}H_{3}$)-**11**, a product of the demethylation pathway. Similarly, feeding of (^{34}S)-**5** to these bacteria leads to the formation of (^{34}S)-DMDS (**159**) and (^{34}S)-**124**.[101,103]

In this chapter, we have demonstrated the enzymatic formation of allyl sulfur volatiles, known from garlic, by feeding of allyl-DMSP derivatives to bacteria of the *Roseobacter* group.

Summary

In earlier studies, it was reported that bacteria of the *Roseobacter* group could accept various DMSP analogs, including **67** and **68** as discussed in chapter 1.[100,101] The degradation of these analogs resulted in the generation of **70**, **124**, **75**, and **77**. To explore further, three bacteria from the *Roseobacter* clade *P. inhibens* DSM 17395, *D. shibae* DSM 16493, and *O. indolifex* DSM 14862 were investigated in relation to the DMSP analogs. Two specific analogs of **5**, 3-(diallylsulfonio)propanoate (DAllSP, **144**) and 3-(allylmethylsulfonio)propanoate (AllMSP, **145**), were synthesized and fed to *P. inhibens*, *D. shibae*, and *O. indolifex*. Upon feeding of **144** and **145**, the bacterial cultures released a strong garlic-like odor. This observation suggested that compounds **144** and **145** underwent degradation leading to the production of sulfur compounds, similar to those found in garlic. A thorough analysis of the emitted volatiles using GC/MS revealed a diverse array of sulfur compounds, including diallyl sulfide (**152**), allyl methyl disulfide (**153**), dimethyl trisulfide (**124**), and various derivatives as shown in Figure 25.

Feeding of **144** to *P. inhibens*, *D. shibae*, and *O. indolifex* resulted in the production of allyl sulfur compounds, along with several other compounds like **124**, dimethyl tetrasulfide (**155**), and *S*-methyl methanethiosulfonate (**151**), already known from *P. inhibens*. *P. inhibens* and *D. shibae* showed a significant formation of diallyl sulfide (**152**), indicating an efficient degradation of **144** through the lysis pathway, facilitated by the *dddP* and *dddL* genes encoded within these strains respectively. Surprisingly,

O. indolfix, lacking a DMSP lyase, still produced **152**, suggesting the presence of another unknown lyase enzyme.

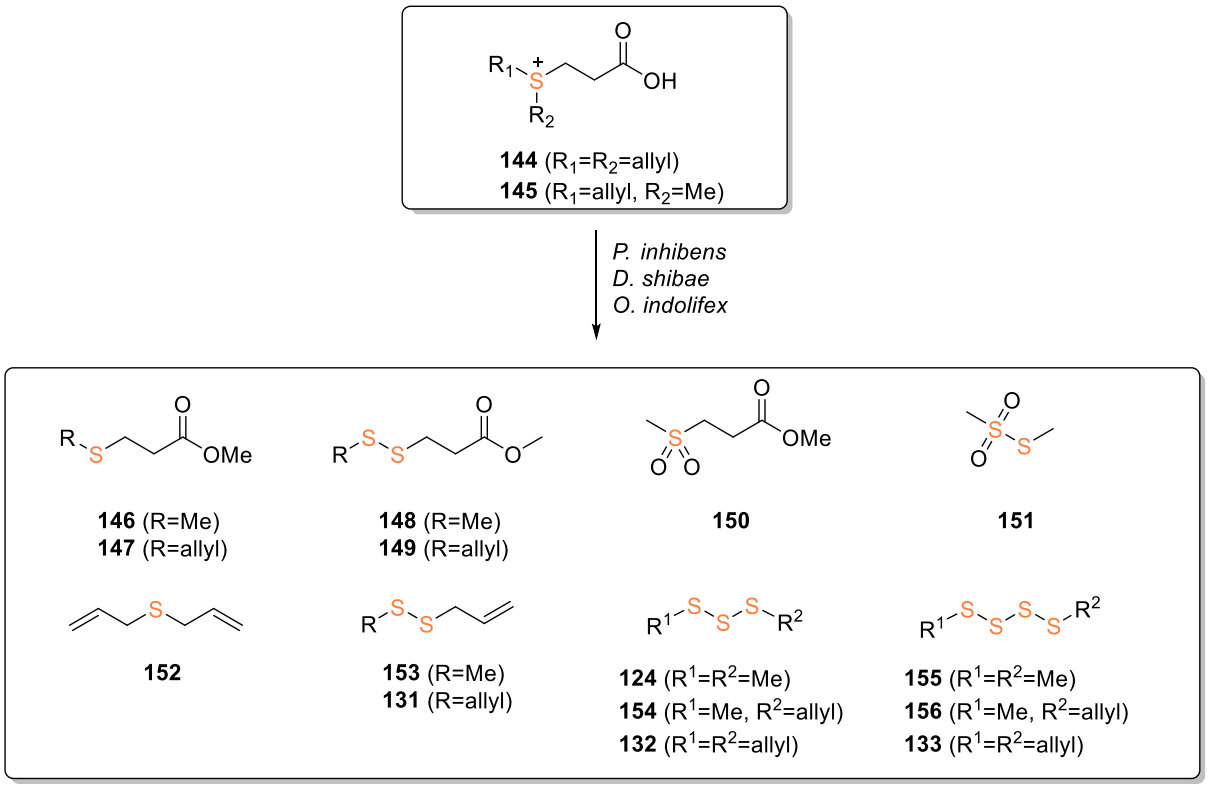

Figure 25. Volatiles released by feeding of **144** and **145** to *P. inhibens*, *D. shibae*, and *O. indolifex*.

Furthermore, the demethylation pathway was fully established in all three strains, as they encoded genes DmdA-D, although the *dmdD* gene was missing in *D. shibae* and *O. indolfex*. It was possible that another enoyl-CoA hydratase from fatty acid degradation was active in these two organisms. Consequently, degradation of **144** via the demethylation pathway released compounds such as **152**, **131**, allyl methyl trisulfide (**154**), traces of **132** and allyl methyl tetrasulfide (**156**). The formation of these compounds could be explained as follows: First, DmdA deallylated **144** to 3-(allylsulfanyl)propanoic acid (**158**), which was further enzymatically degraded by DmdB-D, resulting in formation of allyl thiol (**141**). Allyl thiol (**141**), upon aerial oxidation, underwent dimerization or reacted with **11** to form **131** and allyl methyl disulfide (**153**) (Figure 26A). Sulfur volatile **141**, upon similar oxidation with H_2S, yielded **132** and allyl methyl trisulfide (**154**) (Figure 26B).

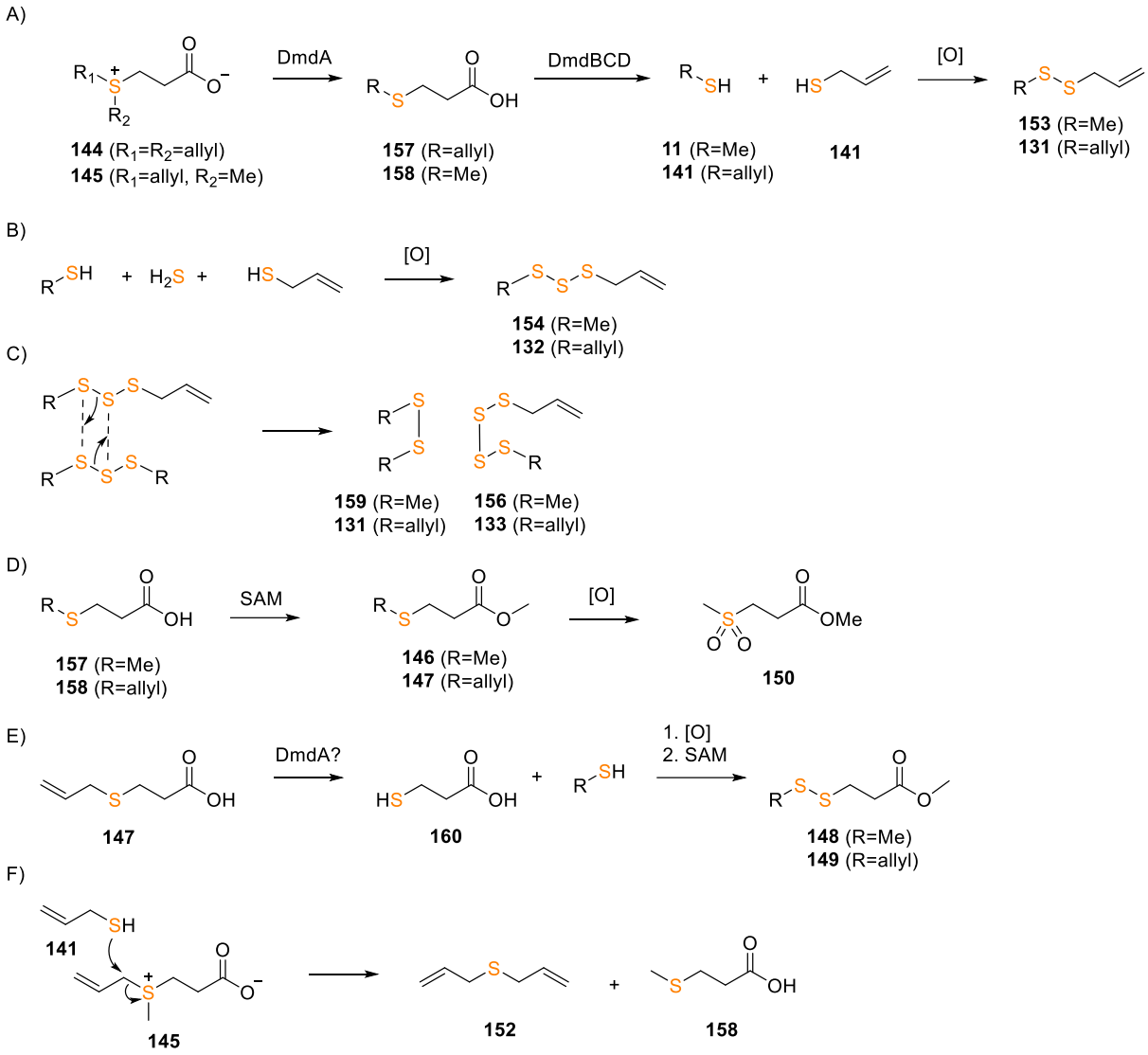

Scheme 26. Proposed mechanisms for the formation of sulfur volatiles from **144** and **145**.

The metathesis reaction between two trisulfides may have resulted in the formation of **133** and **156** (Figure 26C). Additionally, traces of methyl 3-(allylsulfanyl) propanoate (**147**), methyl 3-(methyldisulfanyl)propanoate (**148**), and methyl 3-(allyldisulfanyl)propanoate (**149**) were also observed. While the compound **147** was formed by the *O*-methylation of **158** with SAM, the formation of **148** and **149** was explained by two rounds of deallylation of **144** by DmdA followed by oxidation with corresponding thiol (**11** or **141**) and *O*-methylation (Figure 26D-E).

These compounds were identified by comparing mass spectra in our database or by comparing retention index values with those found in the literature.[100] Only the mass spectrum of **149** returned no database hit. Therefore, a structural proposal for **149** was

made based on the fragmentation pattern in the mass spectrum. This hypothesis was confirmed by synthesizing compound **149**. The mass spectrum and retention index value of synthetic **149** were found identical to those of natural **149** obtained from the feeding experiment.

Feeding of **145** to three strains resulted in a large amount of **146** and a small amount of **147**. While **146** can be formed by deallylation of **145** through DmdA, **147** is likely produced by demethylation of **145** followed by *O*-methylation with SAM. Surprisingly, the significant production of **146** suggests that deallylation was more efficient than demethylation, contrary to the natural function of DmdA catalyzing methyl group transfer. Additionally, di- and trisulfides, including **131**, **149**, **153**, and **154**, were obtained through the DMSP demethylation pathway. Compound **152** resulted from the degradation of **145** into **141** via the demethylation pathway followed by nucleophilic attack on another **145** (Figure 26F).

However, in the case of *D. shibae* and *O. indolifex*, the production of **146** decreased and di-trisulfides increased, suggesting inefficient deallylation of **145** by DmdA in these strains. Only *O. indolifex* produced compound **150**, whose mass spectrum was not in our database. Based on the fragmentation pattern of its mass spectrum, **150** was suggested to be 3-(methylsulfonyl)propanoate (**150**). To confirm this hypothesis, compound **150** was synthesized. The mass spectrum and retention index of synthetic **150** matched to those of naturally obtained **150**, suggesting its formation by the oxidation of **146** through an oxygenase present in *O. indolifex* (Figure 26D).

Chapter 4

Discovery of dimethylsulfoxonium propionate lyases – a missing enzyme relevant to the global sulfur cycle

Anuj K. Chhalodia and Prof. Dr. Jeroen S. Dickschat*

Org. Biomol. Chem. **2023**, *21*, 3083–3089.

The publication “Discovery of dimethylsulfoxonium propionate lyases – a missing enzyme relevant to the global sulfur cycle” can be found in Appendix C.

Introduction

DMSP lyases are enzymes that degrade DMSP (**5**) into DMS (**6**) and acrylate (**9**). DMS (**6**), an important atmospheric gas, oxidizes to form sulfates (**13**) and sulfur dioxide (**14**), which act as cloud condensation nuclei as discussed in chapter 1. However, a significant amount of **6** is oxidized into water-soluble DMSO (**8**) and **13**, either enzymatically or through photochemical reactions.[123,124] Specifically, Trimethylamine monooxygenase (Tmm) from pelagic bacteria oxidizes **6** into **8**. Consequently, the concentration of **8** in marine water samples is observed to be higher than that of **6** and **5**.[125] In 2018, an important new metabolite, DMSOP (**7**), was discovered in various DMSP-producing algae and bacteria, as mentioned in chapter 1. These organisms could potentially produce **8** by oxidizing **5** into **7**, which is then cleaved into **8**. However, the enzymes responsible for these specific reactions have not yet been identified.[15]

In this study, we have identified enzymes capable of catalyzing the degradation of **7** into **8** and **9**. Additionally, we conducted kinetic studies on these enzymes with **7** to determine their catalytic efficiency.

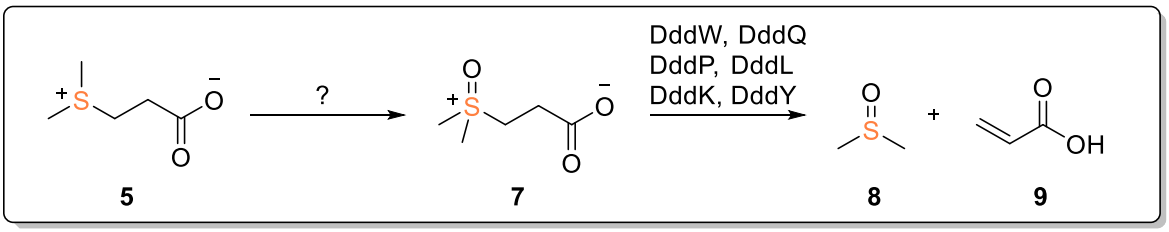

Figure 27. Oxidation of **5** into **7** followed by enzymatic cleavage into **8** and **9** by DMSOP lyases.

Summary

DMSOP (**7**) could be a significant source of marine DMSO (**8**), but the conversion pathway to **8** and **9** remains unclear. Consequently, the activity of DMSP lyases towards **7** was examined. DMSOP (7) was synthesized by oxidizing compound **5** using $RuCl_3$ and NaOCl, resulting in significantly higher purity than previously reported in the literature.[15] Six DMSP lyases (DddW, DddQ, DddP, DddL, DddK, DddY) were initially tested at pH 8 and 30 °C, but analyzing the water-soluble enzyme product (**8**) was challenging. To address this, (*methyl*-$^{13}C_2$)-**7** was synthesized for enzyme activity tests. The Labeled **7** allowed easy monitoring of the enzyme reaction product using

^{13}C NMR spectroscopy without requiring a workup. All six lyases were tested across a pH range of 3 to 9 and temperatures from 10 to 80 °C.

To find the optimal pH, the six enzymes were incubated with (*methyl*-$^{13}C_2$)-**7** at 20 °C across different pH values. It was found that DddW, DddQ, DddK, and DddY were most active at pH 8, while DddP showed highest activity at pH 6, and DddL at pH 9. The conversions were determined by integrating the peaks in the ^{13}C-NMR spectrum of (*methyl*-$^{13}C_2$)-**8** and (*methyl*-$^{13}C_2$)-**7**. DddW had low conversion at pH 6 but high conversion from pH 7 to 9, with the highest at pH 8. DddQ showed low activity between pH 4 and 7, highest at pH 8, and maintained good conversion at pH 9. DddP showed good conversion at pH 5, performed best at pH 6, and had low turnover from pH 7 to 9. DddK activity increased from pH 5, reaching an optimum at pH 8, with only minor activity at pH 9. DddL was consistently active from pH 3 to 8, showing moderate increase and performing best at pH 9. DddY showed moderate and increasing conversion from pH 3 to 7, highest at pH 8, and had moderate conversion at pH 9.

The temperature dependency of all six enzymes with (*methyl*-$^{13}C_2$)-**7** was investigated within a range of 10 °C to 80 °C. DddW was active across the entire range, showing the highest conversion at 10 °C. Similarly, DddQ performed best at 10 °C and nearly achieved complete conversion at 20 °C; its activity was maintained across the range but gradually decreased at higher temperatures. DddP was also active from 10 °C to 80 °C, with the highest conversion at 30 °C. DddK was highly active between 10 °C and 30 °C, highest at 30 °C, but its performance dropped sharply at 40 °C, though some activity was observed at temperatures up to 80 °C. DddL was active throughout the entire temperature range, with optimal substrate turnover at 30 °C. Lastly, DddY was highly active at 10 °C (its optimum) and 20 °C, and retained its conversion rate at higher temperatures.

Enzyme kinetic data were collected at 20 °C and the optimal pH for each enzyme, except for DddL, which could not be purified in an active form. The analysis included both substrates **5** and **7**. The kinetic data for **5** with DddW, DddQ, and DddP were consistent with previous findings.[104] However, DddK and DddY with **5** showed significantly lower K_M values of 0.76 ± 0.08 mM, and 0.23 ± 0.01 mM, respectively, compared to previous reports for *Pelagibacter ubique* (13.6 ± 2.1 mM)[126] and

Acinetobacter bereziniae (5.0 ± 0.6 mM).[127] The reasons for these differences are unclear.

In a similar manner, kinetic data for **7** with five DMSP lyases were obtained. DddY emerged as the most efficient enzyme for **7**, with a catalytic efficiency (k_{cat}/K_M) value of 6.10 ± 0.01 s^{-1} mM^{-1}, slightly lower than **5** (21.6 ± 1.7 s^{-1} mM^{-1}). This result is unexpected, given previous reports by Pohnert et al., which indicated similar production of **8** from **7** in both the wild-type and Δ*dddY* knockout mutant strains of *Alcaligenes faecalis*.[15] One possibility is that another unidentified DMSOP lyase is upregulated in the Δ*dddY* knockout strain during growth on DMSOP (**7**). Alternatively, DddY from *A. faecalis*, and *F. balearica* as used in our study, may exhibit significantly different activities for the cleavage of **7**.

For DddW, **5** was cleaved with moderately higher efficiency (k_{cat}/K_M = 2.51 ± 0.03 s^{-1} mM^{-1}) compared to **7** (k_{cat}/K_M = 1.07 ± 0.01 s^{-1} mM^{-1}), whereas DddK exhibited similar efficiency for both substrates **5** and **7**. However, DddQ and DddP were less efficient enzymes overall, though they both converted **7** more effectively than **5**. Therefore, DddQ and DddP are best characterized as DMSOP lyases. Notably, DddP demonstrated substrate inhibition with **7** at concentrations above 2.5 mM, which likely contributes to its lower performance.

Chapter 5

Functional characterisation of twelve terpene synthases from actinobacteria

Anuj K. Chhalodia, Houchao Xu, Georges B. Tabekoueng, Binbin Gu, Kizerbo A. Taizoumbe, Lukas Lauterbach and Prof. Dr. Jeroen S. Dickschat*

Beilstein J. Org. Chem. **2023,** *19,* 1386–1398.

Gene (WP_153520876) cloning, isolation and structure elucidation of **171** was performed by me. Gene (MBB5895433) cloning, isolation and structure elucidation of **170** was performed by Houchao Xu. Gene (WP_078950427, WP_150516140) cloning, isolation and structure elucidation of **172** was performed by Georges B. Tabekoueng, and cloning of other genes, isolation and structure elucidation of **173**, **174** and **175** were performed by Binbin Gu, Kizerbo A. Taizoumbe, and Lukas Lauterbach.

The publication "**Functional characterisation of twelve terpene synthases from actinobacteria**" can be found in Appendix D.

Introduction

Terpene synthases are enzymes that convert acyclic and achiral oligoprenyl pyrophosphates into complex terpene hydrocarbons or alcohols. This process starts with substrate ionization, either by diphosphate removal (type I terpene synthase) or protonation (type II terpene synthase). The resulting cationic species undergoes reactions involving cyclizations, hydride or proton shifts, and skeletal rearrangements. Many such enzymes have been found in bacteria, plants, and fungi. For example, 5-*epi*-aristolochene (**161**) synthase and casbene (**162**) synthase are plant enzymes from *Nicotiana tabacum* and *Ricinus communis*, respectively.[128,129] Similarly, many fungal enzymes are known to be either mono-functional or bifunctional. Aristolochene (**163**) synthase, a mono-functional enzyme containing only a terpene synthase domain, has been isolated from *Aspergillus terreus*[130] and *Penicillium roqueforti*,[131] however, bifunctional enzymes have a prenyltransferase domain that creates an oligoprenyl pyrophosphate precursor and a terpene synthase domain that cyclizes it into complex structures. Notable examples include fusicoccadiene (**164**) synthase from *Phomopsis amygdali*,[132] and macrophomene (**165**) synthase from *Macrophomina phaseolina*.[133]

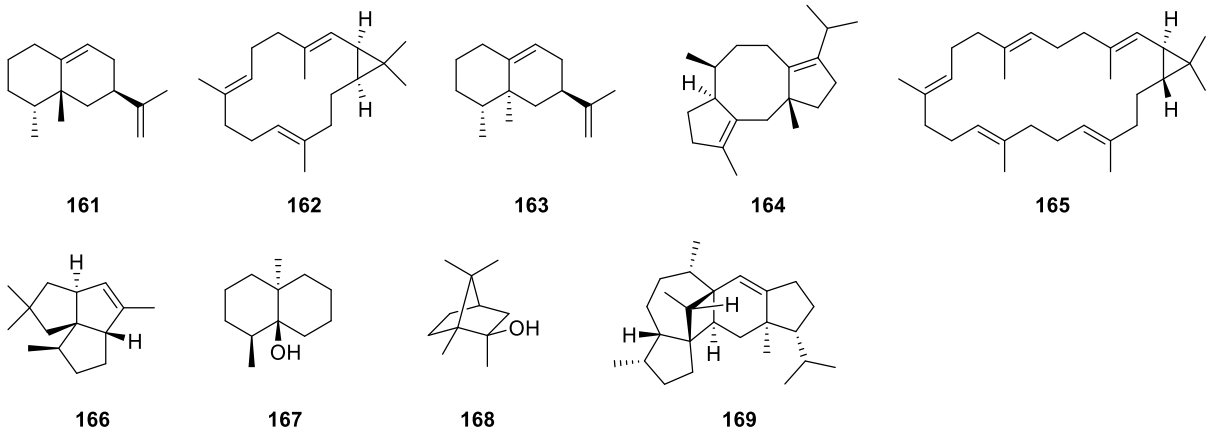

Figure 28. Terpenes produced by characterized terpene synthases.

The identification of pentalenene (**166**) synthase from *Streptomyces exfoliates*,[134] opened the way for the discovery of other bacterial enzymes, including the synthases for geosmin (**167**) and 2-methylisoborneol (**168**) from *Streptomyces coelicolor*.[135,136] Recent discoveries have also disclosed the successful isolation of bacterial sesterterpene synthases, including sesterviridene (**169**) synthase from *Kitasatospora viridis*.[137-139]

In this chapter, we have analyzed fifteen terpene synthases from actinobacteria for their products. Four terpene synthases with previously unknown functions were isolated and characterized using NMR spectroscopy. This led to the discovery of the first terpene synthases for (+)-δ-cadinol (**170**), (+)-α-cadinene (**171**), and the first two bacterial (−)-amorpha-4,11-diene (**172**) synthases. Other characterized enzymes, which had functional homologs identified before, include *epi*-isozizaene synthase,[140] 7-*epi*-α-eudesmol synthase,[141,142] four sesquiterpene synthases producing mixtures of hedycaryol[143] and germacrene A,[144] a diterpene synthase for allokutznerene,[145] and a sesterterpene synthase for sesterviolene.[146]

Summary

In efforts to expand the knowledge on terpene synthases, fifteen uncharacterized homologs were chosen from different branches of a phylogenetic tree constructed from 4018 bacterial terpene synthase homologs. Their encoding genes were cloned and expressed in *Escherichia coli*. Test reactions were conducted using purified recombinant proteins and substrates like GPP, FPP, GGPP, and GFPP. Consequently, the fifteen enzymes were characterized as sesquiterpene, diterpene, and sesterterpene synthases.

The enzyme (MBB5895433) isolated from *Kutzneria kofuensis* was observed to transform FPP into (+)-δ-cadinol (**170**). The optical rotation of **170** ($[\alpha]_D^{25}$= +95.9, *c* 0.55, CH_2Cl_2) closely matched that of the enantiomer found in plants like *Pinus sibirica* ($[\alpha]_D^{20}$ = +118.4) and *Torreya nucifera* ($[\alpha]_D^{18}$ = +118.6),[147] as well as in the fungus *Xylobolus frustulatus* ($[\alpha]_D^{25}$ = +99.9, *c* 0.6, $CHCl_3$).[148] Hence, this enzyme is appropriately termed a (+)-δ-cadinol synthase, marking the first discovery of a terpene synthase responsible for the biosynthesis of **170**.

A terpene synthase (WP_153520876) from *Streptomyces jumonjiensis* was identified as an α-cadinene synthase, converting FPP into α-cadinene (**171**) with high yield. It shares 32% amino acid sequence identity with germacrene A synthase from *M. marina*.[149] The optical rotation of **171** ($[\alpha]_D^{25}$ = +60.0, *c* 0.015, C_6D_6) indicates the opposite enantiomer to that found in *Humulus lupulus* ($[\alpha]_D^{24}$ = −62.4 (*c* 0.868, $CHCl_3$)).[150] This marks the first discovery of an α-cadinene synthase from *Streptomyces jumonjiensis*.

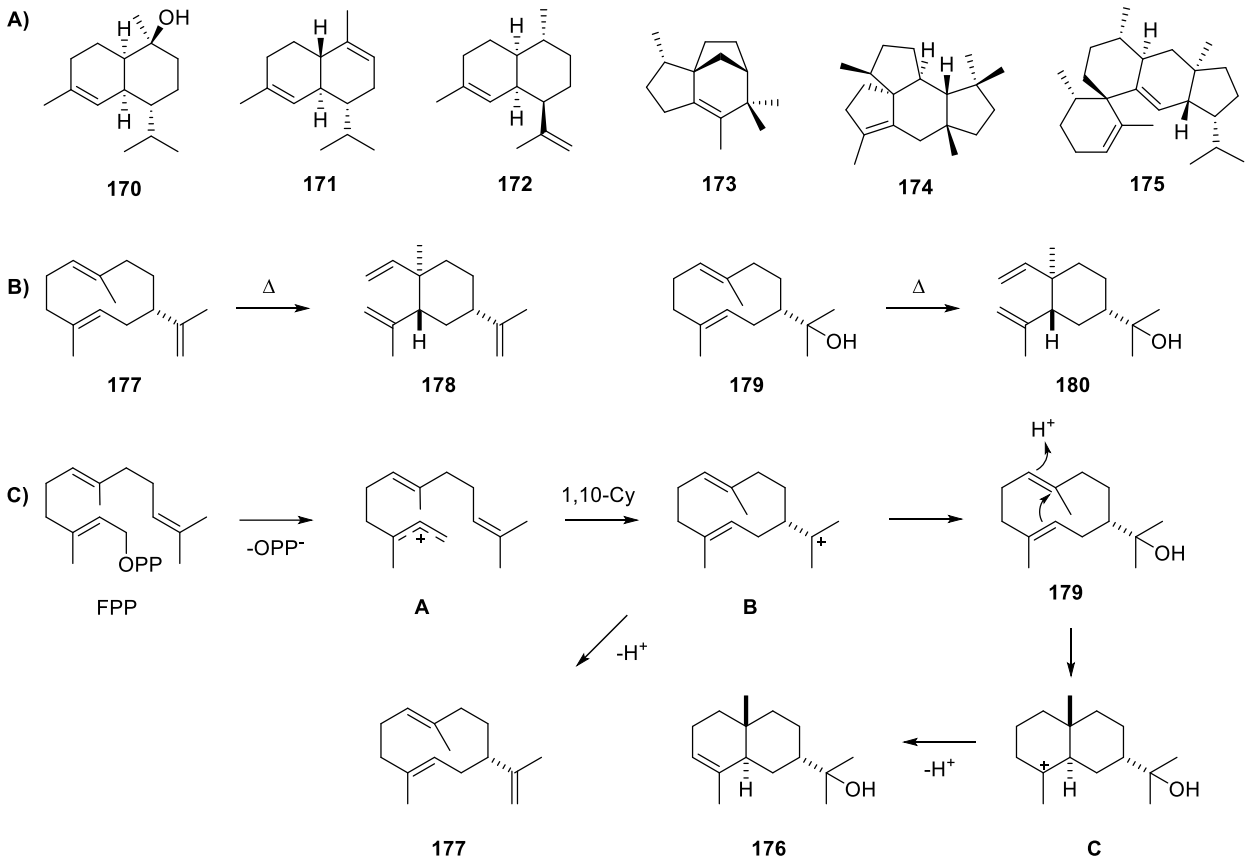

Figure 29. A) Terpenes produced by uncharacterized enzymes. B) Cope rearrangement product of **177** and **179**. B) Cyclisation mechanism for **176**, with the formation of **179** as an intermediate and **176** as a side product.

Two sesquiterpene synthases (WP_078950427, WP_150516140) from *Streptomyces lavendulae* and *Streptomyces subrutilus* produced (−)-amorpha-4,11-diene (**172**). These enzymes differ from known ones, sharing 25% and 28% amino acid sequence identity with spiroalbatene synthase from *Allokutzneria albata*.[151] The optical rotation of **172** ($[\alpha]_D^{25}$ = −9.4, *c* 0.64, CH_2Cl_2) corresponds to that of **172** isolated from *Viguiera oblongifolia* ($[\alpha]_D^{25}$ = −8, *c* 0.4, $CHCl_3$). Thus, they are identified as (−)-amorpha-4,11-diene (**172**) synthases, similar to the one in *Artemisia annua*, which catalyzes the initial step in artemisinin biosynthesis.[152]

The terpene synthase (WP_086008896) from *Nocardia brevicatena*, sharing 48% amino acid sequence identity with *epi*-isozizaene (**173**) synthase (EIZS) from *Streptomyces coelicolor*,[153] produces **173** when incubated with FPP, confirming its function. Surprisingly, it forms a mixture of monoterpenes when incubated with GPP,

unlike EIZS from *Streptomyces bungoensis*. Therefore, the terpene synthase from *N. brevicatena* is identified as an *epi*-isozizaene synthase.

Another terpene synthase (WP_028812116) from *Streptomyces flavidovirens* catalyzes the conversion of FPP, resulting in 7-*epi*-α-eudesmol (**176**) as the main product. Additionally, germacrene A (**177**) and hedycaryol (**179**) are formed, confirmed by the detection of their Cope rearrangement products elemene (**178**) and elemol (**180**) in GC–MS analysis. Sharing 78% amino acid sequence identity with 7-*epi*-α-eudesmol (**176**) synthase from *S. viridochromogenes*,[142,154] this enzyme is accurately characterized as a 7-*epi*-α-eudesmol synthase.

The four terpene synthases isolated from *Streptomyces sclerotialus* (WP_030615021), *Streptomyces catenulae* (WP_051739595), *Streptomyces ficellus* (WP_156694351), and *Streptomyces morookaense* (WP_171082395) exclusively accept FPP, yielding varying mixtures of **179** and **177** with low product formation, detected as Cope rearrangement products **178** and **180**. Consequently, the terpene synthases from *S. sclerotialus*, *S. catenulae*, and *S. ficellus* are identified as hedycaryol (**179**) synthases, while the synthase from *S. morookaense* is described as a germacrene A (**177**) synthase. These synthases share a 63% amino acid sequence identity. Notably, the spiroviolene synthase from *S. violens* is the closest characterized homolog of these enzymes, sharing an amino acid sequence identity ranging from 32% to 36%.

A diterpene synthase (WP_184867163) from *Kutzneria kofuensis* produces a high yield of allokutznerene (**174**) when incubated with GGPP. This enzyme shares 58% amino acid sequence identity with cattleyene synthase (CyS) from *Streptomyces cattleya* and 36% with phomopsene synthase from *Allokutzneria albata*. Thus, it is identified as *Kutzneria kofuensis* allokutznerene synthase (KkAS). Interestingly, KkAS shares low sequence identity with phomopsene synthase, but formed the same product.

Finally, a terpene synthase (WP_159685978) isolated from *Streptomyces* sp. Tü produces sesterviolene (**175**) when incubated with GFPP. This newly identified enzyme is termed as sesterviolene synthase. It closely resembles sesterviolene synthase from *Streptomyces violarus*, sharing 85% sequence identity.

Thus, a phylogenetic analysis of bacterial terpene synthases resulted in the discovery of the first bacterial synthases for (+)-δ-cadinol and (+)-α-cadinene. Additionally, the first bacterial synthase for (−)-amorpha-4,11-diene, which had been initially isolated from *Artemisia annua* and was involved in artemisinin biosynthesis, was also identified.

Chapter 6

The Stereochemical Course of DmdC, an Enzyme Involved in the Degradation of Dimethylsulfoniopropionate

Anuj K. Chhalodia and Prof. Dr. Jeroen S. Dickschat*

Chembiochem **2024***, 25,* e202300795.

The publication “The Stereochemical Course of DmdC, an Enzyme Involved in the Degradation of Dimethylsulfoniopropionate” can be found in Appendix E.

Introduction

Marine bacteria are responsible for degrading DMSP (**5**), with approximately 20% of the material converted into the volatile compound DMS (**6**) and the remaining 80% into MeSH (**11**).[155] The metabolic pathway that leads to the production of **11** from **5** is known as the demethylation pathway. This process is facilitated by four key enzymes: DMSP demethylase (DmdA), MMPA-coenzyme A ligase (DmdB), MMPA-CoA dehydrogenase (DmdC), and either MTA-CoA hydratase (DmdD) or its ortholog, AcuH.[82,155] The enzyme DmdC, which facilitates the intermediate step of the demethylation pathway (Figure 18), is FAD-dependent and a member of the acyl-CoA dehydrogenase family, commonly involved in fatty acid metabolism.[82,89] Acyl-CoA dehydrogenases initiate fatty acid β-oxidation by catalyzing the formation of a double bond between the C_α and C_β positions of CoA-conjugated substrates, with flavin adenine dinucleotide (FAD) acting as a cofactor. Acyl-CoA dehydrogenases are capable of utilizing a variety of substrates, including short, medium, and long-chain fatty acid acyl-CoA, such as butyryl-CoA, C_8-CoA, and C_{11}-CoA.[156-158] The crystal structure of DmdC has been resolved,[89] however a crystal structure with both the substrate and FAD together has not yet been obtained. Thus far, three DmdC isozymes in *R. pomeroyi* DSS-3 have been identified, all exhibiting MMPA-CoA dehydrogenase activity.[82] Despite this, the structural and catalytic mechanisms of these isozymes have not been reported, leaving the stereochemical course of DmdC unknown. In this study, we determined the stereochemical course of the DmdC-catalyzed reaction by synthesizing stereoselectively deuterated N-acetylcysteamine thioester (SNAc ester) analogs of **182**.

Summary

The investigation into the stereochemical behavior of DmdC began with the cloning and expression of the *dmdC* gene in *E. coli*. Subsequently, the DmdC was incubated with the SNAc ester (**182**) of 3-(methylsulfanyl)propionic acid (**181**), leading to its efficient conversion into the desired product (**183**). This successful transformation enabled us to delve into the stereochemical behavior of DmdC.

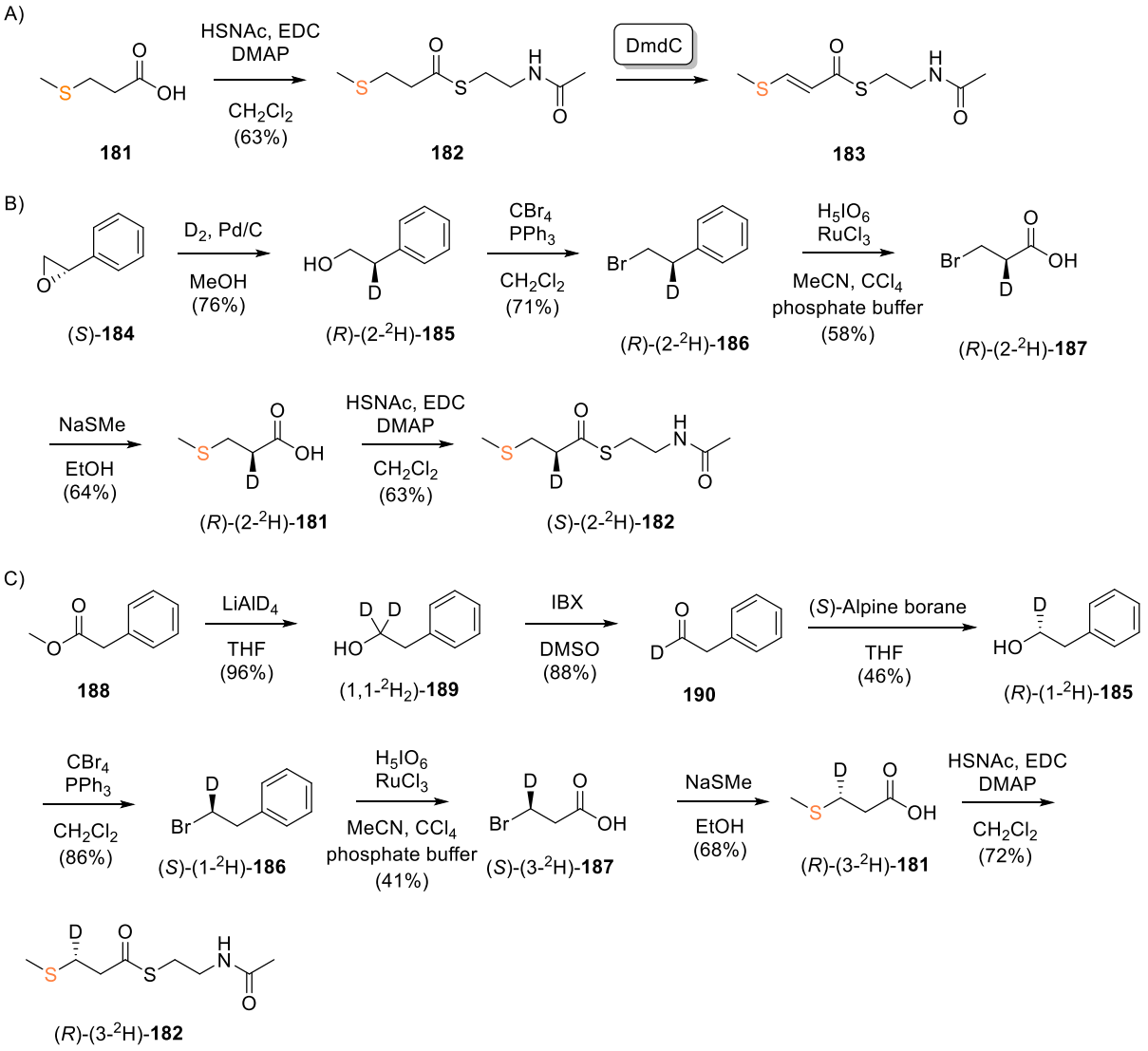

Figure 30. Synthesis of stereoselective deutereted isotopomers of **182**.

To achieve this, four stereoselectively deuterated substrate surrogates of **182** were synthesized with selective deuterations at either the α or β carbon positions. The stereochemically selective deuteration at α carbon began with the controlled opening of the epoxide ring of (*S*)-styrene epoxide (**184**). This was achieved via catalytic hydrogenation utilizing deuterium gas, resulting in the formation of (*R*)-(2-^{2}H)-**185** with an inverted configuration.[159] A subsequent bromination reaction resulted in the formation of (*R*)-(2-^{2}H)-**186**. Oxidative cleavage of the phenyl ring of **186** in the presence of periodic acid and $RuCl_3$ yielded (*R*)-(2-^{2}H)-**187**. Through nucleophilic substitution with NaSMe, compound (*R*)-(2-^{2}H)-**187** was transformed into (*R*)-(2-^{2}H)-**181**. The compound **181** was subjected to an esterification reaction to yield the SNAc ester (*S*)-(2-^{2}H)-**182** (Figure 30). A similar synthetic pathway was utilized to synthesize (*R*)-(2-^{2}H)-**182**, starting from (*R*)-styrene epoxide.

The synthesis of isotopomer **182**, featuring stereoselective deuteration at the β-carbon, was initiated by reducing methyl phenylacetate (**188**) with $LiAlD_4$ to yield (1,1-$^2H_2$)-**189**. Subsequent oxidation of (1,1-$^2H_2$)-**189** with IBX produced **190**, which underwent stereoselective reduction with (*S*)-Alpine borane, resulting in (*R*)-(1-^{2}H)-**185**. Bromination of (*R*)-(1-^{2}H)-**185** yielded (*R*)-(1-^{2}H)-**186**, followed by oxidation of the phenyl ring in the presence of periodic acid and $RuCl_3$, NaSMe substitution, and esterification, ultimately yielding (*R*)-(3-^{2}H)-**182** (Figure 30). A similar synthetic route was utilized for the synthesis of compound (*S*)-(3-^{2}H)-**182**, involving the stereoselective reduction of compound **190** with (*R*)-Alpine borane.

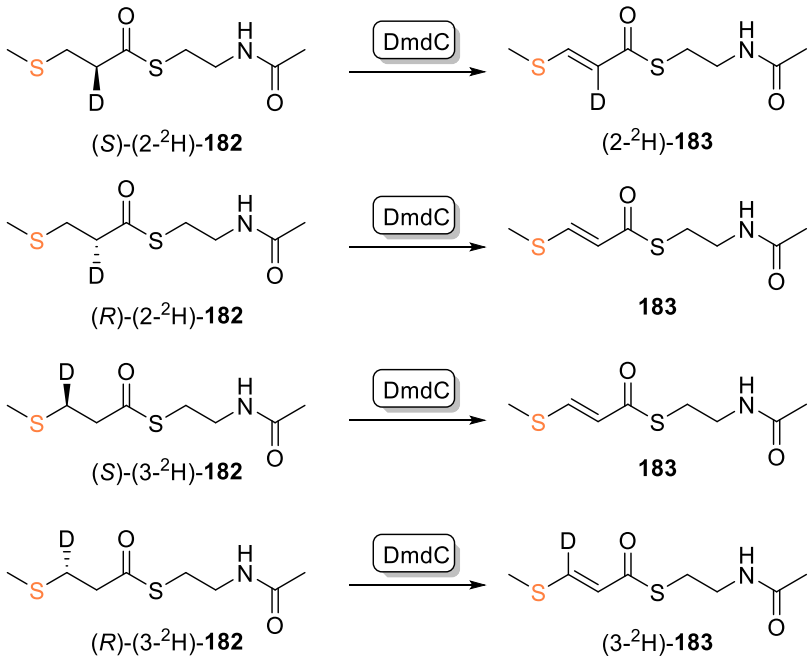

Figure 31. Stereochemical course of DmdC.

Each of the four stereoselectively deuterated isotopomers were incubation individually with DmdC, followed by product extraction using CH_2Cl_2 and subsequent GC/MS analysis. Mass spectrometric analysis revealed distinctive patterns: for (*S*)-(2-^{2}H)-**182**, deuterium remained associated with the product to yielded (2-^{2}H)-**183** (Figure 31), indicated by the molecular ion peak at *m*/*z* 220 and fragment ion peaks at *m*/*z* 102 and 74. However, a minor fragment ion peak at *m*/*z* 101 suggested non-enzymatic partial deuterium loss, which increased over prolonged incubation. Although, (*R*)-(2-^{2}H)-**182** exhibited clear deuterium loss to produce **183**, evidenced by the molecular ion peak at *m*/*z* 219, base ion peak at *m*/*z* 101, and fragment ion peak at *m*/*z* 73. In summary, the incubation of SNAc ester (*R*) and (*S*)-(2-^{2}H)-**182** with DmdC highlighted the enzyme preference for selectively abstracting the 2-*pro*-*R* proton (Figure 31).

Moreover, the hydride abstraction at the β carbon was explored. Incubation of (*R*)-(3-^{2}H)-**182** with DmdC resulted in the formation of (3-^{2}H)-**183** with deuterium retention, evidenced by the presence of a molecular ion peak at *m/z* 220 and a base ion peak at 102 (Figure 31). In case of (*S*)-(3-^{2}H)-**182**, clear deuterium loss was observed, indicated by the molecular ion peak and fragment ion peak at *m*/*z* 219 and 101, respectively.

Thus, these results indicate that the reaction catalyzed by the acyl-CoA dehydrogenase DmdC follows an *anti*-elimination mechanism, selectively abstracting the 2-*pro*-*R* proton and the 3-*pro*-*S* hydride during the dehydrogenation process of substrate surrogate **182** (Figure 31). It is noteworthy that similar stereochemical pathways have been observed in other acyl-CoA dehydrogenases found in pork liver,[160,161] *Clostridium kluyveri*,[162] rat liver,[163] and *Candida polytica*,[163] all involved in the β-oxidation of fatty acids.

Chapter 7

On the Substrate Scope of Dimethylsulfonium Propionate Lyases toward Dimethylsulfoxonium Propionate Derivatives

Anuj K. Chhalodia and Prof. Dr. Jeroen S. Dickschat*

Eur. J. Org. Chem. **2024**, *17*, e202400098

The publication “On the Substrate Scope of Dimethylsulfonium Propionate Lyases toward Dimethylsulfoxonium Propionate Derivatives” can be found in Appendix F.

Introduction

In addition to DMSP (**5**), DMOSP (**7**) is an important metabolite produced by bacteria and algae, which can then be degraded into DMSO (**8**) by marine organisms.[15] DMSO (**8**) can impact Earth's climate by serving as a precursor to marine DMS (**6**), through the reduction by marine bacteria. Additionally, a certain amount of DMSO (**8**) serves as an important source of atmospheric sulfur, which oxidizes into sulfates (**13**), serving as cloud condensation nuclei and potentially impacting Earth's climate dynamics, as discussed in chapter 1.[164-166] Moreover, compound **8** also acts as a source of methane, a potent greenhouse gas.[167,168] Extensive research has been done that focused on the biogeochemical cycling of **8**, although a complex mechanism is involved in the formation and degradation of **8**. However, marine DMSO (**8**) primarily originates from bacteria, algae, and the photochemical oxidation of **6**.[124,169-170]. As discussed in Chapter 1, Thume et al. later found that marine bacteria produce **7**, which could potentially serve as a precursor to marine **8**. Recently, we have discovered the enzymes that can potentially cleave **7** into **8** as presented in chapter 4. In this chapter, we investigated the substrate tolerance of DMSP lyases using four synthesized analogs of **7** with long alkyl chains, and their catalytic efficiency was examined by performing the kinetic study. Additionally, we have explored the enantioselectivity of the most efficient enzyme, DddW, considering the chiral nature of the synthesized analogs of **7**.

Summary

As discussed in Chapter 4, six DMSP lyase enzymes were identified to cleave **7** into **8** and **9**.[16] These enzymes were further investigated for their substrate tolerance. To explore this, four analogs of **7** with long alkyl chain (EMSOP (**191**), PMSOP (**192**), BMSOP (**193**) and IMSOP (**194**) were synthesized and tested for their activity with DMSP lyases.

In the initial experiment, analogs of **7** were incubated with purified recombinant forms of six DMSP lyases (DddW, DddQ, DddP, DddL, DddK, and DddY). However, the analysis of enzyme reaction products encountered challenges due to their solubility in the aqueous phase. To overcome this issue, (*methyl*-^{13}C)-**7** analogs were synthesized using 3-mercaptopropanoic acid with alkyl iodide and $^{13}CH_3$-I.

The enzymatic reactions with (*methyl*-^{13}C)-**7** analogs enabled the monitoring of substrate conversion to ethylmethyl sulfoxide (**195**), propylmethyl sulfoxide (**196**), butylmethyl sulfoxide (**197**), and isopropylmethyl sulfoxide (**198**) through ^{13}C NMR spectroscopy analysis. The activities of DMSP lyases were evaluated with each of the four (*methyl*-^{13}C)-**7** analogs across a pH range from 3 to 9. DddW, DddQ, DddL, DddK, and DddY demonstrated highest activity at pH 8, whereas DddP exhibited optimal performance at pH 6.

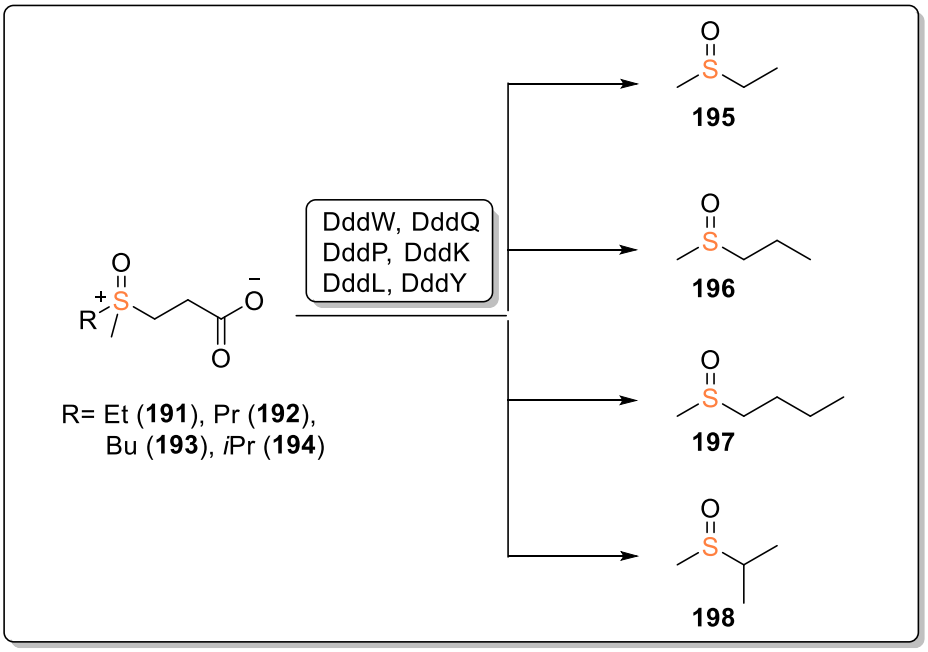

Figure 32. Enzymatic conversion of analogs of **8** by DMSP lyases.

DddQ efficiently converted all four substrates over the pH range of 6 to 9, with optimal activity observed at pH 8. At pH 4, substrate **194** showed poor conversion, whereas at pH 5, all substrates were converted except for **191**. Notably, the reaction was more efficient with shorter alkyl chain substrates. The conversion of substrates was highly efficient with DddW from pH 6 to 9. Only substrate **194** converted at a low rate at pH 6, but **191** and **192** showed full conversion at pH 8 with DddW.

DddP did not accept **194** but exhibited poor conversion rates for **191**, **192**, and **193** across pH 4 to 9, with the highest conversion observed at pH 6, In contrast, DddY showed highest efficiency for all substrates at pH 8. The conversion rates for **191** and **192** were higher compared to **193** and **194**. DddY was active with **191** and **192** from pH 4 to 9, with **193** showing activity from pH 5 to 9, and **194** displaying conversion at pH 7 and 8.

DddK exhibited high conversion rates for **191**, **192**, and **193** at pH 8, but showed slow conversion for **194**. On the other hand, DddL converted **191**, **192**, and **193** at a poor rate and did not accept **194**. Specifically, substrate **191** showed conversion from pH 3 to 9, substrate **192** from pH 4 to 9, and **193** from pH 5 to 9. Consequently, substrates with shorter alkyl chains demonstrated a broader pH range for conversion.

The enzyme kinetics for analogs of **7** were investigated using Michaelis-Menten kinetics with four enzymes: DddW, DddQ, DddK, and DddY. Due to low conversion rates, DddP was excluded from the kinetics study. Unfortunately, DddL could not be included due to purification challenges. The experiments were conducted at pH 8 and 20 °C. The k_{cat}/K_m values revealed lower activity for analogs of **7** compared to **7**,[16] with decreasing catalytic efficiency as the alkyl chain length increased. DddY demonstrated the highest efficiency among the enzymes, while DddW showed best performance with **191** and **192**, although exhibiting high efficiency with **193** and **194**. In contrast, DddQ and DddK displayed lower efficiency.

The synthesized analogs of **7** were chiral, with a stereogenic center at the sulfur atom. DddW, identified as the best enzyme, was selected for preparative-scale reactions. HPLC analysis showed that the products from **191**, **193**, and **194** had low enantiomeric excesses (1% to 17%). However, the product obtained from **192** exhibited a slightly higher enantiomeric excess (25%), with $[\alpha]_D^{25}$ = –33.3 (*c* 0.04, EtOH) indicating (*R*)-methylpropyl sulfoxide (**196**) as the major enantiomer, consistent with literature values $[\alpha]_D^{25}$ = –139.0 (*c* 0.83, EtOH).[171] The product of **193** was mainly (*R*)-butylmethyl sulfoxide (**197**), while the major products form **191** and **194** were (*S*)-ethylmethyl sulfoxide (**195**) and (*S*)-isopropylmethyl sulfoxide (**198**), respectively.

Chapter 8

Summary and outlook

The research presented in this doctoral dissertation primarily focuses on the sulfur metabolism of *Roseobacter* group bacteria, culminating in six publications that include a wide range of topics within sulfur chemistry and bacterial biosynthesis. The studies provide significant insights into the intricate biochemical pathways and environmental roles of sulfur compounds in marine ecosystem.

One publication, titled “Identification of Volatiles from Six Marine *Celeribacter* Strains,” summarizes the volatile compounds, including sulfur volatiles, released by *Celeribacter* strains, and elucidates their biosynthesis pathways as outlined in Chapter 2.[172] Another publication, titled “Breakdown of 3-(allylsulfonio) propanoates in bacteria from the *Roseobacter* group yields garlic oil constituents” investigates the formation of sulfur volatiles similar to those found in garlic through the degradation of allyl-DMSP derivatives by *Roseobacter* bacteria, as detailed in chapter 3.[173] Two publications delve into the degradation of dimethylsulfoxonium propionate (DMSOP, **7**) and its analogs, partially investigating the stereoselectivity of DMSP lyases using chiral analogs of **7**, as presented in chapter 4 and 7.[6,116] This research raises further questions about the stereoselectivity of other DMSP lyases and how to enhance it. Additionally, one publication, titled “The Stereochemical Course of DmdC, an Enzyme Involved in the Degradation of Dimethylsulfoniopropionate” detailed the stereochemical course of DmdC, an enzyme important to the DMSP demethylation pathway as explained in chapter 6,[94] while another publication, titled “Functional characterisation of twelve terpene synthases from actinobacteria” summarize a phylogenetic analysis of terpene synthases from bacteria, leading to the discovery of three new bacterial enzymes: (+)-α-cadinene (**171**), (+)-δ-cadinol (**170**), and (−)-amorpha-4,11-diene (**172**) as discussed in chapter 5.[174] This finding significantly advances the understanding of biosynthesis of natural products.

A substantial portion of the work focuses on the activities of DMSP lyases and DMSP demethylation enzymes, which play crucial roles in the global sulfur cycle by catalyzing the cleavage of DMSP (**5**) into dimethyl sulfide (DMS, **6**) and methanethiol (MeSH, **11**). For instance, DmdC, an acyl-CoA dehydrogenase, that catalyzes the dehydrogenation step in the DMSP demethylation pathway, was first isolated from

Ruegeria pomeroyi DSS-3 in 2011.[82] However, its stereochemical course was unknown due to the lack of a crystal structure of DmdC with its substrate, MMPA-CoA. This dissertation addresses this gap by synthesizing four deuterium-labeled isotopomers of MMPA-SNAc (**182**), using them in enzyme reactions, and analyzing the products by GC-MS. The retention and abstraction of deuterium from the α and β carbon atoms of **182** by DmdC provided a clear overview of the stereochemical course of DmdC.

The study of DMSP lyase activity towards compounds **5**, **7**, and their analogs involves critical factors, including the characterization of DMSP lyases through various analytical techniques and enzyme reactions. The enzyme reaction products of DMSP lyases with DMSP and its analogs result in the formation of volatile compounds, which were captured using advanced techniques such as SPME (Solid Phase Microextraction) fiber[104] and CLSA (Closed Loop Stripping Analysis),[175] followed by GC-MS analysis. These methods offer a direct and efficient way to capture volatiles compared to traditional techniques involving incubation of bacterial cells with substrate in sealed vials followed by analysis of volatiles by gas chromatography. The enzyme reactions of DMSP lyases with **7** and its analogs resulted in water-soluble sulfoxides, which caused analytical challenges. This led to the development of a novel method using ^{13}C-labeled substrates for enzyme reactions, allowing the monitoring of products by ^{13}C NMR spectroscopy. The peak integration of the ^{13}C NMR spectrum, when compared with the unlabeled compound, indicates the quantitative formation of the desired products.

The challenges of using the isotope labeling technique lies in the multi-step synthesis of labeled compounds, which requires handling of highly volatile intermediates and results in high-cost starting materials. Moreover, there is a considerable risk of deuterium loss during the synthesis process.

Celeribacter bacteria, members of the *Rhodobacteraceae* family, have been extensively studied for their diverse metabolic activities. Notable examples include manganese oxidation by *Celeribacter manganoxidans*, which catalyzes the conversion of Mn^{2+} into MnO_2,[176] and polycyclic aromatic hydrocarbon degradation by *Celeribacter indicus*.[177] Additionally, these bacteria encode genes for DMSP lyases, although their role in DMSP cleavage has been poorly understood. As part of

this thesis, six *Celeribacter* strains were analyzed for their volatile compound production. This analysis led to the identification of various sulfur volatiles, with other volatile compounds. Isotope labeling feeding experiments provided critical insights into the biosynthetic pathways of these sulfur volatiles as explained in chapter 2. These findings reveal the metabolic versatility of *Celeribacter* bacteria and their potential role in sulfur cycling in the marine environment. Moreover, this work opens a new path for in-depth studies on the biosynthetic pathways involved in DMSP (**5**) and methionine (**4**) degradation in *Celeribacter* bacteria. The identification and characterization of these pathways are crucial for understanding the ecological role of these bacteria in the marine sulfur cycle. Furthermore, the potential cloning and functional analysis of new genes related to DMSP lyase or DMSP demethylase activities could provide valuable tools for biotechnological applications, such as bioconversion of sulfur compounds. In conclusion, this research enhances the understanding of the metabolic capabilities of *Celeribacter* bacteria and their ecological significance. It also lays the groundwork for future studies aimed at exploring and harnessing their unique biochemical pathways.

Additionally, a significant part of this dissertation focuses on the biosynthesis of sulfur volatiles similar of those found in garlic. For this investigation, two allyl-DMSP derivatives (**144**, **145**) were synthesized and fed to agar cultures of three bacteria belonging to the *Roseobacter* group. These feeding experiments resulted in the emission of a strong garlic-like odor, with the production of sulfur volatile compounds that were collected using the CLSA technique. Subsequent GC-MS analysis confirmed the presence of allyl sulfur volatiles that are known from garlic as introduced in chapter 3. This study emphasizes the capacity of DMSP lyases and DMSP demethylation enzymes in these bacteria to generate sulfur compounds similar to those observed in natural sources. This finding not only enriches the understanding of microbial sulfur metabolism but also highlights potential applications in the production of natural flavors. Thus, this work not only advances fundamental knowledge but also opens avenues for practical applications in environmental and industrial contexts.

In addition to exploring sulfur metabolism, this dissertation includes a significant investigation into terpene biosynthesis, where the first three bacterial enzymes capable of producing sesquiterpenes: (+)-α-cadinene (**171**), (+)-δ-cadinol (**170**), and (−)-amorpha-4,11-diene (**172**) were discovered as explained in chapter 5. The

structures of these novel compounds were elucidated using NMR spectroscopy. The rapid transformation of substrates into products within the active sites of terpene synthases presents challenges in monitoring hydride transfer and the formation of cationic species. To address this, enzyme reactions using ^{13}C and deuterium-labeled substrates were performed, and comparison of NMR spectra with unlabeled compounds facilitated the elucidation of the cyclization mechanisms and absolute configurations of these terpenes. These target ^{13}C and deuterium labeled substrates were obtained by multi steps synthesis. Additionally, to support the findings from isotope labeling experiments, Density Functional Theory (DFT) calculations could be used as an alternative method. DFT calculations are capable of estimating energy barriers for each reaction step, providing insights into the smoothness and feasibility of reaction pathways. This research significantly enhances the understanding of the production of valuable terpenoids and the potential for engineering novel terpene synthase. Moreover, the insights gained contribute to advancing natural product discovery and promoting sustainable chemical synthesis efforts.

The implications of these findings are extensive. The discovery of enzymes for DMSOP (**7**) cleavage and its role in the marine sulfur cycle highlights the complexity of marine sulfur metabolism and its influence on atmospheric chemistry. The ability of DMSP lyases to degrade **7** into **8** opens new pathway for understanding the enzymatic sulfur transformations in marine environments. Future research may be focus on elucidating the complete degradation pathways of DMSOP (**7**) analogs, and investigation of the enhancement of the stereoselectivity of DMSP lyases through enzyme engineering. Additionally, investigating the substrate tolerance of DMSOP (**7**) analogs, including selenium and tellurium substitutions, could uncover new biochemical pathways and enzymatic functions.

This research opens new directions in marine biochemistry, such as studying the ecological roles and chemical ecology of volatile compounds produced by *Celeribacter* strains. The discovery of new bacterial terpene synthases suggests many more undiscovered enzymes with unique functions.

In the long term, this research enhances the understanding of marine ecosystems and global sulfur cycles, with implications for climate science. The insights into sulfur metabolism in *Roseobacter* group bacteria could inform atmospheric chemistry and

climate regulation. Overall, this cumulative thesis advances knowledge of sulfur metabolism in marine bacteria, highlighting intricate biochemical pathways and their broader environmental significance. The findings open the way for future research, addressing remaining questions and exploring new frontiers in marine sulfur chemistry.

References

[1] P. Haas, *Biochem. J*. **1935**, *29*, 1297–1299.

[2] F. Challenger, M. I. Simpson, *J. Chem. Soc.* **1948***,* 1591–1597.

[3] F. C. Van Duyl, W. W. Gieskes, A. J. Kop, W. E. Lewis, *J*. *Sea Res*. **1998**, *40*, 221–231.

[4] G. O. Kirst, *Annu*. *Rev*. *Plant Physiol*. **1990**, *41*, 21–53.

[5] W. K. D. J. Sunda, D. J. Kieber, R. P. keines, S. Huntsman, *Nature* **2002**, *418*, 317–320.

[6] J. E. Lovelock, R. J. Maggs, R. A. Rasmussen, *Nature* **1972**, *237*, 452–453.

[7] S. Hatakeyama, M. Okuda, H. Akimoto, *Geophys*. *Res*. *Lett*. **1982**, *9*, 583–586.

[8] J. S. Dickschat, P. Rabe, C. A. Citron, *Org*. *Biomol*. *Chem*. **2015**, *13*, 1954–1968.

[9] D. K. Shaw, J. Sekar, P. V. Ramalingam, *Environ. Microbiol.* **2022**, *24*, 2669–2700.

[10] A. R. Curson, J. D. Todd, M. J. Sullivan, A. W. Johnston, *Nat*. *Rev*. *Microbiol*. **2011**, *9*, 849–859.

[11] R. P. Kiene, L. J. Linn, *Geochim*. *Cosmochim*. *Acta* **2000**, *64*, 2797–2810.

[12] S. F. Watts, *Atmos*. *Environ*. **2000**, *34*, 761–779.

[13] M. Chin, D. J. Jacob, *J. Geophys. Res.* **1996**, *101*, 18691–18699.

[14] J. Lovelock, (**2006**). *The Revenge of Gaia: Earth's Climate in Crisis and the Fate of Humanity*. New York: Basic Books.

[15] K. Thume, B. Gebser, L. Chen, N. Meyer, D. J. Kieber, G. Pohnert, *Nature* **2018**, *563*, 412–415.

[16] A. K. Chhalodia, J. S. Dickschat, *Org*. *Biomol*. *Chem*. **2023**, *21*, 3083–3089.

[17] M. A. Moran, C. R. Reisch, R. P. Kiene, W. B. Whitman, *Annu. Rev. Mar. Sci.* **2012**, *4*, 523–542.

[18] R. C. Greene, *J*. *Biol*. *Chem*. **1962**, *237*, 2251–2254.

[19] A. D. Hanson, J. Rivoal, L. Paquet, D. A. Gage, *Plant Physiol*. **1994**, *105*, 103–110.

[20] W. R. Barnard, M. O. Andreae, R. L. Iverson, *Cont*. *Shelf*. *Res*. **1984**, *3*, 103–113.

[21] A. Uchida, T. Ooguri, T. Ishida, Y. Ishida, *Nippon Suisan Gakkaishi* **1993**, *59*, 851–855.

[22] J. B. Raina, D. M. Tapiolas, S. Forêt, A. Lutz, D. Abrego, J. Ceh, F. O. Seneca, P. L. Clode, D. G. Bourne, B. L. Willis, C. A. Motti, *Nature* **2013**, *502*, 677–680.

[23] M. G. Kocsis, K. D. Nolte, D. Rhodes, T. L. Shen, D. A. Gage, A. D. Hanson, *Plant Physiol*. **1998**, *117*, 273–281.

[24] D. Rhodes, D. A. Gage, A. J. Cooper, A. D. Hanson, *Plant Physiol*. **1997**, *115*, 1541–1548.

[25] F. James, L. Paquet, S. A. Sparace, D. A. Gage, A. D. Hanson, *Plant Physiol*. **1995**, *108*, 1439–1448.

[26] F. James, K. D. Nolte, A. D. Hanson, *J*. *Biol*. *Chem*. **1995**, *270*, 22344–22350.

[27] A. R. J. Curson, J. Liu, A. Bermejo Martínez, R. T. Green, Y. Chan, O. Carrión, B. T. Williams, S. H. Zhang, G. P. Yang, P. C. Bulman Page, X. H. Zhang, *Nat*. *Microbiol*. **2017**, *2*, 1–9.

[28] C. Liao, F. P. Seebeck, *Angew*. *Chem*. **2019**, *131*, 3591–3594.

[29] D. A. Gage, D. Rhodes, K. D. Nolte, W. A. Hicks, T. Leustek, A. J. Cooper, A. D. Hanson, *Nature* **1997**, *387*, 891–894.

[30] P. S. Summers, K. D. Nolte, A. J. Cooper, H. Borgeas, T. Leustek, D. Rhodes, A. D. Hanson, *Plant Physiol*. **1998**, *116*, 369–378.

[31] M. D. Keller, R. P. Kiene, G. O. Kirst, P. T. Visscher, (**2012**). *Biological and environmental chemistry of DMSP and related sulfonium compounds*. Springer Science & Business Media.

[32] H. Kitaguchi, A. Uchida, Y. Ishida, *Fish. Sci. Res.* **1999**, *65*, 613–617.

[33] M. Steinke, G. Malin, S. D. Archer, P. H. Burkill, P. S. Liss, *Aquat*. *Microb*. *Ecol*. **2002**, *26*, 259–270.

[34] D. M. Yost, C. L. Mitchelmore, *Mar. Ecol. Prog. Ser.* **2009***, 386,* 61–70.

[35] D. J. Franklin, M. Steinke, J. Young, I. Probert, G. Malin, *Mar*. *Ecol*. *Prog*. *Ser*. **2010**, *410*, 13–23.

[36] G. V. Wolfe, M. Steinke, *Limnol. Oceanogr.* **1996***, 41,* 1151-1160.

[37] M. P. De Souza, D. C. Yoch, *Appl. Environ. Microbiol.* **1995**, *61*, 3986–3991.

[38] M. K. Nishiguchi, L. J. Goff, *J. Phycol.* **1995**, *31*, 567–574.

[39] J. W. Dacey, N. V. Blough, *Geophys. Res. Lett.* **1987**, *14*, 1246–1249.

[40] M. P. De Souza, D. C. Yoch, *Appl. Environ. Microbiol.* **1995**, *61*, 21–26.

[41] M. Steinke, G. Malin, S. M. Turner, P. S. Liss, *J. Sea Res.* **2000**, *43*, 233–244.

[42] A. R. J. Curson, M. J. Sullivan, J. D. Todd, A. W. B. Johnston, *ISME J*. **2010**, *4*, 144–146.

[43] C. R. Reisch, W. M. Crabb, S. M. Gifford, Q. Teng, M. J. Stoudemayer, M. A. Moran, W. B. Whitman, *Mol. Microbiol.* **2013**, *89*, 774–791.

[44] N. M. Levine, V. A. Varaljay, D. A. Toole, J. W. Dacey, S. C. Doney, M. A. Moran, *Environ*. *Microbiol*. **2012**, *14*, 1210–1223.

[45] J. D. Todd, R. Rogers, Y. G. Li, M. Wexler, P. L. Bond, L. Sun, A. R. J. Curson, G. Malin, M. Steinke, A. W. B. Johnston, *Science* **2007**, *315*, 666–669.

[46] A. R. J. Curson, R. Rogers, J. D. Todd, C. A. Brearley, A. W. B. Johnston, *Environ*. *Microbiol*. **2008**, 10, 757–767.

[47] J. D. Todd, A. R. J. Curson, C. L. Dupont, P. Nicholson, A. W. B. Johnston, *Environ*. *Microbiol*. **2009**, *11*, 1376–1385.

[48] J. D. Todd, A. R. J. Curson, M. Kirkwood, M. J. Sullivan, R. T. Green, A. W. B. Johnston, *Environ*. *Microbiol*. **2011**, *13*, 427–438.

[49] A. R. J. Curson, M. J. Sullivan, J. D. Todd, A. W. B. Johnston, *ISME J*. **2011**, *5*, 1191–1200.

[50] J. D. Todd, M. Kirkwood, S. Newton-Payne, A. W. B. Johnston, *ISME J*. **2012**, *6*, 223–226.

[51] J. Sun, J. D. Todd, J. C. Thrash, Y. Qian, M. C. Qian, B. Temperton, J. Guo, E. K. Fowler, J. T. Aldrich, C. D. Nicora, M. S. Lipton, R. D. Smith, P. de Leenheer, S. H. Payne, A. W. B. Johnston, C. L. Davie-Martin, K. H. Halsey, S. J. Giovannoni, *Nat. Microbiol.* **2016**, *1*, 1–5.

[52] C. Y. Li, X. J. Wang, X. L. Chen, Q. Sheng, S. Zhang, P. Wang, M. Quareshy, B. Rihtman, X. Shao, C. Gao, F. Li, *Elife* **2021**, *10*, e64045.

[53] S. Y. Wang, N. Zhang, Z. J. Teng, X. D. Wang, J. D. Todd, Y. Z. Zhang, H. Y. Cao, C. Y. Li, *Environ*. *Microbiol*. **2023**, *25*, 1238–1249.

[54] U. Alcolombri, S. Ben-Dor, E. Feldmesser, Y. Levin, D. S. Tawfik, A. Vardi, *Science* **2015**, *348*, 1466–1469.

[55] J. H. Ansede, R. Friedman, D. C. Yoch, *Appl*. *Environ*. *Microbiol*. **2001**, *67*, 1210–1217.

[56] J. B. Raina, D. Tapiolas, B. L. Willis, D. G. Bourne, *Appl*. *Environ*. *Microbiol*. **2009**, *75*, 3492–3501.

[57] J. D. Todd, A. R. J. Curson, N. Nikolaidou-Katsaraidou, C. A. Brearley, N. J. Watmough, Y. Chan, P. C. Page, L. Sun, A. W. Johnston, *Environ*. *Microbiol*. **2010**, *12*, 327–343.

[58] J. B. Raina, D. Tapiolas, C. A. Motti, S. Foret, T. Seemann, J. Tebben, B. L. Willis, D. G. Bourne, *Peer* J. **2016**, *4*, e2275.

[59] T. Elssner, C. Engemann, K. Baumgart, H. P. Kleber, *Biochem*. **2001**, *40*, 11140–11148.

[60] U. Alcolombri, P. Laurino, P. Lara-Astiaso, A. Vardi, D. S. Tawfik, *Biochem*. **2014**, *53*, 5473−5475.

[61] Y. J. Chiou, Y. F. Chan, S. P. Yu, C. Y. Lu, S. S. Y. Hsiao, P. W. Chiang, T. C. Hsu, P. Y. Liu, N. Wada, Y. Lee, W. N. Jane, *Sci*. *Adv*. **2023**, *9*, eadk1910.

[62] J. M. Gonzalez, J. S. Covert, W. B. Whitman, J. R. Henriksen, F. Mayer, B. Scharf, R. Schmitt, A. Buchan, J. A. Fuhrman, R. P. Kiene, M. A. Moran, *Int. J. Syst. Environ. Microbiol.* **2003**, *53*, 1261–1269.

[63] P. Wang, X. L. Chen, C. Y. Li, X. Gao, D. Y. Zhu, B. B. Xie, Q. L. Qin, X. Y. Zhang, H. N. Su, B. C. Zhou, L. Y. Xun, *Mol*. *Microbiol*. **2015**, *98*, 289–301.

[64] J. H. Hehemann, A. Law, L. Redecke, A. B. Boraston, *PLoS One* **2014**, *9*, e103128.

[65] C. Y. Li, T. D. Wei, S. H. Zhang, X. L. Chen, X. Gao, P. Wang, B. B. Xie, H. N. Su, Q. L. Qin, X. Y. Zhang, J. Yu, *Proc*. *Natl*. *Acad*. *Sci*. USA **2014**, *111*, 1026–1031.

[66] B. Holmquist, B. L. Vallee, *J*. *Biol*. *Chem*. **1974**, *249*, 4601–4607.

[67] K. S. Larsen, D. S. Auld, *Biochem*. **1989**, *28*, 9620–9625.

[68] D. R. Holland, A. C. Hausrath, D. Juers, B. W. Matthews, *Protein Sci*. **1995**, *4*, 1955–1965.

[69] M. Gomez-Ortiz, F. X. Gomis-Rüth, R. Huber, F. X. Avilés, *FEBS Lett*. **1997**, *400*, 336–340.

[70] A. E. Brummett, M. Dey, *Biochem*. **2016**, *55*, 6162–6174.

[71] A. E. Brummett, N. J. Schnicker, A. Crider, J. D. Todd, M. Dey, *PloS one* **2015**, *10*, e0127288.

[72] J. M. Dunwell, A. Culham, C. E. Carter, C. R. Sosa-Aguirre, P. W. Goodenough, *Trends Biochem*. *Sci*. **2001**, *26*, 740–746.

[73] M. Peng, M., X. L. Chen, D. Zhang, X. J. Wang, N. Wang, P. Wang, J. D. Todd, Y. Z. Zhang, C. Y. Li, *Environ. Microbiol.* **2019**, *85*, e03127–18.

[74] N. J. Schnicker, S. M. De Silva, J. D. Todd, M. Dey, *Biochem.* **2017**, *56*, 2873–2885.

[75] C. Y. Li, D. Zhang, X. L. Chen, P. Wang, W. L. Shi, P. Y. Li, X. Y. Zhang, Q. L. Qin, J. D. Todd, Y. Z. Zhang, *J. Mol. Biol.* **2017**, *429*, 3850–3862.

[76] J. Jumper, R. Evans, A. Pritzel, T. Green, M. Figurnov, O. Ronneberger, K. Tunyasuvunakool, R. Bates, A. Žídek, A. Potapenko, A. Bridgland, *Nature* **2021**, *596*, 583–589.

[77] J. M. González, R. P. Keine, M. A. Moran, *Environ. Microbiol.* **1999**, *65*, 3810–3819.

[78] P. T. Visscher, M. R. Diaz, B. F. Taylor, *Mar. Ecol. Prog. Ser.* **1992**, *89*, 293–296.

[79] E. C. Howard, J. R. Henriksen, A. Buchan, C. R. Reisch, H. Bürgmann, R. Welsh, W. Ye, J. M. González, K. Mace, S. B. Joye, R. P. Kiene, *Science* **2006**, *314*, 649–652.

[80] D. J. Schuller, C. R. Reisch, M. A. Moran, W. B. Whitman, W. N. Lanzilotta, *Protein Sci.* **2012**, *21*, 289–298.

[81] E. C. Howard, S. Sun, E. J. Biers, M. A. Moran, *Environ*. *Microbiol*. **2008**, *10*, 2397–2410.

[82] C. R. Reisch, M. J. Stoudemayer, V. A. Varaljay, I. J. Amster, M. A. Moran, W. B. Whitman, *Nature* **2011**, *473*, 208–211.

[83] C. R. Reisch, M. A. Moran, W. B. Whitman, *J*. *Bacteriol* **2008**, *190*, 8018–8024.

[84] C. R. Reisch, M. A. Moran, W. B. Whitman, *Front*. *Microbiol*. **2011**, *2*, 172.

[85] R. P. Kiene, *Mar. Chem.* **1996**, *54*, 69–83.

[86] X. Zhang, L. Zhou, X. Cheng, *EMBO J.* **2000**, *19*, 3509–3519.

[87] Y. Huang, J. Komoto, K. Konishi, Y. Takata, H. Ogawa, T. Gomi, M. Fujioka, F. Takusagawa, *J*. *Mol*. *Biol*. **2000**, *298*, 149–162.

[88] J. L. Martin, J. Begun, M. J. McLeish, J. M. Caine, G. L. Grunewald, *Structure* **2001**, *9*, 977–985.

[89] X. Shao, H. Y. Cao, F. Zhao, M. Peng, P. Wang, C. Y. Li, W. L. Shi, T. D. Wei, Z. Yuan, X. H. Zhang, X. L. Chen, *Mol. Microbiol.* **2019**, *111*, 1057–1073.

[90] E. Conti, N. P. Franks, P. Brick, *Structure* **1996**, *4*, 287–298.

[91] J. J. May, N. Kessler, M. A. Marahiel, M. T. Stubbs, *Proc. Natl. Acad. Sci. U. S. A.* **2002**, *99*, 12120–12125.

[92] A. M. Gulick, V. J. Starai, A. R. Horswill, K. M. Homick, J. C. Escalante-Semerena, *Biochem.* **2003**, *42*, 2866–2873.

[93] G. Kochan, E. S. Pilka, F. von Delft, U. Oppermann, W. W. Yue, *J. Mol. Biol.* **2009**, *388*, 997–1008.

[94] A. K. Chhalodia, J. S. Dickschat, *ChemBioChem* **2024**, e202300795.

[95] B. Pohl, T. Raichle, S. Ghisla, *Eur. J. Biochem.* **1986**, *160*, 109–115.

[96] J. J. Kim, M. Wang, R. Paschke, *Proc*. *Natl*. *Acad*. *Sci*. *U. S. A.* **1993**, *90*, 7523–7527.

[97] H. Tamaoki, Y. Nishina, K. Shiga, R. Miura, *J. Biochem.* **1999**, *126*, 285–296.

[98] D. Tan, W. M. Crabb, W. B. Whitman, L. Tong, *PloS one* **2013**, *8*, e63870.

[99] S. J. Giovannoni, U. Stingl, *Nature* **2005**, *437*, 343–348.

[100] J. S. Dickschat, C. Zell, N. L. Brock, *ChemBioChem* **2010**, *11*, 417–425.

[101] N. L. Brock, C. A. Citron, C. Zell, M. Berger, I. Wagner-Döbler, J. Petersen, T. Brinkhoff, M. Simon, J. S. Dickschat, *Beilstein J. Org. Chem.* **2013**, *9*, 942–950.

[102] A. K. Chhalodia, J. S. Dickschat, *Beilstein J. Org. Chem*. **2021**, *17*, 569–580.

[103] N. L. Brock, M. Menke, T. A. Klapschinski, J. S. Dickschat, *Org. Biomol. Chem.* **2014**, *12*, 4318–4323.

[104] I. Burkhardt, L. Lauterbach, N. L. Brock, J. S. Dickschat, *Org. Biomol. Chem.* **2017**, *15*, 4432–4439.

[105] L. Lei, K. P. Cherukuri, U. Alcolombri, D. Meltzer, D. S. Tawfik, *Biochem.* **2018**, *57*, 3364−3377.

[106] A. K. Chhalodia, J. S. Dickschat, *Eur*. *J*. *Org*. *Chem*. **2024**, e202400098.

[107] J. M. González, M. A. Moran, *Appl. Environ. Microbiol.* **1997**, *63*, 4237–4242.

[108] N. Selje, M. Simon, T. Brinkhoff, *Nature* **2004**, *427*, 445–448.

[108] E. Celik, M. Maczka, N. Bergen, T. Brinkhoff, S. Schulz, J. S. Dickschat, *Org. Biomol. Chem.* **2017**, *15*, 2919–2922.

[109] B. P. Durham, S. Sharma, H. Luo, C. B. Smith, S. A. Amin, S. J. Bender, S. P. Dearth, B. A. Van Mooy, S. R. Campagna, E. B. Kujawinski, E. V. Armbrust, *Proc. Natl. Acad. Sci. U. S. A.* **2015**, *112*, 453–457.

[110] M. Berger, N. L. Brock, H. Liesegang, M. Dogs, I. Preuth, M. Simon, J. S. Dickschat, T. Brinkhoff, *Appl. Environ. Microbiol.* **2012**, *78*, 3539–3551.

[111] N. L. Brock, A. Nikolay, J. S. Dickschat, *Chem. Commun.* **2014**, *50*, 5487–5489.

[112] D. Ueda, S. Matsugane, W. Okamoto, M. Hashimoto, T. Sato, *Angew. Chem. Int. Ed.* **2018**, *57*, 10347–10351.

[113] J. S. Dickschat, S. S. Wickel, C. J. Bolten, T. Nawrath, S. Schulz, C. Wittmann, *Eur. J. Org. Chem.* **2010**, 2687–2695.

[114] F. W. Semmler, *Arch. Pharm.* **1892***, 230*, 434–443.

[115] A. Stoll, E. Seebeck, *Helv. Chim. Acta* **1949**, *32*, 197–205.

[116] E. Block, S. Ahmad, M. K. Jain, R. W. Crecely, R. Apitz-Castro, M.R. Cruz, *J. Am. Chem. Soc.* **1984**, *106*, 8295–8296.

[117] E. Block, *Angew. Chem. Int. Ed.* **1992**, *31*, 1135–1178.

[118] J. S. Dickschat, *Nat. Prod. Rep.* **2017**, *34*, 310–328.

[119] S. Schulz, J. S. Dickschat, *Nat. Prod. Rep.* **2007**, *24*, 814–842.

[120] J. S. Dickschat, I. Wagner-Döbler, S. Schulz, *Chem. Ecol.* **2005**, *31*, 925–947.

[121] J. S. Dickschat, H. Reichenbach, I. Wagner-Döbler, S. Schulz, *Eur. J. Org. Chem.* **2005**, 4141–4153.

[122] V. Thiel, T. Brinkhoff, J. S. Dickschat, S. Wickel, J. Grunenberg, I. Wagner-Döbler, M. Simon, S. Schulz, *Org. Biomol. Chem.* **2010**, *8*, 234–246.

[123] D. A. del Valle, D. J. Kieber, R. P. Kiene, *Mar. Chem.* **2007**, *103*, 197–208.

[124] A. D. Hatton, D. H. Shenoy, M. C. Hart, A. Mogg, D. H. Green, *Biogeochemistry* **2012***, 110,* 131–146.

[125] E. C. Asher, J. W. H. Dacey, M. Stukel, M. C. Long, P. D. Tortell, *Limnol. Oceanogr.* **2017**, *62*, 104–124.

[126] M. Peng, X. L. Chen, D. Zhang, X. J. Wang, N. Wang, P. Wang, J. D. Todd, Y. Z. Zhang, C. Y. Li, *Appl. Environ. Microbiol.* **2019**, *85*, e03127–18.

[127] C. Y. Li, D. Zhang, X. L. Chen, P. Wang, W. L. Shi, P. Y. Li, X. Y. Zhang, Q. L. Qin, J. D. Todd, Y. Z. Zhang, *J. Mol. Biol.* **2017**, *429*, 3850–3862.

[128] P. J. Facchini, J. Chappell, *Proc. Natl. Acad. Sci. U. S. A.* **1992**, *89*, 11088–11092.

[129] C. J. Mau, C. A. West, *Proc. Natl. Acad. Sci. U. S. A.* **1994**, *91*, 8497–8501.

[130] D. E. Cane, P. C. PrabhakaranE. J. Salaski, P. H. Harrison, H. Noguchi, B. J. Rawlings, *J. Am. Chem. Soc.* **1989**, *111*, 8914–8916.

[131] R. H. Proctor, T. M. Hohn, *J. Biol. Chem.* **1993**, *268*, 4543–4548.

[132] T. Toyomasu, M. Tsukahara, A. Kaneko, R. Niida, W. Mitsuhashi, T. Dairi, N. Kato, T. Sassa, *Proc. Natl. Acad. Sci. U. S. A.* **2007**, *104*, 3084–3088.

[133] H. Tao, L. Lauterbach, G. Bian, R. Chen, A. Hou, T. Mori, S. Cheng, B. Hu, L. Lu, X. Mu, M. Li, *Nature* **2022**, *606*, 414–419.

[134] D. E. Cane, J. K. Sohng, C. R. Lamberson, S. M. Rudnicki, Z. Wu, M. D. Lloyd, J. S. Oliver, B. R. Hubbard, *Biochemistry* **1994**, *33*, 5846–5857.

[135] J. Jiang, X. He, D. E. Cane, *Nat. Chem. Biol.* **2007**, *3*, 711–715.

[136] C. M. Wang, D. E. Cane, *J. Am. Chem. Soc.* **2008**, *130*, 8908–8909.

[137] A. Hou, J. S. Dickschat, *Angew. Chem. Int. Ed.* **2020**, *59*, 19961–19965.

[138] B. Gu, B. Goldfuss, J. S. Dickschat, *Angew. Chem. Int. Ed.* **2023**, *62*, e202215688.

[139] H. Xu, G. Schnakenburg, B. Goldfuss, J. S. Dickschat, *Angew. Chem. Int. Ed.* **2023**, *62*, e202306429.

[140] X. Lin, R. Hopson, D. E. Cane, *J. Am. Chem. Soc.* **2006**, *128*, 6022–6023.

[141] P. Rabe, J. S. Dickschat, *Angew. Chem., Int. Ed.* **2013**, *52*, 1810–1812.

[142] P. Rabe, T. Schmitz, J. S. Dickschat, *Beilstein J. Org. Chem.* **2016**, *12*, 1839–1850.

[143] H. Xu, N. D. Lackus, T. G. Köllner, J. S. Dickschat, *Org. Lett.* **2022**, *24*, 587–591.

[144] J. Rinkel, J. S. Dickschat, *Org. Lett.* **2019**, *21*, 2426–2429.

[145] L. Lauterbach, J. Rinkel, J. S. Dickschat, *Angew. Chem. Int. Ed.* **2018**, *57*, 8280–8283.

[146] D. K. Ro, E. M. Paradise, M. Ouellet, K. J. Fisher, K. L. Newman, J. M. Ndungu, K. A. Ho, R. A. Eachus, T. S. Ham, J. Kirby, M. C. Chang, *Nature* **2006**, *440*, 940–943.

[147] T. Sakai, K. Nishimura, H. Chikamatsu, Y. Hirose, *Bull. Chem. Soc. Jpn.* **1963**, *36*, 1261–1264.

[148] G. W. Van Eijk, H. J. Roeijmans, P. E. J. Verwiel, *Exp. Mycol.* **1984**, *8*, 273–275.

[149] J. Rinkel, J. S. Dickschat, *Org. Lett.* **2019**, *21*, 2426–2429.

[150] Y. Naya, M. Kotake, *Bull. Chem. Soc. Jpn.* **1969**, *42*, 1468.

[151] J. Rinkel, L. Lauterbach, P. Rabe, J. S. Dickschat, *Angew. Chem. Int. Ed.* **2018**, *57*, 3238–3241.

[152] P. Mercke, M. Bengtsson, H. J. Bouwmeester, M. A. Posthumus, P. E. Brodelius, *Arch. Biochem. Biophys.* **2000**, *381*, 173–180.

[153] X. Lin, R. Hopson, D. E. Cane, *J. Am. Chem. Soc.* **2006**, *128*, 6022–6023.

[154] P. Rabe, J. S. Dickschat, *Angew. Chem. Int. Ed.* **2013**, *52*, 1810–1812.

[155] R. P. Kiene, L. J. Linn, J. González, M. A. Moran, J. A. Bruton, *Appl. Environ. Microbiol*. **1999**, *65*, 4549–4558.

[156] S. Ghisla, C. Thorpe, *Eur. J. Biochem.* **2004**, *271*, 494–508.

[157] K. L. Peterson, E. E. Sergienko, Y. Wu, N. R. Kumar, A. W. Strauss, A. E. Oleson, W. W. Muhonen, J. B. Shabb, D. K. Srivastava, *Biochemistry* **1995**, *34*, 14942–14953.

[158] D. K. Ma, Z. Li, A. Y. Lu, F. Sun, S. Chen, M. Rothe, R. Menzel, F. Sun, H. R. Horvitz, *Cell* **2015**, *161*, 1152–1163.

[159] Z. Yin, E. Liebhart, E. Stegmann, H. Brötz-Oesterhelt, J. S. Dickschat, *Org. Chem. Front.* **2022**, *9*, 2714–2720.

[160] J. F. Biellmann, C. G. Hirth, *FEBS Lett.* **1970**, *8*, 55–56.

[161] J. F. Biellmann, C. G. Hirth, *FEBS Lett.* **1970**, *9*, 335–336.

[162] H.-J. la Roche, M. Kellner, H. Günther, H. Simon, Hoppe-Seyler's *Z. Physiol. Chem.* **1971**, *352*, 399–402.

[163] A. Kawaguchi, S. Tsubotani, Y. Seyama, T. Yamakawa, T. Osumi, T. Hashimoto, T. Kikuchi, M. Ando, S. Okuda, *J. Biochem.* **1980**, *88*, 1481–1486.

[164] I. Barnes, J. Hjorth, N. Mihalopoulos, *Chem. Rev.* **2006**, *106*, 940–975.

[165] I. Faloona, S. A. Conley, B. Blomquist, A. D. Clarke, V. Kapustin, S. Howell, D. H. Lenschow, A. R. Bandy, *J. Atmos. Chem.* **2009**, *63*, 13–32.

[166] R. Von Glasow, P. J. Crutzen, *Atmos. Chem. Phys.* **2004**, *4*, 589–608.

[167] C. Zindler, A. Bracher, C. A. Marandino, B. Taylor, E. Torrecilla, A. Kock, H. W. Bange, *Biogeosciences* **2013**, *10*, 3297–3311.

[168] F. Althoff, K. Benzing, P. Comba, C. McRoberts, D. R. Boyd, S. Greiner, F. Keppler, *Nat. Commun.* **2014**, *5*, 4205.

[169] P. A. Lee, S. J. De Mora, M. Levasseur, *Atmos. ocean* **1999**, *37*, 439–456.

[170] P. A. Lee, S. J. De Mora, *J. Phycol.* **1999**, *35*, 8–18.

[171] K. K. Andersen, B. Bujnicki, J. Drabowicz, M. Mikolajczyk, J. B. O' Brien, *J. Org. Chem.* **1984**, *49*, 4070–4072.

[172] A. K. Chhalodia, J. Rinkel, D. Konvalinkova, J. Petersen, J. S. Dickschat, *Beilstein J. Org. Chem.* **2021**, *17*, 420–430.

[173] A. K. Chhalodia, J. S. Dickschat, *Beilstein J. Org. Chem.* **2021**, *17*, 569–580.

[174] A. K. Chhalodia, H. Xu, G. B. Tabekoueng, B. Gu, K. A. Taizoumbe, L. Lauterbach, J. S. Dickschat, *Beilstein J. Org. Chem.* **2023**, *19*, 1386–1398.

[175] K. Grob, F. J. Zürcher, *Chromatogr.* **1976**, *117*, 285–294.

[176] L. Wang, Y. Liu, Y. Wang, X. Dai, X. H. Zhang, *Int. J. Syst. Evol. Microbiol.* **2015**, *65*, 4180–4185.

[177] Q. Lai, J. Cao, J. Yuan, F. Li, Z. Shao, *Int. J. Syst. Evol. Microbiol.* **2014**, *64* 4160–4167.

Appendices A–F

Appendix A

Identification of volatiles from six marine Celeribacter strains

Beilstein J. Org. Chem. **2021**, *17*, 420–430

DOI: 10.3762/bjoc.17.38

BEILSTEIN JOURNAL OF ORGANIC CHEMISTRY

Identification of volatiles from six marine *Celeribacter* strains

Anuj Kumar Chhalodia[1], Jan Rinkel[1], Dorota Konvalinkova[1], Jörn Petersen[2] and Jeroen S. Dickschat[*1]

Full Research Paper

Open Access

Address:
[1]Kekulé Institute of Organic Chemistry and Biochemistry, University of Bonn, Gerhard-Domagk-Straße 1, 53121 Bonn, Germany and [2]Leibniz-Institut DSMZ - Deutsche Sammlung von Mikroorganismen und Zellkulturen GmbH, Inhoffenstraße 7b, 38124 Braunschweig, Germany

Email:
Jeroen S. Dickschat* - dickschat@uni-bonn.de

* Corresponding author

Keywords:
GC–MS; isotopes; *Roseobacter*; sulfur metabolism; volatiles

Beilstein J. Org. Chem. **2021,** *17,* 420–430.
https://doi.org/10.3762/bjoc.17.38

Received: 07 December 2020
Accepted: 02 February 2021
Published: 11 February 2021

This article is part of the thematic issue "Chemical ecology".

Guest Editor: C. Beemelmanns

Abstract

The volatiles emitted from six marine *Rhodobacteraceae* species of the genus *Celeribacter* were investigated by GC–MS. Besides several known compounds including dimethyl trisulfide and *S*-methyl methanethiosulfonate, the sulfur-containing compounds ethyl (*E*)-3-(methylsulfanyl)acrylate and 2-(methyldisulfanyl)benzothiazole were identified and their structures were verified by synthesis. Feeding experiments with [*methyl*-$^{2}H_3$]methionine, [*methyl*-^{13}C]methionine and [^{34}S]-3-(dimethylsulfonio)propanoate (DMSP) resulted in the high incorporation into dimethyl trisulfide and *S*-methyl methanethiosulfonate, and revealed the origin of the methylsulfanyl group of 2-(methyldisulfanyl)benzothiazole from methionine or DMSP, while the biosynthetic origin of the benzothiazol-2-ylsulfanyl portion could not be traced. The heterocyclic moiety of this compound is likely of anthropogenic origin, because 2-mercaptobenzothiazole is used in the sulfur vulcanization of rubber. Also in none of the feeding experiments incorporation into ethyl (*E*)-3-(methylsulfanyl)acrylate could be observed, questioning its bacterial origin. Our results demonstrate that the *Celeribacter* strains are capable of methionine and DMSP degradation to widespread sulfur volatiles, but the analysis of trace compounds in natural samples must be taken with care.

Introduction

Bacteria from the roseobacter group belong to the most abundant microbial species in marine ecosystems [1,2]. They are present from polar to tropical regions, in marine sediments, in estuarine and open ocean environments in different pelagic zones ranging from surface waters to depths of >2,000 m [3,4]. Some species are associated with other marine organisms, e.g., *Thalassococcus halodurans* DSM 26915^{T} has been isolated from the marine sponge *Halichondria panicea* [5], and *Phaeobacter gallaeciensis* DSM 26640^{T} is an isolate from the scallop *Pecten maximus* [6]. Important interactions are also observed between bacteria from the roseobacter group and various types of marine algae, e.g., the first described organisms

Roseobacter litoralis DSM 6996^T and *R. denitrificans* DSM 7001^T were obtained from seaweed [7], while *Dinoroseobacter shibae* DSM 16493^T and *Marinovum algicola* DSM 10251^T are both isolates from the dinoflagellate *Prorocentrum lima* [8,9]. Especially in algal blooms bacteria of the roseobacter group are highly abundant [10], and here they belong to the main players involved in the enzymatic degradation of the algal sulfur metabolite 3-(dimethylsulfonio)propanoate (DMSP, Scheme 1) [11]. Its catabolism leads either through the demethylation pathway by action of the enzymes DmdABCD to methanethiol (MeSH, Scheme 1A) [12] or through lysis by DddD [13] or hydrolytic cleavage by one of the known DMSP lyases (DddW [14], DddP [15], DddQ [16], DddL [17], DddY [18] or DddK [19]) to dimethyl sulfide (DMS, Scheme 1B).

It has already been pointed out in the 1970s and 1980s that atmospheric DMS is important for the global sulfur cycle [20] and influences the climate on Earth, known as CLAW hypothesis according to the authors' initials (Carlson, Lovelock, Andreae, Warren) [21], which underpins the relevance of this algal–bacterial interaction. Isotopic labeling experiments demonstrated that also in laboratory cultures roseobacter group bacteria efficiently degrade DMSP into sulfur volatiles [22,23], but also from other sulfur sources including 2,3-dihydroxypropane-1-sulfonic acid (DHPS, Scheme 1C) labeling was efficiently incorporated into sulfur volatiles [24,25]. Notably, DHPS is produced in large quantities by the marine diatom *Thalassiosira pseudonana* [26], and diatoms from this genus live in symbiotic relationship with bacteria of the roseobacter group [27]. Another interesting aspect of sulfur metabolism in marine bacteria from the roseobacter group is the production of the sulfur-containing antibiotic tropodithietic acid (TDA) in *Phaeobacter piscinae* DSM 103509^T [28], a compound that is in equilibrium with its tautomer thiotropocin [29] that was first described from *Pseudomonas* sp. CB-104 [30]. Its biosynthesis depends on the clustered *tda* genes [31] and has been studied by

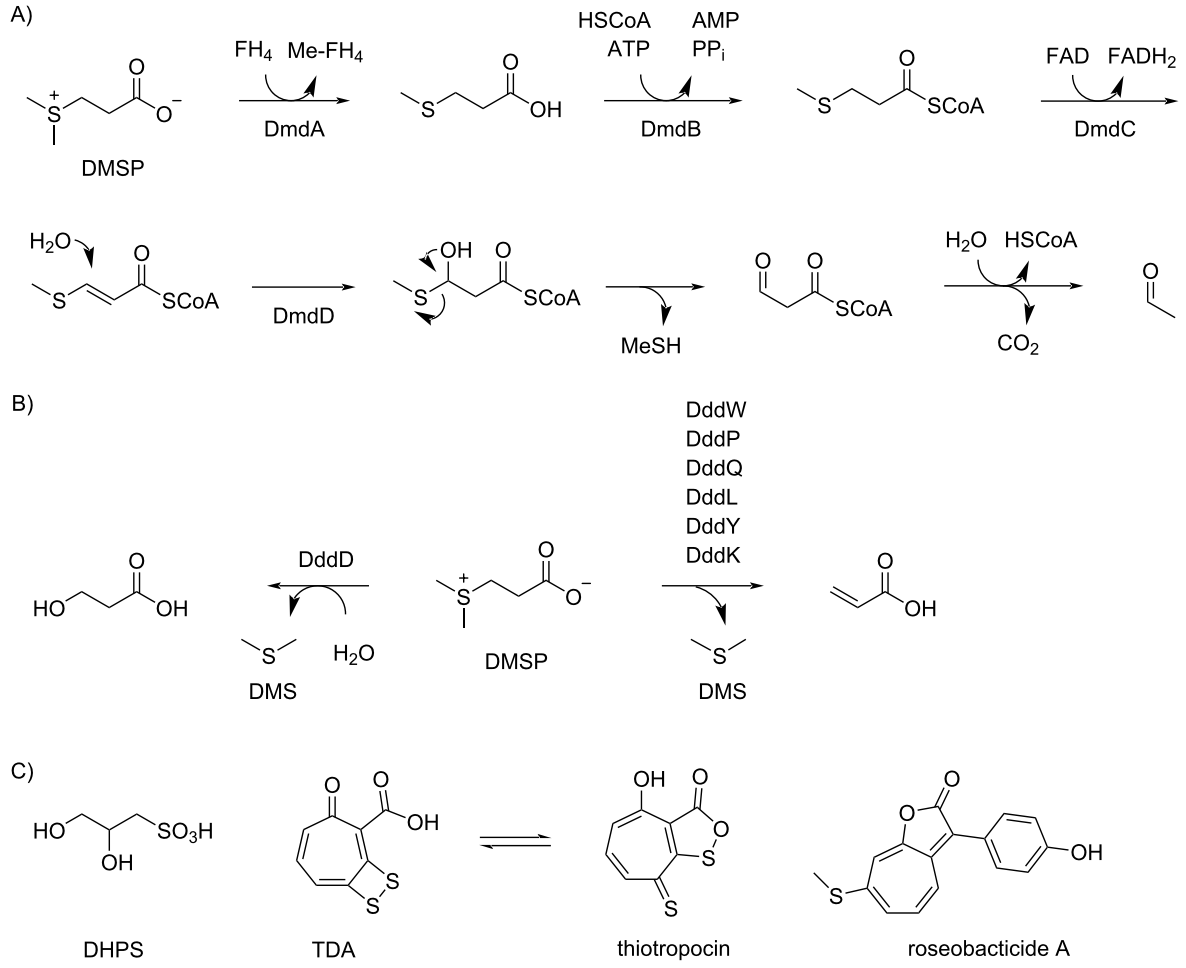

Scheme 1: Sulfur metabolism in bacteria from the roseobacter group. A) DMSP demethylation by DmdABCD, B) DMSP hydrolysis by DddP and lysis by DddW, DddP, DddQ, DddL, DddY or DddK, and C) structures of DHPS and sulfur-containing secondary metabolites.

feeding experiments with labeled precursors to the wildtype and gene knockout strains of *P. inhibens* DSM 17395^T, demonstrating the formation of TDA from phenylalanine through phenylacetyl-CoA and the phenylacetyl-CoA catabolon [32,33]. These experiments also led to a suggestion for the mechanism for sulfur incorporation, but further research is required for a deep understanding of TDA biosynthesis. Besides its function as an antibiotic, TDA acts as a signaling molecule, similar to *N*-acylhomoserine lactones, at concentrations 100 times lower than required for a significant antibiotic activity [34]. The biosynthesis of tropone [35] and of the algicidal sulfur-containing roseobacticides [36] are most likely connected to the TDA pathway. Interestingly, in the interaction with marine algae *P. inhibens* can change its lifestyle from a symbiotic relationship during which the antibiotic TDA and growth stimulants are produced to a pathogenic interaction promoted by lignin degradation products in fading algal blooms that induce roseobacticide biosynthesis [36]. All these examples demonstrate the importance of sulfur metabolism for marine bacteria from the roseobacter group. Here we report on the volatiles emitted by six *Celeribacter* species with a special focus on sulfur volatiles. The results from feeding studies with labeled precursors demonstrate that the *Celeribacter* strains can form sulfur volatiles from methionine and DMSP, but also showed that some of the detected sulfur compounds are not or only partly of bacterial origin.

Results and Discussion

Headspace analysis

The volatiles released by six marine *Celeribacter* type strains, including *C. marinus* DSM 100036^T, *C. neptunius* DSM 26471^T, *C. manganoxidans* DSM 27541^T, *C. baekdonensis* DSM 27375^T, *C. halophilus* DSM 26270^T and *C. indicus* DSM 27257^T, were collected through a closed-loop stripping apparatus (CLSA) on charcoal [37]. After extraction with dichloromethane the obtained extracts were analyzed by GC–MS (Figure 1). The compounds were identified by the comparison of the recorded EI mass spectra to library spectra and of retention indices [38] to tabulated literature data (Table 1), or by a direct comparison to authentic standards. The structures of the identified compounds are shown in Figure 2.

While the headspace extracts from *C. marinus*, *C. neptunius* and *C. manganoxidans* were particularly rich, the extracts from *C. baekdonensis*, *C. halophilus* and *C. indicus* contained fewer compounds. Most of the observed volatiles are well known [56,57] and were thus readily identified from their mass spectra and retention indices. Pyrazines including methylpyrazine (**1**), 2,5-dimethylpyrazine (**2**) and trimethylpyrazine (**3**) were present in the extracts from all six strains. Notably, also several α-hydroxyketones that have been described as biosynthetic precursors to pyrazines [40], represented by 3-hydroxypentan-2-one (**4**), 2-hydroxypentan-3-one (**5**) and 2-hydroxyhexan-3-one (**6**), were observed in some of the investigated strains. A series of aldehydes ranging from hexanal (**7**) to tetradecanal (**13**) was found in strain specific patterns, with all identified compounds present in the bouquet from *C. manganoxidans*. A similar series of γ-lactones spanning from pentan-4-olide (**14**) to dodecan-4-olide (**20**), in addition to 3-methylbutan-4-olide (**21**) and 4-methylhex-5-en-4-olide (**22**), was detected in strain-specific patterns, with almost all of these compounds present in *C. marinus*; only *C. halophilus* did not emit lactones. Furans included furan-2-ylmethanol (**23**), furfural (**24**), and 2-acetylfuran (**25**). Cyclohexanol (**26**) was observed only once in *C. marinus*, and aromatic compounds included benzyl alcohol (**27**), benzaldehyde (**28**) and salicylaldehyde (**29**), acetophenone (**30**) and *o*-aminoacetophenone (**31**), 2-phenylethanol (**32**), and phenylacetone (**33**). 6-Methylhept-5-en-2-one (**34**) was detected in all strains, while its saturated analog 6-methylheptan-2-one (**35**) was only emitted by *C. baekdonensis* and geranylacetone (**36**) only by the three productive species *C. marinus*, *C. neptunius*, and *C. manganoxidans*. Compounds **34** and **36** have been described as non-enzymatic degradation products arising from the side chain in menaquinones [58]. Sulfur-containing compounds included dimethyl trisulfide (**37**), released by all six species, *S*-methyl methanethiosulfonate (**38**), 2-acetylthiazole (**39**), and benzothiazole (**40**), the latter also in the extracts from all six strains. In addition, the extracts from the three species *C. marinus*, *C. neptunius* and *C. baekdonensis* contained an additional volatile (**41**) whose mass spectrum (Figure 3A) was not included in our libraries. Furthermore, ethyl 3-(methylsulfanyl)acrylate (**42**) was found in *C. marinus* and *C. manganoxidans*, but the measured retention index (I = 1177) did not allow to distinguish between the *E* and the *Z* isomer for which retention indices of I = 1144 (*E*) and I = 1158 (*Z*) were reported [53]. Therefore, for an unambiguous structural assignment for compounds **41** and **42** the synthesis of reference compounds was required.

Synthesis of reference compounds

The mass spectrum of the component **41** showed strong similarities to the library mass spectrum of 2-mercaptobenzothiazole that has a molecular weight of 167 Da. The isotope pattern of the molecular ion at m/z = 213 indicated the presence of three sulfur atoms. The strong base peak at m/z = 167 in the mass spectrum of **41** suggested a benzothiazol-2-ylsulfanyl moiety, while the mass difference to the molecular ion pointed to the connection to a methylsulfanyl group. Taken together, this analysis resulted in the structural proposal of 2-(methyldisulfanyl)benzothiazole for **41**. For the structural verification a synthesis was performed by a $BF_3{\cdot}OEt_2$-catalyzed reaction of bis(benzothiazol-2-yl)disulfane with dimethyl disulfide, giving

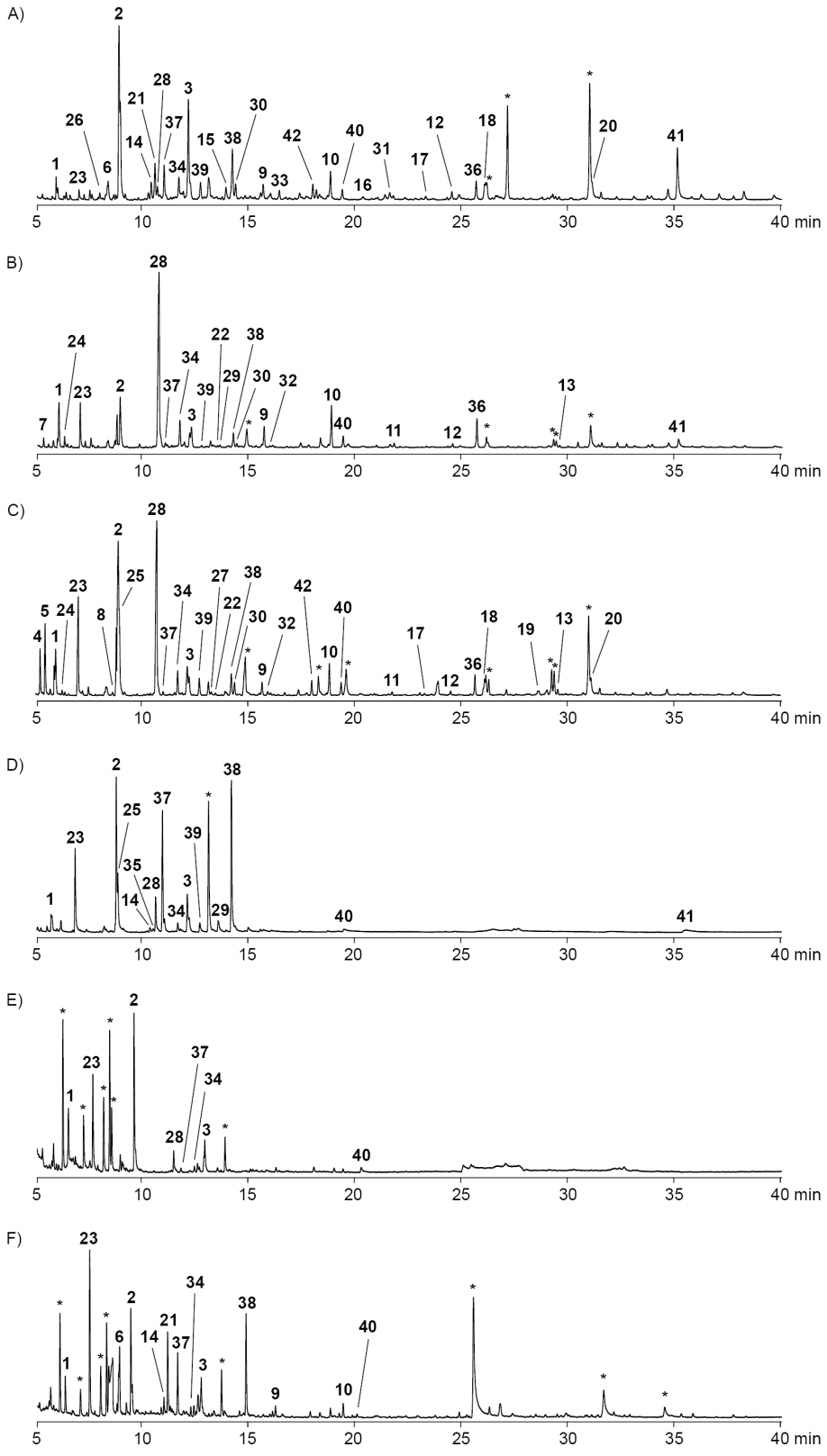

Figure 1: Total ion chromatograms of headspace extracts from A) *C. marinus* DSM 100036^T, B) *C. neptunius* DSM 26471^T, C) *C. manganoxidans* DSM 27541^T, D) *C. baekdonensis* DSM 27375^T, E) *C. halophilus* DSM 26270^T, and F) *C. indicus* DSM 27257^T. Peaks arising from known contaminants are indicated by asterisks.

Table 1: Volatiles from *Celeribacter* spp.

Compound[a]	*I*[b]	*I*(lit.)[b]	Id.[c]	Occurrence[d]					
3-hydroxypentan-2-one (**4**)	812	815 [39]	ri, ms			C			
hexanal (**7**)	813	806 [39]	ri, ms		B				
2-hydroxypentan-3-one (**5**)	818	818 [40]	ri, ms			C			
methylpyrazine (**1**)	831	826 [41]	ri, ms	A	B	C	D	E	F
furfural (**24**)	841	841 [42]	ri, ms		B	C			
furan-2-ylmethanol (**23**)	861	863 [43]	ri, ms	A	B	C	D	E	F
cyclohexanol (**26**)	888	886 [44]	ri, ms	A					
2-hydroxyhexan-3-one (**6**)	899	900 [40]	ri, ms	A					F
heptanal (**8**)	906	901 [45]	ri, ms			C			
2,5-dimethylpyrazine (**2**)	912	908 [45]	ri, ms	A	B	C	D	E	F
2-acetylfuran (**25**)	913	909 [45]	ri, ms			C	D		
pentan-4-olide (**14**)	953	956 [46]	ri, ms	A			D		F
3-methylbutan-4-olide (**21**)	957	958 [47]	ri, ms	A					F
6-methylheptan-2-one (**35**)	959	962 [48]	ri, ms				D		
benzaldehyde (**28**)	961	952 [45]	ri, ms	A	B	C	D	E	
dimethyl trisulfide (**37**)	970	968 [49]	ri, ms	A	B	C	D	E	F
6-methylhept-5-en-2-one (**34**)	988	981 [45]	ri, ms	A	B	C	D	E	F
trimethylpyrazine (**3**)	1000	1000 [45]	ri, ms	A	B	C	D	E	F
2-acetylthiazole (**39**)	1017	1014 [45]	ri, ms	A	B	C	D		
benzyl alcohol (**27**)	1033	1026 [45]	ri, ms			C			
4-methylhex-5-en-4-olide (**22**)	1039	1034 [45]	ri, ms		B	C			
salicylaldehyde (**29**)	1042	1039 [45]	ri, ms		B		D		
hexan-4-olide (**15**)	1052	1056 [50]	ri, ms	A					
S-methyl methanethiosulfonate (**38**)	1061	1068 [51]	ri, ms	A	B	C	D		F
acetophenone (**30**)	1065	1059 [45]	ri, ms	A	B	C			
nonanal (**9**)	1103	1100 [45]	ri, ms	A	B	C			F
2-phenylethanol (**32**)	1111	1106 [45]	ri, ms		B	C			
phenylacetone (**33**)	1127	1124 [52]	ri, ms	A					
ethyl (*E*)-3-(methylsulfanyl)acrylate (**42**)	1177	*1144* [53]	ms	A		C			
decanal (**10**)	1203	1201 [45]	ri, ms	A	B	C			F
benzothiazole (**40**)	1221	1222 [54]	ri, ms	A	B	C	D	E	F
octan-4-olide (**16**)	1252	1250 [45]	ri, ms	A					
o-aminoacetophenone (**31**)	1292	1296 [55]	ri, ms	A					
undecanal (**11**)	1298	1305 [45]	ri, ms		B	C			
nonan-4-olide (**17**)	1354	1358 [45]	ri, ms	A		C			
dodecanal (**12**)	1400	1408 [45]	ri, ms	A	B	C			
geranylacetone (**36**)	1445	1453 [45]	ri, ms	A	B	C			
decan-4-olide (**18**)	1461	1465 [45]	ri, ms	A		C			
undecan-4-olide (**19**)	1568	1569 [45]	ri, ms			C			
tetradecanal (**13**)	1605	1611 [45]	ri, ms		B	C			
dodecan-4-olide (**20**)	1673	1676 [45]	ri, ms	A		C			
2-(methyldisulfanyl)benzothiazole (**41**)	1860		std	A	B		D		

[a]Identified by GC–MS, known typical contaminants such as plasticizers are not included and all listed compounds were not detected in blank runs with medium plates (except traces of benzaldehyde); [b]retention index on a HP5-MS GC column and comparison to literature data from the same or a similar type of GC column; [c]identification based on ri: matching retention index (difference between measured retention index and literature data ≤10 points), ms: mass spectrum matching to a database spectrum, std: direct comparison to an authentic standard; [d]occurrence in A: *C. marinus* DSM 100036^T, B: *C. neptunius* DSM 26471^T, C: *C. manganoxidans* DSM 27541^T, D: *C. baekdonensis* DSM 27375^T, E: *C. halophilus* DSM 26270^T, and F: *C. indicus* DSM 27257^T.

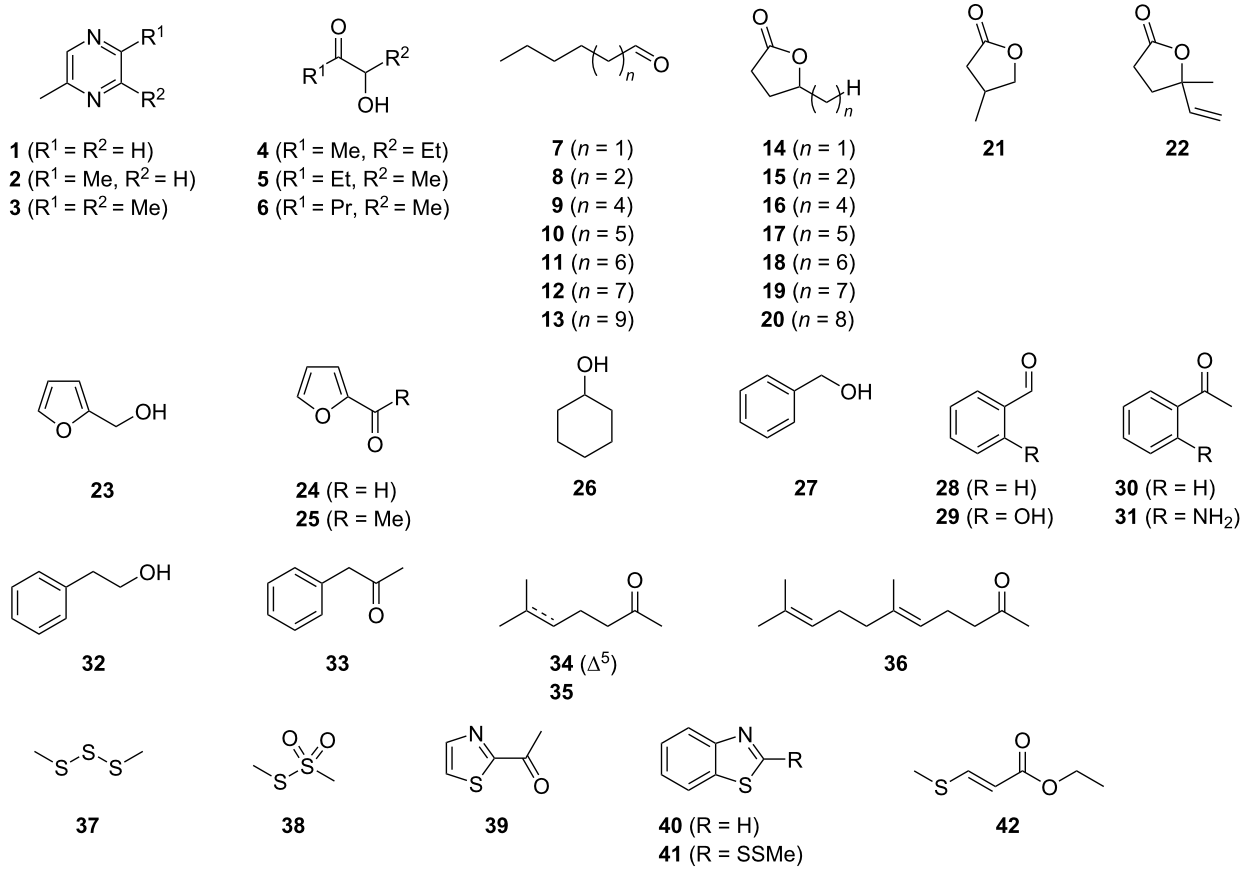

Figure 2: Structures of the identified volatile compounds in the headspace extracts from six *Celeribacter* type strains.

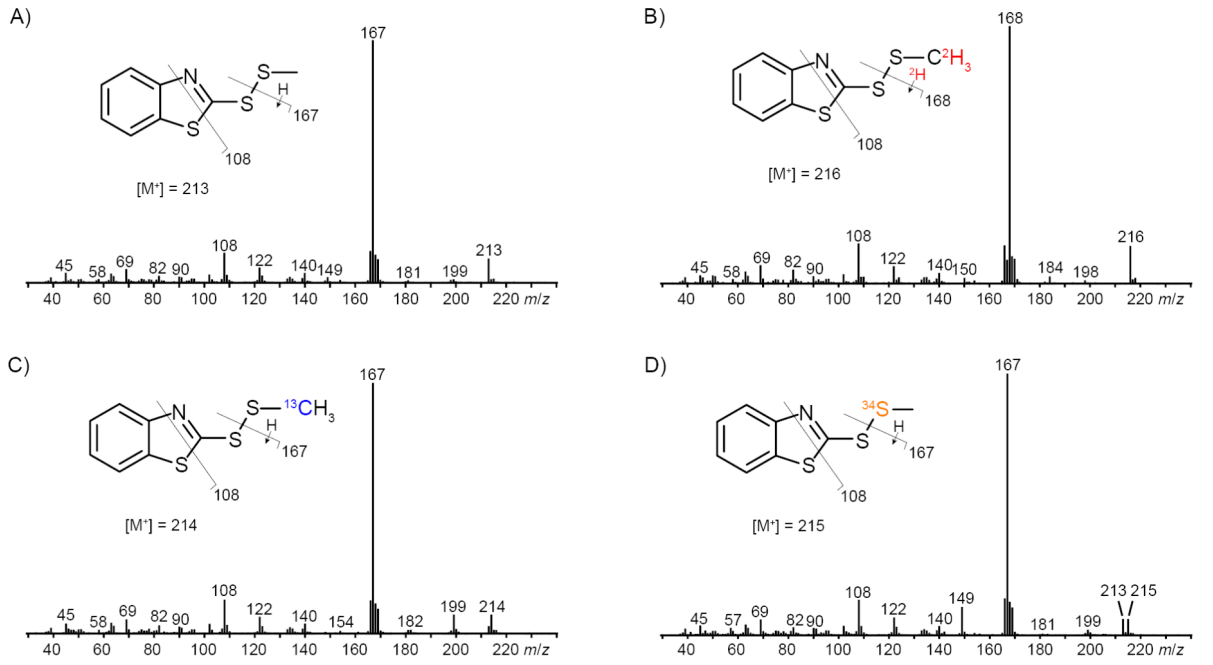

Figure 3: EI mass spectra of A) unlabeled 2-(methyldisulfanyl)benzothiazole (**41**) and of labeled **41** after feeding of B) (*methyl*-$^{2}H_3$)methionine, C) (*methyl*-^{13}C)methionine and D) (^{34}S)DMSP.

access to **41** with a yield of 64% (Scheme 2). The synthetic compound **41** showed an identical mass spectrum and retention index compared to the volatile in the *Celeribacter* extracts. The *Z* and *E* stereoisomers of **42** were obtained by the Michael addition of NaSMe to ethyl propiolate (**45**), yielding a mixture of stereoisomers inseparable by silica gel column chromatography (92%). The major stereoisomer was found to be (*Z*)-**42** (dr 94:6), whose preferred formation may be a result of a chalcogen–chalcogen interaction between the sulfur and an ester oxygen. This phenomenon was first described in supramolecular structures by Gleiter [59] and later also used to explain the outcome of organocatalytic reactions [60]. The pure stereoisomers of **42** were isolated by preparative HPLC, for which the best separation was achieved using a YMC ChiralART Cellulose-SC column. This yielded 70% of (*Z*)-**42** and 6% of (*E*)-**42**, and their analysis by GC–MS showed retention indices of I = 1177 for (*E*)-**42** and I = 1200 for (*Z*)-**42**, revealing that the compound in the headspace extracts of *C. marinus* DSM 100036^T and *C. manganoxidans* DSM 27541^T was identical to (*E*)-**42**.

Feeding experiments with isotopically labeled precursors

The biosynthesis of sulfur volatiles in *C. marinus* was investigated in a series of feeding experiments with isotopically labeled precursors. Feeding of (*methyl*-$^2H_3$)methionine resulted in the efficient incorporation of labeling into **37** (79% incorporation rate, Figure S1B in Supporting Information File 1), **38** (78%, Figure S1F in Supporting Information File 1) and the *S*-methyl group of **41** (84%), as indicated by a shift of the molecular ion from m/z = 213 to 216 (Figure 3B, deuterated compounds can be separated from their non-deuterated analogs by gas chromatography [61]). The base peak appears at m/z = 168, demonstrating its formation with participation of one deuterium from the *S*-methyl group. Analogous results were obtained by feeding of (*methyl*-^{13}C)methionine, showing incorporation into **37** (74%, Figure S1C in Supporting Information File 1), **38** (71%, Figure S1G in Supporting Information), and the MeS group of **41** (71%, Figure 3C; the signal at m/z = 213 represents unlabeled **41** that, in contrast to a deuterated compound, cannot be separated from ^{13}C-labeled **41** by gas chromatography). Furthermore, feeding of [^{34}S]DMSP gave an incorporation into the MeS groups of **37** (50%, Figure S1D), into both sulfur atoms of **38** (47%, Figure S1H in Supporting Information File 1), but only into one sulfur atom of **41** (46%), as indicated by the molecular ion at m/z = 215, while no signals at m/z = 217 and 219 were visible that would account for the incorporation of labeling into two or three of the sulfur atoms in **41** (Figure 3D; also here the signal at m/z = 213 represents inseparable unlabeled **41**). In this experiment, the base peak did not change which allowed the localization of labeling specifically in the MeS group of **41**.

The fact that no incorporation was observed for the other two sulfur atoms of **41** prompted us to further investigate the biosynthetic origin of the benzothiazol-2-ylsulfanyl portion of **41** to establish its natural origin. Several feeding experiments with central primary metabolites including ($^{13}C_6$)glucose, ($^{13}C_5$)ribose and (*indole*-$^2H_5$)tryptophan were performed, but none of these experiments resulted in a detectable incorporation of labeling. Conclusively, a non-biological origin of this part of the molecule seems likely, which may also explain why the detection of **41** in *Celeribacter* was not always reproducible. Notably, 2-mercaptobenzothiazole is used in the sulfur vulcanization of rubber and could react spontaneously with MeSH of bacterial origin in the presence of oxygen to form **41**, giving a reasonable explanation for its formation.

Also none of the feeding experiments with the various labeled precursors resulted in an incorporation of labeling into the

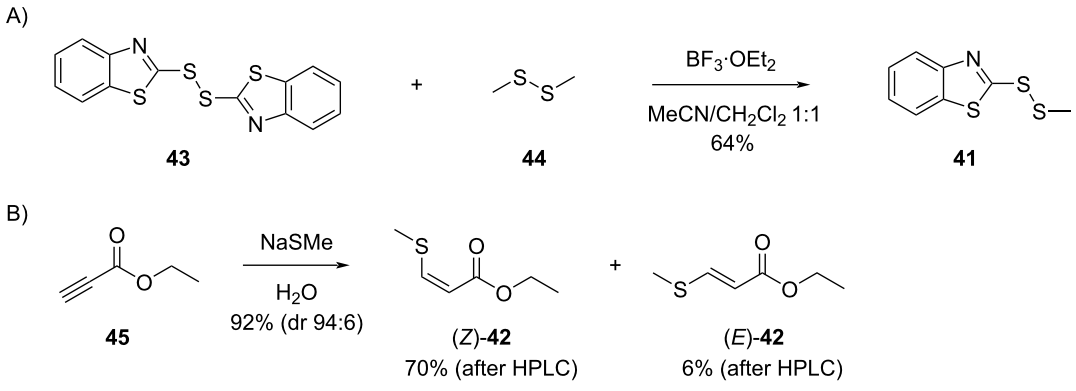

Scheme 2: Synthesis of sulfur-containing compounds detected in the *Celeribacter* headspace extracts. A) Synthesis of 2-(methyldisulfanyl)benzothiazole (**41**) and B) synthesis of ethyl (*Z*)- and (*E*)-3-(methylsulfanyl)acrylate (**42**).

sulfur volatiles **39**, **40**, and **42**, which also questioned their natural origin. This finding is rather surprising for **42**, especially regarding the feeding experiment with (^{34}S)DMSP, because its formation would be explainable by a DMSP degradation through the demethylation pathway, for which all relevant enzymes are encoded in the six *Celeribacter* strains (only a DmdA homolog is missing in *C. indicus*, Table S1 in Supporting Information File 1), and e.g., transesterification of the DmdC product with EtOH (Scheme 1A). Compound **42** is not a widespread sulfur volatile, but has been reported before from pineapples [53], pears [62], passion fruits [63], and apples [64].

Conclusion

Six marine *Celeribacter* strains were investigated for their volatiles, leading to the identification of 42 compounds from different classes, including several sulfur volatiles. However, feeding experiments with isotopically labeled precursors suggested that only the widespread compounds dimethyl trisulfide (**37**) and *S*-methyl methanethiosulfonate (**38**) are of natural origin, while no labeling from any of the fed precursors was incorporated into 2-acetylthiazole (**39**), benzothiazole (**40**), and ethyl (*E*)-3-(methylsulfanyl)acrylate (**42**), thus questioning their natural source from *Celeribacter*. These results demonstrate that the six *Celeribacter* strains are able to degrade methionine and DMSP with formation of MeSH as a source for the likely non-enzymatic oxidation in the presence of air to **37** and **38**, opening possibilities for future studies on methionine and DMSP degrading enzymes and pathways in *Celeribacter*. Our study also shows that the results from trace compound analyses must be taken with care and contaminations from other sources must always be taken into consideration. For the unusual compound 2-(methyldisulfanyl)benzothiazole (**41**) the incorporation of labeling was observed only into the MeS group, while the benzothiazol-2-ylsulfanyl portion is likely of anthropogenic origin from the rubber vulcanization agent 2-mercaptobenzothiazole that reacts with MeSH from the bacterial metabolism.

Experimental

Strains, culture conditions, and feeding experiments

All six *Celeribacter* type strains were cultivated at 28 °C on marine broth agar plates. In case of feeding experiments, the isotopically labeled compound (1 mM) was added to the agar medium before inoculation.

Collection of volatiles

The volatiles emitted by *Celeribacter* spp. agar plate cultures were collected on charcoal filters (Chromtech, Idstein, Germany, precision charcoal filters charged with 5 mg of charcoal) by use of a closed-loop stripping apparatus as developed by Grob and Zürcher [37]. After a collection time of 24 h the charcoal was extracted with CH_2Cl_2 (50 µL) and the extract was analyzed by GC–MS.

GC–MS

GC–MS analyses were carried out through a 7890B GC – 5977A MD system (Agilent, Santa Clara, CA, USA). The GC was equipped with a HP5-MS fused silica capillary column (30 m, 0.25 mm i.d., 0.50 µm film) and operated with the settings 1) inlet pressure: 77.1 kPa, He flow: 23.3 mL min^{-1}, 2) injection volume: 2 µL, 3) splitless injection, 4) temperature program: 5 min isothermic at 50 °C, then increasing with 5 °C min^{-1} to 320 °C, and 5) He carrier gas flow: 1.2 mL min^{-1}. The parameters of the MS were 1) transfer line temperature: 250 °C, 2) ion source temperature: 230 °C, 3) quadrupole temperature: 150 °C, and 4) electron energy: 70 eV. Retention indices were calculated from retention times in comparison to those of a homologous series of *n*-alkanes (C_7–C_{40}).

General synthetic and analytical methods

Reactions were carried out in oven-dried flasks under Ar atmosphere and using distilled and dried solvents. Chemicals were obtained from Sigma-Aldrich (St. Louis, USA). Column chromatography was performed on silica gel (0.04–0.06 nm) purchased from Acros Organics (Geel, Belgium) with distilled solvents. NMR spectroscopy was performed on a Bruker (Billerica, USA) Avance III HD Ascend (500 MHz) spectrometer. Solvent peaks were used for referencing (^{1}H NMR: $CDCl_3$ residual proton signal δ = 7.26 ppm, ^{13}C NMR: $CDCl_3$ δ = 77.16 ppm) [65]. Multiplicities are indicated by s (singlet) and d (doublet), coupling constants *J* are given in Hz. IR spectra were recorded on a Bruker α spectrometer equipped with a diamond-ATR probe, and qualitative signal intensities are reported by w (weak), m (medium), and s (strong). HPLC purification of compound **42** was performed on an Azura HPLC system (Knauer, Berlin, Germany) equipped with a UV–vis detector MWL 2.1L (deuterium lamp, 190–700 nm) and a YMC ChiralART Cellulose-SC column (5 µm; 250 × 20 mm) with a guard column of the same type (30 × 20 mm). The elution was performed with hexane/propanol 60:40 (isocratic) at a flow rate of 10 mL min^{-1} (36 bar). The UV–vis absorption was monitored at 275 nm.

Synthesis of 2-(methyldisulfanyl)benzothiazole (**41**)

1,2-Bis(benzothiazol-2-yl)disulfane (**43**, 1.00 g, 3.00 mmol, 1 equiv) and dimethyl sulfide (**44**, 0.28 g, 3.00 mmol, 1 equiv) were dissolved in dry CH_3NO_2 (10 mL) and dry CH_2Cl_2 (10 mL). The solution was cooled to 0 °C and then treated with $BF_3{\cdot}Et_2O$ (43 mg, 0.3 mmol, 0.1 equiv). After stirring at 0 °C for 3 hours and at room temperature overnight, the reaction was

quenched by the addition of water (10 mL) and extracted with ethyl acetate (3 × 50 mL). The combined extracts were dried with $MgSO_4$ and concentrated. The residue was purified by column chromatography (cyclohexane/ethyl acetate 1:1) to give **41** as a colorless solid (0.82 g, 3.85 mmol, 64%). R_f 0.60 (cyclohexane/ethyl acetate 5:1; TLC visualized with UV illumination at 366 nm); GC (HP-5MS): I = 1854; IR (diamond-ATR) ṽ: 3060 (s), 2916 (s), 1425 (w), 1310 (s), 1236 (s), 1005 (w), 756 (w), 431 (s) cm^{-1}; ^1H NMR (500 MHz, $CDCl_3$, 298 K) δ 7.88 (ddd, J = 8.1, 1.2, 0.7 Hz, 1H, CH), 7.87 (ddd, J = 7.9, 1.2, 0.6 Hz, 1H, CH), 7.43 (ddd, J = 8.3, 7.3, 1.2 Hz, 1H, CH), 7.33 (ddd, J = 8.2, 7.2, 1.2 Hz, 1H, CH), 2.67 (s, 3H, CH_3) ppm; ^{13}C NMR (125 MHz, $CDCl_3$, 298 K) δ 172.50 (C), 155.17 (C), 135.90 (C), 126.37 (CH), 124.70 (CH), 122.24 (CH), 121.27 (CH), 23.62 (CH_3) ppm.

Synthesis of ethyl (*Z*)-3-(methylsulfanyl)acrylate ((*Z*)-**42**) and ethyl (*E*)-3-(methylsulfanyl)acrylate ((*E*)-**42**)

Ethyl propiolate (**45**, 70 mg, 0.71 mmol, 1 equiv) was dissolved in distilled water (5 mL) followed by the addition of sodium methanethiolate (50 mg, 0.71 mmol, 1 equiv). The solution was stirred for 30 minutes at room temperature. Water (5 mL) was added and the product was extracted with ethyl acetate (3 × 10 mL). The combined extracts were dried over $MgSO_4$ and concentrated to afford the crude product. Purification by column chromatography (cyclohexane/ethyl acetate 99:1) gave a mixture of stereoisomers (*Z*)-**42** and (*E*)-**42** as pale yellow oil (96 mg, 0.65 mmol, 92%, dr 94:6 by ^1H NMR). The product mixture was separated by preparative HPLC to give pure (*Z*)-**42** (73 mg, 0.50 mmol, 70%) and (*E*)-**42** (6 mg, 0.04 mmol, 6%).

(*Z*)-42. R_f 0.74 (cyclohexane/ethyl acetate 1:1); GC (HP-5MS): I = 1200; IR (diamond-ATR) ṽ: 2982 (w), 2927 (w),1695 (m), 1569 (m), 1434 (w), 1374 (w), 1300 (w), 1266 (w), 1213 (m), 1166 (s), 1095 (w), 1033 (w), 986 (w), 961 (w), 800 (w), 727 (w), 687 (w) cm^{-1}; ^1H NMR (700 MHz, $CDCl_3$, 298 K) δ 7.04 (d, J = 10.14 Hz, 1H, CH), 5.83 (d, J = 10.14 Hz, 1H, CH), 4.20 (q, J = 7.15 Hz, 2H, CH_2), 2.39 (s, 3H, CH_3), 1.29 (t, J = 7.17 Hz, 3H, CH_3) ppm; ^{13}C NMR (175 MHz, $CDCl_3$, 298 K) δ 166.75 (C), 151.84 (CH), 113.18 (CH), 60.17 (CH_2), 19.28 (CH_3), 14.44 (CH_3) ppm.

(*E*)-42. R_f 0.76 (cyclohexane/ethyl acetate 1:1); GC (HP-5MS): I = 1177; IR (diamond-ATR) ṽ: 2980 (w), 2925 (w), 1701 (s), 1578 (s), 1444 (w), 1366 (w), 1322 (w), 1297 (m), 1251 (s), 1161 (s), 1095 (w), 1037 (m), 945 (m), 886 (w), 832 (w), 799 (w), 702 (w) cm^{-1}; ^1H NMR (700 MHz, $CDCl_3$, 298 K) δ 7.76 (d, J = 14.93 Hz, 1H, CH), 5.68 (d, J = 14.90 Hz, 1H, CH), 4.21 (q, J = 7.14 Hz, 2H, CH_2), 2.35 (s, 3H, CH_3), 1.31 (t, J = 7.13 Hz, 3H, CH_3) ppm; ^{13}C NMR (175 MHz, $CDCl_3$, 297 K) δ 165.59 (C), 147.21 (CH),113.56 (CH), 60.55 (CH_2), 27.26 (CH_3), 14.67 (CH_3) ppm.

Supporting Information

Supporting Information File 1

DMSP demethylation pathway in *Celeribacter* spp. and copies of spectra.
[https://www.beilstein-journals.org/bjoc/content/supplementary/1860-5397-17-38-S1.pdf]

Acknowledgements

We thank Andreas Schneider (Bonn) for HPLC separation of (*E*)- and (*Z*)-**42**.

Funding

This work was funded by the Deutsche Forschungsgemeinschaft (DFG, German Research Foundation) – Project-ID 34509606 – TRR 51 within the frame of the Transregional Collaborative Research Center “Roseobacter”.

ORCID® iDs

Jeroen S. Dickschat - https://orcid.org/0000-0002-0102-0631

References

1. Giovannoni, S. J.; Stingl, U. *Nature* **2005,** *437,* 343–348. doi:10.1038/nature04158
2. González, J. M.; Moran, M. A. *Appl. Environ. Microbiol.* **1997,** *63,* 4237–4242. doi:10.1128/aem.63.11.4237-4242.1997
3. Selje, N.; Simon, M.; Brinkhoff, T. *Nature* **2004,** *427,* 445–448. doi:10.1038/nature02272
4. Brinkhoff, T.; Giebel, H.-A.; Simon, M. *Arch. Microbiol.* **2008,** *189,* 531–539. doi:10.1007/s00203-008-0353-y
5. Lee, O. O.; Tsoi, M. M. Y.; Li, X.; Wong, P.-K.; Qian, P.-Y. *Int. J. Syst. Evol. Microbiol.* **2007,** *57,* 1919–1924. doi:10.1099/ijs.0.64801-0
6. Ruiz-Ponte, C.; Cilia, V.; Lambert, C.; Nicolas, J. L. *Int. J. Syst. Bacteriol.* **1998,** *48,* 537–542. doi:10.1099/00207713-48-2-537
7. Shiba, T. *Syst. Appl. Microbiol.* **1991,** *14,* 140–145. doi:10.1016/s0723-2020(11)80292-4
8. Biebl, H.; Allgaier, M.; Tindall, B. J.; Koblizek, M.; Lünsdorf, H.; Pukall, R.; Wagner-Döbler, I. *Int. J. Syst. Evol. Microbiol.* **2005,** *55,* 1089–1096. doi:10.1099/ijs.0.63511-0
9. Lafay, B.; Ruimy, R.; Rausch de Traubenberg, C.; Breittmayer, V.; Gauthier, M. J.; Christen, R. *Int. J. Syst. Bacteriol.* **1995,** *45,* 290–296. doi:10.1099/00207713-45-2-290
10. Gonzalez, J. M.; Simo, R.; Massana, R.; Covert, J. S.; Casamayor, E. O.; Pedros-Alio, C.; Moran, M. A. *Appl. Environ. Microbiol.* **2000,** *66,* 4237–4246. doi:10.1128/aem.66.10.4237-4246.2000

11. Dickschat, J. S.; Rabe, P.; Citron, C. A. *Org. Biomol. Chem.* **2015,** *13,* 1954–1968. doi:10.1039/c4ob02407a
12. Reisch, C. R.; Stoudemayer, M. J.; Varaljay, V. A.; Amster, I. J.; Moran, M. A.; Whitman, W. B. *Nature* **2011,** *473,* 208–211. doi:10.1038/nature10078
13. Todd, J. D.; Rogers, R.; Li, Y. G.; Wexler, M.; Bond, P. L.; Sun, L.; Curson, A. R. J.; Malin, G.; Steinke, M.; Johnston, A. W. B. *Science* **2007,** *315,* 666–669. doi:10.1126/science.1135370
14. Todd, J. D.; Kirkwood, M.; Newton-Payne, S.; Johnston, A. W. B. *ISME J.* **2012,** *6,* 223–226. doi:10.1038/ismej.2011.79
15. Kirkwood, M.; Le Brun, N. E.; Todd, J. D.; Johnston, A. W. B. *Microbiology (London, U. K.)* **2010,** *156,* 1900–1906. doi:10.1099/mic.0.038927-0
16. Todd, J. D.; Curson, A. R. J.; Kirkwood, M.; Sullivan, M. J.; Green, R. T.; Johnston, A. W. B. *Environ. Microbiol.* **2011,** *13,* 427–438. doi:10.1111/j.1462-2920.2010.02348.x
17. Curson, A. R. J.; Rogers, R.; Todd, J. D.; Brearley, C. A.; Johnston, A. W. B. *Environ. Microbiol.* **2008,** *10,* 757–767. doi:10.1111/j.1462-2920.2007.01499.x
18. Curson, A. R. J.; Sullivan, M. J.; Todd, J. D.; Johnston, A. W. B. *ISME J.* **2011,** *5,* 1191–1200. doi:10.1038/ismej.2010.203
19. Sun, J.; Todd, J. D.; Thrash, J. C.; Qian, Y.; Qian, M. C.; Temperton, B.; Guo, J.; Fowler, E. K.; Aldrich, J. T.; Nicora, C. D.; Lipton, M. S.; Smith, R. D.; De Leenheer, P.; Payne, S. H.; Johnston, A. W. B.; Davie-Martin, C. L.; Halsey, K. H.; Giovannoni, S. J. *Nat. Microbiol.* **2016,** *1,* 16065. doi:10.1038/nmicrobiol.2016.65
20. Lovelock, J. E.; Maggs, R. J.; Rasmussen, R. A. *Nature* **1972,** *237,* 452–453. doi:10.1038/237452a0
21. Charlson, R. J.; Lovelock, J. E.; Andreae, M. O.; Warren, S. G. *Nature* **1987,** *326,* 655–661. doi:10.1038/326655a0
22. Dickschat, J. S.; Zell, C.; Brock, N. L. *ChemBioChem* **2010,** *11,* 417–425. doi:10.1002/cbic.200900668
23. Brock, N. L.; Citron, C. A.; Zell, C.; Berger, M.; Wagner-Döbler, I.; Petersen, J.; Brinkhoff, T.; Simon, M.; Dickschat, J. S. *Beilstein J. Org. Chem.* **2013,** *9,* 942–950. doi:10.3762/bjoc.9.108
24. Brock, N. L.; Menke, M.; Klapschinski, T. A.; Dickschat, J. S. *Org. Biomol. Chem.* **2014,** *12,* 4318–4323. doi:10.1039/c4ob00719k
25. Celik, E.; Maczka, M.; Bergen, N.; Brinkhoff, T.; Schulz, S.; Dickschat, J. S. *Org. Biomol. Chem.* **2017,** *15,* 2919–2922. doi:10.1039/c7ob00357a
26. Durham, B. P.; Sharma, S.; Luo, H.; Smith, C. B.; Amin, S. A.; Bender, S. J.; Dearth, S. P.; Van Mooy, B. A. S.; Campagna, S. R.; Kujawinski, E. B.; Armbrust, E. V.; Moran, M. A. *Proc. Natl. Acad. Sci. U. S. A.* **2015,** *112,* 453–457. doi:10.1073/pnas.1413137112
27. Mönnich, J.; Tebben, J.; Bergemann, J.; Case, R.; Wohlrab, S.; Harder, T. *ISME J.* **2020,** *14,* 1614–1625. doi:10.1038/s41396-020-0631-5
28. Bruhn, J. B.; Nielsen, K. F.; Hjelm, M.; Hansen, M.; Bresciani, J.; Schulz, S.; Gram, L. *Appl. Environ. Microbiol.* **2005,** *71,* 7263–7270. doi:10.1128/aem.71.11.7263-7270.2005
29. Greer, E. M.; Aebisher, D.; Greer, A.; Bentley, R. *J. Org. Chem.* **2008,** *73,* 280–283. doi:10.1021/jo7018416
30. Kintaka, K.; Ono, H.; Tsubotani, S.; Harada, S.; Okazaki, H. *J. Antibiot.* **1984,** *37,* 1294–1300. doi:10.7164/antibiotics.37.1294
31. Geng, H.; Bruhn, J. B.; Nielsen, K. F.; Gram, L.; Belas, R. *Appl. Environ. Microbiol.* **2008,** *74,* 1535–1545. doi:10.1128/aem.02339-07
32. Berger, M.; Brock, N. L.; Liesegang, H.; Dogs, M.; Preuth, I.; Simon, M.; Dickschat, J. S.; Brinkhoff, T. *Appl. Environ. Microbiol.* **2012,** *78,* 3539–3551. doi:10.1128/aem.07657-11
33. Brock, N. L.; Nikolay, A.; Dickschat, J. S. *Chem. Commun.* **2014,** *50,* 5487–5489. doi:10.1039/c4cc01924e
34. Beyersmann, P. G.; Tomasch, J.; Son, K.; Stocker, R.; Göker, M.; Wagner-Döbler, I.; Simon, M.; Brinkhoff, T. *Sci. Rep.* **2017,** *7,* 730. doi:10.1038/s41598-017-00784-7
35. Thiel, V.; Brinkhoff, T.; Dickschat, J. S.; Wickel, S.; Grunenberg, J.; Wagner-Döbler, I.; Simon, M.; Schulz, S. *Org. Biomol. Chem.* **2010,** *8,* 234–246. doi:10.1039/b909133e
36. Seyedsayamdost, M. R.; Case, R. J.; Kolter, R.; Clardy, J. *Nat. Chem.* **2011,** *3,* 331–335. doi:10.1038/nchem.1002
37. Grob, K.; Zürcher, F. *J. Chromatogr.* **1976,** *117,* 285–294. doi:10.1016/0021-9673(76)80005-2
38. Kováts, E. *Helv. Chim. Acta* **1958,** *41,* 1915–1932. doi:10.1002/hlca.19580410703
39. Elmore, J. S.; Mottram, D. S.; Enser, M.; Wood, J. D. *Meat Sci.* **2000,** *55,* 149–159. doi:10.1016/s0309-1740(99)00137-0
40. Dickschat, J. S.; Wickel, S.; Bolten, C. J.; Nawrath, T.; Schulz, S.; Wittmann, C. *Eur. J. Org. Chem.* **2010,** 2687–2695. doi:10.1002/ejoc.201000155
41. Cerny, C.; Guntz-Dubini, R. *J. Agric. Food Chem.* **2006,** *54,* 574–577. doi:10.1021/jf052222s
42. Spadone, J.-C.; Takeoka, G.; Liardon, R. *J. Agric. Food Chem.* **1990,** *38,* 226–233. doi:10.1021/jf00091a050
43. Lee, S.-R.; Macku, C.; Shibamoto, T. *J. Agric. Food Chem.* **1991,** *39,* 1972–1975. doi:10.1021/jf00011a017
44. Pino, J. A.; Mesa, J.; Muñoz, Y.; Martí, M. P.; Marbot, R. *J. Agric. Food Chem.* **2005,** *53,* 2213–2223. doi:10.1021/jf0402633
45. Adams, R. P. *Identification of Essential Oil Components by Gas Chromatography/Mass Spectrometry;* Allured Pub Corp.: Carol Stream, IL, 2009.
46. Ansorena, D.; Gimeno, O.; Astiasarán, I.; Bello, J. *Food Res. Int.* **2001,** *34,* 67–75. doi:10.1016/s0963-9969(00)00133-2
47. Citron, C. A.; Rabe, P.; Dickschat, J. S. *J. Nat. Prod.* **2012,** *75,* 1765–1776. doi:10.1021/np300468h
48. Owens, J. D.; Allagheny, N.; Kipping, G.; Ames, J. M. *J. Sci. Food Agric.* **1997,** *74,* 132–140. doi:10.1002/(sici)1097-0010(199705)74:1<132::aid-jsfa779>3.0.co;2-8
49. Cha, Y. J.; Cadwallader, K. R. *J. Agric. Food Chem.* **1998,** *46,* 1123–1128. doi:10.1021/jf970380g
50. Wickel, S. M.; Citron, C. A.; Dickschat, J. S. *Eur. J. Org. Chem.* **2013,** 2906–2913. doi:10.1002/ejoc.201300049
51. Kubec, R.; Drhová, V.; Velíšek, J. *J. Agric. Food Chem.* **1998,** *46,* 4334–4340. doi:10.1021/jf980379x
52. Ferhat, M. A.; Tigrine-Kordjani, N.; Chemat, S.; Meklati, B. Y.; Chemat, F. *Chromatographia* **2007,** *65,* 217–222. doi:10.1365/s10337-006-0130-5
53. Takeoka, G. R.; Buttery, R. G.; Teranishi, R.; Flath, R. A.; Güntert, M. *J. Agric. Food Chem.* **1991,** *39,* 1848–1851. doi:10.1021/jf00010a032
54. Nawrath, T.; Mgode, G. F.; Weetjens, B.; Kaufmann, S. H. E.; Schulz, S. *Beilstein J. Org. Chem.* **2012,** *8,* 290–299. doi:10.3762/bjoc.8.31
55. Citron, C. A.; Barra, L.; Wink, J.; Dickschat, J. S. *Org. Biomol. Chem.* **2015,** *13,* 2673–2683. doi:10.1039/c4ob02609h
56. Schulz, S.; Dickschat, J. S. *Nat. Prod. Rep.* **2007,** *24,* 814–842. doi:10.1039/b507392h
57. Dickschat, J. S. *Nat. Prod. Rep.* **2017,** *34,* 310–328. doi:10.1039/c7np00003k

58. Ueda, D.; Matsugane, S.; Okamoto, W.; Hashimoto, M.; Sato, T. *Angew. Chem., Int. Ed.* **2018,** *57,* 10347–10351. doi:10.1002/anie.201805383
59. Werz, D. B.; Staeb, T. H.; Benisch, C.; Rausch, B. J.; Rominger, F.; Gleiter, R. *Org. Lett.* **2002,** *4,* 339–342. doi:10.1021/ol016953z
60. Leverett, C. A.; Purohit, V. C.; Romo, D. *Angew. Chem., Int. Ed.* **2010,** *49,* 9479–9483. doi:10.1002/anie.201004671
61. Dickschat, J. S. *Nat. Prod. Rep.* **2014,** *31,* 838–861. doi:10.1039/c3np70080a
62. Takeoka, G. R.; Buttery, R. G.; Flath, R. A. *J. Agric. Food Chem.* **1992,** *40,* 1925–1929. doi:10.1021/jf00022a040
63. Werkhoff, P.; Güntert, M.; Krammer, G.; Sommer, H.; Kaulen, J. *J. Agric. Food Chem.* **1998,** *46,* 1076–1093. doi:10.1021/jf970655s
64. Ferreira, L.; Perestrelo, R.; Caldeira, M.; Câmara, J. S. *J. Sep. Sci.* **2009,** *32,* 1875–1888. doi:10.1002/jssc.200900024
65. Fulmer, G. R.; Miller, A. J. M.; Sherden, N. H.; Gottlieb, H. E.; Nudelman, A.; Stoltz, B. M.; Bercaw, J. E.; Goldberg, K. I. *Organometallics* **2010,** *29,* 2176–2179. doi:10.1021/om100106e

License and Terms

Appendix B

Breakdown of 3-(allylsulfonio)propanoates in bacteria from the Roseobacter group yields garlic oil constituents

Beilstein J. Org. Chem. **2021**, *17*, 569–580

DOI: 10.3762/bjoc.17.51

BEILSTEIN JOURNAL OF ORGANIC CHEMISTRY

Breakdown of 3-(allylsulfonio)propanoates in bacteria from the *Roseobacter* group yields garlic oil constituents

Anuj Kumar Chhalodia and Jeroen S. Dickschat*

Full Research Paper

Open Access

Address:
Kekulé Institute of Organic Chemistry and Biochemistry, University of Bonn, Gerhard-Domagk-Straße 1, 53121 Bonn, Germany

Email:
Jeroen S. Dickschat* - dickschat@uni-bonn.de

* Corresponding author

Keywords:
Allium sativum; allyl sulfides; 3-(dimethylsulfonio)propanoate; *Roseobacter*; volatiles

Beilstein J. Org. Chem. **2021,** *17,* 569–580.
https://doi.org/10.3762/bjoc.17.51

Received: 22 December 2020
Accepted: 19 February 2021
Published: 26 February 2021

This article is part of the thematic issue "Chemical ecology".

Guest Editor: C. Beemelmanns

Abstract

Two analogues of 3-(dimethylsulfonio)propanoate (DMSP), 3-(diallylsulfonio)propanoate (DAllSP), and 3-(allylmethylsulfonio)propanoate (AllMSP), were synthesized and fed to marine bacteria from the *Roseobacter* clade. These bacteria are able to degrade DMSP into dimethyl sulfide and methanethiol. The DMSP analogues were also degraded, resulting in the release of allylated sulfur volatiles known from garlic. For unknown compounds, structural suggestions were made based on their mass spectrometric fragmentation pattern and confirmed by the synthesis of reference compounds. The results of the feeding experiments allowed to conclude on the substrate tolerance of DMSP degrading enzymes in marine bacteria.

Introduction

The name of the allyl group has been introduced by Wertheim in 1844 when he investigated the constituents of garlic oil and derives from the botanical name of garlic (*Allium sativum*) [1]. During that time, the structures of the garlic oil constituents and also of the allyl group remained unknown, but its formula was correctly assigned as C_3H_5. Five decades later, Semmler reported on the nature of allyl propyl disulfide (**1**), diallyl disulfide (**2**), diallyl trisulfide (**3**), and diallyl tetrasulfide (**4**) from garlic oil (Scheme 1A) [2]. The antibacterial principle in garlic was identified in 1944 by Cavallito et al. as allicin (**5**) [3], a formal oxidation product of disulfide **2**. Not only **5**, but also several other sulfur compounds from garlic are today known to exhibit diverse biological activities, including inter alia antibacterial, antifungal, antioxidant, anti-inflammatory, and anticancer effects [4]. Later on, also heterocyclic compounds including 2-vinyl-4*H*-1,3-dithiine (**6**) and 3-vinyl-3,4-dihydro-1,2-dithiine (**7**) were discovered [5]. The formation of these volatile sulfur compounds starts from alliin (**9**) [6], a non-volatile precursor that is stored in garlic and related plants and only degraded into sulfur volatiles upon wounding by the pyridoxal phosphate (PLP) dependent alliinase (Scheme 1B) [7]. This initial enzyme-catalyzed reaction yields one equivalent of allyl-

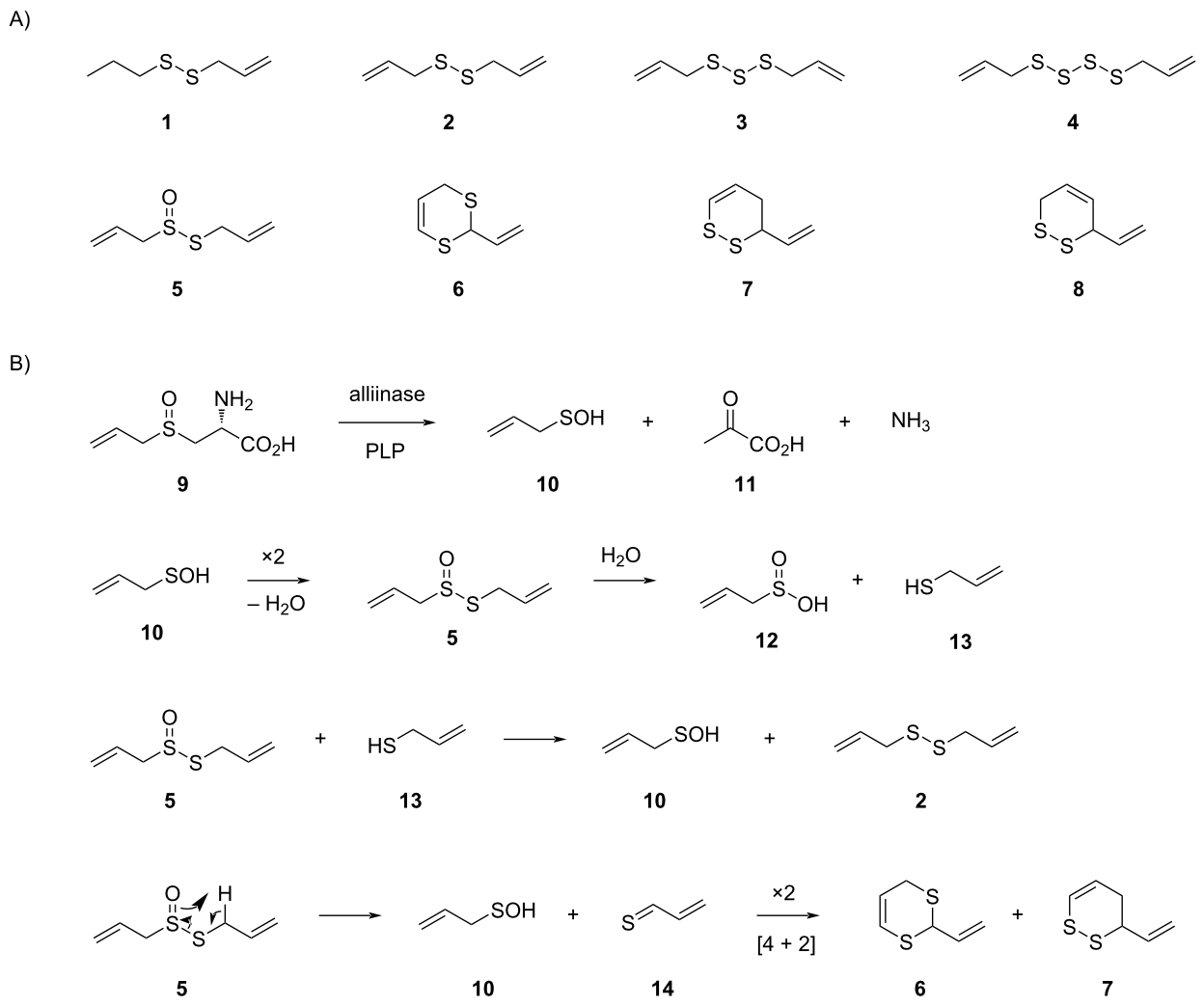

Scheme 1: Volatile allyl sulfides. A) Compounds known from garlic oil, B) mechanism of formation from alliin (**9**) by the PLP-dependent allinase (PLP: pyridoxalphosphate) and subsequent spontaneous reactions.

sulfenic acid (**10**), pyruvic acid (**11**), and ammonia from **9**, followed by a series of proposed spontaneous reactions [5,8]. Through these transformations, acid **10** can undergo a dimerization with elimination of water to allicin (**5**). The hydrolysis of **5** results in allylsulfinic acid (**12**) and allyl thiol (**13**), the latter of which can react with another molecule of **5** to yield **10** and **2**. Alternatively, **5** can decompose to **10** and thioacroleine (**14**) by a Cope elimination, which explains the formation of the heterocycles **6** and **7** by dimerization through a [4 + 2] cycloaddition [5]. Compounds **6** and **7** were also reported to be formed from **5** during gas chromatographic (GC) analysis by an unknown mechanism [9] (**7** was confused with its double bond regioisomer 3-vinyl-3,6-dihydro-1,2-dithiine (**8**) in this study [5]). Under these conditions the formation of the heterocyclic disulfides **7** and **8** may not involve a dimerization of **14**, as a [4 + 2] cycloaddition is not a preferred gas-phase reaction.

The ecology of marine bacteria in their interaction with algae is particularly interesting in which the bacteria can promote the algal growth, but can also kill their host [10,11]. For both processes, the phytohormone indole-3-acetic acid is used as a messenger molecule [10]. For the macroalga *Ulva mutabilis* the presence of bacteria from the *Roseobacter* group is even mandatory for proper algal development, and 3-(dimethylsulfonio)propanoate (DMSP) is used as a chemotactic signal by the bacteria attracting them towards the algal host [12]. Many bacteria and fungi also release sulfur volatiles [13,14] that are especially important headspace constituents from marine bacteria of the *Roseobacter* group [15-17]. In these organisms, sulfur volatiles are to a large extent generated from algal (DMSP), a metabolite that is produced in massive amounts by algae [18], thus giving another example for the complex interactions between marine bacteria and algae. Known DMSP degradation pathways include its hydrolysis to dimethyl sulfide

(DMS) and 3-hydroxypropanoic acid (**15**) by the enzyme DddD [19], or the lysis to DMS and acrylic acid (**16**) for which various enzymes including DddL [20], DddP [21], DddQ [22], DddY [23], DddW [24], and DddK [25] have been described (Scheme 2A). Furthermore, a demethylation pathway is known through which DMSP is first converted into methylmercaptopropanoic acid (**17**) by the tetrahydrofolate (FH_4)-dependent demethylase, DmdA (Scheme 2B) [26]. Compound **17** can be transformed into the coenzyme A thioester **18** by the CoA ligase DmdB, followed by FAD-dependent oxidation to the α,β-unsaturated compound **19** by DmdC. The attack of water to the Michael acceptor catalyzed by the enoyl-CoA hydratase DmdD yields the hemithioacetal **20** that spontaneously collapses to methanethiol (MeSH) and malonyl-CoA semialdehyde (**21**). This compound further degrades to acetaldehyde (**22**) through the thioester hydrolysis and decarboxylation [27].

Feeding of (*methyl*-$^2H_6$)DMSP to *Phaeobacter inhibens* DSM 17395 and *Ruegeria pomeroyi* DSM 15171 resulted in the efficient uptake of labelling into dimethyl disulfide (DMDS), the oxidative dimerization product from MeSH, showing the activity of the demethylation pathway in these bacteria. However, knockout of the *dmdA* gene in *R. pomeroyi* still gave a low incorporation of labelling into DMDS, suggesting the presence of another gene responsible for the demethylation activity [28]. Also the labelling from (^{34}S)DMSP was efficiently incorporated into DMDS and dimethyl trisulfide (DMTS) [29]. Our previous investigations have also demonstrated that synthetic, i.e., non-natural DMSP analogues such as 3-(ethylmethyl)sulfoniopropanoate (EMSP), 3-(diethylsulfonio)propanoate (DESP), 3-(dimethylselenio)propanoate (DMSeP; this compound is also formed naturally in *Spartina alterniflora* in the presence of sodium selenate [30]), and even 3-(dimethyltellurio)propanoate (DMTeP) are converted by the demethylation pathway into ethanethiol, methaneselenol, and methanetellurol, respectively, that further react to various volatiles containing EtS, MeSe, and MeTe groups [31]. The in vitro incubations of these DMSP analogues with recombinant DddQ and DddW from *R. pomeroyi* and DddP from *P. inhibens* demonstrated that all substrate analogues can be degraded through the lysis pathway into the corresponding dialkyl chalcogenides; only DMTeP was not cleaved by DddQ [32]. Here we describe the synthesis of the new DMSP analogues 3-(allylmethylsulfonio)propanoate (AllMSP) and 3-(diallylsulfonio)propanoate (DAllSP) and their

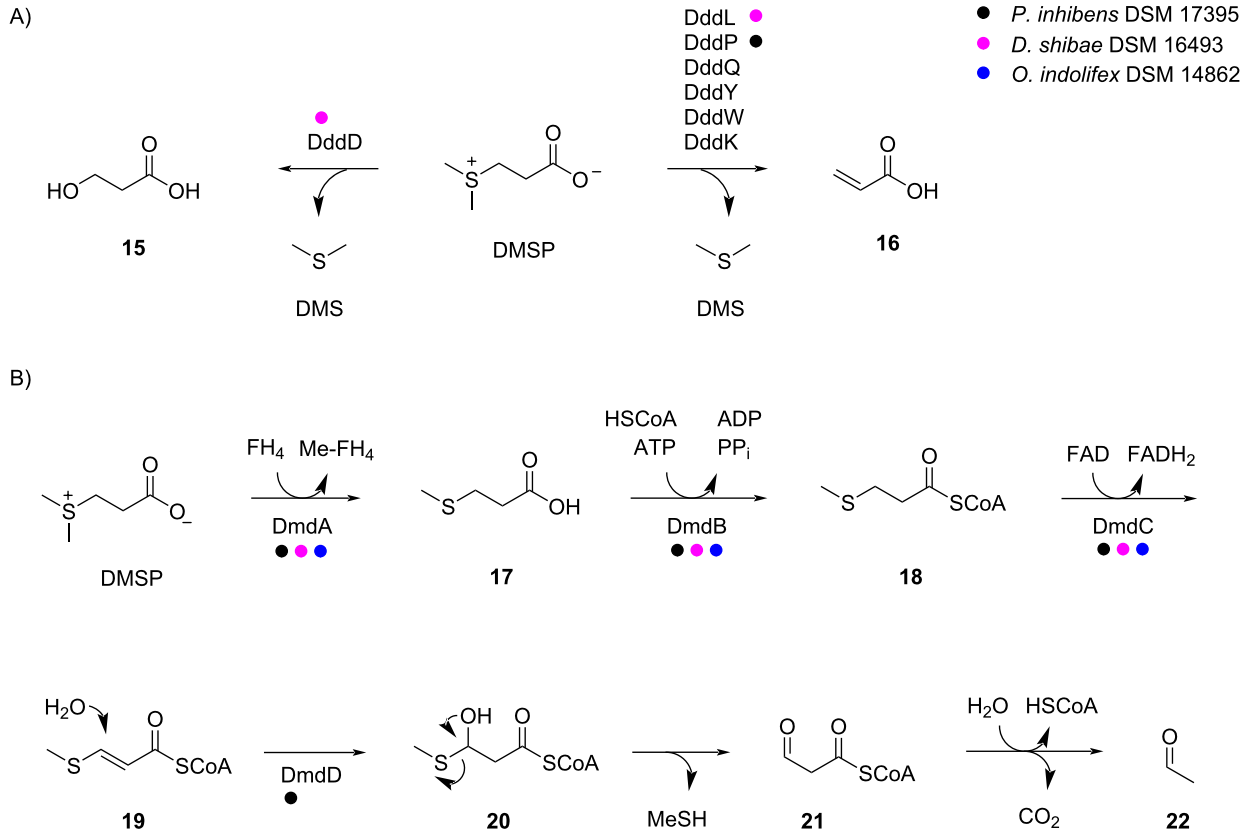

Scheme 2: Degradation of DMSP by marine bacteria. A) Hydrolysis or lysis to DMS, B) demethylation pathway leading to MeSH. The color code shows which enzymes are encoded in the genomes of the strains investigated in this study.

conversion into typical garlic odor constituents by marine bacteria from the *Roseobacter* group that do not naturally occur in these organisms.

Results and Discussion

3-(Diallylsulfonio)propanoate (DAllSP) and 3-(allylmethylsulfonio)propanoate (AllMSP) were synthesized by the acid-catalyzed addition of allyl methyl sulfide and diallyl sulfide, respectively, to acrylic acid (Scheme 3). The obtained DMSP analogues were fed to marine broth agar plate cultures of three strains from the *Roseobacter* group with fully sequenced genomes, including *P. inhibens* DSM 17395, *Dinoroseobacter shibae* DSM 16493, and *Oceanibulbus indolifex* DSM 14862. In all cases the bacterial cultures released a strong garlic-like odor, presumptively due to a degradation of the DMSP derivatives to sulfur-containing volatiles, similar to the compounds known from garlic, through one of the pathways shown in Scheme 2. The emitted volatiles were captured on charcoal filter traps using a closed-loop stripping apparatus (CLSA) [33], followed by the extraction of the filters with CH_2Cl_2 and analysis by gas chromatography–mass spectrometry (GC–MS) of the resulting extracts. Most of the compounds were readily identified by the comparison of their mass spectra and retention indices to published data. Every experiment was performed in triplicate to check for the reproducibility of the results. For comparison, the volatiles from all three strains grown on marine broth medium without the addition of DMSP or its analogues have been reported before [31].

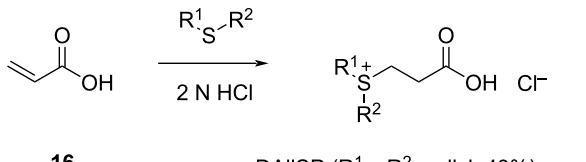

Scheme 3: Synthesis of DMSP derivatives.

Feeding of DAllSP to *P. inhibens* resulted in the production of sulfur volatiles including several allyl derivatives (Figure 1, Figure 2A, Table 1, and Figure S1 in Supporting Information File 1). Besides the methylated sulfur compounds dimethyl trisulfide (**31**), dimethyl tetrasulfide (**33**), and *S*-methyl methanethiosulfonate (**28**) that were reported previously from *P. inhibens* [31], large amounts of diallyl sulfide (**29**) were observed, pointing to an efficient degradation of DAllSP through the lysis pathway, for which the DMSP lyase DddP can account in this organism (Scheme 2). Furthermore, the compounds allyl methyl disulfide (**30**), diallyl disulfide (**2**), allyl methyl trisulfide (**32**), and traces of diallyl trisulfide (**3**) and allyl methyl tetrasulfide (**34**) were observed. The formation of these compounds is explainable by the deallylation of DAllSP to 3-(allylsulfanyl)propanoic acid (**37**) and further degradation to allyl thiol (**13**) through the enzymes of the demethylation pathway that is fully established in *P. inhibens* by genes coding for DmdA–D (Scheme 4A). In the presence of air thiol **13** can then undergo an oxidative dimerization, or react analogously with MeSH to form allyl methyl disulfide (**30**, Scheme 4B). Similar oxidations requiring one additional unit of hydrogen sulfide can lead to the trisulfides **3** and **32** (Scheme 4C), while higher polysulfides such as **34** can arise through a metathesis reaction of two trisulfides (Scheme 4D). Also traces of methyl 3-(allylsulfanyl)propanoate (**24**), methyl 3-(methyldisulfanyl)propanoate (**25**), and methyl 3-(allyldisulfanyl)propanoate (**26**) were observed. While the presence of **24** can be explained by the *O*-methylation of the DmdA product **37** with *S*-adenosylmethionine (SAM, Scheme 4E), compounds **25** and **26** require a second deallylation of **37** to 3-mercaptopropanoic acid (**38**) possibly by DmdA, the reaction with a corresponding thiol MeSH or **13**, and *O*-methylation (Scheme 4F).

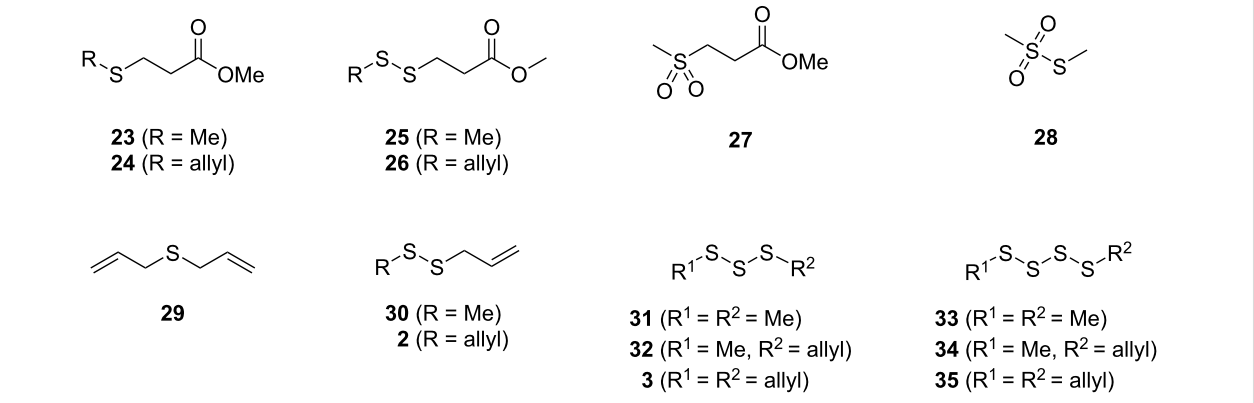

Figure 1: Sulfur volatiles released by agar plate cultures of marine bacteria fed with DAllSP or AllMSP.

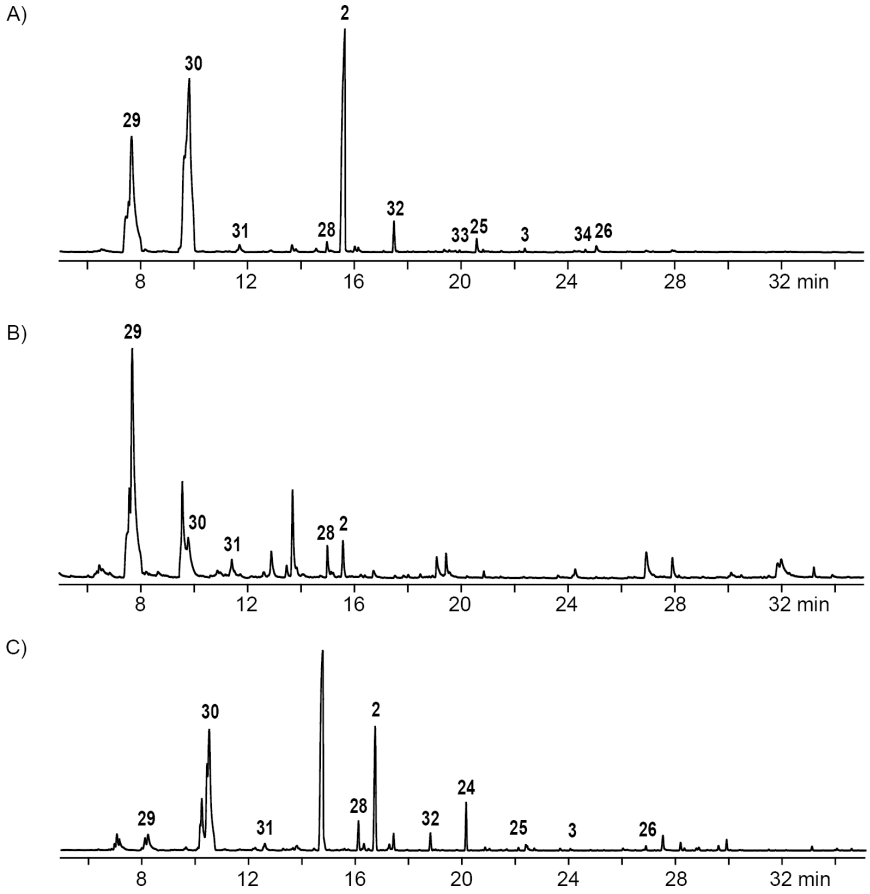

Figure 2: Total ion chromatograms of CLSA extracts obtained from feeding experiments with DAllSP fed to A) *P. inhibens*, B) *D. shibae*, and C) *O. indolifex*. Numbers at peaks refer to compounds in Figure 1. Peaks without numbers are unidentified.

Table 1: Volatiles from agar plate cultures fed with DAllSP.

Compound[a]	*I*	$I_{lit.}$[b]	*P. in.*[c]	*D. sh.*[c]	*O. in.*[c]
diallyl sulfide (**29**)*	849	848 [34]	●●●	●●●	●●●
allyl methyl disulfide (**30**)	910	912 [34]	●●●	●●●	●●●
dimethyl trisulfide (**31**)*	967	970 [35]	●●●	●○●	●●○
S-methyl methanethiosulfonate (**28**)*	1063	1068 [35]	●●●	●●●	●●○
diallyl disulfide (**2**)*	1074	1075 [34]	●●●	●●●	●●●
allyl methyl trisulfide (**32**)	1136	1133 [36]	●●●	○○●	●●●
methyl 3-(allylsulfanyl)-propanoate (**24**)	1177	–	○●○	○○○	●●●
dimethyl tetrasulfide (**33**)	1216	1215 [37]	●●●	○○○	○○○
methyl 3-(methyldisulfanyl)-propanoate (**25**)*	1236	–	●●●	○○●	●○●
diallyl trisulfide (**3**)	1300	1300 [38]	●●●	○○○	●○●
allyl methyl tetrasulfide (**34**)	1382	1371 [39]	●●○	○○○	○○●
methyl 3-(allyldisulfanyl)-propanoate (**26**)*	1397	–	●●●	○○●	●○●
diallyl tetrasulfide (**35**)	1551	1540 [38]	○○○	○○○	○○●

[a]Asterisks indicate the identity to a commercially available or synthetic reference standard. [b]Retention index literature data for a HP5-MS or a similar GC column. [c]Abbreviations are *P. in.* = *Phaeobacter inhibens*, *D. sh.* = *Dinoroseobacter shibae*, and *O. in.* = *Oceanibulbus indolifex*. Filled circles indicate the presence, non-filled circles indicate the absence of a compound in the headspace extract. The colors of the circles refer to the chromatograms in Figure 2 and Figure S1–S3 in Supporting Information File 1 with the same color.

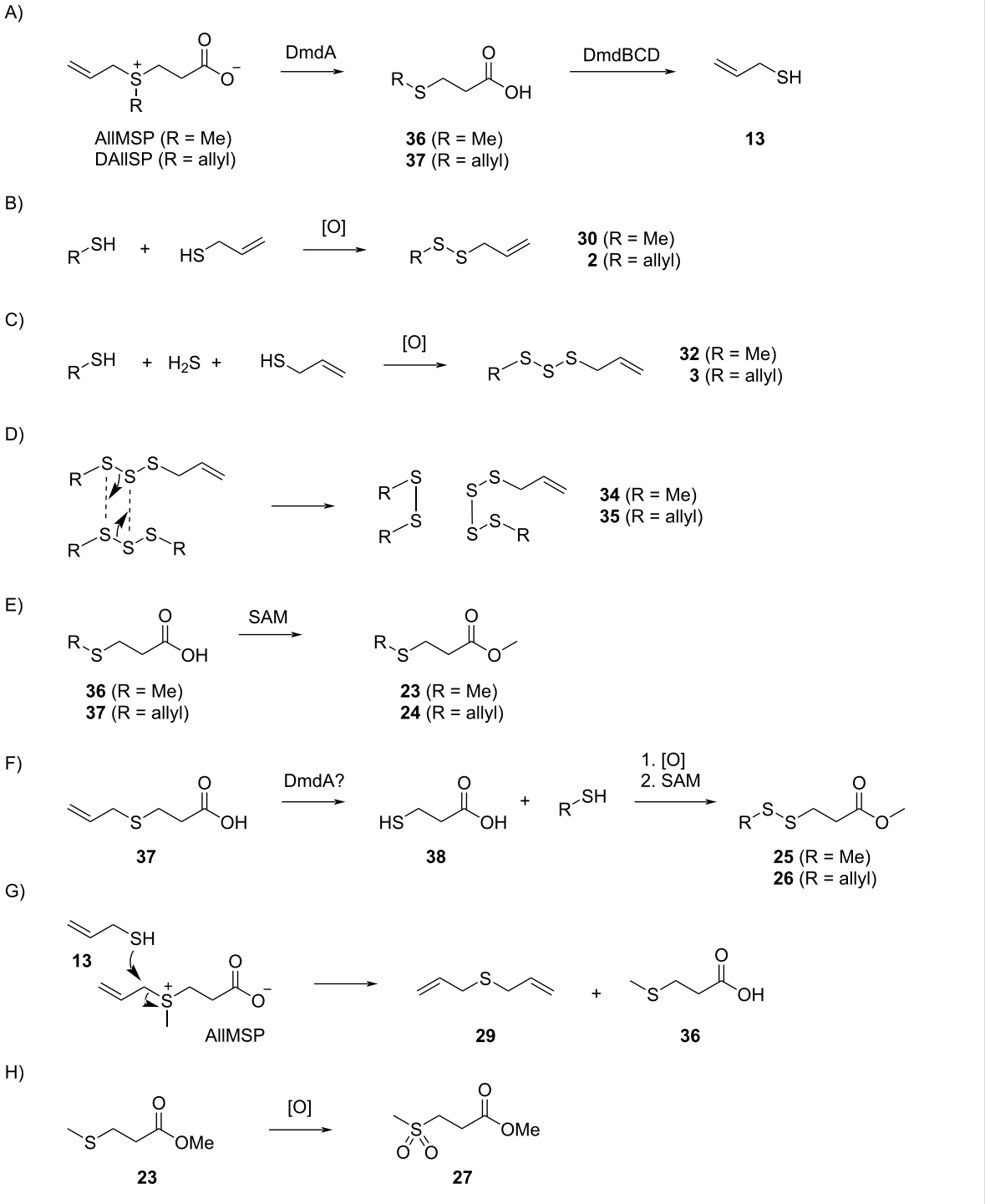

Scheme 4: Proposed mechanisms for the formation of sulfur volatiles from DAllSP and AllMSP.

Very similar patterns of volatiles were obtained in the feeding experiments of DAllSP with *D. shibae* and *O. indolifex* (Figure 2B,C, Table 1 and Figures S2 and S3 in Supporting Information File 1). An additionally observed compound in one analysis of *O. indolifex* was diallyl tetrasulfide (**35**). Both organisms also encode the DMSP demethylation pathway in their genomes, but with missing *dmdD* genes in both cases. A possible explanation is, that another enoyl-CoA hydratase, e.g., from fatty acid degradation, may functionally substitute for DmdD. *Dinoroseobacter shibae* additionally encodes genes for the DMSP hydrolase DddD and the DMSP lyase DddL, explaining the formation of **29**, while no DMSP hydrolase or

lyase is found in *O. indolifex*. Still, compound **29** is observed within this organism, but in lower quantities than in *P. inhibens* or *D. shibae*, and may point to the presence of another, yet unidentified type of DMSP lyase in this organism, because control experiments with medium plates with DAllSP added did not show a spontaneous degradation to **29** that could explain its observation.

The compound identification was based on a comparison to an authentic standard or of mass spectra to data base spectra in our MS libraries and confirmed for most cases by comparison of the retention indices to literature data, only for the mass spectrum of **26** no data base hit was returned. Therefore, a structural suggestion for this compound was based on the observed fragmentation pattern of the mass spectrum (Figure 3A). The molecular ion together with its isotope pattern pointed to two sulfur atoms, while the fragment ion at m/z = 64 ($[S_2]^+$) pointed to a disulfide. The fragment ions at m/z = 59 ($[C_2O_2H_3]^+$) and 161 ($[M - OMe]^+$) indicated a methyl ester, and the series of m/z = 105 ($[C_3H_5S_2]^+$), 73 ($[C_3H_5S]^+$), and 41 ($[C_3H_5]^+$) suggested an allyl disulfide. Taken together, the structure of methyl 3-(allyldisulfa-nyl)propanoate was delineated for compound **26** that was further supported by additional fragmentations as shown in Figure 3A. In addition, compound **26** was synthesized by a method reported previously for the related compound **25** [40], through dimerization of methyl 3-mercaptopropanoate (**39**) to dimethyl 3,3'-disulfanediyldipropanoate (**40**), followed by the $BF_3{\cdot}OEt_2$-mediated metathesis with **2** (Scheme 5A). The synthetic compound **26** was identical by mass spectrum and retention index to the unknown volatile.

The feeding of AllMSP to *P. inhibens* resulted in the formation of large amounts of methyl 3-(methylsulfanyl)propanoate (**23**) in addition to smaller quantities of methyl 3-(allylsulfanyl)propanoate (**24**, Figure 4A, Table 2 and Figure S4 in Supporting Information File 1). While compound **23** can arise from AllMSP by deallylation to 3-(methylsulfanyl)propanoic acid (**36**), potentially through DmdA, and *O*-methylation, the deriva-

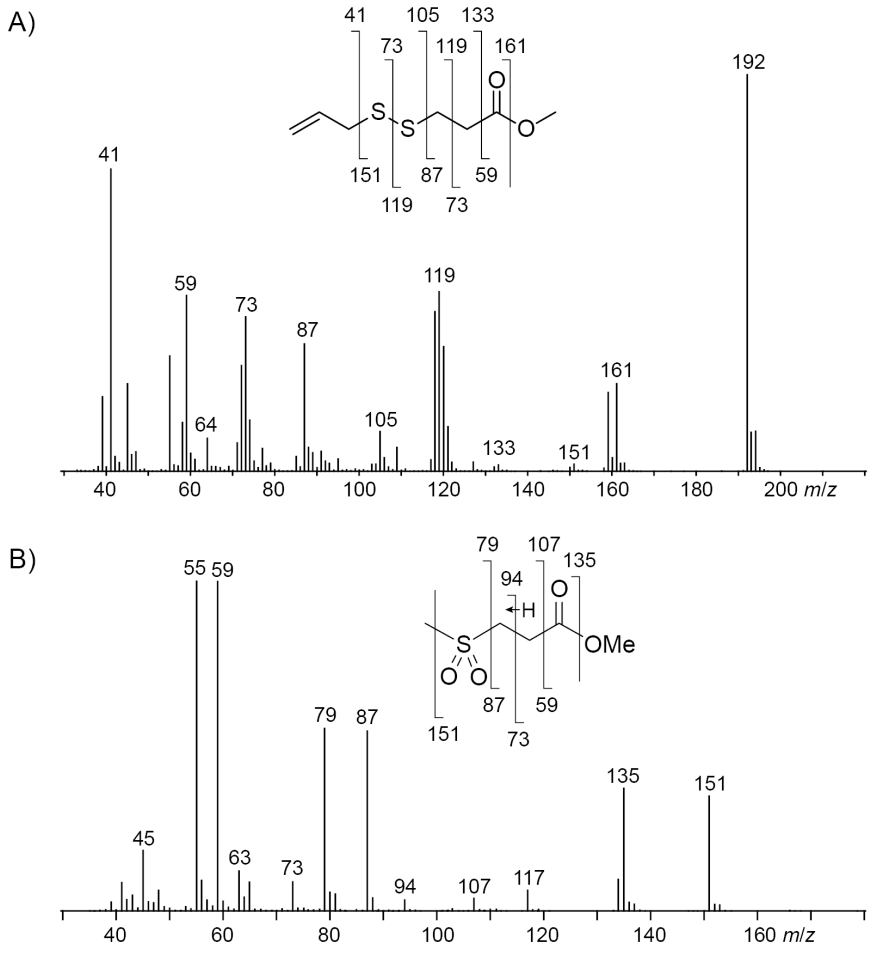

Figure 3: EI mass spectrum and fragmentation pattern of the unknown volatiles A) methyl 3-(allyldisulfanyl)propanoate (**26**) and B) methyl 3-(methylsulfonyl)propanoate (**27**).

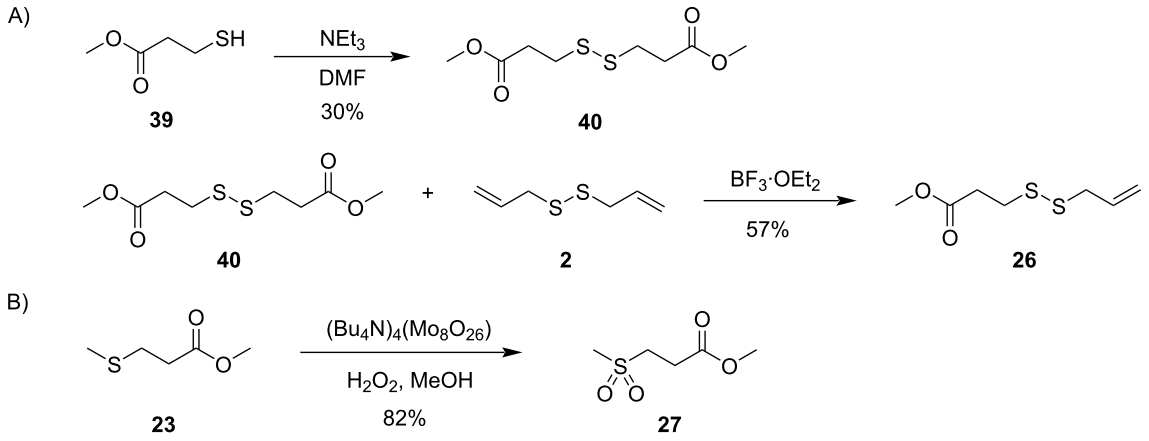

Scheme 5: Synthesis of A) methyl 3-(allyldisulfanyl)propanoate (**26**) and B) methyl 3-(methylsulfonyl)propanoate (**27**).

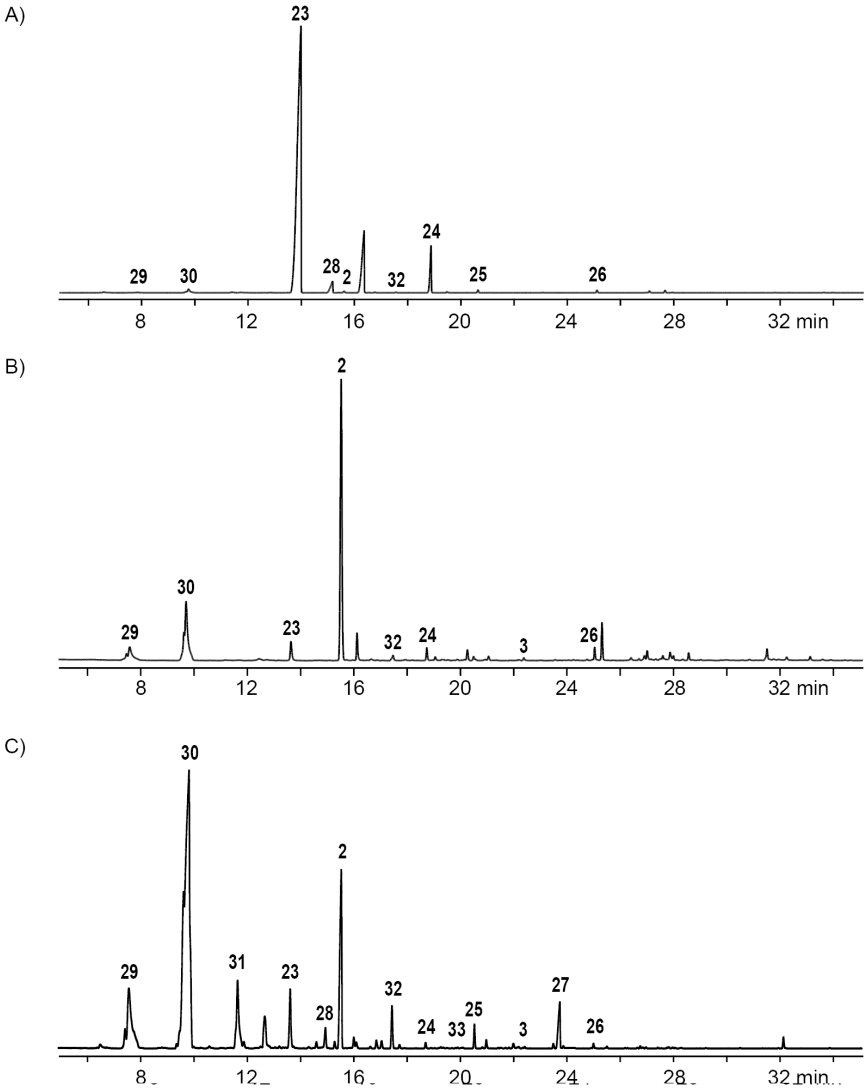

Figure 4: Total ion chromatograms of CLSA extracts obtained from the feeding experiments with AllMSP fed to A) *P. inhibens*, B) *D. shibae*, and C) *O. indolifex*. Numbers at peaks refer to compounds in Figure 1. Peaks without numbers are unidentified.

Table 2: Volatiles from agar plate cultures fed with AllMSP.

Compound[a]	I	$I_{lit.}$[b]		*P. in.*[c]	*D. sh.*[c]	*O. in.*[c]
diallyl sulfide (**29**)*	849	848 [34]	1	●○●	●●●	●●○
allyl methyl disulfide (**30**)	910	912 [34]	2	●●●	●●●	●●●
dimethyl trisulfide (**31**)*	967	970 [35]	3	○○●	○●●	●●○
methyl 3-(methylsulfanyl)-propanoate (**23**)*	1020	1023 [41]	4	●●●	●●●	●●●
S-methyl methanethiosulfonate (**28**)*	1063	1068 [35]	5	●●●	○●●	●●○
diallyl disulfide (**2**)*	1074	1075 [34]	6	●●●	●●●	●●●
allyl methyl trisulfide (**32**)	1136	1133 [36]	7	●●●	●●●	●●●
methyl 3-(allylsulfanyl)propanoate (**24**)	1177	–	8	●●●	●●●	●●●
dimethyl tetrasulfide (**33**)	1216	1215 [37]	9	○○○	○●●	●●○
methyl 3-(methyldisulfanyl)-propanoate (**25**)*	1236	–	10	●●●	○●●	●●●
diallyl trisulfide (**3**)	1300	1300 [38]	11	○○○	●●●	●●●
methyl 3-(methylsulfonyl)propanoate (**27**)*	1353	–	12	○○○	○○○	●●○
methyl 3-(allyldisulfanyl)propanoate (**26**)*	1397	–	13	●●●	●●●	●●●

[a]Asterisks indicate the identity to a commercially available or synthetic reference standard. [b]Retention index literature data for a HP5-MS or a similar GC column. [c]Abbreviations are *P. in.* = *Phaeobacter inhibens*, *D. sh.* = *Dinoroseobacter shibae*, and *O. in.* = *Oceanibulbus indolifex*. Filled circles indicate the presence, non-filled circles indicate the absence of a compound in the headspace extract. The colors of the circles refer to the chromatograms in Figure 4 and Figures S4–S6 in Supporting Information File 1 with the same color.

tive **24** may be formed analogously through intermediate **37** (Scheme 4A and E). The higher production of **23** in comparison to **24** suggests that the deallylation of AllMSP is more efficient than its demethylation, which is surprising, because naturally DmdA catalyzes a methyl-group transfer. This finding may reflect the high reactivity of the allyl group towards nucleophiles. Other compounds originating from AllMSP included the di- and trisulfides **2**, **26**, **30**, and **32** that pointed to a breakdown of AllMSP to **13** through the DMSP demethylation pathway and subsequent oxidative polysulfide formation (Scheme 4A–C), but their formation was lower than from DAllSP, likely because of the discussed efficient deallylation of AllMSP. Small amounts of diallyl sulfide (**29**) were also detected, which is the formal lysis product of DAllSP, but not of AllMSP. In first instance, its formation from AllMSP was surprising, but it is explainable by a degradation of AllMSP to **13**, followed by a nucleophilic attack at the allyl group of another AllMSP molecule (Scheme 4G). For *D. shibae* and *O. indolifex* the same pattern of compounds was found (Figure 4B,C, and Figures S5 and S6 in Supporting Information File 1), only the production of the deallylated compound **23** was lower, while in turn the production of the di- and trisulfides from **13** and of **29** was increased. This suggests that the deallylation of AllMSP by the DmdA variants in these organisms may be less efficient than was observed for *P. inhibens*. Besides these sulfur compounds, only *O. indolifex*, but not the other two strains, released another compound, **27**, whose mass spectrum was not included in our databases. The analysis of the fragmentation pattern (Figure 3B) suggested that **27** could be methyl 3-(methylsulfonyl)propanoate, an oxidation product of **23**. This hypothesis was confirmed by the chemical oxidation of **23**, yielding methyl 3-(methylsulfonyl)propanoate with an identical mass spectrum and retention index to the volatile **27** (Scheme 5B). This compound may arise from **23** by the action of an oxygenase that is restricted to *O. indolifex* and not encoded in the genomes of the other two species. Its spontaneous formation from **23** in the presence of air can be excluded, because other cultures forming **23** did not show the release of **27**.

Conclusion

Bacteria from the *Roseobacter* group can degrade DMSP analogues with *S*-allyl groups including AllMSP and DAllSP, likely with the participation of the enzymes for DMSP (hydro)lysis and from the DMSP demethylation pathway. Because MeSH can also originate from other sources, the DMSP derivatives used in this study can lead to products that can indicate which metabolic pathways are used for their conversion. Interestingly, the volatiles formed from AllMSP and DAllSP closely resemble flavoring compounds from garlic. The demethylation pathway with all four enzymes DmdABCD is fully established in *P. inhibens*, while genes for DmdD are missing in *D. shibae* and *O. indolifex*, suggesting that another enzyme with a low sequence homology may substitute for DmdD, leading to allylthiol and several sulfur volatiles derived from it in all three strains. The DMSP hydrolase DddD and the lyase DddL are present in *D. shibae*, and *P. inhibens* has a DMSP lyase DddP, which can explain the conversion of

DAllSP into diallyl sulfide, while the reason for its formation in *O. indolifex* is currently unclear and may point to an unknown type of DMSP lyase in this organism. Since the observed patterns of allylated sulfur volatiles in the three investigated strains are different, it seems possible that the DMSP (hydro)lases and the enzymes from the DMSP demethylation pathway have different activities towards AllMSP and DAllSP. In vitro studies with recombinant purified enzymes and mutational work will be needed for more detailed insights to support our hypotheses regarding the involved enzymes in AllMSP and DAllSP breakdown and will be performed in our laboratories in the future.

Experimental

Strains and culture condition

Phaeobacter inhibens DSM 14862, *Dinoroseobacter shibae* DSM 16493, *Oceanibulbus indolifex* DSM 14862 were precultured in full strength marine broth medium (MB 2216, Roth) at 28 °C with shaking at 180 rpm until the OD value reached about 1.0.

Feeding experiments and sampling of volatiles

Headspace samplings for each strain were done in triplicates. For the feeding experiments, DAllSP or AlMSP (1 mM) were added to the full strength marine broth agar medium (MB2216) after autoclavation. The medium was then transferred into glass Petri dishes. The agar plates were inoculated with the precultures (400 µL), incubated for two days at 28 °C and then subjected for headspace extraction to a CLSA [33] for 24 h. The released volatiles were collected on charcoal filters (Chromtech, Idstein, Germany), followed by the extraction of the filters with dichloromethane (50 µL), and analysis of the extracts by GC–MS. For comparison, blank experiments with MB medium alone and with MB agar plates spiked with DAllSP or AlMSP were performed in the same way. All the volatiles mentioned in Table 1 and Table 2 were not observed in the blank experiments.

GC–MS

The GC–MS analyses were carried out on a HP7890A GC system connected to a HP5975C mass selective detector fitted with a HP-5MS fused silica capillary column (30 m × 0.22 mm i.d., 0.25 µm film, Hewlett-Packard). The conditions were: inlet pressure: 67 kPa, He 23.3 mL min^{-1}; injection volume: 1 µL; injector: 250 °C; transfer line: 300 °C; electron energy: 70 eV. The GC was programmed as follows: 50 °C (5 min isothermic), increasing at 5 °C min^{-1} to 320 °C and operated in the splitless mode (60 s valve time); carrier gas (He): 1.2 mL min^{-1}. The retention indices were determined from *n*-alkane standards (C_8–C_{32}) [42].

General synthetic methods

All chemicals were purchased from TCI (Deutschland) or Sigma-Aldrich Chemie (Germany), and used without purification. Solvents were distilled and dried by standard methods. NMR spectra were recorded on a Bruker (Billerica, USA) Avance III HD Prodigy (500 MHz) or on an Avance III HD Cryo (700 MHz) NMR spectrometer. The spectra were referenced against solvent signals (^{1}H NMR, residual proton signal: D_2O δ = 4.79 ppm, $CDCl_3$ δ = 7.26 ppm, d_6-DMSO δ = 2.50 ppm; ^{13}C NMR: $CDCl_3$ δ = 77.16 ppm, d_6-DMSO δ = 39.52 ppm). The coupling constants are given in Hz. IR spectra were recorded on a Bruker α spectrometer equipped with a diamond-ATR probe. The relative intensities of signals are indicated by w (weak), m (medium), and s (strong).

Synthesis of allyl DMSP derivatives

A mixture of acrylic acid (0.72 g, 10 mmol) and diallyl sulfide or allylmethyl sulfide (10 mmol) was treated with 2 N HCl at 80 °C for 4 h. The reaction mixture was concentrated in vacuo and the residue was purified by silica gel column chromatography (CH_2Cl_2/MeOH 5:1), followed by recrystallization from methanol/diethyl ether 1:1 to yield the pure compounds.

DAllSP·HCl. Yield: 960 mg (4.32 mmol, 43%). ^{1}H NMR (D_2O, 700 MHz) δ 5.98 (ddt, *J* = 17.5, 10.2, 7.4, 2H), 5.73 (d, *J* = 10.2, 2H), 5.72 (d, *J* = 17.0, 2H), 4.08 (d, *J* = 7.4, 4H), 3.43 (t, *J* = 6.9, 2H), 2.78 (t, *J* = 6.9, 2H); ^{13}C NMR (D_2O, 175 MHz) δ 177.05 (C), 127.65 (2 × CH), 123.54 (2 × CH_2), 41.53 (2 × CH_2), 35.08 (CH_2), 31.68 (CH_2); HRMS–EI (*m*/*z*): calcd for $[C_9H_{15}O_2S]^+$, 187.0787; found, 187.0790.

AllMSP·HCl. Yield: 1.06 g (5.41 mmol, 54%). ^{1}H NMR (D_2O, 700 MHz) δ 5.96 (ddt, *J* = 17.5, 10.2, 7.5, 1H), 5.74 (d, *J* = 10.2, 1H), 5.71 (d, *J* = 17.2, 1H), 4.13 (dd, *J* = 13.4, 7.4, 1H), 4.09 (dd, *J* = 13.4, 7.5, 1H), 3.58 (dt, *J* = 13.7, 6.9, 1H), 3.47 (dt, *J* = 13.5, 6.7, 1H), 3.04 (t, *J* = 6.8, 2H), 2.91 (s, 3H); ^{13}C NMR (D_2O, 175 MHz) δ 173.77 (C), 128.19 (CH), 122.74 (CH_2), 43.82 (CH_2), 35.84 (CH_2), 28.75 (CH_2), 21.72 (CH_3); HRMS–EI (*m*/*z*): calcd for $[C_7H_{13}O_2S]^+$, 161.0631; found, 161.0630.

Synthesis of dimethyl 3,3'-disulfanediyldipropanoate (**40**)

A solution of methyl 3-mercaptopropanoate (6.00 g, 50.0 mmol, 1.0 equiv) and triethylamine (5.05 g, 50.0 mmol) in DMF (10 mL) was treated for 24 h at 40 °C. The reaction was quenched by the addition of water and the aqueous phase extracted with ethyl acetate. The extract was dried with $MgSO_4$ and then concentrated in vacuo. The residue was purified by silica column chromatography (cyclohexane/EtOAc 5:1) to give compound **40** (1.80 g, 7.56 mmol, 30%) as pale yellow oil. TLC

R_f 0.44 (cyclohexane/EtOAc 10:3); IR (diamond-ATR) ṽ: 2998 (w), 2952 (w), 2845 (w), 2256 (w), 1730 (m), 1436 (w), 1354 (w), 1240 (w), 1215(w), 1195 (w), 1171 (w), 1139 (w), 1046 (w), 1017 (w), 979 (w), 907 (w), 822 (w), 726 (m), 648 (w), 435 (w) cm^{-1}; ^1H NMR ($CDCl_3$, 500 MHz) δ 3.64 (s, 6H), 2.87 (t, J = 7.2, 4H), 2.68 (t, J = 7.2, 4H) ppm; ^{13}C NMR ($CDCl_3$, 125 MHz) δ 172.11 (2 × C), 51.90 (2 × CH_3), 33.93 (2 × CH_2), 33.16 (2 × CH_2) ppm.

Synthesis of methyl 3-(allyldisulfanyl)propanoate (**26**)

To a solution of dimethyl 3,3'-disulfanediyldipropanoate (**40**, 0.50 g, 2.10 mmol, 1.0 equiv) and diallyl disulfide (**2**, 0.31 g, 2.10 mmol, 1.0 equiv) in dry DCM (10 mL) and CH_3NO_2 (10 mL) at 0 °C $BF_3{\cdot}OEt_2$ (30 mg, 0.21 mmol, 0.1 equiv) was added. The reaction mixture was stirred at 0 °C for 3 h and at room temperature overnight. The reaction was quenched by the addition of water and extracted with ethyl acetate. The extracts were dried with $MgSO_4$ and concentrated in vacuo. The obtained residue was purified by silica gel column chromatography (cyclohexane/EtOAc 5:1) to give compound **26** (0.23 g, 1.20 mmol, 57%). TLC R_f = 0.72 (cyclohexane/EtOAc = 1:1); IR (diamond-ATR) ṽ: 3082 (w), 2950 (w), 2845 (w), 1736 (s), 1634 (w), 1435 (w), 1354 (w), 1277 (w), 1240 (w), 1216 (w), 1172 (w), 1144 (w), 1017 (w), 985 (w), 922 (w), 859 (w), 820 (w), 756 (w), 722 (w), 669 (w), 582 (w), 478 (w), 435 (w) cm^{-1}; ^1H NMR ($CDCl_3$, 500 MHz) δ 5.83 (ddt, J = 17.1, 9.9, 7.3, 1H), 5.19 (ddt, J = 16.9, 1.3, 1.3, 1H), 5.14 (dm, J = 10.0, 1H), 3.69 (s, 3H), 3.32 (dm, J = 7.3, 2H), 2.91 (t, J = 7.2, 2H), 2.72 (t, J = 7.2, 2H) ppm; ^{13}C NMR ($CDCl_3$, 125 MHz) δ 172.14 (C), 132.71 (CH), 119.40 (CH_2), 52.04 (CH_3), 41.60 (CH_2), 33.87 (CH_2), 33.40 (CH_2) ppm; HRMS–EI (*m/z*): calcd for $[C_7H_{12}O_2S_2]^+$, 192.0273; found, 192.0289.

Synthesis of methyl 3-(methylsulfonyl)propanoate (**27**)

To a stirred solution of $[(n\text{-}C_4H_9)_4N]_4(Mo_8O_{26})$ (5 mg, 2.5 µmol, 0.001 equiv) [43] in methanol (4 mL), methyl 3-methylthiopropanoate (335 mg, 2.50 mmol, 1.0 equiv) was added at 40 °C. After the reaction mixture was stirred for 5 minutes, 30% hydrogen peroxide solution (0.52 mL, 0.57 g, 5.0 mmol, 2.0 equiv) was added dropwise. The color of the reaction mixture changed from colorless to yellow. The reaction mixture was stirred for 30 minutes at room temperature. After completion of the reaction, EtOAc (10 mL) was added, causing precipitation of the catalyst. The catalyst was filtered off, the filtrate was dried with $MgSO_4$ and concentrated in vacuo to give pure **27** (0.34 g, 2.05 mmol, 82%) as colorless solid. TLC R_f 0.17 (cyclohexane/EtOAc 1:1); IR (diamond-ATR) ṽ: 3014 (w), 2948 (w), 2932 (w), 1762 (m), 1687 (w), 1442 (w), 1433 (w), 1418 (w), 1375 (w), 1331 (w), 1306 (m), 1373 (m), 1259 (m), 1203 (w), 1180 (w), 1131 (m), 1056 (w), 1004 (w), 988 (w), 971 (w), 956 (w), 898 (w), 786 (w), 774 (w), 749 (w), 601 (w), 514 (w), 505 (w), 441 (w) cm^{-1}; ^1H NMR (d_6-DMSO, 500 MHz) δ 3.63 (s, 3H), 3.37 (t, J = 7.5, 2H), 3.01 (s, 3H), 2.78 (t, J = 7.5, 2H) ppm; ^{13}C NMR (d_6-DMSO, 125 MHz) δ 170.79 (C), 51.88 (CH_3), 49.14 (CH_2), 40.21 (CH_3), 26.89 (CH_2) ppm.

Supporting Information

Supporting Information File 1

Additional total ion chromatograms and copies of NMR spectra.
[https://www.beilstein-journals.org/bjoc/content/supplementary/1860-5397-17-51-S1.pdf]

Funding

This work was funded by the DFG (SFB TR 51 "*Roseobacter*").

ORCID® iDs

Jeroen S. Dickschat - https://orcid.org/0000-0002-0102-0631

References

1. Wertheim, T. *Ann. Chem. Pharm.* **1844,** *51,* 289–315. doi:10.1002/jlac.18440510302
2. Semmler, F. W. *Arch. Pharm. (Weinheim, Ger.)* **1892,** *230,* 434–443. doi:10.1002/ardp.18922300603
3. Cavallito, C. J.; Buck, J. S.; Suter, C. M. *J. Am. Chem. Soc.* **1944,** *66,* 1952–1954. doi:10.1021/ja01239a049
4. Shang, A.; Cao, S.-Y.; Xu, X.-Y.; Gan, R.-Y.; Tang, G.-Y.; Corke, H.; Mavumengwana, V.; Li, H.-B. *Foods* **2019,** *8,* 246. doi:10.3390/foods8070246
5. Block, E.; Ahmad, S.; Jain, M. K.; Crecely, R. W.; Apitz-Castro, R.; Cruz, M. R. *J. Am. Chem. Soc.* **1984,** *106,* 8295–8296. doi:10.1021/ja00338a049
6. Stoll, A.; Seebeck, E. *Helv. Chim. Acta* **1948,** *31,* 189–210. doi:10.1002/hlca.19480310140
7. Stoll, A.; Seebeck, E. *Helv. Chim. Acta* **1949,** *32,* 197–205. doi:10.1002/hlca.19490320129
8. Block, E. *Angew. Chem., Int. Ed. Engl.* **1992,** *31,* 1135–1178. doi:10.1002/anie.199211351
9. Brodnitz, M. H.; Pascale, J. V.; Van Derslice, L. *J. Agric. Food Chem.* **1971,** *19,* 273–275. doi:10.1021/jf60174a007
10. Segev, E.; Wyche, T. P.; Kim, K. H.; Petersen, J.; Ellebrandt, C.; Vlamakis, H.; Barteneva, N.; Paulson, J. N.; Chai, L.; Clardy, J.; Kolter, R. *eLife* **2016,** *5,* e17473. doi:10.7554/elife.17473
11. Barak-Gavish, N.; Frada, M. J.; Ku, C.; Lee, P. A.; DiTullio, G. R.; Malitsky, S.; Aharoni, A.; Green, S. J.; Rotkopf, R.; Kartvelishvily, E.; Sheyn, U.; Schatz, D.; Vardi, A. *Sci. Adv.* **2018,** *4,* eaau5716. doi:10.1126/sciadv.aau5716
12. Kessler, R. W.; Weiss, A.; Kuegler, S.; Hermes, C.; Wichard, T. *Mol. Ecol.* **2018,** *27,* 1808–1819. doi:10.1111/mec.14472

13. Schulz, S.; Dickschat, J. S. *Nat. Prod. Rep.* **2007,** *24,* 814–842. doi:10.1039/b507392h
14. Dickschat, J. S. *Nat. Prod. Rep.* **2017,** *34,* 310–328. doi:10.1039/c7np00003k
15. Dickschat, J. S.; Wagner-Döbler, I.; Schulz, S. *J. Chem. Ecol.* **2005,** *31,* 925–947. doi:10.1007/s10886-005-3553-9
16. Dickschat, J. S.; Reichenbach, H.; Wagner-Döbler, I.; Schulz, S. *Eur. J. Org. Chem.* **2005,** 4141–4153. doi:10.1002/ejoc.200500280
17. Thiel, V.; Brinkhoff, T.; Dickschat, J. S.; Wickel, S.; Grunenberg, J.; Wagner-Döbler, I.; Simon, M.; Schulz, S. *Org. Biomol. Chem.* **2010,** *8,* 234–246. doi:10.1039/b909133e
18. Dickschat, J. S.; Rabe, P.; Citron, C. A. *Org. Biomol. Chem.* **2015,** *13,* 1954–1968. doi:10.1039/c4ob02407a
19. Todd, J. D.; Rogers, R.; Li, Y. G.; Wexler, M.; Bond, P. L.; Sun, L.; Curson, A. R. J.; Malin, G.; Steinke, M.; Johnston, A. W. B. *Science* **2007,** *315,* 666–669. doi:10.1126/science.1135370
20. Curson, A. R. J.; Rogers, R.; Todd, J. D.; Brearley, C. A.; Johnston, A. W. B. *Environ. Microbiol.* **2008,** *10,* 757–767. doi:10.1111/j.1462-2920.2007.01499.x
21. Todd, J. D.; Curson, A. R. J.; Dupont, C. L.; Nicholson, P.; Johnston, A. W. B. *Environ. Microbiol.* **2009,** *11,* 1376–1385. doi:10.1111/j.1462-2920.2009.01864.x
22. Todd, J. D.; Curson, A. R. J.; Kirkwood, M.; Sullivan, M. J.; Green, R. T.; Johnston, A. W. B. *Environ. Microbiol.* **2011,** *13,* 427–438. doi:10.1111/j.1462-2920.2010.02348.x
23. Curson, A. R. J.; Sullivan, M. J.; Todd, J. D.; Johnston, A. W. B. *ISME J.* **2011,** *5,* 1191–1200. doi:10.1038/ismej.2010.203
24. Todd, J. D.; Kirkwood, M.; Newton-Payne, S.; Johnston, A. W. B. *ISME J.* **2012,** *6,* 223–226. doi:10.1038/ismej.2011.79
25. Sun, J.; Todd, J. D.; Thrash, J. C.; Qian, Y.; Qian, M. C.; Temperton, B.; Guo, J.; Fowler, E. K.; Aldrich, J. T.; Nicora, C. D.; Lipton, M. S.; Smith, R. D.; de Leenheer, P.; Payne, S. H.; Johnston, A. W. B.; Davie-Martin, C. L.; Halsey, K. H.; Giovannoni, S. J. *Nat. Microbiol.* **2016,** *1,* 16065. doi:10.1038/nmicrobiol.2016.65
26. Howard, E. C.; Henriksen, J. R.; Buchan, A.; Reisch, C. R.; Bürgmann, H.; Welsh, R.; Ye, W.; González, J. M.; Mace, K.; Joye, S. B.; Kiene, R. P.; Whitman, W. B.; Moran, M. A. *Science* **2006,** *314,* 649–652. doi:10.1126/science.1130657
27. Reisch, C. R.; Stoudemayer, M. J.; Varaljay, V. A.; Amster, I. J.; Moran, M. A.; Whitman, W. B. *Nature* **2011,** *473,* 208–211. doi:10.1038/nature10078
28. Brock, N. L.; Citron, C. A.; Zell, C.; Berger, M.; Wagner-Döbler, I.; Petersen, J.; Brinkhoff, T.; Simon, M.; Dickschat, J. S. *Beilstein J. Org. Chem.* **2013,** *9,* 942–950. doi:10.3762/bjoc.9.108
29. Brock, N. L.; Menke, M.; Klapschinski, T. A.; Dickschat, J. S. *Org. Biomol. Chem.* **2014,** *12,* 4318–4323. doi:10.1039/c4ob00719k
30. Ansede, J. H.; Pellechia, P. J.; Yoch, D. C. *Environ. Sci. Technol.* **1999,** *33,* 2064–2069. doi:10.1021/es9812296
31. Dickschat, J. S.; Zell, C.; Brock, N. L. *ChemBioChem* **2010,** *11,* 417–425. doi:10.1002/cbic.200900668
32. Burkhardt, I.; Lauterbach, L.; Brock, N. L.; Dickschat, J. S. *Org. Biomol. Chem.* **2017,** *15,* 4432–4439. doi:10.1039/c7ob00913e
33. Grob, K.; Zürcher, F. *J. Chromatogr.* **1976,** *117,* 285–294. doi:10.1016/0021-9673(76)80005-2
34. Ansorena, D.; Astiasarán, I.; Bello, J. *J. Agric. Food Chem.* **2000,** *48,* 2395–2400. doi:10.1021/jf990931y
35. Kubec, R.; Drhová, V.; Velíšek, J. *J. Agric. Food Chem.* **1998,** *46,* 4334–4340. doi:10.1021/jf980379x
36. Ansorena, D.; Gimeno, O.; Astiasarán, I.; Bello, J. *Food Res. Int.* **2001,** *34,* 67–75. doi:10.1016/s0963-9969(00)00133-2
37. Bonaïti, C.; Irlinger, F.; Spinnler, H. E.; Engel, E. *J. Dairy Sci.* **2005,** *88,* 1671–1684. doi:10.3168/jds.s0022-0302(05)72839-3
38. Zoghbi, M. d. G. B.; Andrade, E. H. A.; Maia, J. G. S. *Flavour Fragrance J.* **2002,** *17,* 133–135. doi:10.1002/ffj.1051
39. Mnayer, D.; Fabiano-Tixier, A.-S.; Petitcolas, E.; Hamieh, T.; Nehme, N.; Ferrant, C.; Fernandez, X.; Chemat, F. *Molecules* **2014,** *19,* 20034–20053. doi:10.3390/molecules191220034
40. Hahnke, S.; Brock, N. L.; Zell, C.; Simon, M.; Dickschat, J. S.; Brinkhoff, T. *Syst. Appl. Microbiol.* **2013,** *36,* 39–48. doi:10.1016/j.syapm.2012.09.004
41. Beaulieu, J. C.; Grimm, C. C. *J. Agric. Food Chem.* **2001,** *49,* 1345–1352. doi:10.1021/jf0005768
42. van Den Dool, H.; Dec. Kratz, P. *J. Chromatogr.* **1963,** *11,* 463–471. doi:10.1016/s0021-9673(01)80947-x
43. Yang, C.; Jin, Q.; Zhang, H.; Liao, J.; Zhu, J.; Yu, B.; Deng, J. *Green Chem.* **2009,** *11,* 1401–1405. doi:10.1039/b912521n

License and Terms

Appendix C

Discovery of dimethylsulfoxonium propionate lyases – a missing enzyme relevant to the global sulfur cycle

Org. Biomol. Chem. **2023**, *21*, 3083–3089

DOI: 10.1039/D2OB02288E

Organic & Biomolecular Chemistry

ROYAL SOCIETY OF CHEMISTRY

COMMUNICATION

View Article Online
View Journal

Cite this: DOI: 10.1039/d2ob02288e

Received 20th December 2022,
Accepted 15th March 2023

DOI: 10.1039/d2ob02288e

rsc.li/obc

Discovery of dimethylsulfoxonium propionate lyases – a missing enzyme relevant to the global sulfur cycle†

Anuj K. Chhalodia and Jeroen S. Dickschat *

Six dimethylsulfoniopropionate (DMSP) lyases have been shown to cleave the marine sulfur metabolite dimethylsulfoxonium propionate (DMSOP) into DMSO and acrylate. This discovery characterises a missing enzyme relevant to the global sulfur cycle.

Prompted by the observation of Haas that marine algae release dimethyl sulfide (DMS) upon exposure to air,[1] dimethylsulfoniopropionate (DMSP) was first isolated from the red alga *Polysiphonia fastigiata*.[2] It was subsequently also reported in green algae,[3] dinoflagellates,[4] coccolithophores,[5] higher plants from estuarine habitats,[6] and corals.[7] DMSP mainly functions as an osmolyte[5] and a cryoprotectant.[8] Its cleavage to DMS and acrylic acid (Scheme 1A) by an algal enzyme has been noticed already in 1956[9] and was followed by the isolation of DMSP lyases from algae[10] and marine bacteria.[11,12] This enzymatic reaction is triggered by zooplankton grazing on algae, and the formation of DMS has been made responsible for the antipredatory activity of DMSP.[13] The second cleavage product acrylic acid (**1a**) shows antibacterial activity and is also present in marine algae in substantial amounts.[14] The biosynthesis of DMSP by marine algae,[15] bacteria[16] and corals[17] sums up to amounts in the petagram range,[18] and its degradation to the volatile DMS leads to an estimated annual flux of 13–37 teragrams of sulfur from the oceans into the atmosphere.[19] This process is important not only for the global sulfur cycle,[20] but also for the climate on the Earth, because atmospheric DMS becomes oxidised to sulfate, which leads to sulfate aerosols and cloud formation with a cooling effect on the planet (Scheme 2).[21,22] Besides the DMSP hydrolase DddD that catalyses the hydrolytic cleavage of DMSP through the formation of the coenzyme A thioester to yield DMS and 3-hydroxypropionyl-SCoA (**2**),[23] several DMSP lyases were identified from marine bacteria (DddL, DddP, DddQ, DddW, DddY and DddK)[24–29] and from the coccolithophore *Emiliania huxleyi* (Alma1, Scheme 1A).[30] Recently, another DMSP lyase DddX has been reported in *Psychrobacter* sp. D2 that converts DMSP into

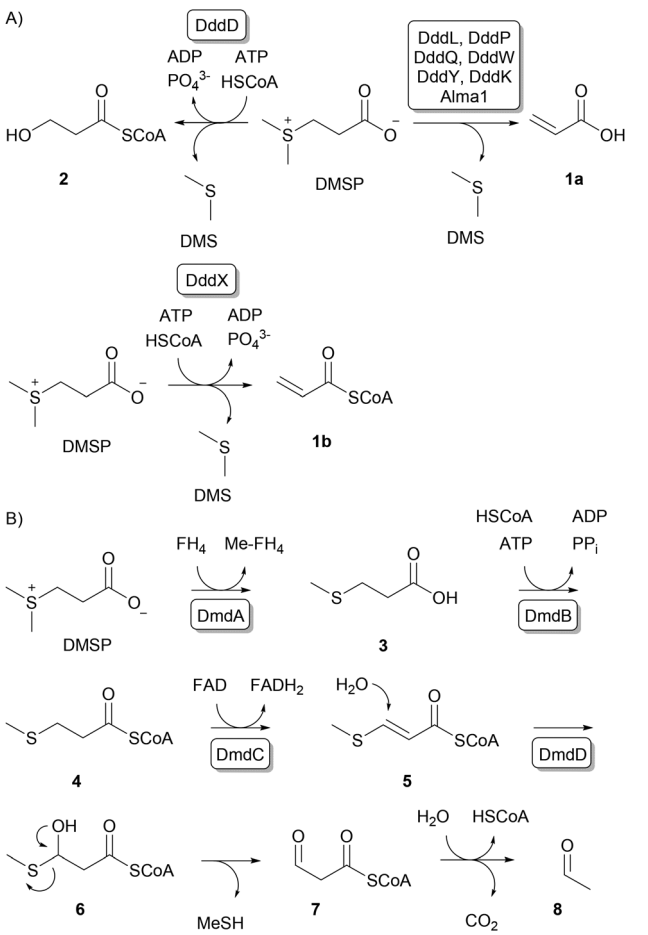

Scheme 1 DMSP degradation pathways. (A) DMSP degradation to DMS through lysis or hydrolysis. (B) DMSP demethylation pathway.

Kekulé-Institute for Organic Chemistry and Biochemistry, University of Bonn, Gerhard-Domagk-Straße 1, 53121 Bonn, Germany. E-mail: dickschat@uni-bonn.de

† Electronic supplementary information (ESI) available: Experimental procedures for gene cloning and expression, synthesis of (methyl-$^{13}C_2$)DMSOP, ^{13}C-NMR spectra of activity assays (pH and temperature dependency), determination of Michaelis–Menten parameters, and NMR spectra of synthetic compounds. See DOI: https://doi.org/10.1039/d2ob02288e

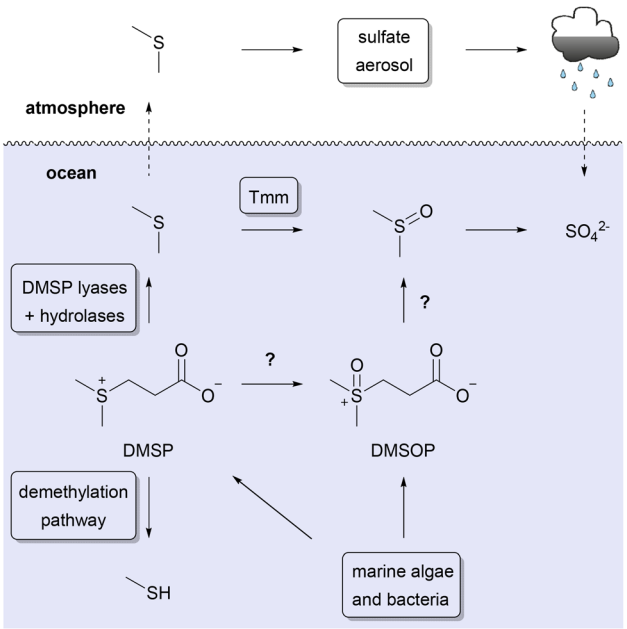

Scheme 2 The global sulfur cycle.

the coenzyme A thioester, followed by cleavage to acryloyl-SCoA (**1b**) and DMS.[31]

Also a DMSP demethylation pathway is known (Scheme 1B) that proceeds through demethylation of DMSP to **3** by DmdA[32] and subsequent conversion into the coenzyme A thioester **4** by DmdB. The FAD-dependent dehydrogenation to **5** by DmdC is followed by hydration to **6** through the enoyl-CoA hydratase DmdD. Spontaneous cleavage of the hemithioacetal in **6** causes the liberation of MeSH and the formation of **7** that upon thioester hydrolysis and decarboxylation leads to acetaldehyde.[33] MeSH is much more water soluble than DMS, and therefore, these reactions contribute to a reduction of the oceanic emission of volatile sulfur compounds into the atmosphere.

Large amounts of DMS are oxidised to the water soluble compounds DMSO and sulfate, either enzymatically or photochemically.[34,35] Specifically, it has been shown that pelagic bacteria can oxidise DMS through trimethylamine monooxygenase (Tmm)[36] to DMSO. The importance of these processes is demonstrated by the fact that the concentration of DMSO in water samples is often even higher than the concentrations of DMS and DMSP.[37] Recently, the DMSP derivative

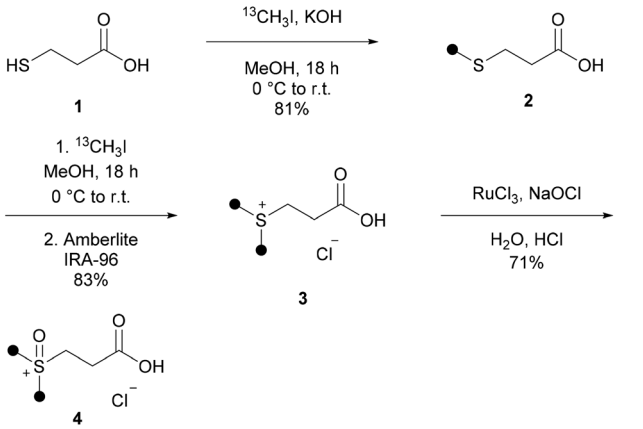

Scheme 3 Synthesis of (methyl-$^{13}C_2$)DMSOP (**4**).

Table 1 Source organisms and properties of enzymes investigated in this study

Enzyme	Source organism	pH optimum[a]	Temperature optimum[b]/°C
DddW	*R. pomeroyi*	pH 8	10 °C
DddQ	*R. pomeroyi*	pH 8	10 °C
DddP	*R. pomeroyi*	pH 6	30 °C
DddK	*C. halophilus*	pH 8	30 °C
DddL	*D. shibae*	pH 9	30 °C
DddY	*F. balearica*	pH 8	10 °C

[a] pH optimum with the substrate DMSOP at 30 °C. [b] Temperature optimum with the substrate DMSOP at pH 8 (for DddP at pH 6).

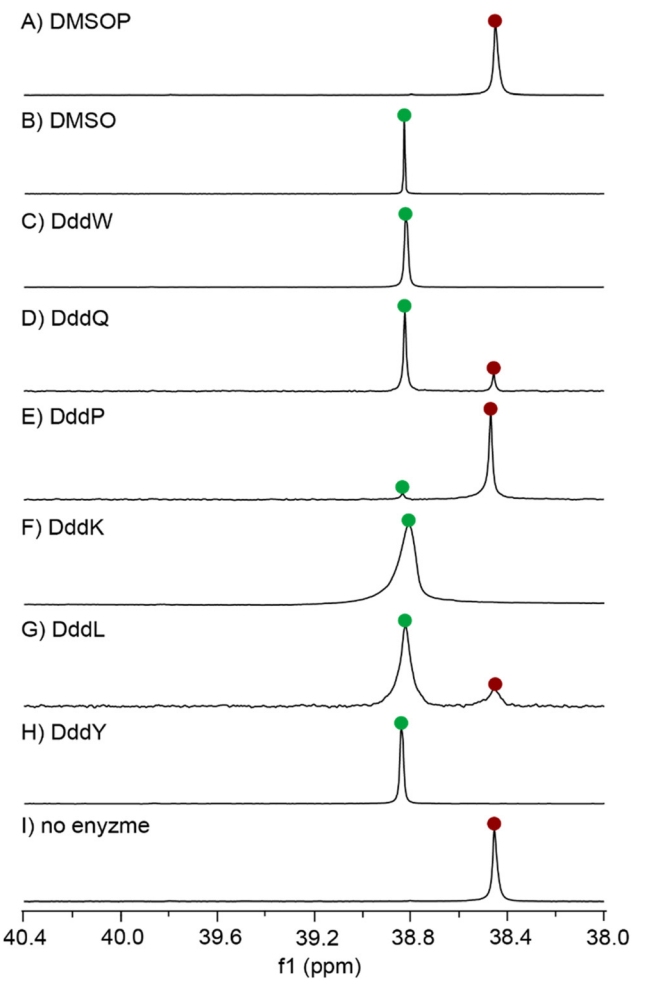

Fig. 1 Enzymatic conversion of (methyl-$^{13}C_2$)DMSOP (**4**). Red dots indicate the peaks for (methyl-$^{13}C_2$)DMSOP, and green dots indicate the peaks for ($^{13}C_2$)DMSO.

dimethylsulfoxonium propionate (DMSOP) has been discovered in several DMSP-producing microalgae and marine bacteria,[38] which could serve as another main source of marine DMSO. However, missing links for our understanding of the global sulfur cycle are the enzymes for the oxidation of DMSP to DMSOP and for the cleavage of DMSOP to DMSO and a C_3 unit such as acrylate. Here we report on the discovery that several of the enzymes described in the literature such as DMSP lyases can convert DMSOP into DMSO. In the case of DddQ, this enzymatic reaction was found to be more efficient than the cleavage of DMSP, so this enzyme is best described as a DMSOP lyase.

To investigate the potential of DMSP lyases to convert DMSOP, the enzymes DddQ, DddW and DddP from *Ruegeria pomeroyi* DSS-3 were expressed in *Escherichia coli* as reported previously.[39] In addition, the genes for DddY from *Ferrimonas balearica* DSM 9799, DddK from *Celeribacter halophilus* DSM 26270, and DddL from *Dinoroseobacter shibae* DSM 16493 were

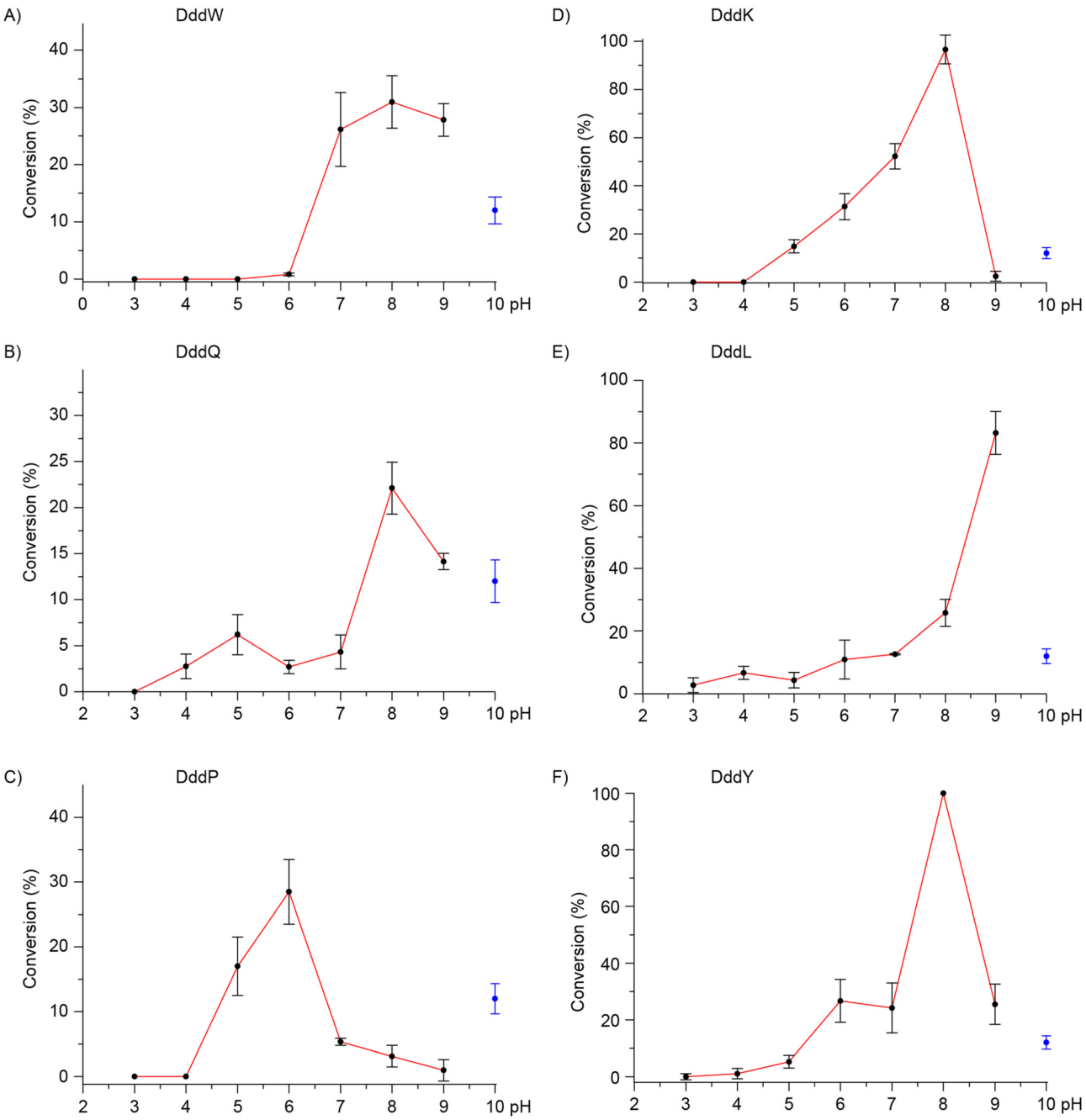

Fig. 2 pH dependency of the investigated enzymes. The panels show the pH dependency of (A) DddW, (B) DddQ, (C) DddP, (D) DddK, (E) DddL, and (F) DddY. Error bars indicate mean conversions determined by ^{13}C NMR and standard deviations from triplicate experiments. The blue bar indicates the base catalysed conversion at pH without the addition of enzymes.

cloned into the pET28c-derived expression vector pYE-Express[40] for heterologous expression in *E. coli* (all enzymes used in this study are tabulated in Table 1). All proteins except DddL were purified by Ni-NTA affinity chromatography (Fig. S1†). Because of a rapid loss of activity of DddL during chromatographic purification, crude cell lysates containing DddL were used for incubation experiments.

In the first series of experiments, all six enzymes were tested for their activity towards DMSOP at pH 8 and 30 °C. The enzyme activity testing using DMSOP as a substrate encounters the special problem that the detection of the reaction product in an aqueous medium is difficult. Therefore, (methyl-$^{13}C_2$) DMSOP (**4**) was synthesised from 3-mercaptopropionic acid (**1**) through a sequence of two methylations using $^{13}CH_3I$ to **2** and (methyl-$^{13}C_2$)DMSP (**3**) and subsequent oxidation (Scheme 3). With the ^{13}C-labelled substrate **4**, a direct monitoring of the enzymatic reaction by ^{13}C-NMR spectroscopy without workup of the sample was possible. Using a substrate concentration of 5 mM, a full conversion of **4** into ($^{13}C_2$)DMSO within 30 min by DddW, DddK and DddY, a partial conversion by DddQ and

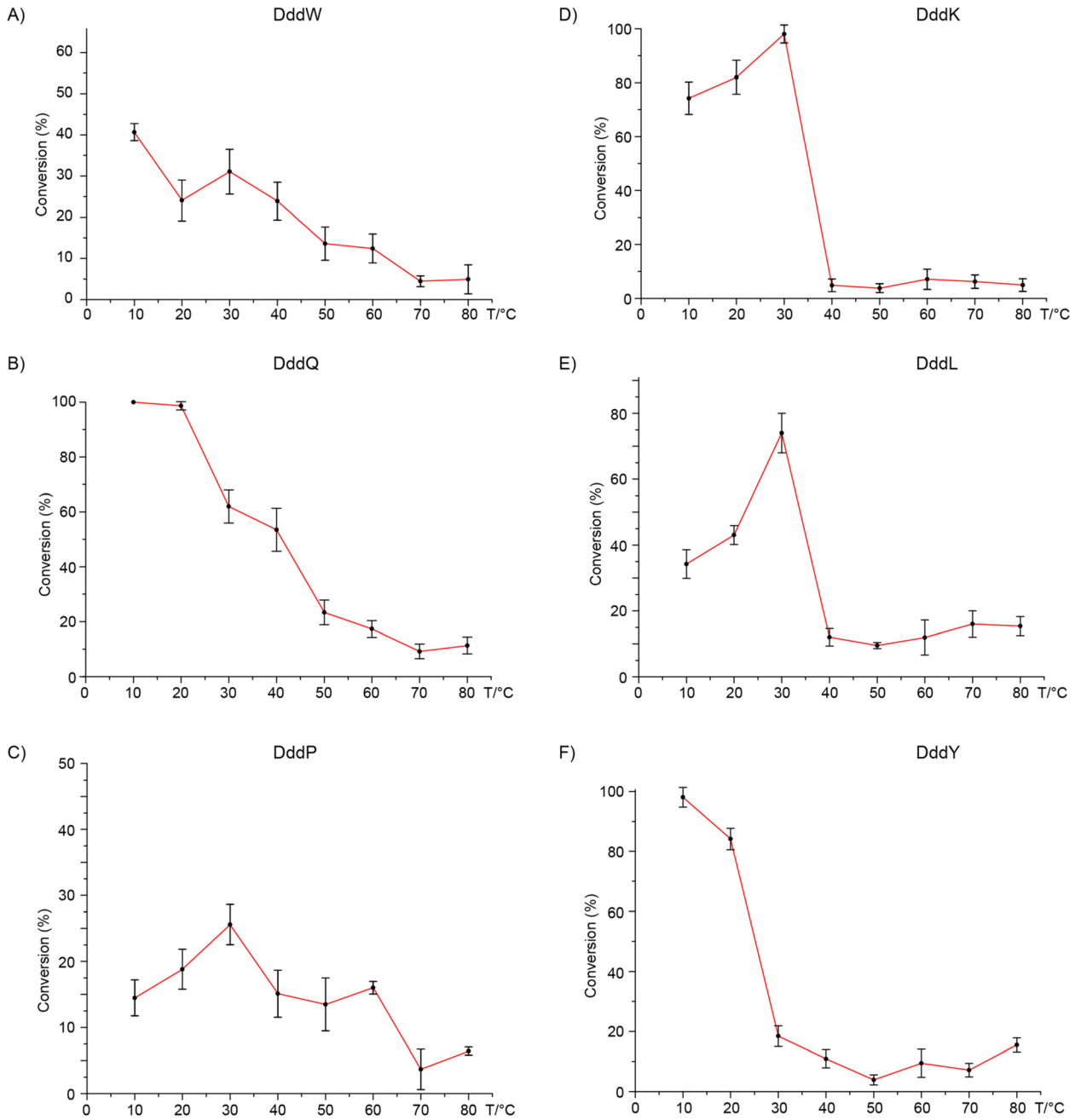

Fig. 3 Temperature dependency of the investigated enzymes. The panels show the temperature dependency of (A) DddW, (B) DddQ, (C) DddP, (D) DddK, (E) DddL, and (F) DddY. Error bars indicate mean conversions determined by ^{13}C NMR and standard deviations from triplicate experiments.

Table 2 Kinetic parameters for DddW, DddQ, DddP (all three enzymes from *R. pomeroyi* DSS-3), DddK (from *C. halophilus* DSM 26270), and DddY (from *F. balearica* DSM 9799) with the substrates DMSOP and DMSP

	DMSOP			DMSP		
Enzyme	K_M [mM]	k_{cat} [s^{-1}]	k_{cat}/K_M [s^{-1} mM^{-1}]	K_M [mM]	k_{cat} [s^{-1}]	k_{cat}/K_M [s^{-1} mM^{-1}]
DddW[a]	45.5 ± 5.0	49.0 ± 0.2	1.07 ± 0.01	16.3 ± 1.2	41.0 ± 0.28	2.51 ± 0.03
DddQ[a]	27.3 ± 2.2	7.4 ± 0.03	0.27 ± 0.01	49.7 ± 3.4	3.93 ± 0.01	0.08 ± 0.001
DddP[b]	1.45 ± 0.16	1.0 ± 0.06	0.69 ± 0.03	24.0 ± 3.6	4.65 ± 0.21	0.19 ± 0.004
DddK[a]	1.47 ± 0.08	2.0 ± 0.02	1.36 ± 0.02	0.76 ± 0.08	1.45 ± 0.03	1.90 ± 0.05
DddY[a]	8.8 ± 1.0	53.7 ± 0.1	6.10 ± 0.01	0.23 ± 0.01	4.94 ± 0.10	21.6 ± 1.7

[a] Determined at pH = 8 and room temperature. [b] Determined at pH = 6 and room temperature. Standard deviations were determined from triplicate experiments.

DddL, and only a poor conversion by DddP were observed (Fig. 1).

All six enzymes were tested for their pH optimum with the substrate DMSOP, and it turned out that several of the investigated enzymes were active over a wide range of pH values (Fig. 2). The pH dependency of all enzymes was tested at 20 °C and from pH 3–9. None of the enzymes showed activity below pH 3, while at pH 10, the spontaneous base-catalysed degradation of DMSOP started (indicated with the blue dot and error bars in Fig. 2). In order to test the pH dependency, enzyme incubations of (methyl-$^{13}C_2$)DMSOP were performed in triplicate, and conversions were determined by peak integrations of the ^{13}C-NMR spectra of (methyl-$^{13}C_2$)DMSO and (methyl-$^{13}C_2$)DMSOP. Low enzyme concentrations were chosen so that only partial conversion was obtained.

DddW showed a minor conversion at pH 6 and a high conversion from pH 7 to 9, with an optimum at pH 8 (Fig. 2A, pH optima are also summarised in Table 1, *vide supra*). DddQ exhibited a low activity in the range of pH 4–7, a clear optimum at pH 8, and also a good conversion at pH 9 (Fig. 2B). DddP revealed a good conversion at pH 5, performed the best at pH 6, and gave a minor substrate turnover in the pH range of 7–9 (Fig. 2C). DddK showed an increasing activity starting from pH 5, culminating in the optimum at pH 8, and had only a minor activity at pH 9 (Fig. 2D). DddL was active over the whole pH range of 3–8 with a moderate increase over this range and performed clearly the best at pH 9 (Fig. 2E). Similarly, DddY resulted in moderate and increasing conversions from pH 3 to 7, with a clear optimum at pH 8 and moderate substrate conversion at pH 9 (Fig. 2F).

The temperature dependency of all six enzymes with the substrate DMSOP was investigated through an analogous approach, *i.e.*, determination of the conversion rates of the substrate (methyl-$^{13}C_2$)DMSOP into (methyl-$^{13}C_2$)DMSO by ^{13}C-NMR from triplicate experiments. The selected temperature range was from 10 °C to 80 °C, and low enzyme concentrations were used in order to ensure only partial conversions to identify the temperature optimum. The temperature optima were tested for all enzymes at pH 8, and only for DddP that acted sluggishly at this pH the optimum was determined at pH 6. The results are shown in Fig. 3, and optimum temperatures are summarised in Table 1.

DddW was active over the whole temperature range and showed the highest conversion at 10 °C (Fig. 3A). Similarly, DddQ performed the best at 10 °C and also showed an almost complete conversion at 20 °C; the activity was retained over the whole temperature range and gradually dropped towards higher temperatures (Fig. 3B). DddP was also active from 10 °C to 80 °C and resulted in the highest conversion at 30 °C (Fig. 3C). The enzyme DddK was highly active between 10 °C and 30 °C, peaking at 30 °C, while its performance dropped dramatically at 40 °C. Despite this finding, a small activity was observed at all higher temperatures up to 80 °C (Fig. 3D). DddL was also active over the whole temperature range with a clearly optimal substrate turnover at 30 °C (Fig. 3E). Finally, DddY was highly active at 10 °C (optimum) and 20 °C and retained the conversion rate at all higher temperatures (Fig. 3F).

Enzyme kinetic data were determined at 20 °C and the optimum pH for all enzymes apart from DddL that could not be purified in the active form. The data were obtained using a concentration range of the substrate DMSOP up to concentrations at which a saturation of the kinetic plot was observed.

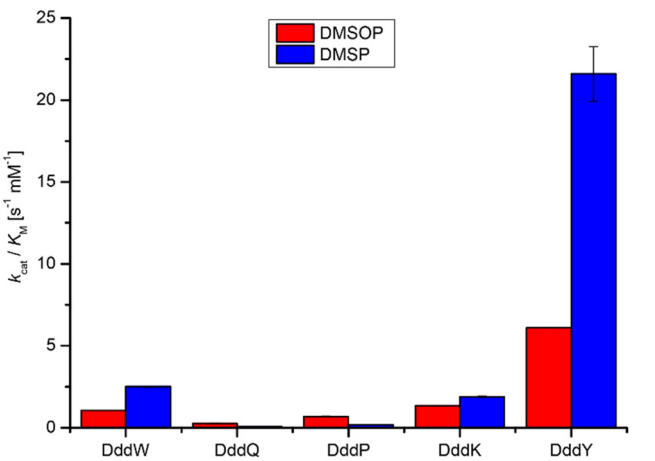

Fig. 4 Enzyme kinetic data (k_{cat}/K_M) for DddW, DddQ, DddP, DddK and DddY. The error bars show standard deviations based on triplicate experiments (some error bars are small, and data are also summarised in Table 2).

Table 3 Literature data for kinetic parameters for DddW, DddQ, DddP, DddK, and DddY with the substrate DMSP

Enzyme	Source organism (conditions)	K_M [mM]	k_{cat} [s^{-1}]	k_{cat}/K_M [s^{-1} mM^{-1}]
DddW	*R. pomeroyi* DSS-3 (pH 8)[39]	12.8 ± 0.8	16.8 ± 0.4	1.32 ± 0.09
DddW	*R. pomeroyi* DSS-3[41]	8.68 ± 0.73	18.3	2.10
DddQ	*R. pomeroyi* DSS-3 (pH 8)[39]	28.6 ± 3.3	0.93 ± 0.04	0.032 ± 0.004
DddQ	*R. lacuscaerulensis* ITI_1157[42]	21.5 ± 6.8		0.047
DddP	*R. pomeroyi* DSS-3 (pH 6)[39]	34.8 ± 4.7	3.85 ± 0.18	0.111 ± 0.013
DddP	*R. nubinhibens* ISM (pH 6, 30 °C)[43]	13.8 ± 5.5		
DddP	*R. lacuscaerulensis* ITI_1157 (pH 6, 60 °C)[44]	17.1 ± 0.98		
DddK	*P. ubique* HTCC 1062 (pH 8, 30 °C)[45]	13.6 ± 2.1	2.1 ± 0.1	
DddK	*P. ubique* HTCC 1062 (pH 7, 30 °C)[45]	3.7 ± 0.6	0.9 ± 0.1	
DddY	*A. bereziniae* NIPH3 (pH 8, 60 °C)[46]	5.0 ± 0.6	8.3 ± 0.5 × 10^3	

Only for DddP, substrate inhibition was observed with DMSOP at concentrations above 2.5 mM, explaining its poor performance in the initial experiments. The relevant kinetic plots for all five enzymes DddW, DddQ, DddP, DddK and DddY are shown in Fig. S4–S8.† For comparison, enzyme kinetic data were also determined for the substrate DMSP (Fig. S9–S13†). The obtained data are summarised in Table 2, and a graphic representation of k_{cat}/K_M values is shown in Fig. 4 (graphs for k_{cat} and K_M are shown in Fig. S14 and S15†). The kinetic parameters with the substrate DMSP were comparable to those reported previously (Table 3). for DddW,[39,41] DddQ,[39,42] and DddP;[43,44] only for DddK, we determined a lower K_M value (0.76 ± 0.08 mM) than that previously reported for DddK from *Pelagibacter ubique* (13.6 ± 2.1 mM),[45] while for DddY from *Acinetobacter bereziniae*, a very high k_{cat} value (8.3 ± 0.5 × 10^3 s^{-1}) has been reported,[46] which is not reflected for DddY from *F. balearica* (4.94 ± 0.10 s^{-1}). The reasons for these different findings are currently unclear.

The best performing enzyme was DddY for both substrates DMSOP and DMSP with a slightly faster conversion of DMSP. This result is surprising, because Pohnert and coworkers reported similar DMSO production from DMSOP by the wild-type strain of *Alcaligenes faecalis* and a ΔdddY knockout mutant.[37] An explanation may be that in the ΔdddY knockout strain, another unidentified DMSOP lyase is upregulated during growth on DMSOP, or the DddY from *A. faecalis* and from *F. balearica* as used in our study may have pronouncedly different activities in DMSOP lysis. Clarification of this point requires further investigation. Also DddW and DddK were highly efficient in the conversion of both substrates. Again, for DddW, DMSP was converted with moderately higher efficiency, while for DddK, both substrates were cleaved with nearly the same rates. DddQ and DddP turned out to be slightly less active, but both enzymes converted DMSOP more efficiently than in the case of DMSP and are therefore best described as DMSOP lyases. Here it should be emphasised that DddP is only active at substrate concentrations below 2.5 mM, but this concentration limit is well above the reported concentrations in sea water that are below 1 nM and intracellular concentrations of up to 1.5 mM in *E. huxleyi*[38] (all enzymes investigated here are of bacterial origin, but nothing is known about the intracellular DMSOP concentrations in bacteria).

Conclusions

Six enzymes including DddW, DddQ, DddP, DddK, DddL and DddY that were originally reported as DMSP lyases were investigated for their potential to cleave the recently discovered marine sulfur metabolite DMSOP. It turned out that all these enzymes are able to catalyse the cleavage of DMSOP into DMSO and acrylate. A plausible mechanism is that this elimination reaction proceeds through abstraction of a proton from the alpha carbon, followed by extrusion of DMSO.[38] Enzyme kinetic data showed that DddQ can cleave DMSOP more efficiently than in the case of DMSP and is therefore best described as a DMSOP lyase. Also for DddP, the kinetic parameters indicated a more efficient conversion of DMSOP than that of DMSP, but this enzyme showed substrate inhibition with DMSOP already at concentrations above 2.5 mM, while this effect was observed previously by us with DMSP only for concentrations above 100 mM.[39] Conclusively, DddP should not be classified as a DMSOP lyase, although it may act efficiently on this substrate at low concentrations that may be physiologically relevant. Because of the large amounts of DMSOP formed in the oceans, this newly discovered enzyme reaction is of global importance for the flux of organic sulfur. While the substrate DMSP yields the apolar and volatile compound DMS that is released into the atmosphere where it influences the global climate, the polar and water soluble compound DMSO is formed from DMSOP and remains in oceanic waters. So far, no enzyme has been known to oxidize DMSP to DMSOP which still represents a missing link in the global sulfur cycle.

Conflicts of interest

There are no conflicts to declare.

Acknowledgements

This work was funded by the Deutsche Forschungsgemeinschaft DFG (SFB TRR 51 “Roseobacter”).

References

1 P. Haas, *Biochem. J.*, 1935, **29**, 1297–1299.
2 F. Challenger and M. I. Simpson, *J. Chem. Soc.*, 1948, 1591–1597.
3 F. Challenger, R. Bywood, P. Thomas and B. J. Hayward, *Arch. Biochem. Biophys.*, 1957, **69**, 514–523.
4 Y. Ishida and H. Kadota, *Agric. Biol. Chem.*, 1967, **31**, 756–757.
5 A. Vairavamurthy, M. O. Andreae and R. L. Iverson, *Limnol. Oceanogr.*, 1985, **30**, 59–70.
6 J. W. H. Dacey, G. M. King and S. G. Wakeham, *Nature*, 1987, **330**, 643–645.
7 A. D. Broadbent, G. B. Jones and R. J. Jones, *Estuarine, Coastal Shelf Sci.*, 2002, **55**, 547–555.
8 G. O. Kirst, C. Thiel, H. Wolff, J. Nothnagel, M. Wanzek and R. Ulmke, *Mar. Chem.*, 1991, **35**, 381–388.
9 G. L. Cantoni and D. G. Anderson, *J. Biol. Chem.*, 1956, **222**, 171–177.
10 M. K. Nishiguchi and L. J. Goff, *J. Phycol.*, 1995, **31**, 567–574.
11 M. P. de Souza and D. C. Yoch, *Appl. Environ. Microbiol.*, 1995, **61**, 21–26.
12 M. J. E. C. van der Maarel, W. Aukema and T. A. Hansen, *FEMS Microbiol. Lett.*, 1996, **143**, 241–245.
13 G. V. Wolfe, M. Steinke and G. O. Kirst, *Nature*, 1997, **387**, 894–897.
14 J. McNeill Sieburth, *Science*, 1960, **132**, 676–677.
15 D. A. Gage, D. Rhodes, K. D. Nolte, W. A. Hicks, T. Leustek, A. J. L. Cooper and A. D. Hanson, *Nature*, 1997, **387**, 891–894.
16 A. R. J. Curson, J. Liu, A. Bermejo Martinez, R. T. Green, Y. Chan, O. Carrion, B. T. Williams, S.-H. Zhang, G.-P. Yang, P. C. Bulman Page, X.-H. Zhang and J. D. Todd, *Nat. Microbiol.*, 2017, **2**, 17009.
17 J. B. Raina, D. M. Tapiolas, S. Foret, A. Lutz, D. Abrego, J. Ceh, F. O. Seneca, P. L. Clode, D. G. Bourne, B. L. Willis and C. A. Motti, *Nature*, 2013, **502**, 677–680.
18 M. Gali, E. Devred, M. Levasseur, S.-J. Royer and M. Babin, *Remote Sens. Environ.*, 2015, **171**, 171–184.
19 A. J. Kettle and M. O. Andreae, *J. Geophys. Res.*, 2000, **105**, 26793–26808.
20 J. E. Lovelock, R. J. Maggs and R. A. Rasmussen, *Nature*, 1972, **237**, 452–453.
21 R. J. Charlson, J. E. Lovelock, M. O. Andreae and S. G. Warren, *Nature*, 1987, **326**, 655–661.
22 S. M. Vallina and R. Simo, *Science*, 2007, **315**, 506–508.
23 J. D. Todd, R. Rogers, Y. G. Li, M. Wexler, P. L. Bond, L. Sun, A. R. J. Curson, G. Malin, M. Steinke and A. W. B. Johnston, *Science*, 2007, **315**, 666–669.
24 A. R. J. Curson, R. Rogers, J. D. Todd, C. A. Brearly and A. W. B. Johnston, *Environ. Microbiol.*, 2008, **10**, 757–767.
25 J. D. Todd, A. R. J. Curson, C. L. Dupont, P. Nicholson and A. W. B. Johnston, *Environ. Microbiol.*, 2009, **11**, 1376–1385.
26 J. D. Todd, A. R. J. Curson, M. Kirkwood, M. J. Sullivan, R. T. Green and A. W. B. Johnston, *Environ. Microbiol.*, 2011, **13**, 427–438.
27 J. D. Todd, M. Kirkwood, S. Newton-Payne and A. W. B. Johnston, *ISME J.*, 2012, **6**, 223–226.
28 A. R. J. Curson, M. J. Sullivan, J. D. Todd and A. W. B. Johnston, *ISME J.*, 2011, **5**, 1191–1200.
29 J. Sun, J. D. Todd, J. C. Thrash, Y. Qian, M. C. Qian, B. Temperton, J. Guo, E. K. Fowler, J. T. Aldrich, C. D. Nicora, M. S. Lipton, R. D. Smith, P. de Leenheer, S. H. Payne, A. W. B. Johnston, C. L. Davie-Martin, K. H. Halsey and S. J. Giovannoni, *Nat. Microbiol.*, 2016, **1**, 16065.
30 U. Alcolombri, S. Ben-Dor, E. Feldmesser, Y. Levin, D. S. Tawfik and A. Vardi, *Science*, 2015, **348**, 1466–1469.
31 C. Y. Li, X. J. Wang, X. L. Chen, Q. Sheng, S. Zhang, P. Wang, M. Quareshy, B. Rihtman, X. Shao, C. Gao, F. Li, S. Li, W. Zhang, X.-H. Zhang, G.-P. Yang, J. D. Todd, Y. Chen and Y.-Z. Zhang, *eLife*, 2021, **10**, e64045.
32 E. C. Howard, J. R. Henriksen, A. Buchan, C. R. Reisch, H. Bürgmann, R. Welsh, W. Ye, J. M. Gonzalez, K. Mace, S. B. Joye, R. P. Kiene, W. B. Whitman and M. A. Moran, *Science*, 2006, **314**, 649–652.
33 C. R. Reisch, M. J. Stoudemayer, V. A. Varaljay, I. J. Amster, M. A. Moran and W. B. Whitman, *Nature*, 2011, **473**, 208–211.
34 D. A. del Valle, D. J. Kieber and R. P. Kiene, *Mar. Chem.*, 2007, **103**, 197–208.
35 A. D. Hatton, D. M. Shenoy, M. C. Hart, A. Mogg and D. H. Green, *Biogeochemistry*, 2012, **110**, 131–146.
36 I. Lidbury, E. Kröber, Z. Zhang, Y. Zhu, J. C. Murrell, Y. Chen and H. Schäfer, *Environ. Microbiol.*, 2016, **18**, 2754–2766.
37 E. C. Asher, J. W. H. Dacey, M. Stukel, M. C. Long and P. D. Tortell, *Limnol. Oceanogr.*, 2017, **62**, 104–124.
38 K. Thume, B. Gebser, L. Chen, N. Meyer, D. J. Kieber and G. Pohnert, *Nature*, 2018, **563**, 412–415.
39 I. Burkhardt, L. Lauterbach, N. L. Brock and J. S. Dickschat, *Org. Biomol. Chem.*, 2017, **15**, 4432–4439.
40 J. S. Dickschat, K. A. K. Pahirulzaman, P. Rabe and T. A. Klapschinski, *ChemBioChem*, 2014, **15**, 810–814.
41 A. E. Brummett, N. J. Schnicker, A. Crider, J. D. Todd and M. Dey, *PLoS One*, 2015, **10**, e0127288.
42 C.-Y. Li, X.-L. Chen, B.-B. Xie, H.-N. Su, Q.-L. Qin and Y.-Z. Zhang, *Proc. Natl. Acad. Sci. U. S. A.*, 2014, **111**, E2080.
43 M. Kirkwood, N. E. Le Brun, J. D. Todd and A. W. B. Johnston, *Microbiology*, 2010, **156**, 1900–1906.
44 P. Wang, X.-L. Chen, C.-Y. Li, X. Gao, D. Zhu, B.-B. Xie, Q.-L. Qin, X.-Y. Zhang, H.-N. Su, B.-C. Zhou, L. Xun and Y.-Z. Zhang, *Mol. Microbiol.*, 2015, **98**, 289–301.
45 M. Peng, X.-L. Chen, D. Zhang, X.-J. Wang, N. Wang, P. Wang, J. D. Todd, Y.-Z. Zhang and C.-Y. Li, *Appl. Environ. Microbiol.*, 2019, **85**, e03127-18.
46 C.-Y. Li, D. Zhang, X.-L. Chen, P. Wang, W.-L. Shi, P.-Y. Li, X.-Y. Zhang, Q.-L. Qin, J. D. Todd and Y.-Z. Zhang, *J. Mol. Biol.*, 2017, **429**, 3850–3862.

Appendix D

Functional characterisation of twelve terpene synthases from actinobacteria

Beilstein J. Org. Chem. **2023**, *19*, 1386–1398

DOI: 10.3762/bjoc.19.100

BEILSTEIN JOURNAL OF ORGANIC CHEMISTRY

Functional characterisation of twelve terpene synthases from actinobacteria

Anuj K. Chhalodia, Houchao Xu, Georges B. Tabekoueng, Binbin Gu, Kizerbo A. Taizoumbe, Lukas Lauterbach and Jeroen S. Dickschat*

Full Research Paper

Open Access

Address:
Kekulé-Institute of Organic Chemistry and Biochemistry, University of Bonn, Gerhard-Domagk-Straße 1, 53121 Bonn, Germany

Email:
Jeroen S. Dickschat* - dickschat@uni-bonn.de

* Corresponding author

Keywords:
actinomycetes; biosynthesis; enzymes; NMR spectroscopy; terpenes

Beilstein J. Org. Chem. **2023,** *19,* 1386–1398.
https://doi.org/10.3762/bjoc.19.100

Received: 21 July 2023
Accepted: 04 September 2023
Published: 15 September 2023

Associate Editor: B. Nay

Abstract

Fifteen type I terpene synthase homologs from diverse actinobacteria that were selected based on a phylogenetic analysis of more than 4000 amino acid sequences were investigated for their products. For four enzymes with functions not previously reported from bacterial terpene synthases the products were isolated and their structures were elucidated by NMR spectroscopy, resulting in the discovery of the first terpene synthases for (+)-δ-cadinol and (+)-α-cadinene, besides the first two bacterial (−)-amorpha-4,11-diene synthases. For other terpene synthases with functions reported from bacteria before the products were identified by GC–MS. The characterised enzymes include a new *epi*-isozizaene synthase with monoterpene synthase side activity, a 7-*epi*-α-eudesmol synthase that also produces hedycaryol and germacrene A, and four more sesquiterpene synthases that produce mixtures of hedycaryol and germacrene A. Three phylogenetically related enzymes were in one case not expressed and in two cases inactive, suggesting pseudogenisation in the respective branch of the phylogenetic tree. Furthermore, a diterpene synthase for allokutznerene and a sesterterpene synthase for sesterviolene were identified.

Introduction

Terpene synthases are remarkable enzymes that can convert acyclic and achiral oligoprenyl pyrophosphates into terpene hydrocarbons or alcohols of high structural complexity. These enzymatic reactions are initiated by ionisation of the substrate either through diphosphate abstraction (for type I terpene synthases) or protonation of the substrate (type II terpene synthases). The resulting cationic species can then react in a cascade reaction via a series of cationic intermediates involving cyclisations, hydride or proton shifts, and skeletal rearrangements. During the past decades numerous enzymes have been characterised from all branches of life. Only considering type I terpene synthases, after the identification of the 5-*epi*-aristolochene (**1**) synthase from *Nicotiana tabacum* [1] and the casbene (**2**) synthase from *Ricinus communis* [2] (Figure 1), hundreds of plant terpene synthases have been identified [3,4], including terpene synthases of microbial type [5]. Also many

fungal terpene synthases are known that can either be monofunctional as in case of the aristolochene (**3**) synthases from *Aspergillus terreus* [6] and *Penicillium roqueforti* [7], or they may be bifunctional and composed of two domains. In these enzymes a prenyltransferase domain catalyses the formation of an oligoprenyl pyrophosphate precursor from dimethylallyl pyrophosphate (DMAPP) and isopentenyl pyrophosphate (IPP) that is subsequently cyclised by the terpene synthase domain. The first discovered example from this class is the fusicoccadiene (**4**) synthase from *Phomopsis amygdali* [8], and even triterpenes such as macrophomene (**5**) can be generated by these bifunctional enzymes [9]. After cloning of the gene for pentalenene (**6**) synthase from *Streptomyces exfoliatus* [10], many bacterial terpene synthases have been identified [11], including enzymes for the non-canonical compounds geosmin (**7**) [12] and 2-methylisoborneol (**8**) [13]. Recent developments also revealed the presence of sesterterpene synthases in bacteria exemplified by the enzymes for sesterviridene (**9**) in *Kitasatospora viridis* [14-16]. Only few terpene synthases have been characterised from other organisms, including enzymes from insects [17], octocorals [18,19], red algae [20,21], and amobae [22,23]. Despite these previous efforts, for many known terpenes still no terpene synthases catalysing their formation have been reported. Here, we report on the discovery and functional characterisation of four sesquiterpene synthases from actinomycetes with novel functions, in addition to several actinomycete terpene synthases for which functional homologs have been identified before.

Results and Discussion

Phylogenetic analysis

A phylogenetic tree was constructed from 4018 bacterial terpene synthase homologs (Figure 2). In this tree all branches of homologous enzymes for which at least one representative was functionally characterised are shown in blue, whereas the uncharacterised enzymes are shown in grey, revealing that the functions of still many terpene synthase homologs are unknown. Some of the largest branches in this tree represent the homologs of *epi*-isozizaene synthase from *Streptomyces coelicolor* [24], caryolan-1-ol synthase from *Streptomyces griseus* [25], selina-4(15),7(11)-diene synthase from *Streptomyces pristinaespiralis* [26], spiroviolene synthase from *Streptomyces violens* [27], micromonocyclol synthase from *Micromonospora marina* [28], α-amorphene synthase from *Streptomyces viridochromogenes* [29,30], *epi*-cubenol synthase from *S. griseus* [31], germacrene A synthase from *M. marina* [32], and 7-*epi*-α-eudesmol synthase from *S. viridochromogenes* [29,30]. In order to expand the knowledge about terpene synthase catalysis, fifteen uncharacterised terpene synthase homologs as listed in Table 1 were selected for further studies from different branches of the tree (indicated by red arrows in Figure 2). The genes coding for all fifteen enzymes were amplified by PCR from genomic DNA, cloned and expressed in *Escherichia coli*. The purified recombinant proteins (Figure S1, Supporting Information File 1) were used in test incubations with geranyl pyrophosphate (GPP), farnesyl pyrophosphate (FPP), geranylgeranyl pyrophosphate (GGPP) and geranylfarnesyl pyrophosphate (GFPP).

Sesquiterpene synthases

The enzyme from *K. kofuensis* (Table 1, entry 1) exhibited all highly conserved motifs required for functionality including the aspartate-rich motif (^{83}DDAYCD) and the NSE triad (^{223}NDIASYYKE, Figure S2, Supporting Information File 1). The closest characterised terpene synthase with an amino acid sequence identity of 25% is the (1(10)*E*,4*E*,6*S*,7*R*)-germacradien-6-ol synthase from *Streptomyces pratensis* [33]. The recombinant enzyme efficiently converted FPP into one

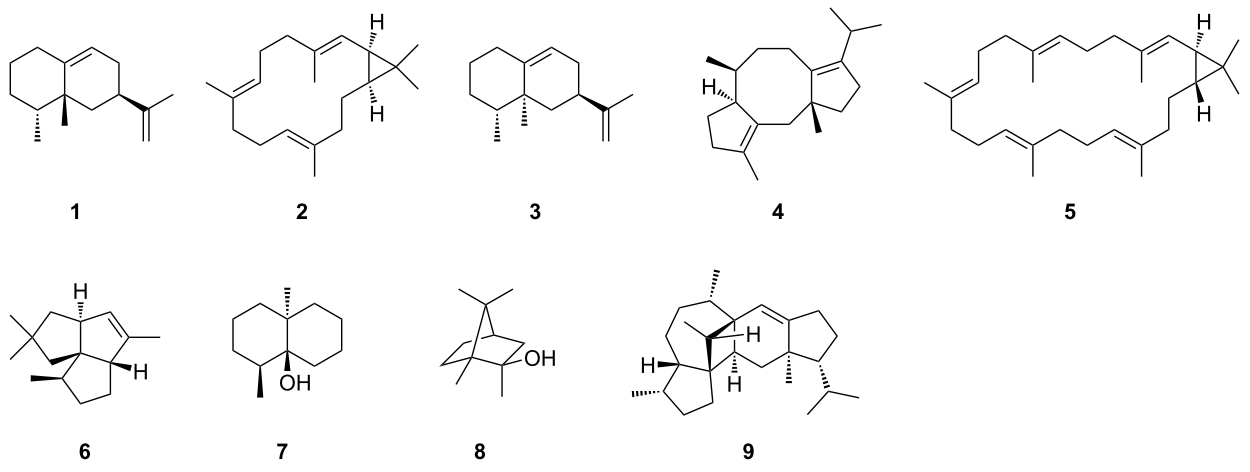

Figure 1: Terpenes produced by characterised terpene synthases.

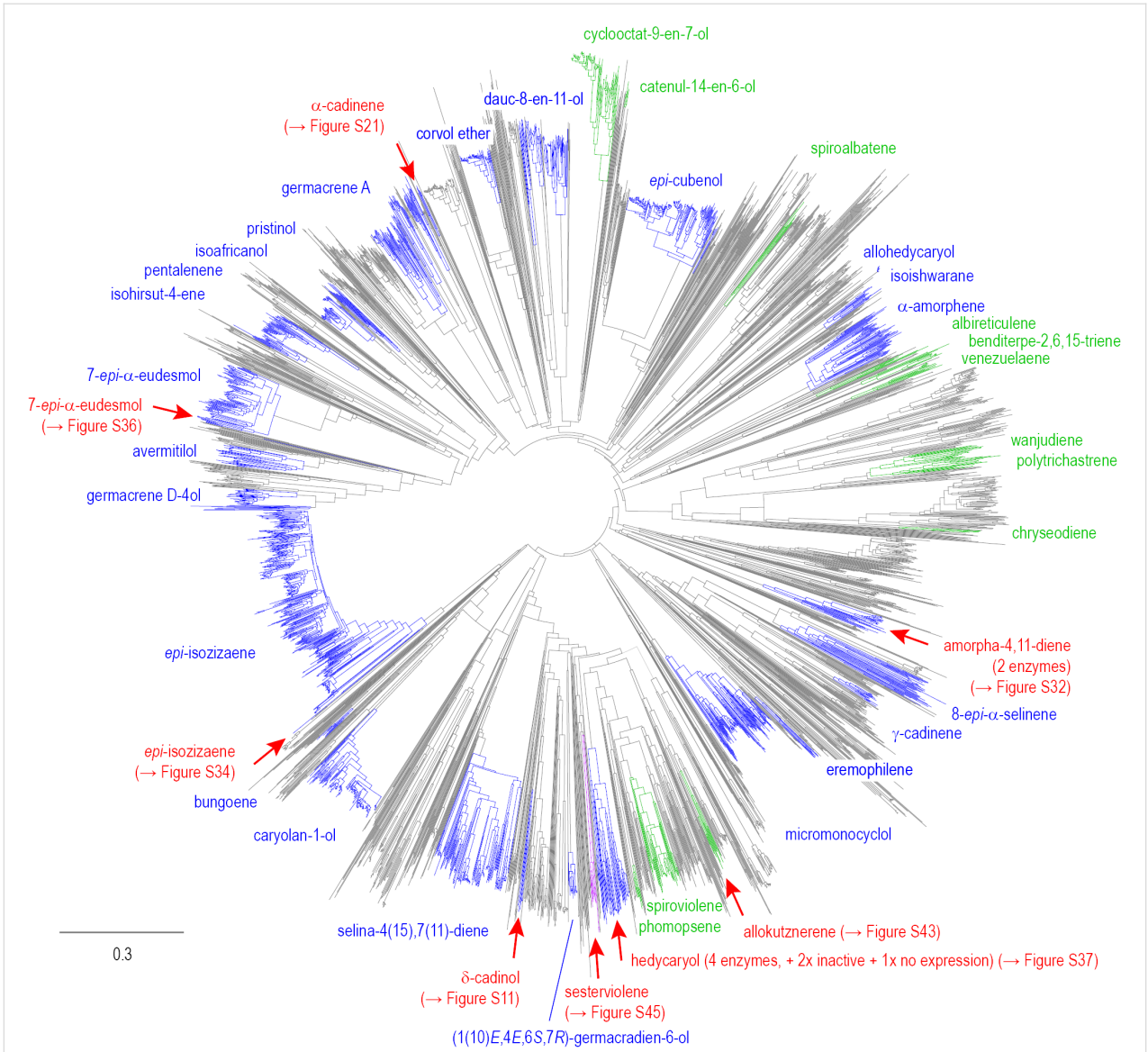

Figure 2: Phylogenetic tree constructed from the amino acid sequences of 4018 terpene synthase homologs. Blue branches indicate groups of homologous sesquiterpene synthases, green branches indicate groups of homologous diterpene synthases, and purple branches indicate groups of homologous sesterterpene synthases from which at least one representative was functionally characterised. The red arrows highlight enzymes characterised in this study (cf. the indicated Figures of Supporting Information File 1 for a detailed view). The scale bar indicates substitutions per site.

sesquiterpene alcohol whose electron ionisation (EI) mass spectrum suggested the structure of δ-cadinol (**10**) by comparison to a mass spectrum included in the NIST Standard Reference Database (Figure 3A and 3B). Only minor amounts of acyclic products were obtained from GPP (myrcene, ocimene, linalool) and GGPP (β-springene), while GFPP was not accepted. A preparative scale incubation of FPP (80 mg, 185 μmol) allowed for the isolation of **10** (5.5 mg, 25 μmol, 14%) for structure elucidation through NMR spectroscopy (Table S2, Figures S3–S10, Supporting Information File 1), confirming the structure of δ-cadinol. The optical rotation of $[\alpha]_D^{25}$ = +95.9 (*c* 0.55, CH_2Cl_2) pointed to the same enantiomer as is known from the plants *Pinus sibirica* ($[\alpha]_D^{20}$ = +118.4) and *Torreya nucifera* ($[\alpha]_D^{18}$ = +118.6) [34], and from the fungus *Xylobolus frustulatus* ($[\alpha]_D^{25}$ = +99.9 (*c* 0.6, $CHCl_3$)) [35]. This finding is rather unusual, as more and more cases were recently identified in which sesquiterpenes from bacteria showed an enantiomeric relationship to plant compounds [36]. The enzyme from *K. kofuensis* represents the first terpene synthase for the biosynthesis of **10** and was thus identified as *Kutzneria kofuensis* (+)-δ-Cadinol Synthase (KkdCS). A few closely related enzymes from other actinomycetes with a pairwise identity of 69% may also function as (+)-δ-cadinol synthases (Figure S11, Supporting Information File 1).

Table 1: Terpene synthase homologs characterised in this study.

entry	organism	accession no.	(main) product
1	*Kutzneria kofuensis* DSM 43851	MBB5895433	(+)-δ-cadinol[a]
2	*Streptomyces jumonjiensis* NRRL 5741	WP_153520876	(+)-α-cadinene[a]
3	*Streptomyces lavendulae* NRRL B-2774	WP_078950427	(−)-amorpha-4,11-diene[a]
4	*Streptomyces subrutilus* ATCC 27467	WP_150516140	(−)-amorpha-4,11-diene[a]
5	*Nocardia brevicatena* NBRC12119	WP_086008896	*epi*-isozizaene[a]
6	*Streptomyces flavidovirens* DSM 40150	WP_028812116	7-*epi*-α-eudesmol[a]
7	*Streptomyces sclerotialus* NRRL ISP-5269	WP_030615021	hedycaryol[a]
8	*Streptomyces catenulae* NRRL B-2342	WP_051739595	hedycaryol[a]
9	*Streptomyces ficellus* NRRL 8067	WP_156694351	hedycaryol[a]
10	*Streptomyces morookaense* DSM 40503	WP_171082395	germacrene A[a]
11	*Streptomyces subrutilus* ATCC 27467	WP_150522245	no expression
12	*Streptomyces natalensis* NRRL B-5314	WP_037793252	inactive
13	*Streptomyces violens* NRRL ISP-5597	WP_030249874	inactive
14	*Kutzneria kofuensis* DSM 43851	WP_184867163	allokutznerene[b]
15	*Streptomyces* sp. Tü 2975	WP_159685978	sesterviolene[c]

[a]From FPP as substrate (sesquiterpene synthase). [b]From GGPP as substrate (diterpene synthase). [c]From GFPP as substrate (sesterterpene synthase).

The enzyme from *S. jumonjiensis* (Table 1, entry 2) showed the fully established conserved motifs including the aspartate-rich region (^{83}DDVRSE) and the NSE triad (^{225}NDIHSYEKE, Figure S12, Supporting Information File 1) and its closest characterised relative is with 32% identity the germacrene A synthase from *M. marina* [32]. The incubation with GPP resulted in minor amounts of acyclic compounds (myrcene, ocimene, linalool), while FPP gave a high yield of α-cadinene (**11**) (Figure 3C and 3D), and GGPP and GFPP were not accepted as substrate. For verification of the GC–MS-based identification the product was isolated from a preparative scale incubation of FPP (80 mg, 185 μmol) to obtain pure **11** (1.3 mg, 6.4 μmol, 3.5%). Structure elucidation by NMR spectroscopy confirmed the identity of the enzyme product α-cadinene (Table S3, Figures S13–S20, Supporting Information File 1). The optical rotation of $[\alpha]_D^{25}$ = +60.0 (*c* 0.015, C_6D_6) indicated the opposite enantiomer as in the plant *Humulus lupulus* ($[\alpha]_D^{24}$ = −62.4 (*c* 0.868, $CHCl_3$)) [37]. (+)-δ-Cadinene synthases have been described from *Gossypium arboreum* [38] and *Gossypium hirsutum* [39], a (−)-δ-cadinene synthase was identified in *Streptomyces clavuligerus* [40], and (−)-γ-cadinene synthases are known from the termite associated fungus *Termitomyces* sp. [41] and the bacterium *Chitinophaga pinensis* [29,30], but no α-cadinene synthase has been reported to date. The enzyme newly described here was designated as *Streptomyces jumonjiensis* (+)-α-Cadinene Synthase (SjaCS). A few more enzymes with a pairwise identity of 83% are observed in other actinomycetes that likely also function as (+)-α-cadinene synthases (Figure S21, Supporting Information File 1).

The enzyme from *S. lavendulae* (Table 1, entry 3) exhibited all highly conserved motifs including the aspartate-rich sequence (^{83}DDQHD) and the NSE triad (^{226}NDVFSLPKE, Figure S22, Supporting Information File 1). The closely related homolog from *S. subrutilus* (Table 1, entry 4) showed the same sequences for these motifs (Figure S23, Supporting Information File 1). Both enzymes are distant from all previously characterised terpene synthases and show a sequence identity of only 25% and 28%, respectively, to their closest characterised homolog spiroalbatene synthase from *Allokutzneria albata* [42]. Test incubations with GPP resulted in the formation of acyclic products besides minor amounts of limonene, while GGPP and GFPP were not converted by both enzymes. With FPP both enzymes resulted in the formation of a sesquiterpene hydrocarbon that was identified by GC–MS as amorpha-4,11-diene (**12**, Figure 4). The structure of the product was confirmed through a preparative scale incubation of FPP (80 mg, 185 μmol) yielding pure **12** (1 mg, 4.9 μmol, 2.6%) for NMR spectroscopic analysis (Table S4, Figures S24–S31, Supporting Information File 1). The optical rotation of $[\alpha]_D^{25}$ = –9.4 (*c* 0.64, CH_2Cl_2) pointed to the same enantiomer as in the plant *Viguiera oblongifolia* ($[\alpha]_D^{24}$ = –8 (*c* 0.4, $CHCl_3$)) [43]. A (−)-amorpha-4,11-diene synthase (ADS) is also known from *Artemisia annua* and catalyses the first committed step in the biosynthesis of artemisinin [44]. From bacteria only the α-amorphene synthase from *S. viridochromogenes* is known [29,30], but no enzyme for the biosynthesis of **12** has been reported before. The enzymes described here were named *Streptomyces lavendulae* (−)-Amorpha-4,11-diene Synthase (SlADS) and *Streptomyces*

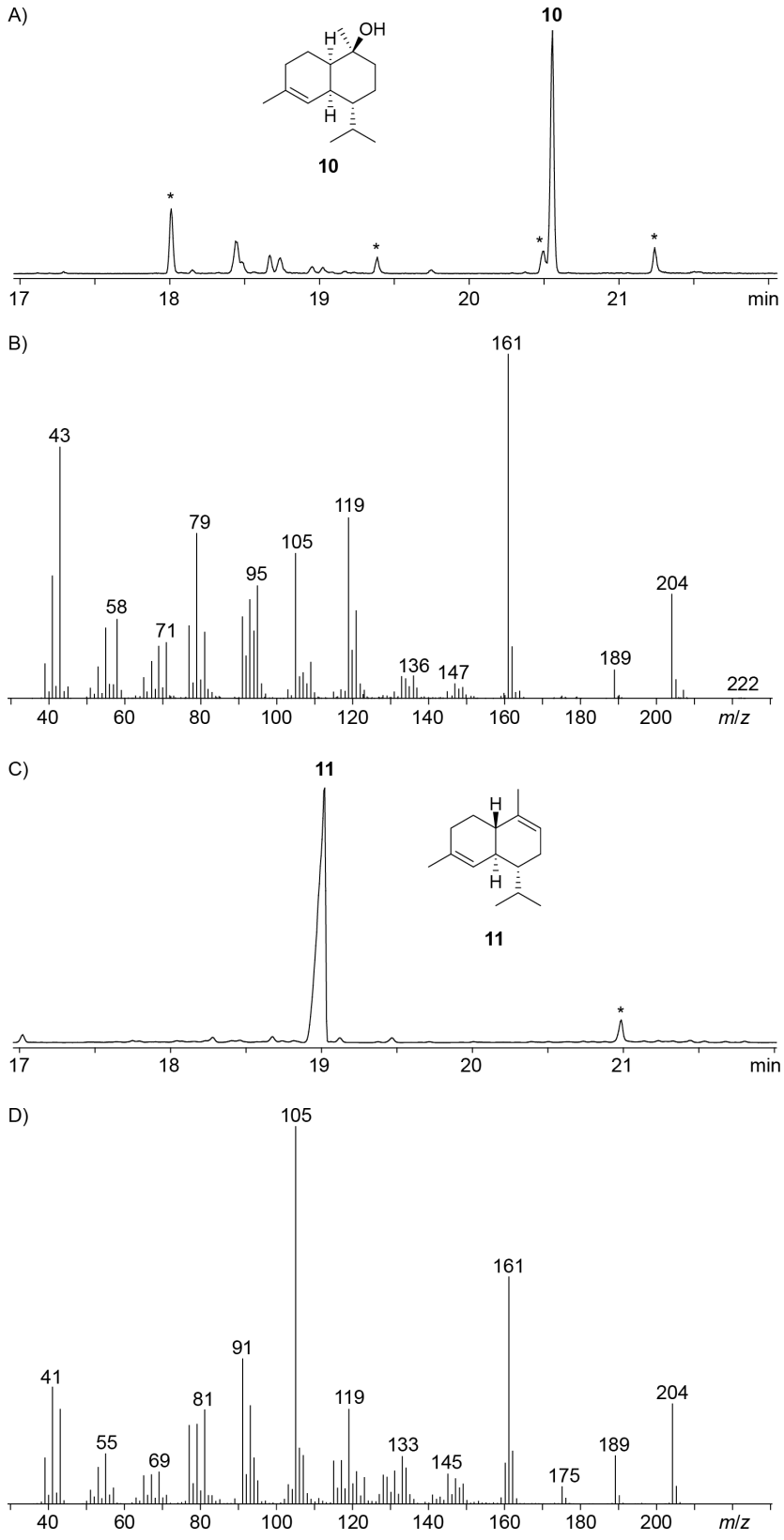

Figure 3: A) Total ion chromatogram of the products obtained from FPP with KkdCS, B) EI mass spectrum of **10**, C) total ion chromatogram of the products obtained from FPP with SjaCS, D) EI mass spectrum of **11**. Asterisks indicate acyclic products and contaminants such as plasticisers.

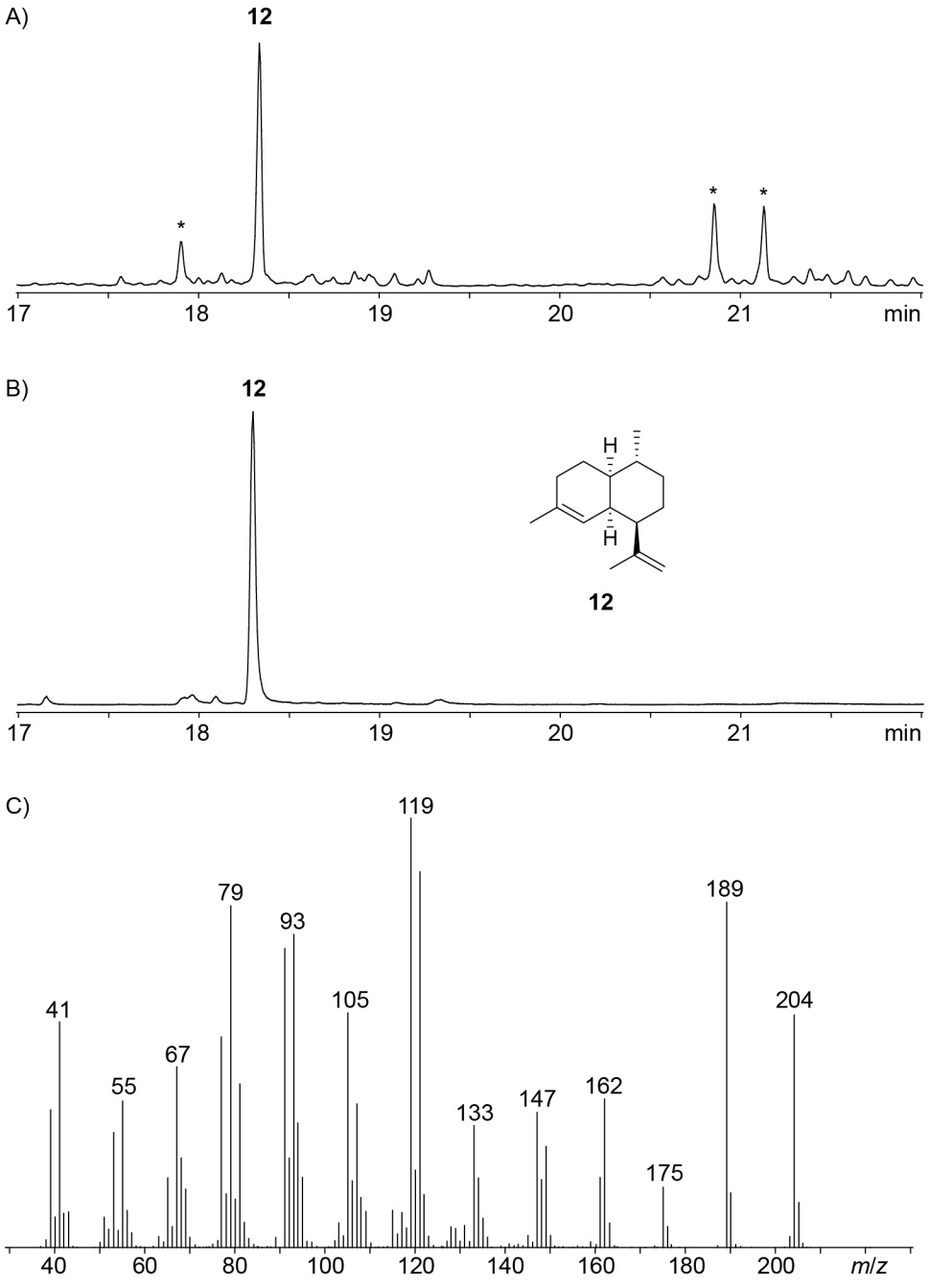

Figure 4: Total ion chromatograms of the products obtained from FPP A) with SlADS and B) with SsADS, C) EI mass spectrum of **12**. Asterisks indicate acyclic products and contaminants such as plasticisers.

subrutilus (−)-Amorpha-4,11-diene Synthase (SsADS). These two enzymes belong to a clade of closely related enzymes with a pairwise identity of 70%, suggesting that (−)-amorpha-4,11-diene synthases also occur in several other streptomycetes (Figure S32, Supporting Information File 1).

The terpene synthase homolog from *N. brevicatena* (Table 1, entry 5) showed the highly conserved motifs with a modified aspartate-rich region (^{86}DDHRN) and the NSE triad ^{227}NDLHSMPKE (Figure S33, Supporting Information File 1). This enzyme is closely related to the *epi*-isozizaene synthase from *S. coelicolor* (EIZS) [24], but is with an amino acid identity of only 48% sufficiently distant so that another function could be expected (Figure S34, Supporting Information File 1). However, the incubation with FPP resulted in the efficient formation of *epi*-isozizaene (**13**) as a single product (Figure 5),

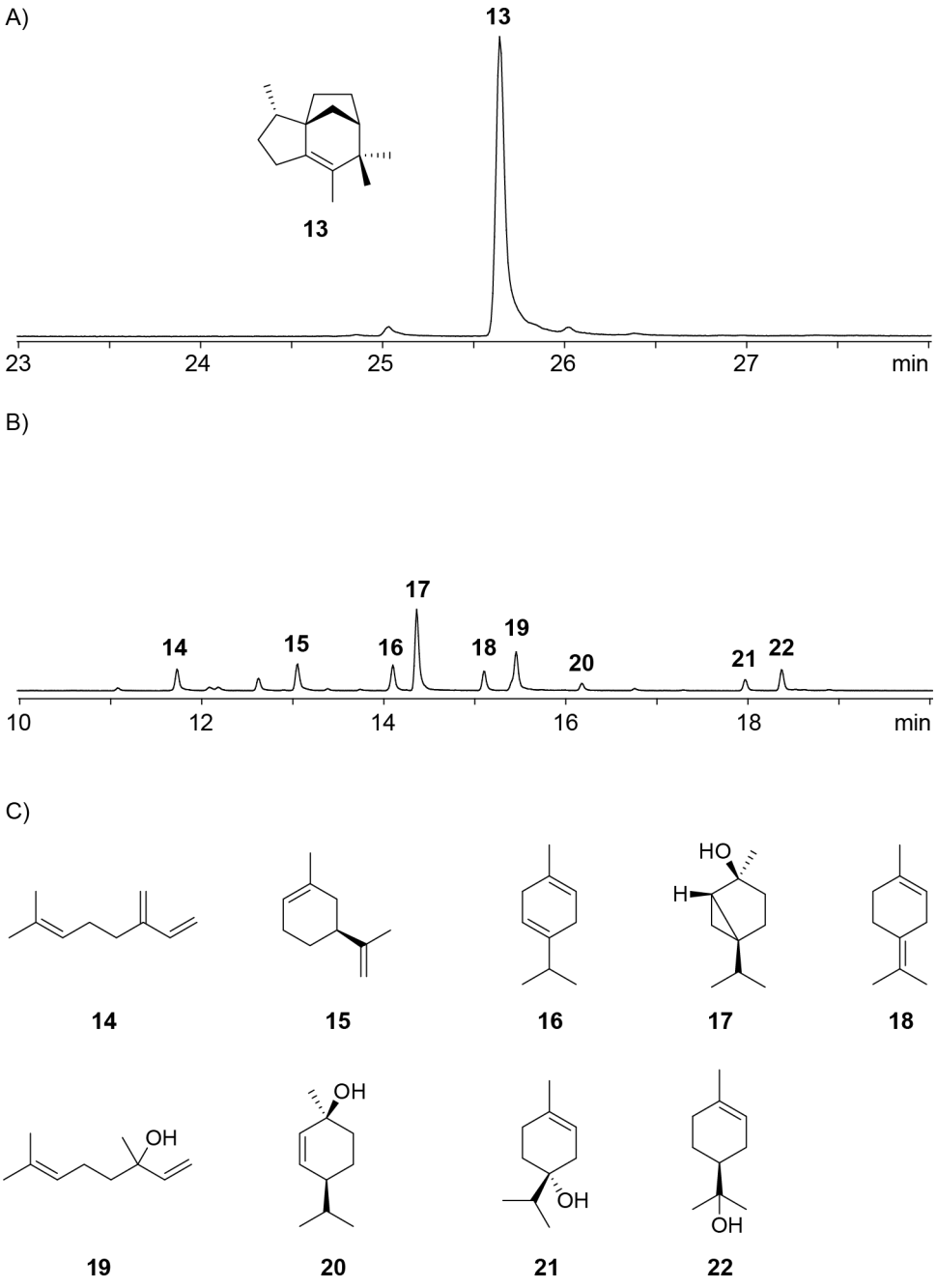

Figure 5: Total ion chromatograms of the products obtained with NbEIZS A) from FPP and B) from GPP, and C) structures of identified monoterpenes (only relative configurations are known). Peak numbers in B) refer to compound numbers in C).

confirming the same function as for known EIZS and identifying the investigated enzyme as *Nocardia brevicatena epi*-isozizaene synthase (NbEIZS). GGPP was not converted, but the incubation with GPP resulted in the production of a complex mixture of monoterpenes including myrcene (**14**), sylvestrene (**15**), γ-terpinene (**16**), *cis*-sabinene hydrate (**17**), terpinolene (**18**), linalool (**19**), *cis*-*p*-ment-2-en-1-ol (**20**), terpinen-4-ol (**21**) and α-terpineol (**22**). All these compounds were identified by comparison of their mass spectra to library spectra and of their gas chromatographic retention indices to literature data (Table S5, Supporting Information File 1). This result stands in contrast to the inability of *epi*-isozizaene synthase from *Streptomyces bungoensis* to accept GPP as a substrate [45].

The terpene synthase homolog from *S. flavidovirens* (Table 1, entry 6) exhibited all highly conserved residues required for enzyme function including the aspartate-rich motif ^{80}DDQFD and the NSE triad ^{221}NDIHSFERE (Figure S35, Supporting Information File 1). This enzyme is with an identity of 78% closely related to the 7-*epi*-α-eudesmol synthase from *S. viridochromogenes* (SvES) [29,30], but forms a separate clade with nine other terpene synthase homologs (Figure S36, Supporting Information File 1), suggesting that it could have a different function. The incubation with FPP yielded 7-*epi*-α-eudesmol (**23**) as the main product, besides germacrene A (**24**) and hedycaryol (**26**) that were detected by their Cope rearrangement products elemene (**25**) and elemol (**27**) formed during GC–MS analysis (Figure 6 and Scheme 1A). These compounds are also observed with 7-*epi*-α-eudesmol synthase from *S. viridochromogenes*, demonstrating that the phylogenetic distance of the enzyme from *S. flavidovirens* is not associated with a different enzyme function. The conversion of GPP gave only trace amounts of acyclic products (geraniol and linalool), while GGPP and GFPP were not accepted as substrate. Taken together, the newly

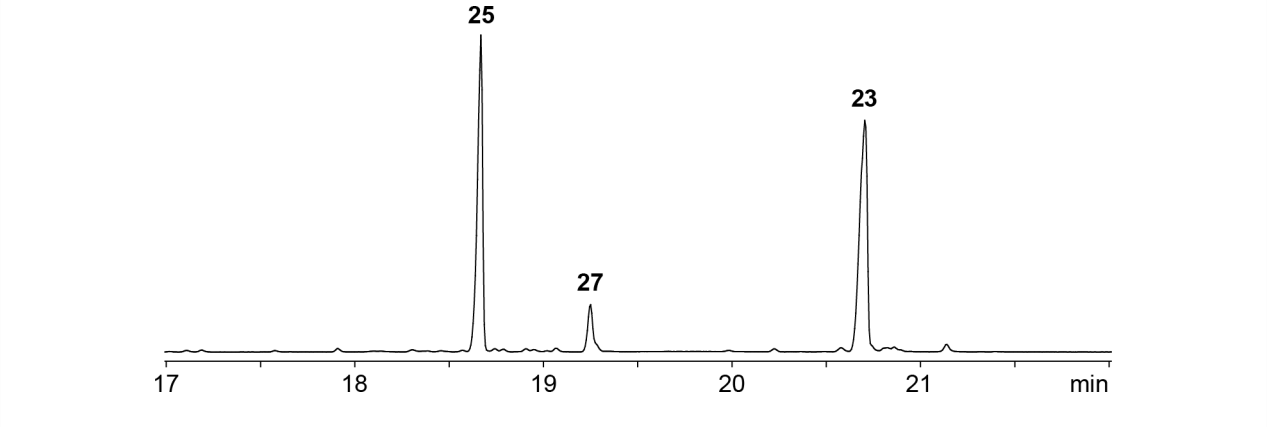

Figure 6: Total ion chromatogram of the products obtained with SfES. Peak numbers refer to compound numbers in Scheme 1.

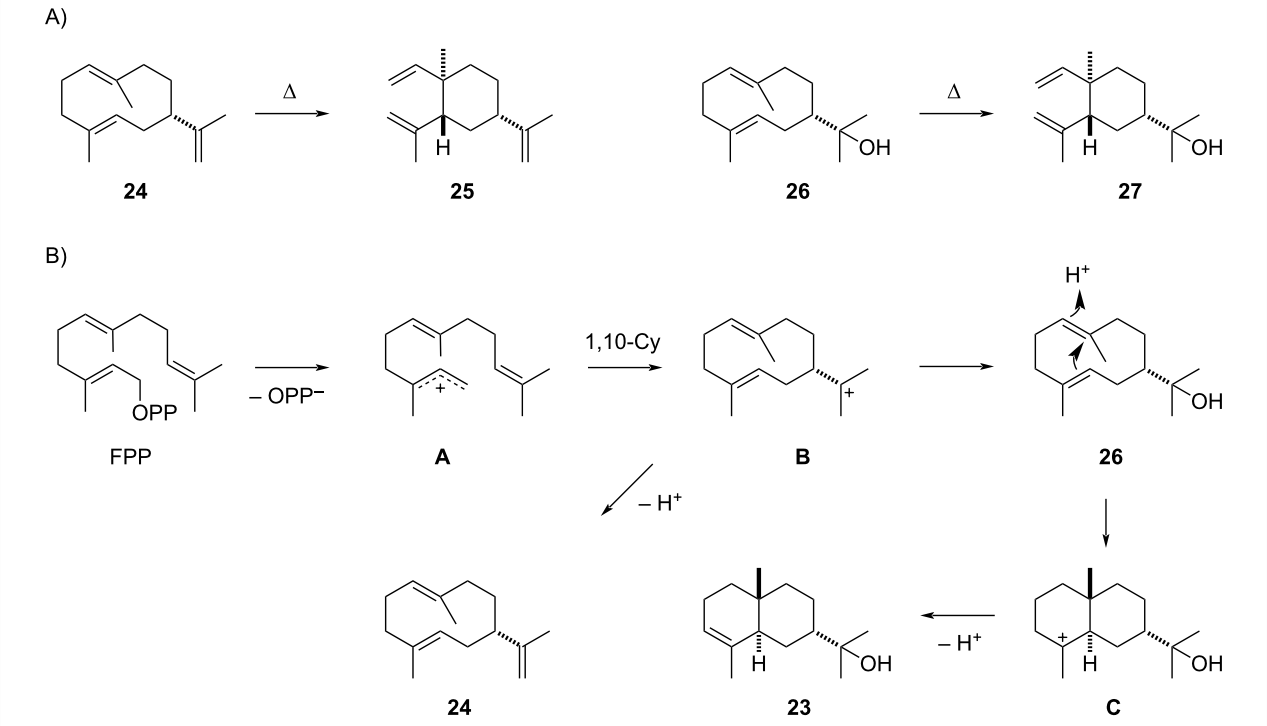

Scheme 1: A) Cope rearrangement of **24** and **26**. B) Cyclisation mechanism from FPP to **23**, identifying compound **26** as a biosynthetic intermediate and **24** as a side product.

characterised enzyme has a main activity for the formation of **23** and can thus be described as *Streptomyces flavidovirens* 7-*epi*-α-Eudesmol Synthase (SfES).

The formation of **24** and **26** can be well understood from the cyclisation mechanism towards **23** (Scheme 1B). After substrate ionisation to **A** a 1,10-cyclisation leads to the (*E*,*E*)-germacradienyl cation (**B**) that can either be deprotonated to **24** or captured with water to yield **26**. Both compounds are important neutral intermediates in sesquiterpene biosynthesis that can be reactivated by reprotonation for a second cyclisation to eudesmane (6,6-bicyclic) or guaiane (7,5-bicyclic) sesquiterpene hydrocarbons or alcohols, respectively [46,47]. Starting from **26**, such a protonation induced cyclisation can lead to **C** that is the direct precursor of **23** by deprotonation.

Furthermore, four closely related terpene synthase homologs from one clade in the phylogenetic tree were investigated (Figure S37, Supporting Information File 1), including enzymes from *S. sclerotialus*, *S. catenulae*, *S. ficellus* and *S. morookaense* (Table 1, entries 7–10). These enzymes showed a pairwise identity of 63% and all exhibited the highly conserved motifs of type I terpene synthases (Figures S38–S41, Supporting Information File 1), only for the enzyme from *S. sclerotialus* the pyrophosphate sensor is missing (Figure S38, Supporting Information File 1) and for the enzyme from *S. catenulae* the RY pair is modified to RF (Figure S39, Supporting Information File 1). The closest characterised homolog of these enzymes is the spiroviolene synthase from *S. violens* [27] with amino acid sequence identities between 32% and 36%. All four enzymes did not accept GPP, GGPP or GFPP, but converted FPP with low product formation into varying mixtures of hedycaryol and germacrene A, detected as Cope rearrangement products **25** and **27**, eventually besides acyclic products (Figure 7). According to the source organism, the enzymes were named as hedycaryol synthases (HS) SsHS, ScHS and SfHS, and the enzyme from *S. morookaense* with **24** as main product was named *Streptomyces morookaense* Germacrene A Synthase (SmGAS). Notably, these enzymes are unrelated to the previously characterised hedycaryol synthase from *Kitasatospora setae* [48] and the germacrene A synthase from *M. marina* [32]. The low productivity of the four enzymes together with the low sequence conservation between them and the deviations in their conserved motifs may point to a pseudogenisation within this branch of the phylogenetic tree. This view is further supported by the observation that three more genes from the same branch from *S. subrutilus*, *S. natalensis* and *S. violens* were in one case not expressed and in two cases only yielded soluble, but inactive enzymes with any of the tested substrates GPP, FPP, GGPP and GFPP (Table 1, entries 11–13).

Diterpene and sesterterpene synthases

One more terpene synthase homolog from *K. kofuensis* (Table 1, entry 14) revealed all highly conserved motifs (Figure S42, Supporting Information File 1) with the aspartate-rich region ^{81}DDINCD and a slightly modified NSE triad (^{224}DDLFSYGKE). This enzyme is most closely related to the cattleyene synthase (CyS) from *Streptomyces cattleya* that shows the same sequence deviation in the NSE triad and has 58% identity [49], and to phomopsene synthase from *A. albata* with 36% identity (Figure S43, Supporting Information File 1) [50]. The incubation of GPP, FPP and GFPP with the purified protein only resulted in acyclic products, while with GGPP an efficient conversion with high selectivity into allokutznerene (**28**), known as a minor product of bacterial phomopsene synthase [50], was observed (Figure 8A and 8B). It is interesting to note that the low sequence identity between phomopsene synthase and *Kutzneria konfuensis* Allokutznerene Synthase (KkAS) still leads to the same product. The phylogenetic tree in Figure S43 (Supporting Information File 1) implies that three more enzymes from the genus *Kutzneria* may act as allokutznerene synthases. While also a fungal phomopsene synthase is known from *Phomopsis amygdali* [51], the biosynthesis of **28** is so far limited to bacteria.

Finally, a terpene synthase homolog from *Streptomyces* sp. Tü 2975 was investigated in this study (Table 1, entry 15). The enzyme contains all conserved sequences with a slightly modified aspartate-rich motif (^{88}DDFIV) and the NSE triad ^{227}NDRYSFCKE, and is with an amino acid sequence identity of 85% closely related to the recently reported sesterviolene synthase from *Streptomyces violarus* (SvSS) [52]. Accordingly, also the enzyme from *Streptomyces* sp. Tü 2975 catalysed the conversion of GFPP into sesterviolene (**29**, Figure 8C and 8D), but GPP, FPP and GGPP were not taken as substrate. The newly identified enzyme was designated *Streptomyces* sp. Tü 2975 Sesterviolene Synthase (StSS).

Conclusion

Despite the accumulated knowledge on bacterial terpene synthases, the scattered distribution of sesqui-, di- and sesterterpene synthases in the phylogenetic tree of Figure 2 demonstrates that it is not possible to predict the substrate chain length of bacterial terpene synthases from a phylogenetic analysis. However, the phylogeny driven investigation of bacterial type I terpene synthase homologs can give access to terpene synthases with novel functions with a good success rate. This approach resulted in the identification of the first sesquiterpene synthases for (+)-δ-cadinol and (+)-α-cadinene, in addition to the first bacterial (−)-amorpha-4,11-diene synthase. This enzyme function was previously only known from *Artemisia annua* in which the (−)-amorpha-4,11-diene synthase is involved in the biosynthe-

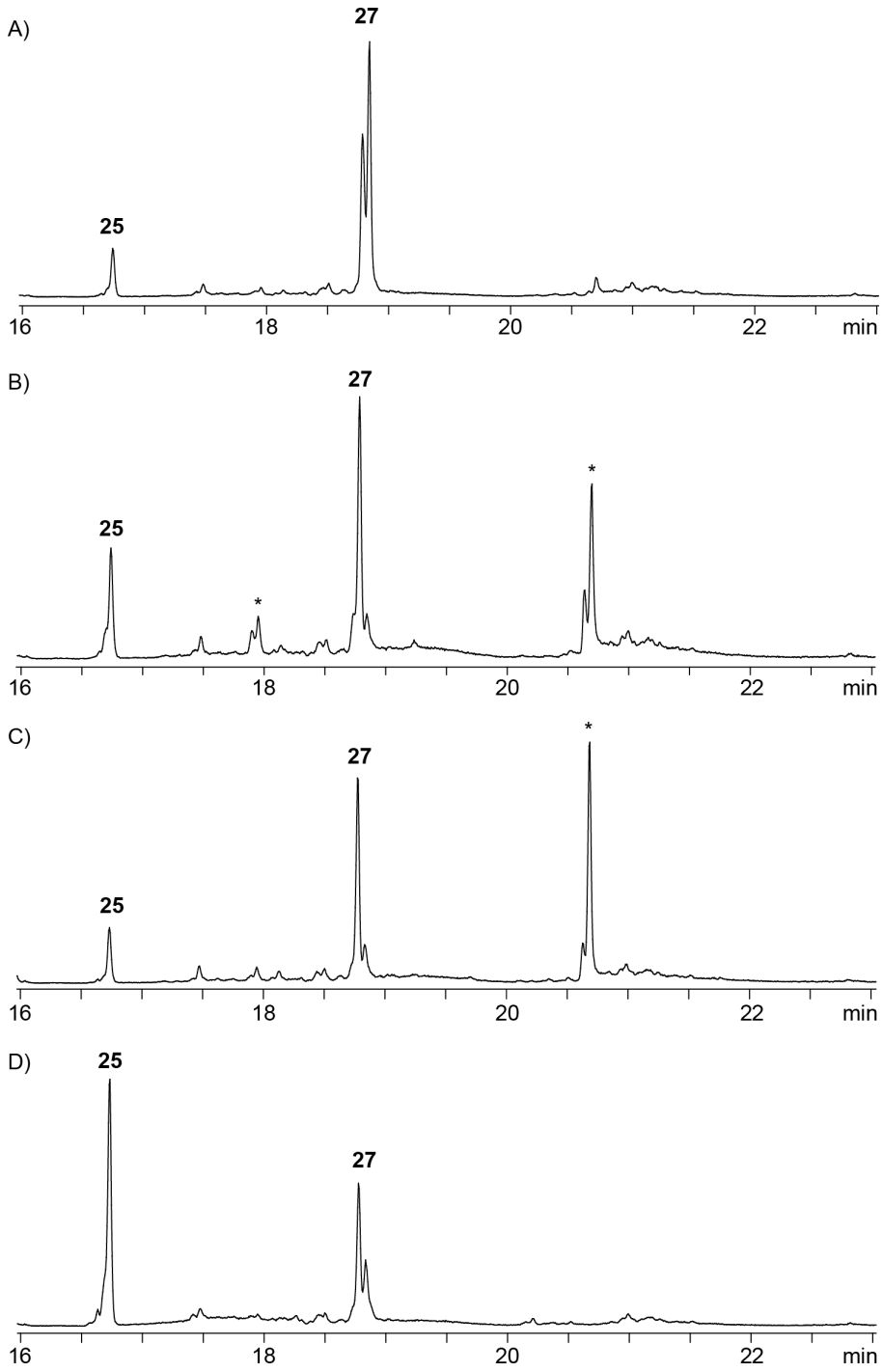

Figure 7: Total ion chromatograms of the products obtained with A) SsHS, B) ScHS, C) SfHS, and D) SmGAS. Peak numbers refer to compound numbers in Scheme 1. Asterisks indicate acyclic products and contaminants such as plasticisers.

sis of artemisinin. The newly discovered bacterial enzyme may be useful for future heterologous pathway reconstitution towards this important drug [52-54]. Enzymes rather closely related to known *epi*-isozizaene [24] and 7-*epi*-α-eudesmol synthases [29,30], but sufficiently distant to expect novel functions, were shown to still form the same products as the previously characterised enzymes. However, the *epi*-isozizaene synthase from *Nocardia brevifolia* exhibited in contrast to the known enzyme from *Streptomyces bungoensis* [45] a substantial monoterpene synthase activity with formation of a product mixture. The 7-*epi*-α-eudesmol synthase from *Streptomyces flavidovirens* showed a loss of function and selectivity with

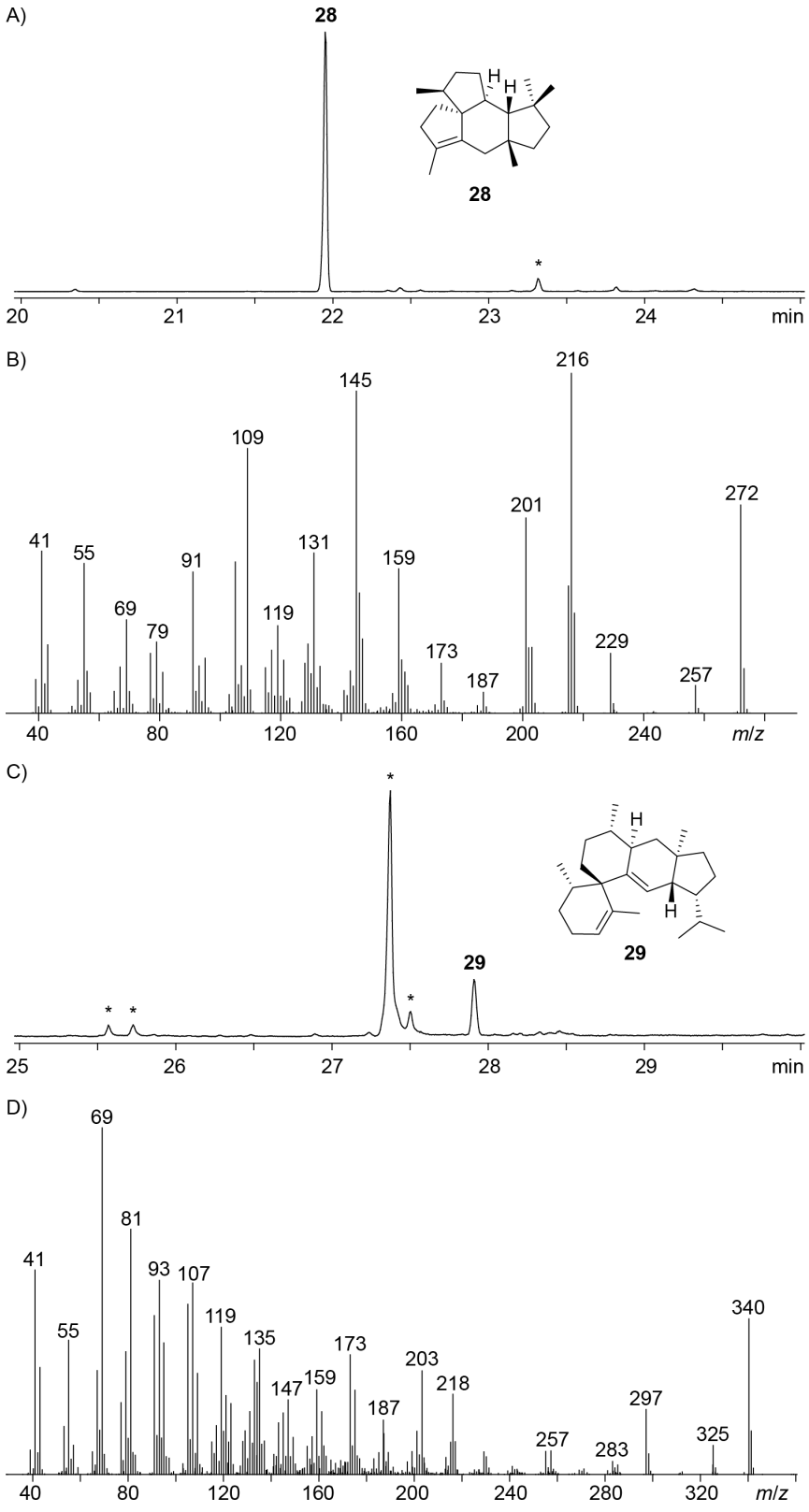

Figure 8: A) Total ion chromatogram of the products obtained from GGPP with KkAS, B) EI mass spectrum of allokutznerene (**28**), C) total ion chromatogram of the products obtained from GFPP with sesterviolene synthase from *Streptomyces* sp. Tü 2975, and D) EI mass spectrum of sesterviolene (**29**). Asterisks indicate acyclic products and contaminants such as plasticisers.

formation of hedycaryol and germacrene A. This observation may be interpreted as the starting point towards pseudogenisation within the branch of 7-*epi*-α-eudesmol synthases. Pseudogenisation may be more advanced within a previously uninvestigated clade of terpene synthase homologs that is distant to other characterised enzymes. Within this clade not only four enzymes producing mixtures of hedycaryol and germacrene A were identified, but also two inactive enzymes were obtained and one enzyme was not expressed. Another interesting discovery was the identification of a diterpene synthase from *Kutzneria kofuensis* that selectively produces allokutznerene. This compound was previously only known as a side product from a closely related phomopsene synthase from *Allokutzneria albata*. The availability of a selective enzyme for allokutznerene is particularly interesting, because the separation of phomopsene and allokutznerene is reportedly very difficult [50]. Last but not least, a sesterterpene synthase for sesterviolene was discovered from *Streptomyces* sp. Tü 2975 that is closely related to the known enzyme from *Streptomyces violarus* [15].

The description of terpene synthases with novel functions as reported in this study is not only important for specific potential applications such as the usage of the bacterial (−)-amorpha-4,11-diene synthase for a pathway reconstruction towards artemisinin. The increased knowledge about terpene synthases together with the structures of their products will also be of interest for machine learning approaches to enable the prediction of terpene synthase functions from their amino acid sequences. Both aspects are relevant arguments to continue the research on terpene synthases, despite the fact that already many enzymes of this class have been described.

Supporting Information

Supporting Information File 1

Additional information and spectra.
[https://www.beilstein-journals.org/bjoc/content/supplementary/1860-5397-19-100-S1.pdf]

Acknowledgements

We thank Heike Brötz-Oesterhelt for strain *Streptomyces* sp. Tü 2975.

Funding

This work was funded by the Deutsche Forschungsgemeinschaft (DFG), project number 513548540, and by the Alexander von Humboldt Foundation with a Georg Forster Research Fellowship granted to Georges B. Tabekoueng.

ORCID® iDs

Kizerbo A. Taizoumbe - https://orcid.org/0009-0000-2756-3354
Lukas Lauterbach - https://orcid.org/0000-0002-6924-2337
Jeroen S. Dickschat - https://orcid.org/0000-0002-0102-0631

References

1. Facchini, P. J.; Chappell, J. *Proc. Natl. Acad. Sci. U. S. A.* **1992,** *89,* 11088–11092. doi:10.1073/pnas.89.22.11088
2. Mau, C. J.; West, C. A. *Proc. Natl. Acad. Sci. U. S. A.* **1994,** *91,* 8497–8501. doi:10.1073/pnas.91.18.8497
3. Zhou, F.; Pichersky, E. *Curr. Opin. Plant Biol.* **2020,** *55,* 1–10. doi:10.1016/j.pbi.2020.01.005
4. Degenhardt, J.; Köllner, T. G.; Gershenzon, J. *Phytochemistry* **2009,** *70,* 1621–1637. doi:10.1016/j.phytochem.2009.07.030
5. Li, G.; Köllner, T. G.; Yin, Y.; Jiang, Y.; Chen, H.; Xu, Y.; Gershenzon, J.; Pichersky, E.; Chen, F. *Proc. Natl. Acad. Sci. U. S. A.* **2012,** *109,* 14711–14715. doi:10.1073/pnas.1204300109
6. Cane, D. E.; Prabhakaran, P. C.; Salaski, E. J.; Harrison, P. H. M.; Noguchi, H.; Rawlings, B. J. *J. Am. Chem. Soc.* **1989,** *111,* 8914–8916. doi:10.1021/ja00206a022
7. Proctor, R. H.; Hohn, T. M. *J. Biol. Chem.* **1993,** *268,* 4543–4548. doi:10.1016/s0021-9258(18)53644-9
8. Toyomasu, T.; Tsukahara, M.; Kaneko, A.; Niida, R.; Mitsuhashi, W.; Dairi, T.; Kato, N.; Sassa, T. *Proc. Natl. Acad. Sci. U. S. A.* **2007,** *104,* 3084–3088. doi:10.1073/pnas.0608426104
9. Tao, H.; Lauterbach, L.; Bian, G.; Chen, R.; Hou, A.; Mori, T.; Cheng, S.; Hu, B.; Lu, L.; Mu, X.; Li, M.; Adachi, N.; Kawasaki, M.; Moriya, T.; Senda, T.; Wang, X.; Deng, Z.; Abe, I.; Dickschat, J. S.; Liu, T. *Nature* **2022,** *606,* 414–419. doi:10.1038/s41586-022-04773-3
10. Cane, D. E.; Sohng, J.-K.; Lamberson, C. R.; Rudnicki, S. M.; Wu, Z.; Lloyd, M. D.; Oliver, J. S.; Hubbard, B. R. *Biochemistry* **1994,** *33,* 5846–5857. doi:10.1021/bi00185a024
11. Dickschat, J. S. *Nat. Prod. Rep.* **2016,** *33,* 87–110. doi:10.1039/c5np00102a
12. Jiang, J.; He, X.; Cane, D. E. *Nat. Chem. Biol.* **2007,** *3,* 711–715. doi:10.1038/nchembio.2007.29
13. Wang, C.-M.; Cane, D. E. *J. Am. Chem. Soc.* **2008,** *130,* 8908–8909. doi:10.1021/ja803639g
14. Hou, A.; Dickschat, J. S. *Angew. Chem., Int. Ed.* **2020,** *59,* 19961–19965. doi:10.1002/anie.202010084
15. Gu, B.; Goldfuss, B.; Dickschat, J. S. *Angew. Chem., Int. Ed.* **2023,** *62,* e202215688. doi:10.1002/anie.202215688
16. Xu, H.; Schnakenburg, G.; Goldfuss, B.; Dickschat, J. S. *Angew. Chem., Int. Ed.* **2023,** *62,* e202306429. doi:10.1002/anie.202306429
17. Beran, F.; Rahfeld, P.; Luck, K.; Nagel, R.; Vogel, H.; Wielsch, N.; Irmisch, S.; Ramasamy, S.; Gershenzon, J.; Heckel, D. G.; Köllner, T. G. *Proc. Natl. Acad. Sci. U. S. A.* **2016,** *113,* 2922–2927. doi:10.1073/pnas.1523468113
18. Scesa, P. D.; Lin, Z.; Schmidt, E. W. *Nat. Chem. Biol.* **2022,** *18,* 659–663. doi:10.1038/s41589-022-01027-1
19. Burkhardt, I.; de Rond, T.; Chen, P. Y.-T.; Moore, B. S. *Nat. Chem. Biol.* **2022,** *18,* 664–669. doi:10.1038/s41589-022-01026-2
20. Kersten, R. D.; Lee, S.; Fujita, D.; Pluskal, T.; Kram, S.; Smith, J. E.; Iwai, T.; Noel, J. P.; Fujita, M.; Weng, J.-K. *J. Am. Chem. Soc.* **2017,** *139,* 16838–16844. doi:10.1021/jacs.7b09452
21. Wei, G.; Jia, Q.; Chen, X.; Köllner, T. G.; Bhattacharya, D.; Wong, G. K.-S.; Gershenzon, J.; Chen, F. *Plant Physiol.* **2019,** *179,* 382–390. doi:10.1104/pp.18.01413

22. Chen, X.; Köllner, T. G.; Jia, Q.; Norris, A.; Santhanam, B.; Rabe, P.; Dickschat, J. S.; Shaulsky, G.; Gershenzon, J.; Chen, F. *Proc. Natl. Acad. Sci. U. S. A.* **2016,** *113,* 12132–12137. doi:10.1073/pnas.1610379113
23. Rabe, P.; Rinkel, J.; Nubbemeyer, B.; Köllner, T. G.; Chen, F.; Dickschat, J. S. *Angew. Chem., Int. Ed.* **2016,** *55,* 15420–15423. doi:10.1002/anie.201608971
24. Lin, X.; Hopson, R.; Cane, D. E. *J. Am. Chem. Soc.* **2006,** *128,* 6022–6023. doi:10.1021/ja061292s
25. Nakano, C.; Horinouchi, S.; Ohnishi, Y. *J. Biol. Chem.* **2011,** *286,* 27980–27987. doi:10.1074/jbc.m111.265652
26. Baer, P.; Rabe, P.; Fischer, K.; Citron, C. A.; Klapschinski, T. A.; Groll, M.; Dickschat, J. S. *Angew. Chem., Int. Ed.* **2014,** *53,* 7652–7656. doi:10.1002/anie.201403648
27. Rabe, P.; Rinkel, J.; Dolja, E.; Schmitz, T.; Nubbemeyer, B.; Luu, T. H.; Dickschat, J. S. *Angew. Chem., Int. Ed.* **2017,** *56,* 2776–2779. doi:10.1002/anie.201612439
28. Rinkel, J.; Dickschat, J. S. *Org. Lett.* **2019,** *21,* 9442–9445. doi:10.1021/acs.orglett.9b03654
29. Rabe, P.; Dickschat, J. S. *Angew. Chem., Int. Ed.* **2013,** *52,* 1810–1812. doi:10.1002/anie.201209103
30. Rabe, P.; Schmitz, T.; Dickschat, J. S. *Beilstein J. Org. Chem.* **2016,** *12,* 1839–1850. doi:10.3762/bjoc.12.173
31. Nakano, C.; Tezuka, T.; Horinouchi, S.; Ohnishi, Y. *J. Antibiot.* **2012,** *65,* 551–558. doi:10.1038/ja.2012.68
32. Rinkel, J.; Dickschat, J. S. *Org. Lett.* **2019,** *21,* 2426–2429. doi:10.1021/acs.orglett.9b00725
33. Rabe, P.; Barra, L.; Rinkel, J.; Riclea, R.; Citron, C. A.; Klapschinski, T. A.; Janusko, A.; Dickschat, J. S. *Angew. Chem., Int. Ed.* **2015,** *54,* 13448–13451. doi:10.1002/anie.201507615
34. Sakai, T.; Nishimura, K.; Chikamatsu, H.; Hirose, Y. *Bull. Chem. Soc. Jpn.* **1963,** *36,* 1261–1264. doi:10.1246/bcsj.36.1261
35. Van Eijk, G. W.; Roeijmans, H. J.; Verwiel, P. E. J. *Exp. Mycol.* **1984,** *8,* 273–275. doi:10.1016/0147-5975(84)90012-4
36. Xu, H.; Rinkel, J.; Dickschat, J. S. *Org. Chem. Front.* **2021,** *8,* 1177–1184. doi:10.1039/d0qo01583k
37. Naya, Y.; Kotake, M. *Bull. Chem. Soc. Jpn.* **1969,** *42,* 1468. doi:10.1246/bcsj.42.1468
38. Chen, X.-Y.; Chen, Y.; Heinstein, P.; Davisson, V. J. *Arch. Biochem. Biophys.* **1995,** *324,* 255–266. doi:10.1006/abbi.1995.0038
39. Davis, E. M.; Tsuji, J.; Davis, G. D.; Pierce, M. L.; Essenberg, M. *Phytochemistry* **1996,** *41,* 1047–1055. doi:10.1016/0031-9422(95)00771-7
40. Hu, Y.; Chou, W. K. W.; Hopson, R.; Cane, D. E. *Chem. Biol.* **2011,** *18,* 32–37. doi:10.1016/j.chembiol.2010.11.008
41. Burkhardt, I.; Kreuzenbeck, N. B.; Beemelmanns, C.; Dickschat, J. S. *Org. Biomol. Chem.* **2019,** *17,* 3348–3355. doi:10.1039/c8ob02744g
42. Rinkel, J.; Lauterbach, L.; Rabe, P.; Dickschat, J. S. *Angew. Chem., Int. Ed.* **2018,** *57,* 3238–3241. doi:10.1002/anie.201800385
43. Bohlmann, F.; Gerke, T.; Jakupovic, J.; King, R. M.; Robinson, H. *Phytochemistry* **1984,** *23,* 1183–1184. doi:10.1016/s0031-9422(00)82638-2
44. Mercke, P.; Bengtsson, M.; Bouwmeester, H. J.; Posthumus, M. A.; Brodelius, P. E. *Arch. Biochem. Biophys.* **2000,** *381,* 173–180. doi:10.1006/abbi.2000.1962
45. Lauterbach, L.; Dickschat, J. S. *Org. Biomol. Chem.* **2020,** *18,* 4547–4550. doi:10.1039/d0ob00606h
46. Xu, H.; Dickschat, J. S. *Chem. – Eur. J.* **2020,** *26,* 17318–17341. doi:10.1002/chem.202002163
47. Xu, H.; Dickschat, J. S. *Chem. – Eur. J.* **2022,** *28,* e202200405. doi:10.1002/chem.202200405
48. Xu, H.; Lackus, N. D.; Köllner, T. G.; Dickschat, J. S. *Org. Lett.* **2022,** *24,* 587–591. doi:10.1021/acs.orglett.1c04021
49. Rinkel, J.; Steiner, S. T.; Dickschat, J. S. *Angew. Chem., Int. Ed.* **2019,** *58,* 9230–9233. doi:10.1002/anie.201902950
50. Lauterbach, L.; Rinkel, J.; Dickschat, J. S. *Angew. Chem., Int. Ed.* **2018,** *57,* 8280–8283. doi:10.1002/anie.201803800
51. Toyomasu, T.; Kaneko, A.; Tokiwano, T.; Kanno, Y.; Kanno, Y.; Niida, R.; Miura, S.; Nishioka, T.; Ikeda, C.; Mitsuhashi, W.; Dairi, T.; Kawano, T.; Oikawa, H.; Kato, N.; Sassa, T. *J. Org. Chem.* **2009,** *74,* 1541–1548. doi:10.1021/jo802319e
52. Ro, D.-K.; Paradise, E. M.; Ouellet, M.; Fisher, K. J.; Newman, K. L.; Ndungu, J. M.; Ho, K. A.; Eachus, R. A.; Ham, T. S.; Kirby, J.; Chang, M. C. Y.; Withers, S. T.; Shiba, Y.; Sarpong, R.; Keasling, J. D. *Nature* **2006,** *440,* 940–943. doi:10.1038/nature04640
53. Paddon, C. J.; Westfall, P. J.; Pitera, D. J.; Benjamin, K.; Fisher, K.; McPhee, D.; Leavell, M. D.; Tai, A.; Main, A.; Eng, D.; Polichuk, D. R.; Teoh, K. H.; Reed, D. W.; Treynor, T.; Lenihan, J.; Jiang, H.; Fleck, M.; Bajad, S.; Dang, G.; Dengrove, D.; Diola, D.; Dorin, G.; Ellens, K. W.; Fickes, S.; Galazzo, J.; Gaucher, S. P.; Geistlinger, T.; Henry, R.; Hepp, M.; Horning, T.; Iqbal, T.; Kizer, L.; Lieu, B.; Melis, D.; Moss, N.; Regentin, R.; Secrest, S.; Tsuruta, H.; Vazquez, R.; Westblade, L. F.; Xu, L.; Yu, M.; Zhang, Y.; Zhao, L.; Lievense, J.; Covello, P. S.; Keasling, J. D.; Reiling, K. K.; Renninger, N. S.; Newman, J. D. *Nature* **2013,** *496,* 528–532. doi:10.1038/nature12051
54. Yuan, J.; Ching, C.-B. *Metab. Eng.* **2016,** *38,* 303–309. doi:10.1016/j.ymben.2016.07.008

License and Terms

Appendix E

The Stereochemical Course of DmdC, an Enzyme Involved in the Degradation of Dimethylsulfoniopropionate

Chembiochem **2024**, *25*, e202300795

DOI: 10.1002/cbic.202300795

ChemBioChem

Research Article
doi.org/10.1002/cbic.202300795

Chemistry Europe
European Chemical Societies Publishing

www.chembiochem.org

The Stereochemical Course of DmdC, an Enzyme Involved in the Degradation of Dimethylsulfoniopropionate

Anuj K. Chhalodia[a] and Jeroen S. Dickschat*[a]

The acyl-CoA dehydrogenase DmdC is involved in the degradation of the marine sulfur metabolite dimethylsulfonio propionate (DMSP) through the demethylation pathway. The stereochemical course of this reaction was investigated through the synthesis of four stereoselectively deuterated substrate surrogates carrying stereoselective deuterations at the α- or the β-carbon. Analysis of the products revealed a specific abstraction of the 2-*pro-R* proton and of the 3-*pro-S* hydride, establishing an *anti* elimination for the DmdC reaction.

Introduction

After the discovery that *Polysiphonia fastigiata* and *P. nigrescens* produce the gas dimethylsulfide,[1] dimethylsulfonium propionate (DMSP) was identified as the storage form in these red algae.[2] DMSP functions as an osmolyte[3] and cryoprotectant[4] and is an important signalling molecule in the chemotaxis of marine bacteria towards polysaccharides.[5] DMSP is one of the most abundant sulfur compounds in marine ecosystems that has been identified in green algae,[6] dinoflagellates,[7] coccolitophores,[3] the salt marsh plant *Spartina alternifolia*,[8] and corals.[9] Different pathways have been described for the biosynthesis of DMSP in green algae,[10] higher plants,[11–13] bacteria,[14,15] and corals,[16] that all start from L-methionine and involve an S-methylation, a decarboxylation and a functional group manipulation at the original α-carbon, but in different orders of steps. It is estimated that the total annual production of DMSP reaches petagram amounts,[17] and a substantial fraction of it is converted into DMS, leading to an estimated annual release of 13–37 teragrams of sulfur from oceanic waters into the atmosphere,[18] with importance for the global sulfur cycle[19] and climate.[20,21]

Several enzymes have been discovered for the breakdown of DMSP, including seven bacterial DMSP lyases (DddL, DddP, DddQ, DddW, DddY, DddK and DddU)[22–28] and Alma1 from the coccolithophore *Emiliana huxleyi*[29] that catalyse an elimination reaction to DMS and acrylate (**1**) (Scheme 1A). In contrast, the DMSP lyase DddD catalyses the hydrolysis of DMSP to DMS and 3-hydroxypropionate (**2**),[30] while the recently described lyase DddX is a bifunctional enzyme that first converts DMSP into the corresponding coenzyme A thioester before cleavage into DMS and acyloyl-CoA (**3**).[31] Another fraction of DMSP is oxidised to dimethylsulfoxonium propionate (DMSOP),[32] but no enzyme is

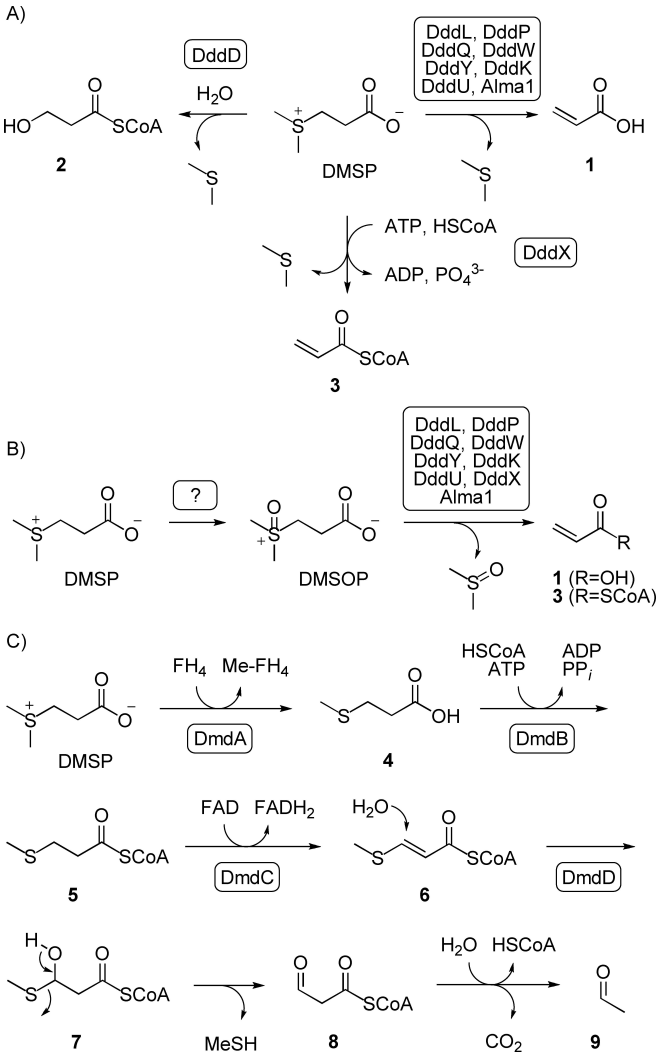

Scheme 1. DMSP degradation pathways. A) Cleavage of DMSP with formation of DMS, B) oxidation to DMSOP and cleavage with formation of DMSO, C) demethylation pathway.

[a] *A. K. Chhalodia, Prof. Dr. J. S. Dickschat*
Kekulé Institute of Organic Chemistry and Biochemistry
University of Bonn
Gerhard-Domagk-Straße 1, 53121 Bonn, Germany
E-mail: dickschat@uni-bonn.de

Supporting information for this article is available on the WWW under https://doi.org/10.1002/cbic.202300795

known for this important transformation. The cleavage of DMSOP leads to the non-volatile and water soluble metabolite dimethylsulfoxide (DMSO), a reaction that can be catalysed by DMSP lyases in vitro and in vivo.[32–34] These reactions limit the sulfur flux from the oceans, as does the breakdown through the demethylation pathway that proceeds with the action of four enzymes[35,36] and is the major pathway for DMSP degradation.[37] The first enzyme catalyses the demethylation of DMSP with tetrahydrofolate (FH_4) to 3-(methylsulfanyl)propionate (**4**), followed by conversion into the coenzyme A thioester **5** by the CoA ligase DmdB. Oxidation by the FAD dependent dehydrogenase DmdC leads to **6** that is hydrolysed by the enoyl-CoA hydratase and thioester hydrolase DmdD. The addition of water first results in the hemithioacetal **7** that collapses to methanethiol (MeSH) and **8**. Hydrolysis of the CoA thioester and decarboxylation finally yield acetaldehyde.[36] Here we report on the synthesis of four stereoselectively deuterated N-acetylcysteamine thioester (SNAc ester) analogs of **5** and their application in the determination of the stereochemical course of the reaction catalysed by DmdC.

Results and Discussion

To investigate the stereochemical course of the DmdC reaction, the coding sequence from *Ruegeria pomeroyi* DSS-3 (accession number AAV97018) was cloned into the expression vector pYE-Express through heterologous recombination in yeast and expressed in *Escherichia coli* BL21 (DE3). The purified recombinant protein (Figure S1) was then incubated with the SNAc ester of 3-(methylsulfanyl)propionic acid (**10**), a surrogate of the natural substrate **5** that was synthesised as shown in Scheme 2A, resulting in the efficient conversion into **11**.

The successful conversion of **10** allowed for an investigation of the stereochemical course of DmdC using stereoselectively deuterated isotopologues of **10**. A stereoselective deuteration at the α-carbon was introduced starting from (*S*)-styrene epoxide (**12**) in which the epoxide was opened through catalytic hydrogenation using deuterium gas (Scheme 2B). This reaction is known to proceed with a clean inversion of configuration[38] to yield the alcohol **13**. Bromination to **14**, oxidative cleavage of the phenyl ring with periodic acid and $RuCl_3$ to **15** and nucleophilic substitution with NaSMe gave (*R*)-(2-^{2}H)-**4** that was converted into the SNAc ester (*S*)-(2-^{2}H)-**10** under standard conditions. Along the same lines, (*R*)-(2-^{2}H)-**10** was synthesised staring from (*R*)-styrene epoxide.

For the synthesis of **10** with a stereoselective deuteration at the β-carbon a similar approach was used (Scheme 2C). Methyl phenylacetate (**16**) was reduced with $LiAlD_4$ to obtain (1,1-$^2H_2$)-**13**. Oxidation with IBX to **17** and a stereoselective reduction with (*S*)-Alpine borane gave (*R*)-(1-^{2}H)-**13**, with a high enantiomeric purity as evident from a Mosher ester analysis (Figure S2). The same sequence of bromination, oxidative phenyl group degradation, nucleophilic substitution and esterification yielded (*R*)-(3-^{2}H)-**10**. Its enantiomer (*S*)-(3-^{2}H)-**10** was prepared analogously using (*R*)-Alpine borane in the stereoselective reduction of **17**.

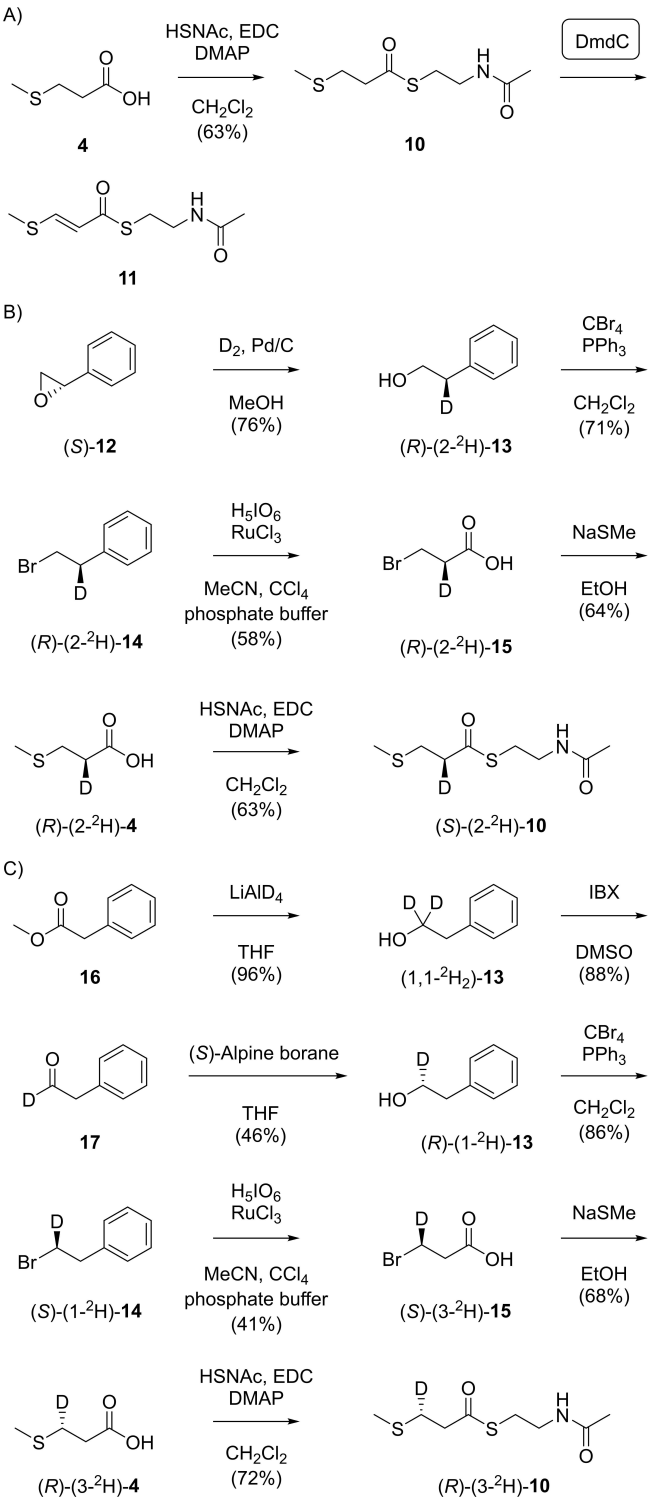

Scheme 2. Synthesis of SNAc ester **10** and its deuterated isotopologues. A) Synthesis of unlabelled **10** and conversion with DmdC into **11**. B) Route for the stereoselective deuteration at C2, C) route for the stereoselective deuteration at C3.

All four stereoselectively deuterated isotopomers of **10** were incubated with DmdC, followed by extraction and GC/MS analysis of the products. The electron ionisation (EI) mass spectrometric analysis revealed a retainment of deuterium in **11**

from (*S*)-(2-^{2}H)-**10** by the molecular ion at *m/z* 220 and diagnostic fragment ions at *m/z* 102 and 74 (Figure 1A; for unlabelled **11** these ions are detected at *m/z* 219, 101, and 73 respectively). The minor fragment ion at *m/z* 101 indicated also a partial loss of deuterium, but this loss is likely non-enzymatic, because its intensity was higher upon prolonged incubation times (Figure S3). Furthermore, a control experiment with unlabelled **10** in deuterium oxide resulted in the incorporation of deuterium from bulk water (Figure S3).

For the conversion of (*R*)-(2-^{2}H)-**10** a clear loss of deuterium was indicated by the molecular ion at *m/z* 219, the base peak at *m/z* 101, and an additional fragment ion at *m/z* 73 (Figure 1B).

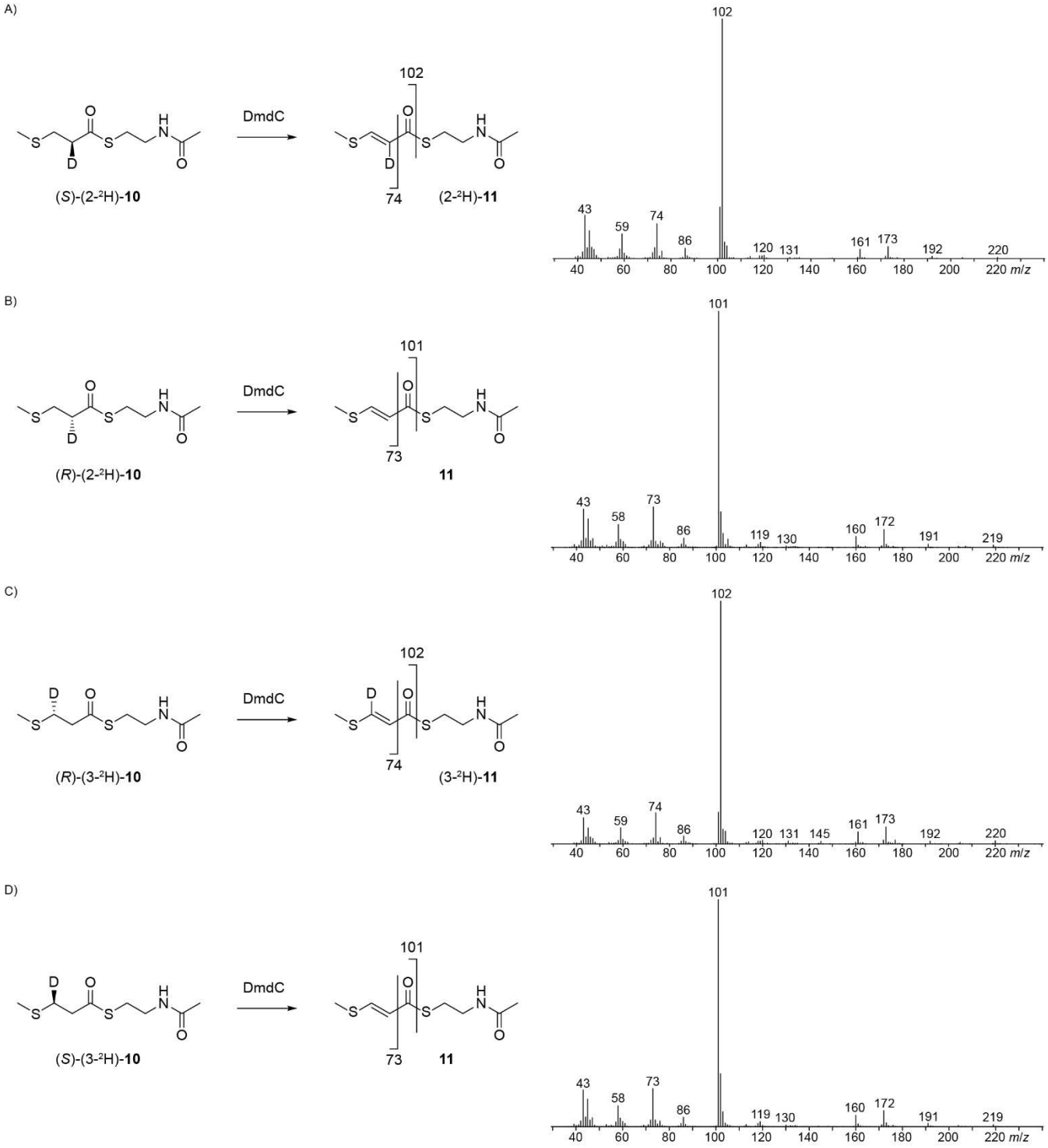

Figure 1. The stereochemical course of DmdC. The incubation of the SNAc esters of A) (*S*)-(2-^{2}H)-3-(methylsulfanyl)propionic acid and B) (*R*)-(2-^{2}H)-3-(methylsulfanyl)propionic acid demonstrate the abstraction of the 2-*pro-R* hydrogen, and of C) (*R*)-(3-^{2}H)-3-(methylsulfanyl)propionic acid and D) (*S*)-(3-^{2}H)-3-(methylsulfanyl)propionic acid demonstrate the abstraction of the 3-*pro-S* hydrogen.

Taken together, these data demonstrate the selective abstraction of the 2-*pro-R* proton in the DmdC reaction.

With respect to the course of the hydride abstraction from the β-carbon, the incubation of (*R*)-(3-^{2}H)-**10** revealed a full retainment of deuterium (*m/z* 220, 102, and 74 Figure 1C), whereas with (*S*)-(3-^{2}H)-**10** the loss of deuterium was observed (*m/z* 219, 101, and 73 Figure 1D). In combination, these results show the abstraction of the 3-*pro-S* hydride, and thus the overall DmdC reaction proceeds with *anti* elimination.

Conclusions

The stereoselective labelling experiments presented in this study have shown that the acyl-CoA dehydrogenase DmdC catalyses an *anti*-elimination and abstracts the 2-*pro-R* proton and the 3-*pro-S* hydride in the dehydrogenation of the substrate surrogate **10**. The same stereochemical course can be assumed for the natural substrate coenzyme A thioester **5** (Scheme 3). Analogous findings with the same stereochemical course have also been reported for acyl-CoA dehydrogenases from pork liver,[39,40] from *Clostridium kluyveri*,[41] from rat liver[42] and *Candida lipolytica*[42] involved in the ß-oxidation of fatty acids (these enzymes formally abstract the 2-*pro-R* proton and the 3-*pro-R* hydride, but these are because of a change in the priority of substituents the same hydrogens). This stereochemical course was later also confirmed by a crystal structure of the pig liver enzyme in complex with the substrate.[43] A crystal structure is also available for DmdC,[44] but unfortunately no structure has been obtained together with the substrate and FAD. Therefore, the data presented here give first conclusive insights into the stereochemical course of the dehydrogenation by DmdC.

Experimental Section

General synthetic and analytical methods. All chemicals were purchased from TCI Deutschland (Eschborn, Germany) or Sigma Aldrich (Darmstadt, Germany) and used without purification. Solvents were dried according to standard procedures and purified by distillation. Silica gel 60 (100–200 mesh) was used for column chromatography. Thin-layer chromatography was performed with 0.2 mm pre-coated plastic sheets Polygram Sil G/UV254 (Machery-Nagel, Düren, Germany). ^{1}H-NMR and ^{13}C-NMR spectra were recorded on a Bruker AV I (500 MHz) or AV III HD Prodigy (700 MHz) spectrometer in $CDCl_3$ or C_6D_6. Spectra were referenced against solvent signals (^{1}H-NMR: $CDCl_3$ δ = 7.26 ppm, C_6D_6 δ = 7.16 ppm; ^{13}C-NMR: $CDCl_3$ δ = 77.01 ppm, C_6D_6 δ = 128.06 ppm) for ^{13}C-NMR.[45] IR spectra were recorded on a Bruker α infrared spectrometer with a diamond ATR probe head. Peak intensities are given as s (strong), m (medium), w (weak) and br (broad). HRMS (ESI) data were recorded on an LTQ Orbitrap XL mass spectrometer using acetonitrile as solvent.

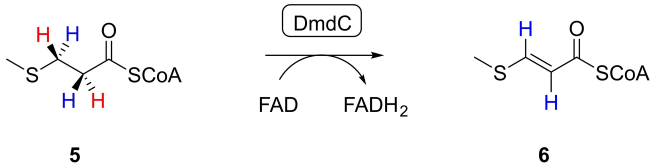

5 6

Scheme 3. The stereochemical course of the dehydrogenation of DMSP by DmdC.

Synthesis of (*R*)- and (*S*)-(2-^{2}H)-2-phenylethanol (13). (*S*)-Styrene epoxide (**12**) (1.90 g, 15.8 mmol, 1.0 equiv.) was dissolved in dry methanol (50 mL). Pd/C (0.2 g, 1.9 mmol, 0.12 equiv.) was added, followed by stirring in a D_2 atmosphere (1 bar) at room temperature overnight. After completion of reaction, the reaction mixture was filtered through a pad of celite. The filtrate was collected and the solvent was evaporated in vacuo. Purification of the crude product by silica gel column chromatography (15% EtOAc/petrol ether) yielded (*R*)-(2-^{2}H)-**13** (1.83 g, 14.9 mmol, 94%) as a colourless oil. TLC (30% EtOAc/petrol ether): R_f = 0.35. ^{1}H-NMR (C_6D_6, 500 MHz):δ = 7.15-7.10 (m, 2H), 7.08-7.04 (m, 1H), 7.03-6.99 (m, 2H), 3.52–3.46 (m, 2H), 2.57-2.50 (m, 1H), 0.81 (br s, 1H) ppm. ^{13}C-NMR (C_6D_6, 126 MHz):δ = 139.27 (C_q), 129.33 (2×CH), 128.69 (2×CH), 126.52 (CH), 63.64 (CH_2), 39.32 (t, $^1J_{C\text{-}D}$ = 19.4 Hz, CHD) ppm. IR (diamond-ATR): $\tilde{\nu}$ = 3356 (br), 3060 (w), 3026 (w), 2924 (w), 2875 (w), 1689 (w), 1603 (w), 1495 (w), 1451 (w), 1026 (m), 741 (w), 697 (m), 490 (w) cm^{-1}. Optical rotation: $[\alpha]_D^{25} = -3.4$ (*c* 0.08, C_6H_6). HRMS (APCI): $[M+H]^+$ calcd. for $C_8H_{10}{}^2HO^+$ *m/z* 124.0867; found *m/z* 124.0868.

The same procedure was used to convert (*R*)-**12** (4.00 g, 33.3 mmol) into (*S*)-(2-^{2}H)-**13** (3.10 g, 25.2 mmol, 76%). All spectral data were identical to those of (*R*)-(2-^{2}H)-**13**. Optical rotation: $[\alpha]_D^{25} = +4.0$ (*c* 0.05, C_6H_6). HRMS (APCI): $[M+H]^+$ calcd. for $C_8H_{10}{}^2HO^+$ *m/z* 124.0867; found *m/z* 124.0869.

Synthesis of (*R*)- and (*S*)-(2-^{2}H)-2-phenylethyl bromide (14). To the solution of (*R*)-(2-^{2}H)-**13** (1.50 g, 12.2 mmol, 1.0 equiv.) in dry CH_2Cl_2 (25 mL) was added CBr_4 (4.44 g, 13.4 mmol, 1.1 equiv.) at room temperature. The reaction mixture was cooled to 0 °C and PPh_3 (3.51 g, 13.4 mmol, 1.1 equiv.) was added portionwise over 10 min. The reaction mixture was warmed to room temperature and stirred overnight. After completion of the reaction, petrol ether was added, leading to precipitation of triphenylphosphine oxide. After filtration the solvents were evaporated in vacuo. The crude compound was purified by silica gel column chromatography (petrol ether) to obtain (*R*)-(2-^{2}H)-**14** (1.95 g, 10.5 mmol, 86%) as a colourless oil. TLC (petrol ether): R_f = 0.68. ^{1}H-NMR (C_6D_6, 500 MHz): δ = 7.09-7.00 (m, 3H), 6.83–6.78 (m, 2H), 3.06 (m, 2H), 2.74–2.69 (m, 1H) ppm.^{13}C-NMR (C_6D_6, 126 MHz): δ = 139.13 (C_q), 128.85 (2×CH), 128.72 (2×CH), 127.01 (CH), 39.12 (t, $^1J_{C\text{-}D}$ = 19.9 Hz, CHD), 32.70 (CH_2) ppm. IR (diamond-ATR): $\tilde{\nu}$ = 3084 (w), 3061 (w), 3027 (w), 2961 (w), 2926 (w), 2858 (w), 1704 (w), 1602 (w), 1495 (w), 1451 (w), 1434 (w), 1279 (w), 1219 (w), 1109 (w), 1076 (w), 746 (w), 698 (m), 669 (w), 536 (w) cm^{-1}. Optical rotation:$[\alpha]_D^{25} = -3.5$ (*c* 0.06, C_6H_6).

The same procedure was used to convert (*S*)-(2-^{2}H)-**13** (2.20 g, 17.9 mmol) into (*S*)-(2-^{2}H)-**14** (2.95 g, 15.8 mmol, 88%). All spectral data were identical to those of (*R*)-(2-^{2}H)-**14**. Optical rotation: $[\alpha]_D^{25} = +4.1$ (*c* 0.05, C_6H_6).

Synthesis of (*R*)- and (*S*)-(2-^{2}H)-3-bromopropionic acid (15). The bromide (*R*)-(2-^{2}H)-**14** (1.00 g, 5.37 mmol, 1.0 equiv.) was dissolved in acetonitrile (10 mL), CCl_4 (10 mL) and phosphate buffer (pH 7, 10 mL). The reaction mixture was cooled to 0 °C and H_5IO_6 (12.3 g, 53.7 mmol, 10.0 equiv.) was added portionwise over 15 min. The reaction mixture was stirred at 0 °C for 20 min followed by the addition of $RuCl_3$ (56 mg, 0.26 mmol, 0.05 equiv.). The reaction mixture was warmed to room temperature and stirred for 16 h, followed by quenching through the addition of water, and extraction with Et_2O (3×50 mL). The combined extracts were adjusted to pH 8–9 by the addition of NH_4OH and then extracted with water (3×50 mL). The combined aqueous phases were acidified with 1N HCl (pH 4–5) and extracted with diethyl ether

(3×50 mL). The combined extracts were dried with $MgSO_4$ and the solvent was evaporated in vacuo to obtain pure (*R*)-(2-^{2}H)-**15** (390 mg, 2.53 mmol, 47%) as a colourless solid. TLC (petrol ether/EtOAc = 1:1): R_f = 0.62.^{1}H-NMR ($CDCl_3$, 500 MHz): δ = 3.56 (d, *J* = 6.9 Hz, 2H), 3.0-2.95 (m, 1H) ppm. ^{13}C-NMR ($CDCl_3$, 126 MHz): δ = 176.06 (COOH), 37.29 (t, $^1J_{C\text{-}D}$ = 20.1 Hz, CHD), 25.07 (CH_2) ppm. IR (diamond-ATR): $\tilde{\nu}$ = 2928 (br), 1717 (m), 1686 (s), 1425 (m), 1300 (w), 1259 (m), 1242 (m), 1149 (w), 897 (m), 859 (w), 832 (w), 638 (w) cm^{-1}. Optical rotation: $[\alpha]_D^{25} = -1.8$ (*c* 0.06, C_6H_6). HRMS (ESI): $[M-H]^-$ calcd. for $C_3H_3{}^2HBrO_2^-$ *m/z* 151.9463; found *m/z* 151.9464.

The same procedure was used to convert (*S*)-(2-^{2}H)-**14** (2.75 g, 14.8 mmol) into (*S*)-(2-^{2}H)-**15** (1.33 g, 8.63 mmol, 58%). All spectral data were identical to those of (*R*)-(2-^{2}H)-**15**. Optical rotation: $[\alpha]_D^{25} = +1.3$ (*c* 0.15, C_6H_6). HRMS (ESI): $[M-H]^-$ calcd. for $C_3H_3{}^2HBrO_2^-$ *m/z* 151.9463; found *m/z* 151.9464.

Synthesis of (*R*)- and (*S*)-(2-^{2}H)-3-(methylsulfanyl)propionic acid (4). Compound (*R*)-(2-^{2}H)-**15** (200 mg, 1.29 mmol, 1.0 equiv.) was dissolved in ethanol (10 mL) followed by addition of sodium methanethiolate (0.27 g, 3.9 mmol, 3.0 equiv.). The reaction mixture stirred under refluxed for 24 h and then quenched by the addition of water. The aqueous phase was acidified to pH 4–5 by the addition of 1N HCl and extracted with EtOAc (3×). The extracts were collected and dried with $MgSO_4$. The solvents were evaporated in vacuo to obtain (*R*)-(2-^{2}H)-**4** (99 mg, 0.81 mmol, 63%) as a pale yellow oil. TLC (30% EtOAc/petrol ether): R_f = 0.36.^{1}H-NMR ($CDCl_3$, 500 MHz): δ = 2.77 (br s, 2H), 2.70-2.63 (m, 1H), 2.14 (s, 3H) ppm. ^{13}C-NMR ($CDCl_3$, 126 MHz): δ = 177.25 (COOH), 34.00 (t, $^1J_{C\text{-}D}$ = 20.0 Hz, CHD), 28.81 (CH_2), 15.64 (CH_3) ppm. IR (diamond-ATR): $\tilde{\nu}$ = 3043 (br), 2919 (w), 1706 (s), 1427 (w), 1228 (w), 1167 (w), 998 (w), 936 (w), 857 (w), 808 (w) cm^{-1}. Optical rotation: $[\alpha]_D^{25} = -1.0$ (*c* 0.10, EtOAc). HRMS (ESI): $[M-H]^-$ calcd. for $C_4H_6{}^2HO_2S^-$ *m/z* 120.0235; found *m/z* 120.0236.

The same procedure was used to convert (*S*)-(2-^{2}H)-**15** (1.30 g, 8.44 mmol) into (*S*)-(2-^{2}H)-**4** (650 mg, 5.37 mmol, 64%). All spectral data were identical to those of (*R*)-(2-^{2}H)-**4**. Optical rotation: $[\alpha]_D^{25} = +1.7$ (*c* 0.06, EtOAc). HRMS (ESI): $[M-H]^-$ calcd. for $C_4H_6{}^2HO_2S^-$ *m/z* 120.0235; found *m/z* 120.0235.

Synthesis of *S*-(2-acetamidoethyl) (*S*)- and (*R*)-(2-^{2}H)-3-(methylsulfanyl)propanethioate (10). To a cooled (0 °C) solution of (*R*)-(2-^{2}H)-**4** (80 mg, 0.66 mmol, 1.0 equiv.) in dry CH_2Cl_2 (8 mL) was added 2-acetamidoethanethiol (HSNAc, 79 mg, 0.66 mmol, 1.0 equiv.), followed by the addition of EDC (152 mg, 0.79 mmol, 1.2 equiv.) and DMAP (16 mg, 0.13 mmol, 0.2 equiv.). The reaction was stirred at 0 °C for 15 min and then at room temperature overnight. The reaction was quenched by the addition of water and extracted with EtOAc (3×). The combined extracts were dried with $MgSO_4$ and the solvents were evaporated in vacuo. Purification by column chromatography on silica gel (60-80% EtOAc/petrol ether) yielded (*S*)-(2-^{2}H)-**10** (118 mg, 0.53 mmol, 81%) as a pale yellow oil. TLC (EtOAc): R_f = 0.34. ^{1}H-NMR (C_6D_6, 500 MHz): δ = 5.01 (br s, 1H), 3.19 (q, *J* = 6.5 Hz, 2H), 2.79 (t, *J* = 6.7 Hz, 2H), 2.49-2.42 (m, 3H), 1.65 (s, 3H), 1.54 (s, 3H) ppm. ^{13}C-NMR (C_6D_6, 126 MHz): δ = 197.29 (CO), 169.08 (CO), 43.38 (t, $^1J_{C\text{-}D}$ = 20.1 Hz, CHD), 39.53 (CH_2), 29.45 (CH_2), 28.80 (CH_2), 22.78 (CH_3), 15.20 (CH_3) ppm. IR (diamond-ATR): $\tilde{\nu}$ = 3281 (br), 3082 (w), 2920 (w), 2851 (w), 1683 (m), 1654 (s), 1549 (m), 1432 (w), 1373 (w), 1287 (w), 1196 (w), 1101 (w), 1051 (w), 991 (w), 957 (w) cm^{-1}. Optical rotation: $[\alpha]_D^{25} = -2.5$ (*c* 0.12, EtOAc). HRMS (ESI): $[M+H]^+$ calcd. for $C_8H_{15}{}^2HNO_2S_2^+$ *m/z* 223.0680; found *m/z* 223.0676.

The same procedure was used to convert (*S*)-(2-^{2}H)-**4**(70 mg, 0.57 mmol) into (*R*)-(2-^{2}H)-**10** (81 mg, 0.36 mmol, 64%). All spectral data were identical to those of (*S*)-(2-^{2}H)-**10**. Optical rotation: $[\alpha]_D^{25} = +2.5$ (*c* 0.08, C_6H_6). HRMS (ESI): $[M+H]^+$ calcd. for $C_8H_{15}{}^2HNO_2S_2^+$ *m/z* 223.0680; found *m/z* 223.0678.

Synthesis of (1,1-^{2}H$_2$)phenylethanol (13).[46] $LiAl^2H_4$ (1.00 g, 24.0 mmol, 0.8 equiv.) was dissolved in dry THF (40 mL) under Ar atmosphere. A solution of methyl phenylacetate (4.50 g, 30.0 mmol, 1.0 equiv.) in dry THF (5 mL) was added dropwise at 0 °C. The reaction was stirred at 0 °C for 30 min. After completion, the reaction was quenched by the addition of a saturated aqueous solution of NH_4Cl, followed by the extraction with Et_2O (3×50 mL). The extracts were collected, dried over $MgSO_4$ and the solvents were evaporated in vacuo. The crude product was purified by silica gel column chromatography (15% EtOAc/petrol ether) to yield (1,1-^{2}H$_2$)-**13** (3.54 g, 28.5 mmol, 96%) as a colourless oil. TLC (30% EtOAc/petrol ether): R_f = 0.36.^{1}H-NMR (C_6D_6, 500 MHz): δ = 7.15-7.10 (m, 2H), 7.08–7.02 (m, 1H), 7.03-6.99 (m, 2H), 2.55 (s, 2H), 1.01 (br s, 1H) ppm. ^{13}C-NMR (C_6D_6, 126 MHz): δ = 139.31 (C_q), 129.34 (2×CH), 128.70 (2×CH), 126.51 (CH), 63.13 (p, $^1J_{C\text{-}D}$ = 21.7 Hz, CDD), 39.48 (CH_2) ppm. IR (diamond-ATR): $\tilde{\nu}$ = 3336 (br), 3062 (w), 3027 (w), 2929 (w), 2861 (w), 2216 (w), 2100 (w), 1738 (w), 1584 (w), 1496 (w), 1453 (w), 1376 (w), 1216 (w), 1122 (w), 1096 (w), 968 (w), 955 (w), 744 (m), 698 (m) cm^{-1}.

Synthesis of (1-^{2}H)-2-phenylacetaldehyde (17).[46] IBX (6.76 g, 24.2 mmol, 3.0 equiv.) was dissolved in DMSO (30 mL) at room temperature. A solution of (1,1-^{2}H$_2$)-**13** (1.00 g, 8.05 mmol, 1.0 equiv.) in DMSO (3 mL) was added dropwise. The reaction mixture was stirred for 2 h at room temperature until the alcohol was consumed. The reaction was quenched by the addition of water and extracted with Et_2O (3×50 mL). The extracts were collected, dried with $MgSO_4$ and the solvents were evaporated in vacuo. The crude product was purified through column chromatography on silica gel (25% Et_2O/petrol ether) to obtain **17** as a colourless oil (0.82 g, 6.7 mmol, 83%). TLC (25% Et_2O/petrol ether): R_f = 0.32. ^{1}H-NMR (C_6D_6, 500 MHz): δ = 7.10–6.97 (m, 3H), 6.85-6.76 (m, 2H), 3.02 (s, 2H) ppm. ^{13}C-NMR (C_6D_6, 126 MHz): δ = 197.30 (t, $^1J_{C\text{-}D}$ = 26.8 Hz, CDO), 132.53 (C_q), 129.78 (2×CH), 129.0 (2×CH), 127.29 (CH), 50.28 (CH_2), ppm. IR (diamond-ATR): $\tilde{\nu}$ = 2924 (m), 2853 (w), 1716 (m), 1584 (w), 1466 (w), 1430 (w), 1288 (w), 1244 (m), 1140 (w), 1015 (m), 949 (w), 791 (w), 743 (w), 668 (w) cm^{-1}. Optical rotation: $[\alpha]_D^{25} = +2.0$ (*c* 0.06, EtOAc).

Synthesis of (*R*)- and (*S*)-(1-^{2}H)-2-phenylethanol (13). In a flame dried flask, compound **17** (1.00 g, 8.26 mmol, 1.0 equiv.) was dissolved in dry THF (10 mL) under Ar atmosphere. (*S*)-Alpine borane (19.0 mL, 0.5 Msolution in THF, 1.2 equiv.) was added dropwise and the reaction mixture was stirred at room temperature for 16 h. Acetaldehyde (0.55 mL, 9.91 mmol, 1.2 equiv.) was added, the reaction mixture was stirred for another 20 min and the solvents were evaporated. The residue was dissolved in dry Et_2O (5 mL) and the solution was cooled to 0 °C, followed by the dropwise addition of ethanolamine (0.60 mL, 9.91 mmol, 1.2 equiv.). Stirring was continued at the same temperature for 30 min. The reaction was quenched by the addition of water and extracted with Et_2O (3×50 mL). The combined extracts were dried with $MgSO_4$ and the solvents were evaporated in vacuo. Purification of the crude productthrough silica gel column chromatography (5% EtOAc/petrol ether) yielded (*R*)-(1-^{2}H)-**13** as a colourless oil (466 mg, 3.78 mmol, 46%). TLC (30% EtOAc/petrol ether): R_f = 0.35. ^{1}H-NMR (C_6D_6, 500 MHz): δ = 7.15–7.10 (m, 2H), 7.08-7.03 (m, 1H), 7.03-6.99 (m, 2H), 3.50-3.43 (m, 1H), 2.54 (d, $^3J_{H,H}$ = 5.0 Hz, 2H), 0.71 (br s, 1H) ppm. ^{13}C-NMR (C_6D_6, 126 MHz): δ = 139.30 (C_q), 129.33 (2×CH), 128.70 (2×CH), 126.52 (CH), 63.32 (t, $^1J_{C\text{-}D}$ = 21.8 Hz, CHD), 39.59 (CH_2) ppm. IR (diamond-ATR): $\tilde{\nu}$ = 3348 (br), 3007 (w), 2921 (m), 2851 (w), 1738 (w), 1632 (w), 1468 (w), 1366 (w), 1231 (w) cm^{-1}. Optical rotation: $[\alpha]_D^{25} = +1.4$ (*c* 0.07, EtOAc). HRMS (APCI): $[M+H]^+$ calcd. for $C_8H_9{}^2HO$ *m/z* 124.0867; found *m/z* 124.0865.

The same procedure was used to convert compound **17** (450 mg, 3.71 mmol) into (*S*)-(1-^{2}H)-**13** (240 mg, 1.95 mmol, 53%). All spectral data were identical to those of (*R*)-(1-^{2}H)-**13**. Optical rotation: $[\alpha]_D^{25} = -2.0$ (*c* 0.18, EtOAc). HRMS (APCI): $[M+H]^+$ calcd. for $C_8H_9{}^2HO$ *m/z* 124.0867; found *m/z* 124.0868.

Determination of the enantiomeric purity of synthetic (*R*)- and (*S*)-(1-^{2}H)-2-phenylethanol (13). To determine the enantiomeric excess of the alcohols (*R*)- and (*S*)-(1-^{2}H)-2-phenylethanol (**13**), both alcohols were converted into Mosher esters. For this purpose, the alcohols (2.0 mg each) were dissolved in $CDCl_3$ (0.5 mL), followed by the addition of (*R*)-Mosher chloride (2.0 mg) and pyridine (2 μL). The reaction mixtures were stirred at room temperature for 1 h and directly analysed by ^{1}H-NMR spectroscopy, showing a high enantiomeric purity for both alcohols (> 99% *ee*, Figure S2).

Synthesis of (*S*)- and (*R*)-(1-^{2}H)-2-phenylethyl bromide (14). Compound (*R*)-(1-^{2}H)-**13** (400 mg, 3.24 mmol, 1.0 equiv.) was dissolved in dry CH_2Cl_2 (15 mL) and CBr_4 (1.18 g, 3.56 mmol, 1.1 equiv.) was added. The reaction mixture was cooled to 0 °C and PPh_3 (934 mg, 3.56 mmol, 1.1 equiv.) was added portionwise. The reaction mixture was stirred at room temperature for 4 h and then quenched by the addition of water, followed by extractionwithCH_2Cl_2 (3×50 mL). The combined extracts were collected, dried with $MgSO_4$ and evaporated in vacuo. The crude product was purified through silica gel column chromatography (petrol ether) to obtain (*S*)-(1-^{2}H)-**14** as a colourless oil (0.52 g, 2.76 mmol, 86%). TLC (petrol ether): $R_f = 0.66$. ^{1}H-NMR (C_6D_6, 500 MHz): δ = 7.20-7.09 (m, 3H), 6.93-6.88 (m, 2H), 3.19-3.12 (m, 1H), 2.82 (d, $^3J_{H,H}$ = 7.5 Hz, 2H) ppm. ^{13}C-NMR (C_6D_6, 126 MHz): δ = 139.16 (C_q), 128.86 (2×CH), 128.72 (2×CH), 127.01 (CH), 39.42 (CH_2), 32.65 (t, $^1J_{C\text{-}D}$ = 23.4 Hz, CHD) ppm. IR (diamond-ATR): $\tilde{\nu}$ = 2925 (m), 2853 (w), 1715 (w), 1602 (w), 1495 (w), 1453 (m), 1376 (w), 1238 (w), 1163 (w), 1079 (w), 1031 (w), 846 (w), 799 (w), 747 (m), 698 (m), 630 (w), 538 (w) cm^{-1}. Optical rotation: $[\alpha]_D^{25} = -4.6$ (*c* 0.07, C_6H_6).

The same procedure was used to convert (*S*)-(1-^{2}H)-**13** (200 mg, 1.62 mmol) into (*R*)-(1-^{2}H)-**14** (260 mg, 1.40 mmol, 84%). All spectral data were identical to those of (*S*)-(1-^{2}H)-**14**. Optical rotation: $[\alpha]_D^{25} = +3.2$ (*c* 0.08, EtOAc).

Synthesis of (*S*)- and (*R*)-(3-^{2}H)-3-bromopropionic acid (15). Compound (*S*)-(1-^{2}H)-**14** (300 mg, 1.61 mmol, 1.0 equiv.) was dissolved in acetonitrile (8 mL), CCl_4 (8 mL) and phosphate buffer (pH 7, 8 mL). The reaction mixture was cooled to 0 °C followed by the addition of H_5IO_6 (3.79 g, 16.1 mmol, 10.0 equiv.) portionwise over 15 min. The reaction mixture was stirred at the same temperature for 20 min and $RuCl_3$ (17 mg, 0.08 mmol, 0.05 equiv.) was added. The reaction mixture was warmed to room temperature and stirred for 16 h, followed by quenching through the addition of water and extraction with diethyl ether (3×50 mL). The extracts were collected and adjusted to pH 8–9 by the addition of NH_4OH and then extracted with water (3×50 mL). The combined aqueous phases were collected and acidified by the addition of 1 N HCl to pH 4–5, followed by the extraction with diethyl ether (3×50 mL). The combined extracts were dried with $MgSO_4$ and evaporated in vacuo to obtain (*S*)-(3-^{2}H)-**15** as a colourless solid (102 mg, 0.67 mmol, 41%). TLC (30% EtOAc/petrol ether): $R_f = 0.51$. ^{1}H-NMR ($CDCl_3$, 500 MHz): δ = 7.82 (br s, 1H), 3.58-3.54 (m, 1H), 2.98 (m, 2H) ppm. ^{13}C-NMR ($CDCl_3$, 126 MHz): δ = 176.48 (CO), 37.47 (CH_2), 25.05 (t, $^1J_{C\text{-}D}$ = 23.6 Hz, CHD) ppm. IR (diamond-ATR): $\tilde{\nu}$ = 2952 (w), 2924 (m), 2854 (w), 1710 (s), 1412 (w), 1288 (w), 1229 (w), 934 (w), 600 (w) cm^{-1}. Optical rotation: $[\alpha]_D^{25} = -1.8$ (*c* 0.11, EtOAc). HRMS (ESI): $[M-H]^-$ calcd. for $C_3H_3{}^2HBrO_2^-$ *m/z* 151.9463; found *m/z* 151.9464.

The same procedure was used to convert (*R*)-(1-^{2}H)-**14** (150 mg, 0.80 mmol) into (*R*)-(3-^{2}H)-**15** (54 mg, 0.35 mmol, 44%). All spectral data were identical to those of (*R*)-(3-^{2}H)-**15**. Optical rotation: $[\alpha]_D^{25} = +0.8$ (*c* 0.13, EtOAc). HRMS (ESI): $[M-H]^-$ calcd. for $C_3H_4{}^2HBrO_2^-$ *m/z* 151.9463; found *m/z* 151.9464.

Synthesis of (*R*)- and (*S*)-(3-^{2}H)-3-(methylsulfanyl)propionic acid (4). Compound (*S*)-(3-^{2}H)-**15** (100 mg, 0.65 mmol, 1.0 equiv.) was dissolved in ethanol (10 mL) and sodium methanethiolate (137 mg, 1.96 mmol, 3.0 equiv.) was added. The reaction mixture was refluxed at 85 °C for 24 h and then quenched by the addition of water, acidified with 1N HCl to pH 4–5, and then extracted with EtOAc (3×50 mL). The combined extracts were dried over $MgSO_4$ and the solvents were evaporated in vacuo to obtained (*R*)-(3-^{2}H)-**4** as a pale yellow oil (54 mg, 0.45 mmol, 68%). TLC (30% EtOAc/petrol ether): $R_f = 0.43$. ^{1}H-NMR ($CDCl_3$, 500 MHz): δ = 2.76 (brs, 1H), 2.67 (m, 2H), 2.14 (s, 3H) ppm. ^{13}C-NMR ($CDCl_3$, 126 MHz): δ = 177.36 (CO), 34.14 (CH_2), 28.65 (t, $^1J_{C\text{-}D}$ = 21.7 Hz, CHD), 15.60 (CH_3) ppm. IR (diamond-ATR): $\tilde{\nu}$ = 3360 (w), 3313 (w), 3192 (br), 2955 (w), 2919 (s), 2850 (w), 1737 (w), 1658 (w), 1633 (w), 1467 (w), 1376 (w), 1298 (w), 1238 (w), 1137 (w) cm^{-1}. $[\alpha]_D^{25} = +2.9$ (*c* 0.07, EtOAc). HRMS (ESI): $[M-H]^-$ calcd. for $C_4H_6{}^2HO_2S^-$ *m/z* 120.0235; found *m/z* 120.0236.

The same procedure was used to convert (*R*)-(3-^{2}H)-**15** (50 mg, 0.32 mmol) into (*S*)-(3-^{2}H)-**4** (25 mg, 0.20 mmol, 64%). All spectral data were identical to those of (*R*)-(3-^{2}H)-**4**. Optical rotation: $[\alpha]_D^{25} = -2.0$ (*c* 0.2, EtOAc). HRMS (ESI): $[M-H]^-$ calcd. for $C_4H_6{}^2HO_2S^-$ *m/z* 120.0235; found *m/z* 120.0235.

Synthesis of *S*-(2-acetamidoethyl) (*R*)- and (*S*)-(3-^{2}H)-3-(methylsulfanyl)propanethioate (10). Compound (*R*)-(3-^{2}H)-**4** (50 mg, 0.41 mmol, 1.0 equiv.) was dissolved in dry CH_2Cl_2 (5 mL) and the solution was cooled to 0 °C. HSNAc (49 mg, 0.41 mmol, 1.0 equiv.) was added, followed by the addition of EDC (94 mg, 0.49 mmol, 1.2 equiv.) and DMAP (10 mg, 0.08 mmol, 0.2 equiv.). The reaction was stirred at 0 °C for 15 min, warmed to room temperature and stirred overnight. The reaction was quenched by the addition of water, followed by the extraction with EtOAc (3×50 mL). The combined extracts were dried with $MgSO_4$ and the solvent was evaporated in vacuo. The product was purified by silica gel column chromatography (60-80% EtOAc/petrol ether) to yield (*R*)-(3-^{2}H)-**10** as a pale yellow oil (66 mg, 0.30 mmol, 72%). TLC (EtOAc): $R_f = 0.38$. ^{1}H-NMR (C_6D_6, 500 MHz): δ = 4.60 (br s, 1H), 3.16 (q, *J* = 6.6 Hz, 2H), 2.77 (t, *J* = 6.7 Hz, 2H), 2.53-2.37 (m, 3H), 1.64 (s, 3H), 1.47 (s, 3H) ppm. ^{13}C-NMR ($CDCl_3$, 126 MHz): δ = 197.26 (CO), 168.79 (CO), 43.59 (CH_2), 39.51 (CH_2), 29.28 (t, $^1J_{C\text{-}D}$ = 21.5 Hz, CHD), 28.81 (CH_2), 22.75 (CH_3), 15.15 (CH_3) ppm. IR (diamond-ATR): $\tilde{\nu}$ = 3291 (br), 3079 (w), 2919 (w), 1685 (m), 1652 (s), 1549 (m), 1432 (m), 1432 (w), 1373 (w), 1360 (w), 1289 (w), 1100 (w), 1042 (w), 955 (w), 798 (w), 625 (w) cm^{-1}. $[\alpha]_D^{25} = +2.1$ (*c* 0.08, C_6H_6). HRMS (ESI): $[M+H]^+$ calcd. for $C_8H_{14}{}^2HNO_2S_2^+$ *m/z* 223.0680; found *m/z* 223.0674.

The same procedure was used to convert (*S*)-(3-^{2}H)-**4** (20 mg, 0.17 mmol) into (*S*)-(3-^{2}H)-**10** (27 mg, 0.12 mmol, 74%). All spectral data were identical to those of (*R*)-(3-^{2}H)-**10**. Optical rotation: $[\alpha]_D^{25} = -1.3$ (*c* 0.06, C_6H_6). HRMS (ESI): $[M+H]^+$ calcd. for $C_8H_{15}{}^2HNO_2S_2^+$ *m/z* 223.0680; found *m/z* 223.0678.

Strains and culture conditions. *Ruegeria pomeroyi* DSS-3 was purchased from DSMZ (Leibniz Institute DSMZ-German Collection of Microorganisms and Cell Cultures GmbH). The strain was grown in marine broth at 30 °C. *E. coli* BL21 (DE3) was purchased from Thermo Scientific (Waltham, Massachusetts, USA), and cultured in LB medium (10 g tryptone, 5 g yeast extract, 5 g NaCl, pH 7.2, 1 L water) at 37 °C. *Saccharomyces cerevisiae* FY834 was cultured in YPD medium (1% yeast extract, 2% peptone, 2% glucose) at 30 °C. For cultivations on agar plates 1.5% agar was added to the medium.

Gene cloning. *Ruegeria pomeroyi* DSS-3 was grown in marine broth for 3 days at 30 °C. The cells were collected by centrifugation and gDNA was isolated by application of the phenol/chloroform

method.[47] The coding gene for DmdC (AAV97018) was amplified from genomic DNA by PCR using Q5 polymerase (New England Biolabs, Ipswich, MA, USA) and the short primers DK005f_DmdC and DK005r_DmdC (Table S1). The PCR conditions were: initial denaturation at 98 °C for 40 s, followed by 30 cycles of a 3 steps program (denaturation at 98 °C for 10 s, annealing at 62–67 °C for 30 s, elongation at 72 °C for 45 s), and a final elongation at 72 °C for 2 min. The long primers DK006f_DmdC and DK006r_DmdC were used for a second PCR in which the product of the first PCR was used as a template to attach homology arms (bold underlined, Table S1) for homologous recombination in yeast with the linearised pYE-Express vector (EcoRI and HindIII digestion).[48] Homologous recombination was performed by the PEG/LiOAc method.[49] After culturing of *Saccharomyces cerevisiae* FY834 in YPD medium for 3 days, the plasmid containing the integrated gene was isolated by using the Zymoprep Yeast Plasmid Miniprep II kit (Zymoresearch, Irvine, CA, USA), followed by introduction into *E. coli* BL21 (DE3) through electroporation. The transformants were cultured on LB agar plates with kanamycin (50 μg/mL) at 37 °C overnight. Single colonies were selected and grown in liquid LB medium overnight for plasmid DNA isolation by using the PureYield Plasmid Miniprep System (Promega, Madison, WI, USA). The sequences of the cloned genes were verified by DNA sequencing.

Gene expression and protein purification. *E. coli* BL21 (DE3) cells carrying the DmdC plasmid were cultured in LB medium (10 mL) containing kanamycin (50 μg/mL) at 37 °C and 160 rpm overnight. The small scale culture was used to inoculate expression cultures in LB medium (1 L) containing kanamycin (50 μg/mL). The expression cultures were grown to $OD_{600} = 0.5–0.6$ at 37 °C at 160 rpm and then cooled to 18 °C before addition of a solution of IPTG (0.4 mM in water, 1 mL L^{-1}). The expression culture was incubated at 18 °C for 18 h at 160 rpm and cells were collected by centrifugation (3500 rpm, 1 h, 4 °C). The cell pellets were resuspended in lysis buffer (50 mM Tris, 100 mM NaCl, 0.5 % glycerol, 20 mM imidazole, pH 8, 15 mL for 1 L of cell culture) and ultra-sonicated (5×1 min intervals). The cell debris was removed by centrifugation (10000×g, 10 min, 4 °C). The supernatant was passed through a cellulose filter (20 μm) and loaded onto a Ni^{2+}-NTA affinity chromatography column. The column was washed using lysis buffer (2×2 mL), followed by elution of the target protein using elution buffer (50 mM Tris, 100 mM NaCl, 0.5 % glycerol, 300 mM imidazole, pH 8). The enzyme concentrations were determined through Bradford assay.[50] The freshly prepared enzyme was typically obtained in a concentration of 4 mg/mL and used immediately for the enzyme reactions.

Enzyme incubations of stereoselectively deuterated SNAc esters 10. Purified DmdC in elution buffer (250 μL, 4 mg/mL) was added to a solution of unlabelled **10** or the stereoselectively deuterated isotopomers of **10** (0.25 mg) and FAD (0.39 mg) in HEPES buffer (500 μL; 100 mM HEPES, adjusted to pH 6.5 with 1 N NaOH). The reaction mixture was incubated at 40 °C for 8 h. The product was extracted with EtOAc (200 μL) and analysed by GC/MS. In control experiments carried out in the same way, prolonged incubation times (48 h) showed a loss of deuterium from (*S*)-(2-^{2}H)-**10**. Furthermore, under the same conditions using HEPES buffer prepared with D_2O an incorporation of deuterium into unlabelled **10** was observed.

GC/MS. GC/MS analyses were carried out on a 5977 A GC/MSD system (Agilent, Santa Clara, CA, USA) with a 7890B GC and a 5977 A mass selective detector. The GC was equipped with a HP5-MS fused silica capillary column (30 m, 0.25 mm i. d., 0.50 μm film). GC settings were 1) inlet pressure: 77.1 kPa, He at 23.3 mL min^{-1}, 2) injection volume: 1 μL, 3) temperature program: 5 min at 50 °C increasing at 10 °C min^{-1} to 320 °C, 4) 60 s valve time, and 5) carrier gas: He at 1.2 mL min^{-1}. MS settings were 1) source temperature: 230 °C, 2) transfer line: 250 °C, 3) quadrupole: 150 °C and 4) electron energy: 70 eV.

Acknowledgements

This work was funded by the Deutsche Forschungsgemeinschaft DFG (SFB TRR 51 "Roseobacter"). Open Access funding enabled and organized by Projekt DEAL.

Conflict of Interests

The authors declare no conflict of interest.

Data Availability Statement

The data that support the findings of this study are available in the supplementary material of this article.

Keywords: dehydrogenases · dimethylsulfonio propionate · enzyme mechanisms · stereochemistry · sulfur volatiles

[1] P. Haas, *Biochem. J.* **1935**, *29*, 1297–1299.
[2] F. Challenger, M. I. Simpson, *J. Chem. Soc.* **1948**, 1591–1597.
[3] A. Vairavamurthy, M. O. Andreae, R. L. Iverson, *Limnol. Oceanogr.* **1985**, *30*, 59–70.
[4] G. O. Kirst, C. Thiel, H. Wolff, J. Nothnagel, M. Wanzek, R. Ulmke, *Mar. Chem.* **1991**, *35*, 381–388.
[5] E. E. Clerc, J.-B. Raina, J. M. Keegstra, Z. Landry, S. Pontrelli, U. Alcolombri, B. S. Lambert, V. Anelli, F. Vincent, M. Masdeu-Navarro, A. Sichert, F. De Schaetzen, U. Sauer, R. Simo, J.-H. Hehemann, A. Vardi, J. R. Seymour, R. Stocker, *Nat. Commun.* **2023**, *14*, 8080.
[6] F. Challenger, R. Bywood, P. Thomas, B. J. Hayward, *Arch. Biochem. Biophys.* **1957**, *69*, 514–523.
[7] Y. Ishida, H. Kadota, *Agric. Biol. Chem.* **1967**, *31*, 756–757.
[8] J. W. H. Dacey, G. M. King, S. G. Wakeham, *Nature* **1987**, *330*, 643–645.
[9] A. D. Broadbent, G. B. Jones, R. J. Jones, *Estuarine Coastal Shelf Sci.* **2002**, *55*, 547–555.
[10] D. A. Gage, D. Rhodes, K. D. Nolte, W. A. Hicks, T. Leustek, A. J. L. Cooper, A. D. Hanson, *Nature* **1997**, *387*, 891–894.
[11] D. Rhodes, D. A. Gage, A. J. L. Cooper, A. D. Hanson, *Plant Physiol.* **1997**, *115*, 1541–1548.
[12] M. G. Kocsis, K. D. Nolte, D. Rhodes, T.-L. Shen, D. A. Gage, A. D. Hanson, *Plant Physiol.* **1998**, *117*, 273–281.
[13] M. G. Kocsis, A. D. Hanson, *Plant Physiol.* **2000**, *123*, 1153–1161.
[14] A. R. J. Curson, J. Liu, A. Bermejo Martinez, R. T. Green, Y. Chan, O. Carrion, B. T. Williams, S.-H. Zhang, G.-P. Yang, P. C. Bulman Page, X.-H. Zhang, J. D. Todd, *Nat. Microbiol.* **2017**, *2*, 17009.
[15] C. Liao, F. P. Seebeck, *Angew. Chem.* **2019**, *131*, 3591–3594; *Angew. Chem. Int. Ed.* **2019**, *58*, 3553–3556.
[16] J. B. Raina, D. M. Tapiolas, S. Foret, A. Lutz, D. Abrego, J. Ceh, F. O. Seneca, P. L. Clode, D. G. Bourne, B. L. Willis, C. A. Motti, *Nature* **2013**, *502*, 677–680.
[17] M. Gali, E. Devred, M. Levasseur, S.-J. Royer, M. Babin, *Remote Sens. Environ.* **2015**, *171*, 171–184.
[18] A. J. Kettle, M. O. Andreae, *J. Geophys. Res.* **2000**, *105*, 26793–26808.
[19] J. E. Lovelock, R. J. Maggs, R. A. Rasmussen, *Nature* **1972**, *237*, 452–453.
[20] R. J. Charlson, J. E. Lovelock, M. O. Andreae, S. G. Warren, *Nature* **1987**, *326*, 655–661.
[21] S. M. Vallina, R. Simo, *Science* **2007**, *315*, 506–508.
[22] A. R. J. Curson, R. Rogers, J. D. Todd, C. A. Brearly, A. W. B. Johnston, *Environ. Microbiol.* **2008**, *10*, 757–767.
[23] J. D. Todd, A. R. J. Curson, C. L. Dupont, P. Nicholson, A. W. B. Johnston, *Environ. Microbiol.* **2009**, *11*, 1376–1385.

[24] J. D. Todd, A. R. J. Curson, M. Kirkwood, M. J. Sullivan, R. T. Green, A. W. B. Johnston, *Environ. Microbiol.* **2011**, *13*, 427–438.
[25] J. D. Todd, M. Kirkwood, S. Newton-Payne, A. W. B. Johnston, *ISME J.* **2012**, *6*, 223–226.
[26] A. R. J. Curson, M. J. Sullivan, J. D. Todd, A. W. B. Johnston, *ISME J.* **2011**, *5*, 1191–1200.
[27] J. Sun, J. D. Todd, J. C. Thrash, Y. Qian, M. C. Qian, B. Temperton, J. Guo, E. K. Fowler, J. T. Aldrich, C. D. Nicora, M. S. Lipton, R. D. Smith, P. de Leenheer, S. H. Payne, A. W. B. Johnston, C. L. Davie-Martin, K. H. Halsey, S. J. Giovannoni, *Nat. Microbiol.* **2016**, *1*, 16065.
[28] S.-Y. Wang, N. Zhang, Z.-J. Teng, X.-D. Wang, J. D. Todd, Y.-Z. Zhang, H.-Y. Cao, C.-Y. Li, *Environ. Microbiol.* **2023**, *25*, 1238–1249.
[29] U. Alcolombri, S. Ben-Dor, E. Feldmesser, Y. Levin, D. S. Tawfik, A. Vardi, *Science* **2015**, *348*, 1466–1469.
[30] a) J. D. Todd, R. Rogers, Y. G. Li, M. Wexler, P. L. Bond, L. Sun, A. R. J. Curson, G. Malin, M. Steinke, A. W. B. Johnston, *Science* **2007**, *315*, 666–669; b) U. Alcolombri, P. Laurino, P. Lara-Astiaso, A. Vardi, D. S. Tawfik, *Biochemistry* **2014**, *53*, 5473–5475.
[31] C. Y. Li, X. J. Wang, X. L. Chen, Q. Sheng, S. Zhang, P. Wang, M. Quareshy, B. Rihtman, X. Shao, C. Gao, F. Li, S. Li, W. Zhang, X.-H. Zhang, G.-P. Yang, J. D. Todd, Y. Chen, Y.-Z. Zhang, *eLife* **2021**, *10*, e64045.
[32] K. Thume, B. Gebser, L. Chen, N. Meyer, D. J. Kieber, G. Pohnert, *Nature* **2018**, *563*, 412–415.
[33] A. K. Chhalodia, J. S. Dickschat, *Org. Biomol. Chem.* **2023**, *21*, 3083–3089.
[34] O. Carrion, C.-Y. Li, M. Peng, J. Wang, G. Pohnert, M. Azizah, X.-Y. Zhu, A. R. J. Curson, Q. Wang, K. S. Walsham, X.-H. Zhang, S. Monaco, J. M. Harvey, X.-L. Chen, C. Gao, N. Wang, X.-J. Wang, P. Wang, S. J. Giovannoni, C.-P. Lee, C. P. Suffridge, Y. Zhang, Z. Luo, D. Wang, J. D. Todd, Y.-Z. Zhang, *Nat. Microbiol.* **2023**, *8*, 2326–2337.
[35] E. C. Howard, J. R. Henriksen, A. Buchan, C. R. Reisch, H. Bürgmann, R. Welsh, W. Ye, J. M. Gonzalez, K. Mace, S. B. Joye, R. P. Kiene, W. B. Whitman, M. A. Moran, *Science* **2006**, *314*, 649–652.
[36] C. R. Reisch, M. J. Stoudemayer, V. A. Varaljay, I. J. Amster, M. A. Moran, W. B. Whitman, *Nature* **2011**, *473*, 208–211.
[37] R. P. Kiene, L. J. Linn, J. Gonzalez, M. A. Moran, J. A. Bruton, *Appl. Environ. Microbiol.* **1999**, *65*, 4549–4558.
[38] Z. Yin, E. Liebhart, E. Stegmann, H. Brötz-Oesterhelt, J. S. Dickschat, *Org. Chem. Front.* **2022**, *9*, 2714–2720.
[39] J. F. Biellmann, C. G. Hirth, *FEBS Lett.* **1970**, *8*, 55–56.
[40] J. F. Biellmann, C. G. Hirth, *FEBS Lett.* **1970**, *9*, 335–336.
[41] H.-J. la Roche, M. Kellner, H. Günther, H. Simon, *Hoppe-Seyler's Z. Physiol. Chem.* **1971**, *352*, 399–402.
[42] A. Kawaguchi, S. Tsubotani, Y. Seyama, T. Yamakawa, T. Osumi, T. Hashimoto, T. Kikuchi, M. Ando, S. Okuda, *J. Biochem.* **1980**, *88*, 1481–1486.
[43] J. J. Kim, M. Wang, R. Paschke, *Proc. Natl. Acad. Sci. USA* **1993**, *90*, 7523–7527.
[44] X. Shao, H.-Y. Cao, F. Zhao, M. Peng, P. Wang, C.-Y. Li, W.-L. Shi, T.-D. Wei, Z. Yuan, X.-H. Zhang, X.-L. Chen, J. D. Todd, Y.-Z. Zhang, *Mol. Microbiol.* **2019**, *111*, 1057–1073.
[45] G. R. Fulmer, A. J. M. Miller, N. H. Sherden, H. E. Gottlieb, A. Nudelman, B. M. Stoltz, J. E. Bercaw, K. I. Goldberg, *Organometallics* **2010**, *29*, 2176–2179.
[46] A. A. Scholte, J. C. Vederas, *Org. Biomol. Chem.* **2006**, *4*, 730–742.
[47] B. Neumann, A. Pospiech, H. U. Schairer, *Trends Genet.* **1992**, *8*, 332.
[48] J. S. Dickschat, K. A. K. Pahirulzaman, P. Rabe, T. A. Klapschinski, *ChemBioChem* **2014**, *15*, 810.
[49] R. D. Giets, R. H. Schiestl, *Nat. Protoc.* **2007**, *2*, 31.
[50] M. M. Bradford, *Anal. Biochem.* **1976**, *72*, 248.

Manuscript received: November 23, 2023
Revised manuscript received: December 11, 2023
Accepted manuscript online: December 12, 2023
Version of record online: ■■, ■■

RESEARCH ARTICLE

The stereochemical course of the dehydrogenase DmdC involved in the degradation of the marine sulfur compound dimethyl sulfoniopropionate (DMSP) along the demethylation pathway has been investigated using stereoselectively deuterated substrate surrogates. The results revealed an *anti* elimination with removal of the 2-*pro-R* and the 3-*pro-S* hydrogen atoms.

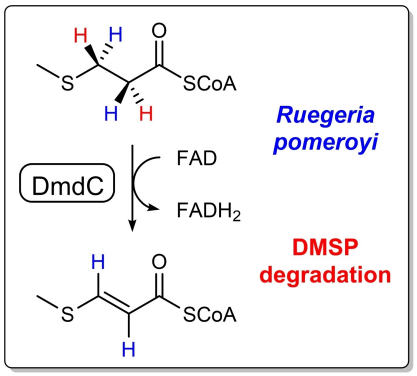

*A. K. Chhalodia, Prof. Dr. J. S. Dickschat**

1 – 9

The Stereochemical Course of DmdC, an Enzyme Involved in the Degradation of Dimethylsulfoniopropionate

Appendix F

On the Substrate Scope of Dimethylsulfonium Propionate Lyases toward Dimethylsulfoxonium Propionate Derivatives

Eur. J. Org. Chem. **2024**, *27*, e202400098

DOI: 10.1002/ejoc.202400098

EurJOC
European Journal of Organic Chemistry

Research Article
doi.org/10.1002/ejoc.202400098

Chemistry Europe
European Chemical Societies Publishing

www.eurjoc.org

On the Substrate Scope of Dimethylsulfonium Propionate Lyases toward Dimethylsulfoxonium Propionate Derivatives

Anuj K. Chhalodia[a] and Jeroen S. Dickschat*[a]

The six dimethylsulfonium propionate (DMSP) lyases DddQ, DddW, DddP, DddY, DddK and DddL catalyze the elimination of dimethyl sulfide from DMSP and can also cleave the marine metabolite dimethylsulfoxonium propionate (DMSOP) to DMSO and acrylate. In this study the potency of all six enzymes for the conversion of four DMSOP analogs with longer alkyl chains that were synthesized in three steps from 3-mercaptopropionic acid was investigated. For this purpose, the pH dependency of the enzyme reactions was determined, showing optimal conditions at pH 8 for all enzymes but DddP, for which an optimum of pH 6 was found. Efficient transformations were observed for DddQ, DddW, DddY and DddK, for which the Michaelis-Menten kinetics were determined for all four substrate analogs. HPLC analysis of the dialkylsulfoxides obtained with the most efficient enzyme DddW revealed that these compounds were obtained with a low to moderate enantiomeric excess (up to 25% *ee*), demonstrating that this enzyme has a preference for one of the enantiomers of the DMSOP analogs.

Introduction

The marine sulfur metabolite dimethylsulfonium propionate (DMSP) was first isolated in 1948 from the red alga *Polysiphonia fastigiata*.[1] This physiologically important molecule not only serves as an important marine nutrient,[2] an osmolyte,[3] cryoprotectant,[4] grazing deterrent,[5] and antioxidant,[6] but is also a chemical signal that directs marine bacteria towards food sources.[7,8] DMSP belongs with an estimated annual production by marine organisms in the petagram range to the most abundant sulfur metabolites on earth[9] and is present in many marine and estuarine organisms including green algae,[10] dinoflagellates,[11] coccolithophores,[3] higher plants,[12] and corals.[13] The biosynthetic pathways toward DMSP have been investigated in green algae,[14] plants,[15–17] corals[18] and bacteria,[19,20] revealing differences for DMSP biosynthesis in these organisms, but all pathways start from L-methionine and proceed in different orders of steps through S-methylation, decarboxylation, and deamination with oxidation.

DMSP is also the source for the climatically relevant gas dimethyl sulfide (DMS) that is released in large amounts from ocean waters into the atmosphere.[21] In higher atmosperic layers and under the influence of sun irradition DMS becomes oxidized to sulfate. This atmospheric sulfate formation has two effects: Firstly, the sulfate aerosol leads to cloud formation which has a cooling effect on the planet,[22,23] and secondly, with the rain sulfate rains down to the continents which is an important transport mechanism within the global sulfur cycle.[24] The cleavage of DMS from DMSP by bacteria is either catalyzed by the type III acyl-CoA transferase DddD with hydrolytic DMS release from a covalently enzyme bound intermediate with formation of 3-hydroxypropionate (**1**, Scheme 1A),[25,26] or by one of the distinct DMSP lyases (DddL, DddP, DddQ, DddY, DddW, DddK and DddU) that have been reported to date.[27–33] In addition, the DMSP lyase Alma1 is known from the coccolithophore *Emiliania huxleyi*.[34] All these DMSP lyases cause the elimination of DMS with formation of acrylate (**2**). In contrast, the recently characterized bifunctional enzyme DddX cleaves DMSP after its conversion into the coenzyme A thioester, leading to the formation of DMS and acryloyl-CoA (**3**).[35]

Two pathways can redirect the metabolism of DMSP and limit the sulfur flux from the ocean to the atmosphere through the formation of water soluble products. Along the DMSP demetylation pathway (Scheme 1B) DMSP is first demethylated by DmdA to 3-(methylsulfanyl)propionate (**4**) which is subsequently converted into the coenzyme A thioester **5** by DmdB.[36,37] The DmdC mediated dehydrogenation with *anti*-elimination of hydrogen[38] then results in **6** that upon the addition of water to the hemithioacetal **7**, elimination of methanethiol (MeSH) to **8**, and decarboxylation by DmdD leads to acetaldehyde (**9**).[36,37] More recently, the oxidized DMSP derivative dimethylsulfoxonium propionate (DMSOP) has been discovered that is also highly abundant in the marine environment (Scheme 1C).[39] While no enzymes for the oxidation of DMSP to DMSOP have been described so far, recent research has demonstrated that the known DMSP lyases can cleave DMSOP with formation of dimethylsulfoxide (DMSO) and acrylate.[40,41]

[a] *A. K. Chhalodia, Prof. Dr. J. S. Dickschat*
Kekulé-Institute for Organic Chemistry and Biochemistry
University of Bonn
Gerhard-Domagk-Straße 1, 53121 Bonn, Germany
E-mail: dickschat@uni-bonn.de

Supporting information for this article is available on the WWW under https://doi.org/10.1002/ejoc.202400098

Research Article
doi.org/10.1002/ejoc.202400098

Chemistry Europe
European Chemical Societies Publishing

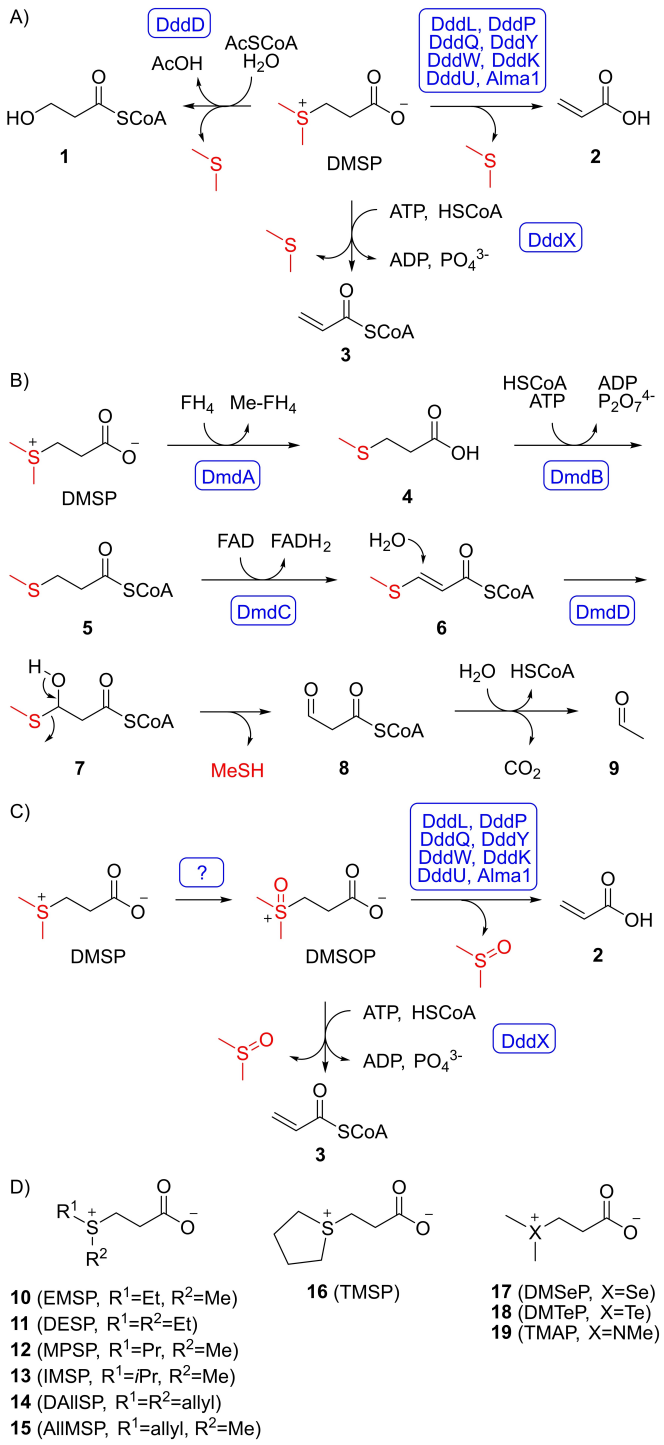

Scheme 1. The degradation of DMSP. A) Cleavage pathway to DMS, B) demethylation pathway to MeSH, C) oxidation pathway with oxidation to DMSOP and cleavage to DMSO, D) structures of DMSP derivatives that were previously shown to be converted by DMSP lyases.

DMSP lyases do not only accept their native substrates DMSP and DMSOP, but are also able to catalyze the cleavage of various DMSP analogs with larger S-alkyl substituents including ethylmethylsulfonium propionate (**10**, EMSP),[42] diethylsulfonium propionate (**11**, DESP),[42] methylpropylsulfonium propionate (**12**, MPSP),[43] and isopropylmethylsulfonium propionate (**13**, IMSP)[43] (Scheme 1D). Interestingly, feeding experiments with DMSP analogs containing an S-allyl group including diallylsulfonium propionate (**14**, DAllSP) and allylmethylsulfonium propionate (**15**, AllMSP) result in the formation of garlic odour constituents, with the consequence that cultures of bacteria that are able to degrade DMSP fed with these substances release the smell of garlic.[44] Also DMSP analogs containing sulfur heterocycles as in tetramethylenesulfonium propionate (**16**, TMSP),[43] or with the sulfur atom substituted by other atoms or groups as represented by dimethylselenium propionate (**17**, DMSeP),[42] dimethyltellurium propionate (**18**, DMTeP),[42] and trimethylammonium propionate (**19**, TMAP)[45] are accepted by various DMSP lyases. In contrast, nothing is known about the substrate tolerance and efficiency of the cleavage of DMSOP analogs mediated by DMSP lyases. Here we report on the synthesis of such DMSOP analogs and investigations on the efficiency of their enzymatic conversion through DMSP lyases.

Results and Discussion

To investigate the substrate scope of DMSP lyases in the conversion of DMSOP analogs, four derivatives were synthesized starting from 3-mercaptopropionic acid (**20**) (Scheme 2). Alkylation under basic conditions with ethyl iodide, propyl iodide, butyl iodide, or isopropyl iodide, respectively, gave the 3-(alkylsulfanyl)propionic acids **21 a**–**21 d**. Their treatment with methyl iodide afforded EMSP (**10**), MPSP (**11**), butylmethylsulfonium propionate (**22**, BMSP) and IMSP (**13**), that were oxidized with $RuCl_3$/NaOCl[39] to obtain the corresponding DMSOP derivatives ethylmethylsulfoxonium propionate (**23 a**, EMSOP), methylpropylsulfoxonium propionate (MPSOP, **23 b**), butylmethylsulfoxonium propionate (BMSOP, **23 c**), and isopropylmethylsulfoxonium propionate (IMSOP, **23 d**).

In a first series of experiments the pH dependency of the enzymatic conversion of the DMSOP analogs with DMSP lyases was investigated. For this purpose, the four DMSOP analogs

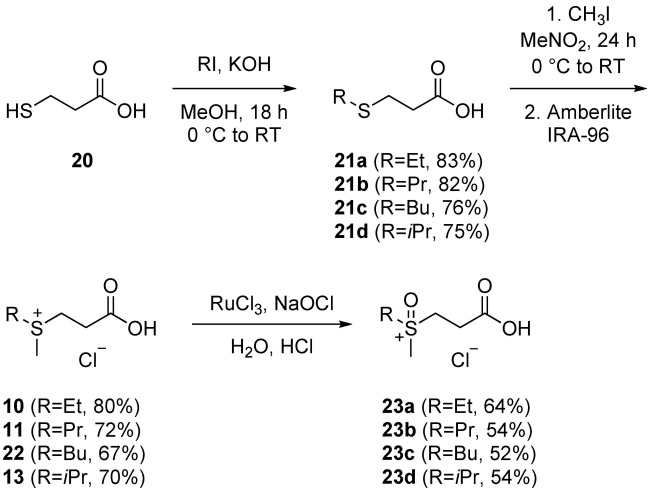

Scheme 2. Synthesis of DMSOP analogs.

were incubated with the purified recombinant enzymes DddQ, DddW and DddP from *Ruegeria pomeroyi* DSS-3,[45] DddY from *Ferrimonas balearica* DSM 9799,[40] and DddK from *Celeribacter halophilus* DSM 26270 (Figure S1, Table S1).[40] Furthermore, DddL from *Dinoroseobacter shibae* DSM 16493 was included, but in this case crude cell lysates from an *Escherichia coli* expression culture were used, because this enzyme is known to undergo degradation during the purification process.[40] These experiments encountered the special problem that the elimination products are water soluble DMSO derivatives that are difficult to extract from the aqueous incubation buffer. Therefore, the four (*methyl*-^{13}C)DMSOP analogs were synthesized using $^{13}CH_3I$ in the methylation of **21 a**–**21 d**. These ^{13}C-labeled substrates allowed for a determination of the conversion rates through ^{13}C-NMR analysis of the enzyme reaction mixtures and peak integration of the signals for the products and remaining starting material. These experiments can be done using buffers and enzyme preparations based on normal water that is a suitable solvent for ^{13}C-NMR analysis. The pH dependency of all enzymes was determined at 30 °C and in a range from pH 3 to pH 9. Control experiments without enzyme revealed a spontaneous cleavage of all DMSOP derivatives at pH 10. The results of these experiments are summarized in Figure 1.

For DddQ (Figure 1A) a conversion of all four substrates was observed between pH 6 and pH 9, with the highest activity at pH 8, in agreement with the previously reported pH optimum of this enzyme towards DMSOP.[40] At pH 5 all substrates but EMSOP were converted and at pH 4 only BMSOP was cleaved with poor efficiency. With the short chain derivatives EMSOP and MPSOP the elimination reaction was slightly more efficient than with BMSOP and IMSOP.

The reported pH optimum for DddW with DMSOP is pH 8.[40] With the substrate analogs for this enzyme a high activity was observed over the whole range from pH 6 to pH 9, only with IMSOP the cleavage reaction was of low efficiency at pH 6 (Figure 1B). At pH 8 a full conversion was observed for EMSOP and MPSOP, and also for the long chain substrates the optimum conditions were found at pH 8.

DddP (Figure 1C) did not accept IMSOP as a substrate. All other substrate analogs were converted with a poor rate ranging from slightly acidic conditions to pH 9. The highest activity was observed for all three substrates at pH 6, in agreement with the known pH optimum of this enzyme with DMSOP.[40]

With DMSOP as substrate DddY is known to be most efficient at pH 8.[40] This is also reflected here by the observed highest conversion rate at pH 8 for all four substrates (Figure 1D). Notably, the cleavage of the short chain substrates EMSOP and MPSOP was generally much more efficient than observed for BMSOP and IMSOP, and also the pH range for which DddY showed activity was widest for EMSOP and MPSOP (pH 4–pH 9), followed by BMSOP (pH 5–pH 9), while IMSOP was only converted at pH 7 and pH 8.

DddK (Figure 1E) showed a low conversion of EMSOP, MPSOP and BMSOP under slightly acidic or neutral conditions, but a significant enhancement at pH 8. Furthermore, IMSOP was only accepted at neutral or slightly basic pH, again with an optimum at pH 8. This reflects the reported optimum at pH 8 for this enzyme with DMSOP.[40]

Finally, DddL did not accept IMSOP and converted all three other substrate analogs with low rates (Figure 1F). Activity was observed with BMSOP ranging from pH 6 to pH 9, and the shorter the alkyl chain in the substrate analog was, the wider this range of activity was extended towards more acidic conditions. Also with the native substrate DMSOP a cleavage was observed previously over the whole range from pH 3 to pH 9, with highest conversion rates at pH 9.[40]

The efficiency of the enzymatic conversion of the DMSOP analogs was also investigated through determination of the Michaelis-Menten kinetics in comparison to previously reported data for the native substrate DMSOP[40] (Table 1). This included investigations on the enzymes DddQ, DddW, DddY and DddK, while the conversion rates for the substrate analogs were too low to measure the enzyme kinetics for DddP, and DddL was not included because this enzyme could not be purified. All kinetic parameters were determined at pH 8 (the pH optimum of all four enzymes) and at 20 °C. Kinetic measurements were based on the UV-spectrometric detection of the formation of

Table 1. Enzyme kinetic data for the conversion of DMSOP and its analogs by various DMS(O)P lyases.

Enzyme[a]	K_M/mM	k_{cat}/s^{-1}	k_{cat}/K_M/s^{-1} mM^{-1}
	DddQ		
DMSOP[b]	27.3 ± 2.2	7.4 ± 0.03	0.27 ± 0.01
EMSOP	12.2 ± 2.8	2.7 ± 0.04	0.22 ± 0.00
MPSOP	23.1 ± 3.9	4.4 ± 0.10	0.19 ± 0.00
BMSOP	22.6 ± 2.6	3.8 ± 0.13	0.16 ± 0.01
IMSOP	13.8 ± 2.1	1.2 ± 0.11	0.08 ± 0.01
	DddW		
DMSOP[b]	45.5 ± 5.0	49.0 ± 0.2	1.07 ± 0.01
EMSOP	17.0 ± 1.7	12.1 ± 0.2	0.71 ± 0.02
MPSOP	28.1 ± 3.3	18.9 ± 0.3	0.67 ± 0.01
BMSOP	67.3 ± 7.5	31.5 ± 0.6	0.47 ± 0.02
IMSOP	14.1 ± 2.9	7.1 ± 1.5	0.50 ± 0.02
	DddY		
DMSOP[b]	8.8 ± 1.0	53.7 ± 0.1	6.1 ± 0.0
EMSOP	6.5 ± 1.4	6.8 ± 0.1	1.1 ± 0.0
MPSOP	3.0 ± 0.2	1.2 ± 0.0	0.41 ± 0.02
BMSOP	9.1 ± 1.6	3.4 ± 0.1	0.37 ± 0.01
IMSOP	14.5 ± 1.5	1.9 ± 0.1	0.13 ± 0.01
	DddK		
DMSOP[b]	1.5 ± 0.1	2.0 ± 0.0	1.4 ± 0.0
EMSOP	23.4 ± 4.3	7.1 ± 0.1	0.34 ± 0.01
MPSOP	24.9 ± 5.0	7.4 ± 0.1	0.32 ± 0.01
BMSOP	11.5 ± 1.0	2.9 ± 0.0	0.25 ± 0.01
IMSOP	19.3 ± 3.2	5.9 ± 0.3	0.30 ± 0.01

[a] All data were determined from triplicates. [b] Data for DMSOP were taken from reference [40].

Research Article
doi.org/10.1002/ejoc.202400098

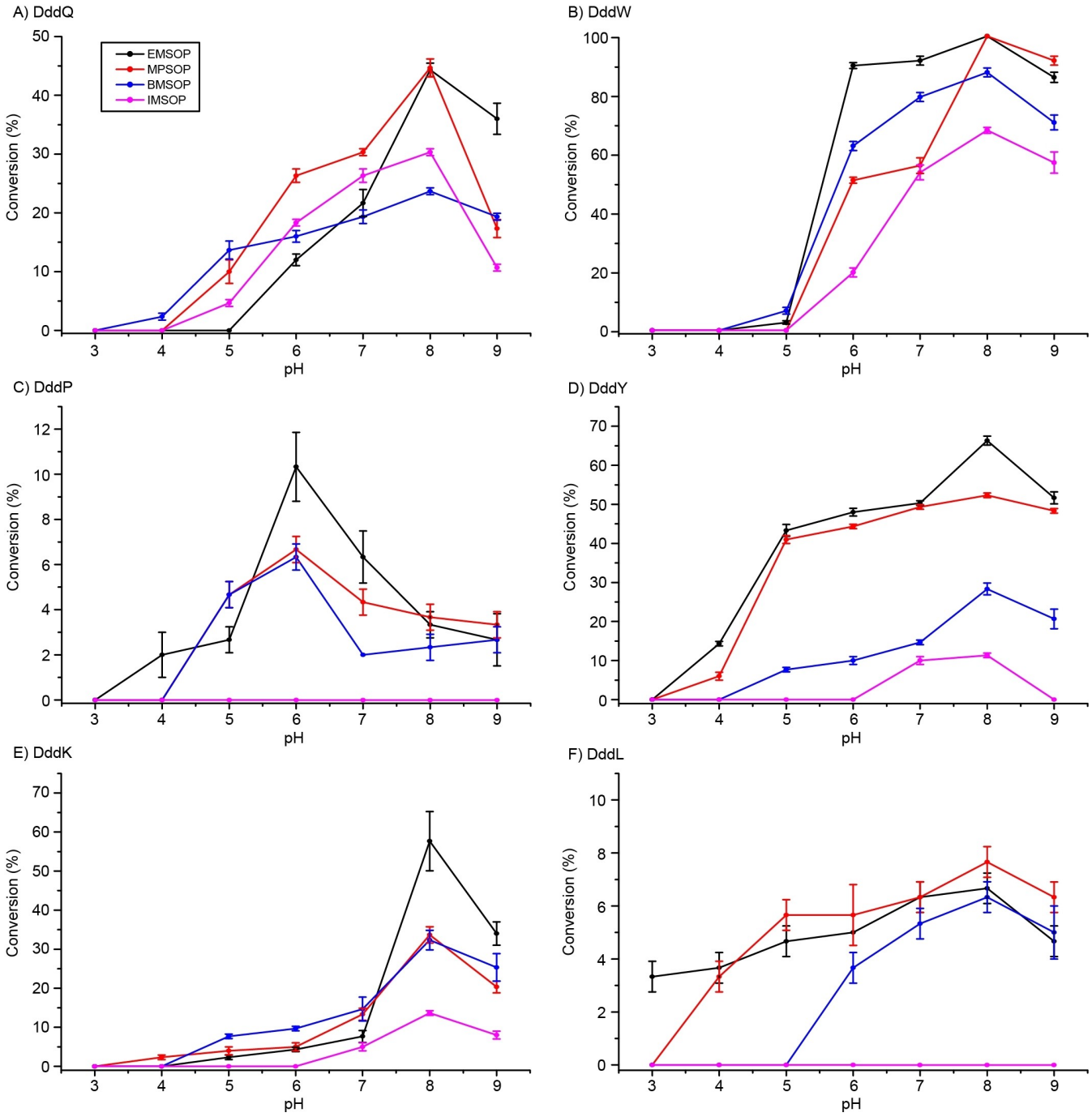

Figure 1. The pH dependency of DMSP lyases with DMSOP analogs. The dots and error bars show mean and standard deviations from triplicates. Please note the different efficiencies of the enzymes reflected by the different y-axis scalings.

acrylic acid at $\lambda = 232$ nm (Figure S2; the maximum absorption of acrylic acid is observed for $\lambda_{max} = 221$ nm, but at this wavelength at high substrate concentrations the measurement range of the UV-spectrometer was exceeded; note that the substrate shows only a low absorption at $\lambda = 232$ nm; Figures S2–S6).

For all four enzymes the k_{cat}/K_M values indicated the highest activity with the substrate DMSOP and showed a decreasing activity with the increasing alkyl chain length of the substrate analogs. The most efficient enzyme for the conversion of DMSOP is DddY ($k_{cat}/K_M = 6.1 \pm 0.0\ s^{-1}\ mM^{-1}$), which is also together with DddW the best performing enzyme for the substrate analogs EMSOP and MPSOP. While DddW retains a high activity also with BMSOP and IMSOP, the activity of DddY towards these substrates, especially towards IMSOP, is reduced. DddQ has a generally lower activity with all four substrate analogs in comparison to DddW and DddY, but this finding is not surprising, because DddQ is also less efficient with the

Research Article
doi.org/10.1002/ejoc.202400098

natural substrate DMSOP. Finally, DddK shows activity in the conversion of all four substrate analogs and can especially for the long chain molecules BMSOP and IMSOP compete with DddW and DddY.

A comparison of the kinetic data obtained in this study for DddW, DddQ, DddK and DddY with DMSOP analogs to previously reported data for DMSP analogs is given in Figure 2. This overview reveals that generally DMSOP and DMSP are the most efficiently converted substrates in the series of DMSOP and DMSP analogs, respectively. Furthermore, DddW is more efficient in the conversion of DMSP analogs in comparison to the corresponding DMSOP analogs. This also seems to be the case for DddK and DddY, but for these enzymes only kinetic data for the conversion of DMSP and not of its analogs are available. In contrast, DddQ is generally more efficient in the conversion of DMSOP analogs in comparison to the corresponding DMSP analogs. This further supports the previous view that DddQ is better described as a DMSOP lyase than a DMSP lyase.[40]

The DMSOP analogs used in this study are chiral compounds with a stereogenic center located at the sulfur atom. Potentially, the cleavage of the DMSOP analogs may proceed with preference for one of the enantiomers and lead to enantiomerically enriched dialkyl sulfoxides. This was investigated using DddW that shows the broadest substrate tolerance in combination with good conversion rates. For this purpose, preparative scale incubations were performed with 50 mg of substrate, followed by product isolation and analysis through HPLC using a chiral stationary phase (Figure 3). While for the products obtained from EMSOP, IMSOP and BMSOP only very low enantiomeric excesses between 1% *ee* and 17% *ee* were obtained, the isolated product methylpropyl sulfoxide showed a slightly higer enantiomeric excess (25% *ee*). The optical rotation of $[\alpha]_D^{25} = -33.3$ (*c* 0.04, EtOH) pointed to the formation of (*R*)-methylpropyl sulfoxide (lit.: $[\alpha]_D = -139.0$, *c* 0.83, EtOH)[46] as the major enantiomer. Notably, the major enantiomer from BMSOP was also (*R*)-butylmethyl sulfoxide, while from EMSOP and IMSOP the *S*-configured dialkyl sulfoxides were the major products.

Conclusions

DMSP is a long known marine metabolite and several DMSP lyases have been described in the literature for its cleavage into the climatically relevant gas dimethyl sulfide.[27–34] Recently, the oxidized derivative DMSOP was discovered in the marine environment that may play a similarly important role in the marine sulfur metabolism as DMSP. As we[40] and others[41] have shown, DMSOP can also be cleaved by DMSP lyases. Furthermore, in our previous research we have demonstrated that DMSP lyases can also cleave various DMSP analogs e.g. with longer alkyl chains or with the sulfur atom exchanged with other heteroatoms, demonstrating that DMSP lyases exhibit a broad substrate tolerance.[42–45] The present study has demonstrated that also DMSOP analogs with longer alkyl chains can be converted by DMSP lyases, with a poor enantioselectivity for

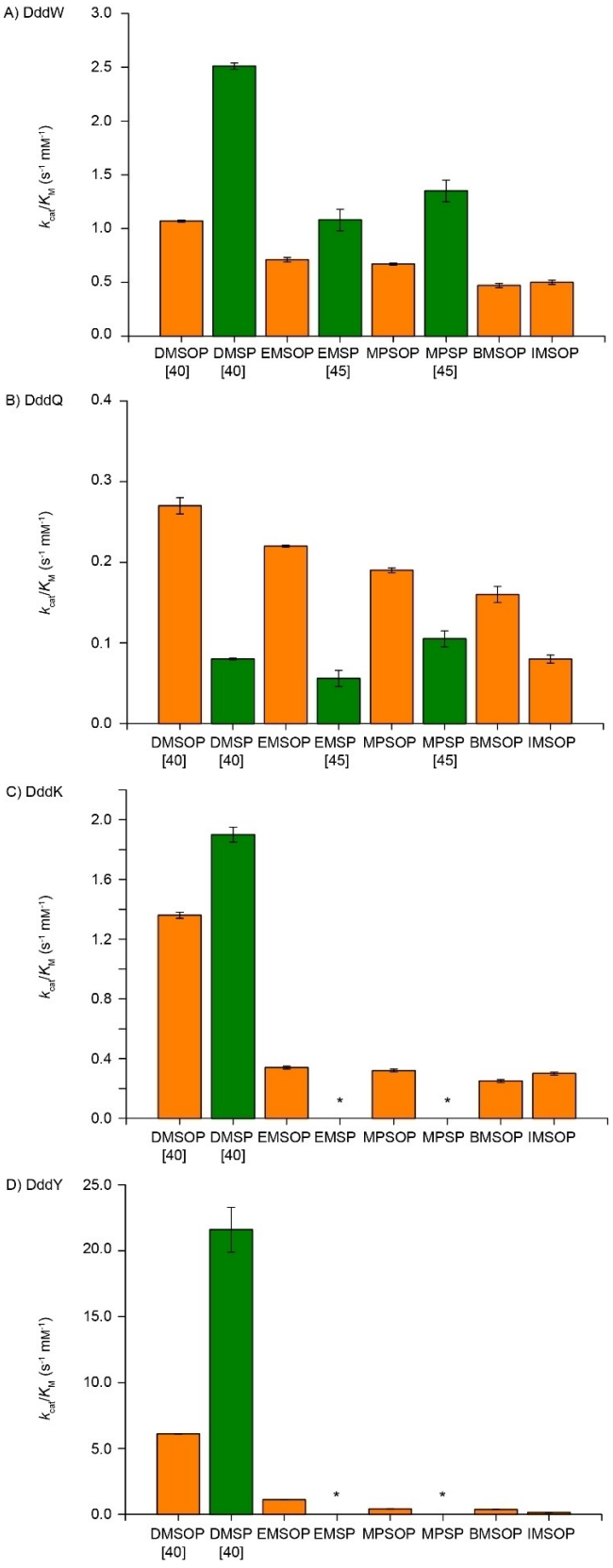

Figure 2. Comparison of enzyme kinetics for DddW, DddQ, DddK and DddY with DMSOP analogs (orange bars) and DMSP analogs (green bars). Error bars indicate mean and standard deviations from triplicates. Please note that the four sections make use of different y-axis scalings. Asterisks indicate enzyme-substrate combinations for which no data are available. References for data taken from the literature are given underneath each substrate.

Research Article
doi.org/10.1002/ejoc.202400098

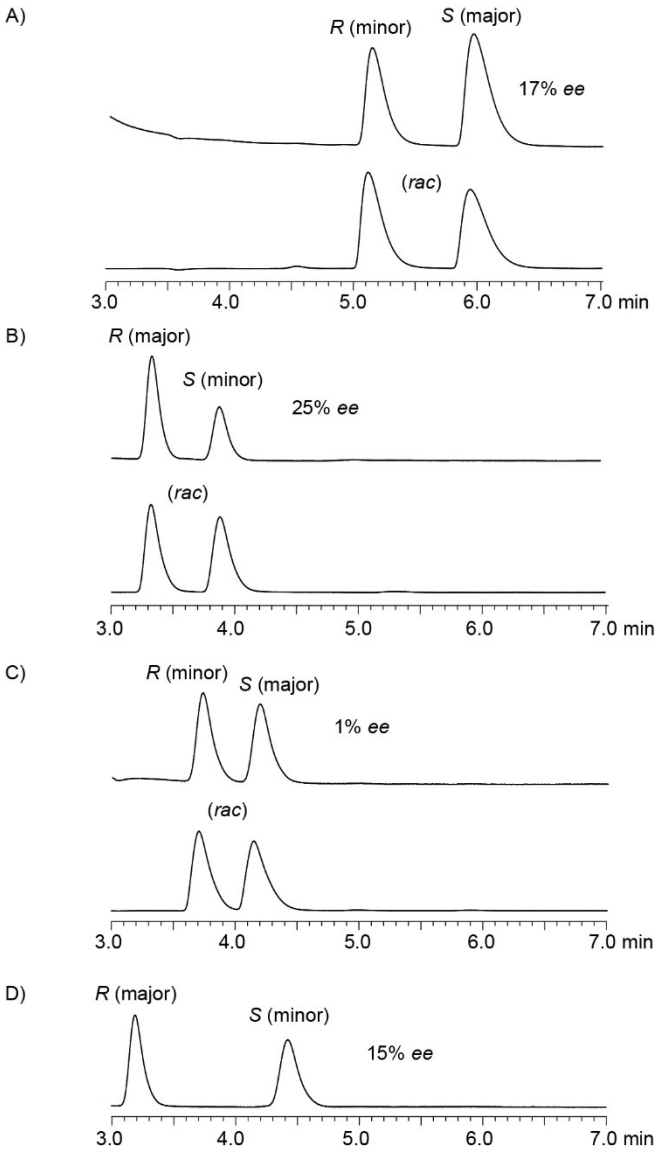

Figure 3. Determination of enantiomeric excesses of alkylmethyl sulfoxides enzymatically obtained with DddW by HPLC using a chiral stationary phase in combination with different solvent systems. Chromatograms of A) the product obtained from EMSOP (17% *ee*, top) and racemic ethylmethyl sulfoxide (bottom), B) the product obtained from MPSOP (25% *ee*, top) and racemic propylmethyl sulfoxide (bottom), C) the product obtained from IMSOP (1% *ee*, top) and racemic isopropylmethyl sulfoxide (bottom), and D) the product obtained from BMSOP (15% *ee*). A racemic standard for butylmethyl sulfoxide was not available.

the chiral substrates, which further expands the generally broad substrate spectrum of this remarkably diverse family of enzymes.

Experimental Section

Gene Expression and Protein Purification

E. coli BL21 (DE3) cells carrying the respective lyase gene were cultured in LB medium (10 mL; 10 g tryptone, 5 g yeast extract, 5 g NaCl, pH 7.2, 1 L water) containing kanamycin (50 μg/mL) at 37 °C and 160 rpm overnight. This starter culture (1 mL) was used to inoculate an expression culture in LB medium (1 L) containing kanamycin. The expression culture was grown until $OD_{600} = 0.5–0.6$ (37 °C, 160 rpm) and then cooled to 18 °C before expression was induced by the addition of a solution of IPTG (1 mL; 0.4 mm in water). The expression culture was incubated for 18 h (18 °C, 160 rpm). The cells were collected by centrifugation (5,500×g, 1 h, 4 °C), the supernatant was discarded and the cell pellet was resuspended in lysis buffer (15 mL; for DddW and DddQ: 10 mm Tris, 200 mm NaCl, 20 mm imidazole, pH 8; for DddP: 20 mm MES, 50 mm NaCl, 20 mm imidazole, pH 6; for DddK: 50 mm HEPES, 300 mm NaCl, 5 mm imidazole, pH 7.5; for DddL and DddY: 100 mm Tris, 100 mm NaCl, 1 mm $CaCl_2$, 10 mg lysozyme, pH 8). The cells were lysed by ultra-sonication under ice cooling (sonication frequency: 20 kHz; DddW, DddQ, DddP, DddL and DddY: 5x 30 sec, DddK: 5x 4 sec). The cell debris was separated by centrifugation (10,000×g, 10 min, 4 °C) and the soluble fraction was passed through a cellulose filter (20 μm). Enzyme purification was carried out by Ni^{2+}-NTA affinity chromatography. For this purpose, the soluble fraction was loaded onto a Ni^{2+}-NTA column, followed by washing with lysis buffer (2x 10 mL) and elution of the target protein using elution buffer (for DddW: 10 mm Tris, 200 mm NaCl, 500 mm imidazole, pH 8, 10 mL; for DddQ: 10 mm Tris, 200 mm NaCl, 100 mm imidazole, pH 8, 10 mL; for DddP: 20 mm MES, 50 mm NaCl, pH 6, 10 mL; for DddK: 50 mm HEPES, 300 mm NaCl, 500 mm imidazole, pH 7.5, 10 mL; for DddY: 100 mm Tris-HCl, 100 mm NaCl, 1 mm $CaCl_2$, 10 mg lysozyme, 150 mm imidazole, pH 8, 10 mL). DddL was used without chromatographic purification, because this enzyme loses activity during purification. The enzyme concentrations were determined through Bradford assay.[47] (DddW: 2.65 mg/mL, DddQ: 1.26 mg/mL, DddP: 3.48 mg/mL, DddK: 4.62 mg/mL, DddY: 1.43 mg/mL). The enzyme solutions were stored at −80 °C with glycerol (10% v/v) added.

General Synthetic and Analytical Methods

All chemicals were purchased from TCI Deutschland GmbH (Eschborn, Germany) or Sigma-Aldrich Deutschland GmbH (Schnelldorf, Germany) and used without purification. Solvents were dried according to standard procedures and purified by distillation. Merck silica gel 60 (100–200 mesh) was used for column chromatography. Thin-layer chromatography was performed with 0.2 mm pre-coated plastic sheets Polygram Sil G/UV254 or for dialkyl sulfoxides with Alugram RP-18 0.15 mm pre-coated aluminum sheets (Machery-Nagel, Düren, Germany). ^{1}H-NMR and ^{13}C-NMR spectra were recorded on a Bruker AV I (400 MHz) or AV III HD Prodigy (500 MHz) spectrometer in $CDCl_3$ or D_2O. Spectra were referenced against solvent signals of $CDCl_3$ ($\delta = 7.26$ ppm) and D_2O ($\delta = 4.79$ ppm) for ^{1}H-NMR and $CDCl_3$ ($\delta = 77.01$ ppm) for ^{13}C-NMR.[48] Mass spectra were recorded on an LTQ Orbitrap XL (ESI-POS, Fisher Scientific) using acetonitrile as solvent.

Enzyme Activity Assay at Different pH Values

To investigate the pH dependency, the enzyme reactions were conducted with DddW, DddQ, DddP, DddK, DddL and DddY at variable pH. All experiments were performed using buffers and enzyme preparations in normal water. In a 1.5 mL tube, the enzyme preparation in the respective buffer used for protein purification (16 μL; concentration set to 3.0 μm) was added to a variable pH buffer (0.5 mL; 10 mm sodium citrate dihydrate, 10 mm citric acid, pH 3, pH 4, pH 5 or pH 6; or 50 mm Tris, pH 8 or pH 9), followed by incubation for 30 min at 30 °C. Then the (*methyl*-^{13}C)DMSOP analog (2.5 mmol; 5 mm final concentration) was added and incubation

was continued for 30 min at 30 °C. The reaction was stopped by heating to 90 °C for 5 min. Without any workup, the reaction product was measured immediately by ^{13}C-NMR spectroscopy. Peak integrations of the signals for the ^{13}C-labeled carbons of the substrate and the product were used to calculate % conversions. A control experiment was performed in the absence of enzyme by incubating (*methyl*-^{13}C)DMSOP analogs at variable pH (pH 3 to pH 9) for 30 min at 30 °C, showing no spontaneous conversion of the substrates over the whole pH range, while all four substrate analogs showed spontaneous degradation at pH 10.

Determination of Enzyme Kinetic Parameters (Michaelis-Menten)

Solutions of DMSOP analogues in kinetic assay buffer (50 mm HEPES, 50 mm NaCl, pH 8; substrate concentration 0.5 mm to 120 mm) were prepared freshly before the assay. Kinetic measurements were performed at 20 °C by mixing different concentrations of DMSOP analogs with enzyme (initial enzyme concentration $[E]_0 =$ 0.9 μM) in a UV cuvette (1 mL reaction volume). Formation of the product acrylic acid was monitored at $\lambda = 232$ nm (HEPES, pH 8) for 5 min. The used wavelengths for absorption measurements of the formed product acrylic acid were chosen higher than the λ_{max} in the corresponding buffer (Figure S2) to prevent exceeding the measurement range of the UV-spectrometer at high substrate concentrations.

Linear regression of the absorption plot recorded by the Cary WinUV kinetics application (Agilent) was used to calculate the initial speed of the reaction (v_0). Correlation factors ($F_{abs->[c]}$) to convert measured absorptions into product concentrations were determined by measuring absorptions of different concentrations at the chosen wavelength in a concentration range for the product of 0.2–1.0 mm in the respective buffer. Absorptions were plotted against concentrations and the slope was determined via linear regression, giving $F_{abs->[c]}$ (Table S2).

For each enzyme-substrate combination the kinetic measurements were performed in triplicates for each set of conditions (substrate concentration). From these replicates average and standard deviation for each data point in Figures S3–S18, reaction rates (v_0) versus substrate concentration ([S]), were determined.The Hill function

$$v_0 = v_{max}\frac{([S]^n)}{K^n + [S]^n} \quad (1)$$

was fitted to the data using OriginPro 8.5 (Origin Lab Corporation, Northampton, MA, USA), defining $n = 1$ to give the Michaelis-Menten equation. From these plots the Michaelis-Menten constant (K_M) and the maximum reaction rate (v_{max}) were determined using the implemented OriginPro 8.5 functions. The turnover number (k_{cat}) was then calculated using the equation

$$k_{cat} = \frac{v_{max}}{[E]_0} \quad (2).$$

Determination of the Enantiomeric Excesses of Dialkyl Sulfoxides

A DddW protein preparation (300 μL, 5.6 mg/mL) was added to incubation buffer (2 mL; 50 mm Tris, pH 8) and incubated for 30 min at 30 °C. Then a solution of **23 a** (50.0 mg, 0.25 mmol), **23 b** (50.0 mg, 0.23 mmol), **23 c** (50.0 mg, 0.22 mmol) or **23 d** (50.0 mg, 0.23 mmol) in incubation buffer (3 mL) was added and the incubation was continued at 30 °C overnight. The reaction mixtures were concentrated in vacuo and the residue was purified by reverse phase (RP-18) column chromatography (0.5 % H_2O/acetonitrile) to obtain the dialkyl sulfoxides.

Ethylmethyl sulfoxide: Yield: 2.2 mg, 0.024 mmol, 10 %; TLC (RP-18, 0.5 % H_2O/acetonitrile): $R_f = 0.33$; ^{1}H-NMR ($CDCl_3$, 500 MHz): $\delta = 2.73$ (q, $^3J_{H,H} = 7.4$ Hz, 2H), 2.55 (s, 3H), 1.33 (t, $^3J_{H,H} = 7.50$ Hz, 3H) ppm; ^{13}C-NMR ($CDCl_3$, 125 MHz): $\delta = 41.33$ (CH_2), 34.10 (CH_3), 11.41 (CH_3) ppm;[52] optical rotation: $[\alpha]_D^{25} = +5.0$ (*c* 0.06, EtOH, 17 % *ee*), lit. for the enriched *S* enantiomer: $[\alpha]_D^{25} = +7.69$ (*c* 1.26, EtOH, 8.1 % *ee*).[49]

Methylpropyl sulfoxide: Yield: 1.7 mg, 0.016 mmol, 7.0 %, TLC (RP-18, 0.5 % H_2O/acetonitrile): $R_f = 0.35$; ^{1}H-NMR ($CDCl_3$, 500 MHz): $\delta = 2.84$–2.71 (m, 1H), 2.68–2.60 (m, 1H), 2.59 (s, 3H), 1.86–1.76 (m, 2H), 1.10 (t, $^3J_{H,H} = 7.4$ Hz, 2H) ppm; ^{13}C-NMR ($CDCl_3$, 125 MHz): $\delta = 56.65$ (CH_2), 38.52 (CH_3), 16.24 (CH_2), 13.34 (CH_3) ppm;[50] optical rotation: $[\alpha]_D^{25} = -33.3$ (*c* 0.04, EtOH, 25 % *ee*), lit. for the pure *R* enantiomer: $[\alpha]_D = -139.0$ (*c* 0.83, EtOH).[46]

Isopropylmethyl sulfoxide: Yield: 3.9 mg, 0.036 mmol, 16 %, TLC (RP-18, 0.5 % H_2O/acetonitrile): $R_f = 0.35$; ^{1}H-NMR ($CDCl_3$, 500 MHz): $\delta = 2.76$ (hept, $^3J_{H,H} = 6.9$ Hz, 1H), 2.48 (s, 3H), 1.31 (d, $^3J_{H,H} = 6.9$ Hz, 3H), 1.27 (d, $^3J_{H,H} = 6.9$ Hz, 3H) ppm; ^{13}C-NMR ($CDCl_3$, 125 MHz): $\delta = 51.98$ (CH), 34.63 (CH_3), 15.48 (CH_3), 14.83 (CH_3) ppm;[51] optical rotation: $[\alpha]_D^{25} = +4.0$ (*c* 0.2, EtOH, 1 % *ee*).

Butylmethyl sulfoxide: Yield: 2.3 mg, 0.019 mmol, 9.0 %, TLC (RP-18, 0.5 % H_2O/acetonitrile): $R_f = 0.32$; ^{1}H-NMR (CD_3OD, 500 MHz): $\delta = 2.83$ (ddd, $^2J_{H,H} = 13.1$ Hz, $^3J_{H,H} = 8.9$, 7.3 Hz, 1H), 2.76 (ddd, $^2J_{H,H} = 13.1$ Hz, $^3J_{H,H} = 8.3$, 6.4 Hz, 1H), 2.63 (s, 3H), 1.78–1.67 (m, 2H), 1.58–1.42 (m, 2H), 0.99 (t, $^3J_{H,H} = 7.43$ Hz, 2H) ppm; ^{13}C-NMR (CD_3OD, 125 MHz): $\delta = 54.62$ (CH_2), 38.10 (CH_3), 25.69 (CH_2), 22.89 (CH_2), 13.97 (CH_3) ppm;[52] optical rotation: $[\alpha]_D^{25} = -11.0$ (*c* 0.10, EtOH, 15 % *ee*), lit. for the pure *S* enantiomer: $[\alpha]_D = +109.9$ (*c* 1.53, EtOH).[46]

Chiral HPLC

To obtain standard compounds, racemic alkylmethyl sulfoxides (ethylmethyl sulfoxide, propylmethyl sulfoxide, and isopropylmethyl sulfoxide) were synthesized as reported previously.[51] The determination of the enantiomeric ratios of the products obtained from the DMSOP analogs with DddW was performed on an Azura HPLC system (Knauer, Berlin, Germany) equipped with a UV-vis detector MWL 2.1 L (deuterium lamp, 190–600 nm) and a DAICEL Chiralpak IA–U column (1.6 μm; 3.0×100 mm). The elution was performed for the product obtained from EMSOP and racemic ethylmethyl sulfoxide with n-hexane/ethanol 95 : 5 (isocratic) at a flow rate of 0.85 mL min^{-1} (279 bar), for the product obtained from MPSOP and racemic propylmethyl sulfoxide with n-hexane/ethanol 85 : 15 (isocratic) at a flow rate of 0.85 mL min^{-1} (228 bar), for the product obtained from IMSOP and racemic isopropylmethyl sulfoxide with n-hexane/ethanol 90 : 10 (isocratic) at a flow rate of 0.85 mL min^{-1} (211 bar), and for the product obtained from BMSOP with n-hexane/ethanol 85 : 15 (isocratic) at a flow rate of 0.85 mL min^{-1} (228 bar).

Acknowledgements

This work was funded by the Deutsche Forschungsgemeinschaft DFG (SFB TRR 51 *"Roseobacter"*). We thank Andreas Schneider for HPLC analyses. Open Access funding enabled and organized by Projekt DEAL.

Conflict of Interests

The authors declare no conflict of interest.

Data Availability Statement

The data that support the findings of this study are available in the supplementary material of this article.

Keywords: enzymes · isotopes · lyases · substrate analogs · sulfur compounds

[1] F. Challenger, M. I. Simpson, *J. Chem. Soc.* **1948**, 1591–1597.
[2] D. C. Yoch, *Appl. Environ. Microbiol.* **2002**, *68*, 5805–5815.
[3] A. Vairavamurthy, M. O. Andreae, R. L. Iverson, *Limnol. Oceanogr.* **1985**, *30*, 59–70.
[4] G. O. Kirst, C. Thiel, H. Wolff, J. Nothnagel, M. Wanzek, R. Ulmke, *Mar. Chem.* **1991**, *35*, 381–388.
[5] G. V. Wolfe, M. Steinke, G. O. Kirst, *Nature* **1997**, *387*, 894–897.
[6] W. Sunda, D. J. Kieber, R. P. Kiene, S. Huntsman, *Nature* **2002**, *418*, 317–320.
[7] J. R. Seymour, R. Simo, T. Ahmed, R. Stocker, *Science* **2010**, *329*, 342–345.
[8] E. E. Clerc, J.-B. Raina, J. M. Keegstra, Z. Landry, S. Pontrelli, U. Alcolombri, B. S. Lambert, V. Anelli, F. Vincent, M. Masdeu-Navarro, A. Sichert, F. De Schaetzen, U. Sauer, R. Simo, J.-H. Hehemann, A. Vardi, J. R. Seymour, R. Stocker, *Nat. Commun.* **2023**, *14*, 8080.
[9] M. Gali, E. Devred, M. Levasseur, S.-J. Royer, M. Babin, *Remote Sens. Environ.* **2015**, *171*, 171–184.
[10] F. Challenger, R. Bywood, P. Thomas, B. J. Hayward, *Arch. Biochem. Biophys.* **1957**, *69*, 514–523.
[11] Y. Ishida, H. Kadota, *Agric. Biol. Chem.* **1967**, *31*, 756–757.
[12] J. W. H. Dacey, G. M. King, S. G. Wakeham, *Nature* **1987**, *330*, 643–645.
[13] A. D. Broadbent, G. B. Jones, R. J. Jones, *Estuarine Coastal Shelf Sci.* **2002**, *55*, 547–555.
[14] D. A. Gage, D. Rhodes, K. D. Nolte, W. A. Hicks, T. Leustek, A. J. L. Cooper, A. D. Hanson, *Nature* **1997**, *387*, 891–894.
[15] D. Rhodes, D. A. Gage, A. J. L. Cooper, A. D. Hanson, *Plant Physiol.* **1997**, *115*, 1541–1548.
[16] M. G. Kocsis, K. D. Nolte, D. Rhodes, T.-L. Shen, D. A. Gage, A. D. Hanson, *Plant Physiol.* **1998**, *117*, 273–281.
[17] M. G. Kocsis, A. D. Hanson, *Plant Physiol.* **2000**, *123*, 1153–1161.
[18] J. B. Raina, D. M. Tapiolas, S. Foret, A. Lutz, D. Abrego, J. Ceh, F. O. Seneca, P. L. Clode, D. G. Bourne, B. L. Willis, C. A. Motti, *Nature* **2013**, *502*, 677–680.
[19] A. R. J. Curson, J. Liu, A. Bermejo Martinez, R. T. Green, Y. Chan, O. Carrion, B. T. Williams, S.-H. Zhang, G.-P. Yang, P. C. Bulman Page, X.-H. Zhang, J. D. Todd, *Nat. Microbiol.* **2017**, *2*, 17009.
[20] C. Liao, F. P. Seebeck, *Angew. Chem.* **2019**, *131*, 3591–3594; *Angew. Chem. Int. Ed.* **2019**, *58*, 3553–3556.
[21] A. J. Kettle, M. O. Andreae, *J. Geophys. Res.* **2000**, *105*, 26793–26808.
[22] R. J. Charlson, J. E. Lovelock, M. O. Andreae, S. G. Warren, *Nature* **1987**, *326*, 655–661.
[23] S. M. Vallina, R. Simo, *Science* **2007**, *315*, 506–508.
[24] J. E. Lovelock, R. J. Maggs, R. A. Rasmussen, *Nature* **1972**, *237*, 452–453.
[25] J. D. Todd, R. Rogers, Y. G. Li, M. Wexler, P. L. Bond, L. Sun, A. R. J. Curson, G. Malin, M. Steinke, A. W. B. Johnston, *Science* **2007**, *315*, 666–669.
[26] U. Alcolombri, P. Laurino, P. Lara-Astiaso, A. Vardi, D. S. Tawfik, *Biochemistry* **2014**, *53*, 5473–5475.
[27] A. R. J. Curson, R. Rogers, J. D. Todd, C. A. Brearly, A. W. B. Johnston, *Environ. Microbiol.* **2008**, *10*, 757–767.
[28] J. D. Todd, A. R. J. Curson, C. L. Dupont, P. Nicholson, A. W. B. Johnston, *Environ. Microbiol.* **2009**, *11*, 1376–1385.
[29] J. D. Todd, A. R. J. Curson, M. Kirkwood, M. J. Sullivan, R. T. Green, A. W. B. Johnston, *Environ. Microbiol.* **2011**, *13*, 427–438.
[30] A. R. J. Curson, M. J. Sullivan, J. D. Todd, A. W. B. Johnston, *ISME J.* **2011**, *5*, 1191–1200.
[31] J. D. Todd, M. Kirkwood, S. Newton-Payne, A. W. B. Johnston, *ISME J.* **2012**, *6*, 223–226.
[32] J. Sun, J. D. Todd, J. C. Thrash, Y. Qian, M. C. Qian, B. Temperton, J. Guo, E. K. Fowler, J. T. Aldrich, C. D. Nicora, M. S. Lipton, R. D. Smith, P. de Leenheer, S. H. Payne, A. W. B. Johnston, C. L. Davie-Martin, K. H. Halsey, S. J. Giovannoni, *Nat. Microbiol.* **2016**, *1*, 16065.
[33] S.-Y. Wang, N. Zhang, Z.-J. Teng, X.-D. Wang, J. D. Todd, Y.-Z. Zhang, H.-Y. Cao, C.-Y. Li, *Environ. Microbiol.* **2023**, *25*, 1238–1249.
[34] U. Alcolombri, S. Ben-Dor, E. Feldmesser, Y. Levin, D. S. Tawfik, A. Vardi, *Science* **2015**, *348*, 1466–1469.
[35] C. Y. Li, X. J. Wang, X. L. Chen, Q. Sheng, S. Zhang, P. Wang, M. Quareshy, B. Rihtman, X. Shao, C. Gao, F. Li, S. Li, W. Zhang, X.-H. Zhang, G.-P. Yang, J. D. Todd, Y. Chen, Y.-Z. Zhang, *eLife* **2021**, *10*, e64045.
[36] E. C. Howard, J. R. Henriksen, A. Buchan, C. R. Reisch, H. Bürgmann, R. Welsh, W. Ye, J. M. Gonzalez, K. Mace, S. B. Joye, R. P. Kiene, W. B. Whitman, M. A. Moran, *Science* **2006**, *314*, 649–652.
[37] C. R. Reisch, M. J. Stoudemayer, V. A. Varaljay, I. J. Amster, M. A. Moran, W. B. Whitman, *Nature* **2011**, *473*, 208–211.
[38] A. K. Chhalodia, J. S. Dickschat, *ChemBioChem* **2024**, *25*, e202300795.
[39] K. Thume, B. Gebser, L. Chen, N. Meyer, D. J. Kieber, G. Pohnert, *Nature* **2018**, *563*, 412–415.
[40] A. K. Chhalodia, J. S. Dickschat, *Org. Biomol. Chem.* **2023**, *21*, 3083–3089.
[41] O. Carrion, C.-Y. Li, M. Peng, J. Wang, G. Pohnert, M. Azizah, X.-Y. Zhu, A. R. J. Curson, Q. Wang, K. S. Walsham, X.-H. Zhang, S. Monaco, J. M. Harvey, X.-L. Chen, C. Gao, N. Wang, X.-J. Wang, P. Wang, S. J. Giovannoni, C.-P. Lee, C. P. Suffridge, Y. Zhang, Z. Luo, D. Wang, J. D. Todd, Y.-Z. Zhang, *Nat. Microbiol.* **2023**, *8*, 2326–2337.
[42] J. S. Dickschat, C. Zell, N. L. Brock, *ChemBioChem* **2010**, *11*, 417–425.
[43] N. L. Brock, M. Menke, T. A. Klapschinski, J. S. Dickschat, *Org. Biomol. Chem.* **2014**, *12*, 4318–4323.
[44] A. K. Chhalodia, J. S. Dickschat, *Beilstein J. Org. Chem.* **2021**, *17*, 569–580.
[45] I. Burkhardt, L. Lauterbach, N. L. Brock, J. S. Dickschat, *Org. Biomol. Chem.* **2017**, *15*, 4432–4439.
[46] K. K. Andersen, B. Bujnicki, J. Drabowicz, M. Mikolajczyk, J. B. O'Brien, *J. Org. Chem.* **1984**, *49*, 4070–4072.
[47] M. M. Bradford, *Anal. Biochem.* **1976**, *72*, 248–254.
[48] G. R. Fulmer, A. J. M. Miller, N. H. Sherden, H. E. Gottlieb, A. Nudelman, B. M. Stoltz, J. E. Bercaw, K. I. Goldberg, *Organometallics* **2010**, *29*, 2176–2179.
[49] M. Akazome, A. Hirabayashi, K. Takaoka, S. Nomura, K. Ogura, *Tetrahedron* **2005**, *61*, 1107–1113.
[50] S. A. Schwengers, C. K. De, O. Grossmann, J. A. Grimm, N. R. Sadlowski, G. G. Gerosa, B. List, *J. Am. Chem. Soc.* **2021**, *143*, 14835–14844.
[51] J. Wu, Z. Wang, X. Y. Chen, Y. Wu, D. Wang, Q. Peng, P. Wang, *Sci. China Chem.* **2020**, *63*, 336–340.
[52] X. B. Li, J. T. Liu, *Chin. J. Chem.* **2007**, *25*, 1309–1311.

Manuscript received: January 26, 2024
Revised manuscript received: March 12, 2024
Accepted manuscript online: March 12, 2024
Version of record online: March 28, 2024

Publications

[1] A. K. Chhalodia, J. Rinkel, D. Konvalinkova, J. Petersen, J. S. Dickschat, *Beilstein J. Org. Chem.* **2021**, *17*, 420–430.

[2] A. K. Chhalodia, J. S. Dickschat, *Beilstein J. Org. Chem.* **2021**, *17*, 569–580.

[3] A. K. Chhalodia, J. S. Dickschat, *Org. Biomol. Chem.* **2023**, *21*, 3083–3089.

[4] A. K. Chhalodia, H. Xu, G. B. Tabekoueng, B. Gu, K. A. Taizoumbe, L. Lauterbach, J. S. Dickschat, *Beilstein J. Org. Chem.* **2023**, *19*, 1386–1398.

[5] A. K. Chhalodia, J. S. Dickschat, *ChemBioChem* **2024**, *25*, e202300795.

[6] A. K. Chhalodia, J. S. Dickschat, *Eur. J. Org. Chem.* **2024***, 17*, e202400098.

[7] K. A. Taizoumbe, A. K. Chhalodia, B. Goldfuss, J. S. Dickschat, *Eur. J. Org. Chem.* **2024**, e202400583.

Abstract

This cumulative doctoral thesis encompasses six research articles focused on mechanistic investigations of sulfur metabolism and terpene biosynthesis. The primary focus of this research is on enzymes involved in the degradation of sulfur metabolites, which play a critical role in the marine sulfur cycle. A part of this research is about the study of DMSP lyases that facilitate the breakdown of DMSP analogs into compounds with natural flavors. An Interesting contribution of this thesis is the detailed investigation into the degradation of a newly discovered sulfur metabolite, dimethylsulfoxonium propionate (DMSOP) by DMSP lyases. This represents the first comprehensive analysis of how DMSP lyases interact with and break down the DMSOP. Additionally, the research partially investigated the stereoselectivity of DMSP lyases by synthesizing the chiral DMSOP analogs. This aspect of the study highlights the DMSP lyases ability to distinguish and act upon different stereoisomers.

Another key enzyme explored in this thesis is DmdC, which plays an important role in the DMSP demethylation pathway. The lack of a crystal structure for DmdC together with its substrate poses a significant challenge to understanding its catalytic mechanism. To address this, deuterium-labeled isotopomers were synthesized, enabling detailed stereochemical investigations. In addition to sulfur metabolism, this thesis also explores terpene biosynthesis. It shows the isolation and characterization of the first bacterial enzymes capable of synthesizing sesquiterpenes, including (+)-α-cadinene, (+)-δ-cadinol, and (−)-amorpha-4,11-diene.

All in all, this thesis provides a comprehensive and detailed investigations of sulfur metabolism and terpene biosynthesis. It advances the understanding of the enzymatic processes involved in these essential biochemical pathways, offering new insights into the natural mechanisms that drive these reactions.